

# DOCTORAL THESIS

## Formulation and the characterisation of a cationic liposomal adjuvants for the delivery of a promising subunit tuberculosis vaccine

Mohammed Hussain

If you have discovered material in AURA which is unlawful e.g. breaches copyright, (either yours or that of a third party) or any other law, including but not limited to those relating to patent, trademark, confidentiality, data protection, obscenity, defamation, libel, then please read our takedown policy at <http://www1.aston.ac.uk/research/aura/aura-take-down-policy/> and contact the service immediately [eprints@aston.ac.uk](mailto:eprints@aston.ac.uk).

**FORMULATION AND CHARACTERISATION OF CATIONIC LIPOSOMAL  
ADJUVANTS FOR THE DELIVERY OF A PROMISING SUBUNIT  
TUBERCULOSIS VACCINE**

**M. JUBAIR HUSSAIN**

**Doctor of Philosophy**

**ASTON UNIVERSITY**

November 2011

This copy of the thesis has been supplied on condition that anyone who consults it is understood to recognise that its copyright rests with its author and that no quotation from the thesis and no information derived from it may be published without proper acknowledgement.

**Aston University**

**Formulation and characterisation of cationic liposomal adjuvants for the delivery of a promising subunit tuberculosis vaccine**

**M. Jubair Hussain**

**Doctor of Philosophy  
2011**

Cationic liposomes of dimethyldioctadecylammonium bromide (DDA) incorporating the glycolipid trehalose 6,6-dibehenate (TDB) forms a promising liposomal vaccine adjuvant. To be exploited as effective subunit vaccine delivery systems, the physicochemical characteristics of liposomes were studied in detail and correlated with their effectiveness *in vivo*, in an attempt to elucidate key aspects controlling their efficacy. This research took the previously optimised DDA-TDB system as a foundation for a range of formulations incorporating additional lipids of 1,2-dipalmitoyl-sn-glycero-3-phosphocholine (DPPC) or 1,2-distearoyl-sn-glycero-3-phosphocholine (DSPC), by incrementally replacing the cationic content within DDA-TDB or reducing the total DDA-TDB dose upon its substitution, to ascertain the role of DDA and the effect of DDA-TDB concentration in influencing the resultant immunological performance upon delivery of the novel subunit TB vaccine, Ag85B-ESAT-6-Rv2660c (H56 vaccine).

With the aim of using the DPPC based systems for pulmonary vaccine delivery and the DSPC systems for application via the intramuscular route, initial work focused on physicochemical characterisation of the systems with incorporation of DPPC or DSPC displaying comparable physical stability, morphological structure and levels of antigen retention to that of DDA-TDB. Thermodynamic analysis was also conducted to detect main phase transition temperatures and subsequent *in vitro* cell culture studies demonstrated a favourable reduction in cytotoxicity, stimulation of phagocytic activity and macrophage activation in response to the proposed liposomal immunoadjuvants.

Immunisation of mice with H56 vaccine via the proposed liposomal adjuvants showed that DDA was an important factor in mediating resultant immune responses, with partial replacement or substitution of DDA-TDB stimulating Th1 type cellular immunity characterised by elevated levels of IgG2b antibodies and IFN- $\gamma$  and IL-2 cytokines, essential for providing protective efficacy against TB. Upon increased DSPC content within the formulation, either by DDA replacement or reduction of DDA and TDB, responses were skewed towards Th2 type immunity with reduced IgG2b antibody levels and elevated IL-5 and IL-10 cytokine production, as resultant immunological responses were independent of liposomal zeta potential.

The role of the cationic DDA lipid and the effect of DDA-TDB concentration were appreciated as the proposed liposomal formulations elicited antigen specific antibody and cellular immune responses, demonstrating the potential of cationic liposomes to be utilised as adjuvants for subunit vaccine delivery. Furthermore, the promising capability of the novel H56 vaccine candidate in eliciting protection against TB was apparent in a mouse model.

Key words: cationic liposomes, adjuvant, subunit vaccine, immunisation, tuberculosis.

## Acknowledgements

I would like to take this opportunity to thank Yvonne for giving me the chance to study such a great project, which has allowed me to develop an array of skills, travel and present work abroad and enjoy a great experience at Aston University, all of which would not be possible without her valuable supervision and support throughout my PhD. Yvonne is not just a great scientist but also an incredible inspiration...and how anyone can complete so many tasks and manage so many people without even breaking into a sweat still amazes me to this day!

A special thanks goes to Dr Vincent Bramwell for his undeniable wealth of knowledge and assistance throughout the immunisation study and I must also acknowledge the Statens Serum Institut (Copenhagen, Denmark), in particular Dennis Christensen for providing the H56 vaccine.

At Aston, I would also like to thank Gill Pilfold for all her time and support over the years, it is very much appreciated. I must also thank Jiteen and Roy for their technical assistance (and patience!), Mel, Brian and Wayne for their guidance during my *in vivo* studies and all the staff, post docs and my lab colleagues for making it such a fantastic working environment ☺

Lastly, but by no means least, there are not enough words to express my gratitude to my parents for their ever-present (and unconditional!) support, and to my brother, sister and the rest of my family for always looking after me. There is no doubt that I could not have attained half of my achievements to date if it wasn't for all their love, care and attention x

*“An investment in knowledge pays the best interest”*

(Benjamin Franklin)

## **Publications resulting from this and related work**

**Hussain, M.J.**, Seville, P.C., Rades, T., and Perrie, Y. Development of liposomes to enhance the delivery of sub-unit vaccines. **J. Pharm. Pharmacol.** 2008; 60 (Suppl. 1): A-39.

**Hussain, M.J.**, Seville, P.C., Rades, T., and Perrie, Y. Correlation of physicochemical properties of cationic liposome adjuvants with their in-vitro activation of macrophages. **J. Pharm. Pharmacol.** 2009; 61: A79-A80.

## **Related abstracts, posters and presentations**

**Hussain, M.J.**, Seville, P.C., Rades, T., and Perrie, Y. (2011) Characterisation of cationic liposomal adjuvants for the delivery of a promising sub-unit tuberculosis vaccine. *38<sup>th</sup> Annual Meeting and Exposition of the Controlled Release Society, Maryland, U.S.A., 2011.* (Poster presentation)

**Hussain, M.J.**, Seville, P.C., Rades, T., and Perrie, Y. (2011) The use of cationic liposomes for the delivery of a novel sub-unit tuberculosis vaccine. *UKICRS Symposium, Queen's University Belfast, 2011.* (Poster presentation)

**Hussain, M.J.**, Seville, P.C., Rades, T., and Perrie, Y. (2009) Characterisation of vaccine delivery systems based on cationic liposomal adjuvants. *Proceedings of the 4<sup>th</sup> International Liposome Society Conference, Liposome Advances: Progress in Drug and Vaccine Delivery, London, 2011.* (Poster presentation)

**Hussain, M.J.**, Seville, P., and Perrie, Y. (2009) Liposomes as Vehicles for Vaccine Delivery. *36<sup>th</sup> Annual Meeting and Exposition of the Controlled Release Society, Copenhagen, Denmark, 2009.* (Poster presentation)

**Hussain, M.J.**, Seville, P.C., Rades, T., and Perrie, Y. (2009) Characterisation of cationic liposomal vaccine adjuvants. *Young Pharmaceutical Scientists Meet, Nice, France, 2009.* (Oral presentation)

**Hussain, M.J.**, Seville, P.C., Rades, T., and Perrie, Y. (2009) Development of Cationic Liposomes as Carriers for Sub-unit Drug Delivery. *UKICRS Symposium, Kings College, London, 2009.* (Poster presentation)

**Hussain, M.J.**, Seville, P.C., Rades, T., and Perrie, Y. (2009) Formulation and Optimisation of Liposomal Adjuvant Systems for Pulmonary Delivery. *APS Inhalation, University of Nottingham, 2009.* (Poster presentation)

**Hussain, M.J.**, Seville, P.C., Rades, T., and Perrie, Y. (2008) Characterisation of DDA/TDB vesicles upon the addition of stabilising lipids in the advancement of a liposomal based adjuvant system. *NHS Quality Assurance Service Annual symposium, Manchester, 2008.* (Poster presentation)

## **Table of Contents**

<b>Title</b> .....	<b>1</b>
<b>Summary</b> .....	<b>2</b>
<b>Acknowledgements</b> .....	<b>3</b>
<b>List of publications</b> .....	<b>4</b>
<b>List of figures</b> .....	<b>9</b>
<b>List of tables</b> .....	<b>15</b>
<b>Abbreviations</b> .....	<b>17</b>
<b>Chapter 1: General Introduction</b> .....	<b>23</b>
1.1. Vaccines.....	24
1.1.1. Vaccines for the prevention of disease.....	24
1.1.2. Types of vaccines.....	25
1.2. Stimulating the immune system.....	29
1.2.1. Innate immunity: the first line of defence.....	29
1.2.2. Adaptive immunity: a specific and highly specialised response.....	30
1.2.3. Immunological memory.....	34
1.2.4. The emergence of Th17.....	34
1.3. Vaccine adjuvants.....	37
1.3.1. Delivery systems.....	39
1.3.1.1. Nano and microparticles.....	39
1.3.1.2. Oil and water emulsions.....	40
1.3.1.3. Immune stimulating complexes.....	40
1.3.1.4. VLP and IRIV.....	41
1.3.2. Immunostimulatory adjuvants and their combination with delivery systems.....	41
1.3.2.1. The use of Monophosphoryl Lipid A as an immunostimulatory adjuvant.....	44
1.3.2.2. The future of adjuvants and the success of AS04: a combined vaccine adjuvant.....	44
1.4. Liposomes: an effective vehicle for drug delivery.....	46
1.4.1. Liposomes as vaccine delivery systems.....	50
1.4.2. Cationic liposomal vaccine delivery systems.....	51
1.4.3. The promising potential of DDA-TDB as a liposomal adjuvant delivery system.....	51
1.5. Vaccination for protection against tuberculosis.....	56
1.5.1. Tuberculosis infection.....	59
1.5.2. Protection against TB: past, present and future promise.....	60
1.6. Aims and Objectives.....	65

<b>Chapter 2: Materials &amp; Methods.....</b>	<b>66</b>
2.1. Materials.....	67
2.2. Methods.....	68
2.2.1. Production of liposomes via lipid hydration.....	68
2.3. Dynamic light scattering: Characterisation of liposome systems.....	70
2.3.1. Determination of particle size.....	70
2.3.2. Determination of zeta potential.....	71
2.4. Differential Scanning Calorimetry (DSC) of liposomal dispersions.....	73
2.5. Protein loading studies.....	74
2.5.1. Separation of liposome associated and non-associated protein.....	74
2.5.2. Sodium dodecyl sulphate polyacrylamide gel electrophoresis.....	74
2.5.3. Bicinchoninic acid (BCA) assay: quantification of non-adsorbed protein.....	75
2.6. Quantification of adsorbed OVA protein via radiolabelling.....	77
2.6.1. Radiolabelling OVA.....	77
2.6.2. Determination of in vitro release via dialysis of liposomes adsorbed with OVA-I <sup>125</sup> .....	79
2.7. Serum stability studies: interaction of serum proteins with liposomes.....	79
2.8. Transmission electron microscopy (TEM).....	80
2.9. Cell culture/in vitro studies.....	81
2.10. CellTiter 96 aqueous non-radioactive cell proliferation assay (MTS assay).....	81
2.11. $\beta$ -N-Acetylglucosaminidase assay.....	85
2.12. Determination of tumour necrosis factor-alpha (TNF- $\alpha$ ) cytokine release.....	86
2.13. In vivo studies: immunological analysis of DDA-TDB based liposomes.....	89
2.13.1. Immunisation of mice.....	89
2.13.2. Spleenocyte proliferation.....	90
2.13.3. Evaluation of H56 antigen specific antibody isotypes.....	91
2.13.4. Quantification of cytokines via the ELISA (Sandwich ELISA).....	92
2.14. Statistical analysis.....	93

**Chapter 3: Characterisation of the effect of introducing supplementary lipids to DDA-TDB based liposomes.....94**

3.1. Introduction: characterisation of liposomal delivery systems.....	95
3.2. Characterisation of liposomes composed of DDA and TDB.....	97
3.2.1. The effect of buffers on the cationic liposome characteristics.....	97
3.2.2. The effect of buffer concentration upon the measured zeta potential.....	99
3.3. Replacement of DDA within DDA-TDB with DPPC or DSPC lipid.....	102
3.4. Substituting DDA-TDB with DPPC or DSPC lipid.....	106
3.4.1. The effect of buffer upon DDA-TDB substituted with additional lipids.....	107
3.4.2. Stability of DDA-TDB liposomes substituted with additional lipids.....	110
3.4.2.1. DDA-TDB based formulations incorporating DPPC.....	110
3.4.2.2. DDA-TDB based formulations incorporating DSPC.....	112
3.5. Morphological analysis of DDA-TDB based liposomes.....	115
3.5.1. TEM of DDA-TDB upon cationic replacement with additional lipids.....	115
3.5.2. TEM of DDA-TDB and its substitution with additional lipids.....	117
3.6. Protein adsorption studies.....	119
3.6.1. Physicochemical characterisation of liposomal systems in dosage form.....	120
3.6.1.1. Liposomal interactions with serum proteins and OVA-I <sup>125</sup> release over time.....	120

3.6.2. Physicochemical characterisation of liposomes adsorbed with OVA at 1 mg/ml.....	128
3.6.2.1. Vesicle size, zeta potential and protein adsorption upon DDA replacement.....	128
3.6.2.2. Vesicle size, zeta potential and protein adsorption upon DDA-TDB substitution.....	132
3.7. Further replacement of DDA within DDA-TDB.....	136
3.7.1. Physicochemical characterisation upon further DDA replacement.....	136
3.8. Conclusions.....	140

**Chapter 4: Thermodynamic analysis of the gel-to-liquid phase transition of DDA-TDB based liposomes.....142**

4.1. Introduction.....	143
4.1.1 Differential scanning calorimetry for thermodynamic analysis.....	143
4.1.2. Thermal characteristics of liposomes.....	144
4.2. DSC of DDA and the effect of TDB on the gel-to-liquid phase transition.....	148
4.3. Investigations using Nano DSC.....	149
4.4. DSC of DDA-TDB based liposomes replacing DDA with DPPC or DSPC lipid.....	152
4.5. DSC of DDA-TDB liposomes substituted with DPPC or DSPC lipid.....	158
4.6. Conclusions.....	163

**Chapter 5: Liposomal immunoadjuvants and their ability to activate macrophages in vitro.....165**

5.1. Introduction.....	166
5.1.1. Therapeutic applications of liposomal delivery systems.....	166
5.1.2. Liposomes as immunoadjuvants.....	166
5.2. Cytotoxicity studies: MTS cell proliferation assay.....	168
5.2.1. Calibration of BALC/c cell number.....	168
5.2.2. Determination of liposome sample concentration.....	169
5.2.3. Cell toxicity studies: DDA replacement within DDA-TDB.....	171
5.2.4. Cell toxicity studies: substitution of DDA-TDB.....	174
5.3. Determination of phagocytic activity: $\beta$ -N-Acetylglucosaminidase (NAG) assay.....	176
5.3.1. Effect of sample concentration upon resultant NAG release.....	176
5.3.2. Induced phagocytic activity upon replacement of DDA or substitution of DDA-TDB.....	178
5.4. Determination of macrophage activation upon quantification of TNF- $\alpha$ .....	181
5.4.1. Effect of sample concentration on mouse TNF- $\alpha$ cytokine production.....	181
5.4.2. Activation of TNF- $\alpha$ in response to DDA-TDB and its cationic replacement.....	183
5.4.3. TNF- $\alpha$ stimulation from DDA-TDB substituted with additional lipids.....	184
5.5. Further studies into determining whether the in vitro cellular activity is due to DDA replacement or removal.....	186
5.6. Conclusions.....	189

<b>Chapter 6: Characterisation and immunological analysis of liposomal TB vaccine delivery systems.....</b>	<b>191</b>
6.1. Introduction.....	192
6.1.1. Hybrid 56 vaccine antigen.....	192
6.2. Preliminary studies – optimisation of the splenocyte proliferation assay.....	193
6.2.1. Effect of cell number and concanavalin A upon splenocyte proliferation.....	193
6.2.2. Effect of pulsing activity and incubation time upon splenocyte proliferation.....	196
6.3. Immunisation study: determination of immune responses to a novel TB vaccine.....	198
6.3.1. H56 vaccine groups.....	198
6.3.2. Characterisation of liposomes upon H56 vaccine antigen adsorption.....	199
6.3.3. Production of anti-H56 IgG, IgG1 and IgG2b antibodies.....	202
6.3.3.1. Replacement of DDA in DDA-TDB: effect upon H56 specific antibody production.....	202
6.3.3.2. Substitution of DDA-TDB: effect upon H56 specific antibody production.....	204
6.3.4. H56 antigen specific splenocyte proliferation.....	207
6.3.4.1. The effect of replacing DDA content within the DDA-TDB adjuvant...207	
6.3.4.2. Substitution of DDA-TDB with varying levels of DSPC lipid.....	209
6.3.5. Quantification of cytokines.....	211
6.3.5.1. Replacement of DDA in DDA-TDB: effect upon H56 specific cytokine production.....	212
6.3.5.2. Substitution of DDA-TDB: effect upon H56 specific cytokine production.....	218
6.4. Conclusions.....	223
<b>Chapter 7: The potential of liposomes as systems for pulmonary vaccine delivery.....</b>	<b>224</b>
7.1. Introduction: vaccination via the pulmonary route.....	225
7.2. Liposomal compatibility with ethanol.....	226
7.3. The effect of ethanol on the particle size and zeta potential of empty liposomes.....	228
7.4. Effect of ethanol exposure to liposomes adsorbed with protein.....	231
7.5. Radiolabelled antigen retention.....	236
7.6. Drawbacks and disadvantages associated to liposomal pulmonary vaccine delivery.....	238
7.7. Conclusions.....	240
<b>Chapter 8: General discussion and conclusions.....</b>	<b>241</b>
<b>References.....</b>	<b>256</b>
<b>Appendix 1.....</b>	<b>281</b>
<b>Appendix 2.....</b>	<b>282</b>

## List of Figures

<b>Chapter 1</b>	<b>General Introduction</b>	<b>Page</b>
Figure 1.1	The main signalling events required to initiate T cell activation	32
Figure 1.2	Schematic overview of T cell activation and effector function	33
Figure 1.3	The classification of liposomes characterised by size and physical structure	47
Figure 1.4	Estimated cases of tuberculosis reported in 2009 by country	57
Figure 1.5	The deadly cycle of tuberculosis	58
<b>Chapter 2</b>	<b>Materials &amp; Methods</b>	
Figure 2.1	The production of liposomes via lipid hydration	69
Figure 2.2	A schematic illustration of the zeta potential of a particle	72
Figure 2.3	An example OVA protein standard curve for the BCA assay	76
Figure 2.4	Determination of $\gamma$ -radiation activity for iodine labelled OVA samples eluted through a sephadex column	78
Figure 2.5	Confirmatory BCA assay results for suspected protein labelled samples	78
Figure 2.6	The structure and conversion of MTS into formazan	82
Figure 2.7	Schematic diagram summarising the main steps of the MTS cell proliferation assay	84
Figure 2.8	The enzymatic hydrolysis of NAG substrate	85
Figure 2.9	Schematic summary of the mouse TNF- $\alpha$ enzyme-linked immunosorbent assay (ELISA) development kit	88
<b>Chapter 3</b>	<b>Characterisation of the effect of introducing supplementary lipids to DDA-TDB based liposomes</b>	
Figure 3.1	The effect of hydrating medium during liposome production characterised for particle size, polydispersity and zeta potential, together with visual observations of liposomes prepared in <b>A: Tris buffer</b> , <b>B: 5% Dextrose</b> and <b>C: PBS</b>	99
Figure 3.2	The effect of <b>Tris buffer</b> or <b>PBS</b> concentration on the measurement	102

	of zeta potential for DDA-TDB liposomes	
Figure 3.3	Replacement of DDA within DDA-TDB characterised for particle size, polydispersity and zeta potential, together with visual observations with <b>A: DPPC</b> or <b>B: DSPC</b>	<b>105</b>
Figure 3.4	The effect of <b>Tris buffer</b> vs. <b>PBS</b> (10 mM, pH 7.4) in the hydration of DDA-TDB substituted with <b>A: DPPC</b> or <b>B: DSPC</b> and characterised for particle size, polydispersity and zeta potential with corresponding sample images	<b>109</b>
Figure 3.5	Time development of particle size and zeta potential for DDA-TDB and its substitution with 25-75 mol% <b>DPPC</b> stored at 4 °C ( <b>A &amp; B</b> ) and at 25 °C ( <b>C &amp; D</b> )	<b>111</b>
Figure 3.6	Time development of particle size and zeta potential for DDA-TDB and its substitution with 25-75 mol% <b>DSPC</b> stored at 4 °C ( <b>A &amp; B</b> ) and at 25 °C ( <b>C &amp; D</b> )	<b>113</b>
Figure 3.7	Images of DDA-TDB in Tris buffer and its substitution at 25-75 mol% with <b>DPPC</b> at <b>A: day 0</b> and <b>B: day 28</b> or with <b>DSPC</b> at <b>C: day 0</b> and <b>D: day 28</b> , stored at 25 °C	<b>114</b>
Figure 3.8	TEM micrographs of DDA-TDB replaced with either <b>DPPC</b> or <b>DSPC</b> lipid	<b>116</b>
Figure 3.9	TEM micrographs of <b>A: DDA-TDB</b> , <b>B: DDA-TDB-50% DPPC</b> and <b>C: DDA-TDB-50% DSPC</b>	<b>118</b>
Figure 3.10	OVA/I <sup>125</sup> release profile in Tris buffer or FBS	<b>124</b>
Figure 3.11	Vesicle size, zeta potential and antigen release of liposomes adsorbed with 10 µg/ml OVA in Tris or FBS	<b>124-126</b>
Figure 3.12	Particle size, polydispersity and zeta potential upon replacement of DDA in DDA-TDB with <b>DPPC</b> or <b>DSPC</b> and adsorption of OVA at 1 mg/ml	<b>129</b>
Figure 3.13	Quantification of non-adsorbed OVA protein in the supernatants of DDA-TDB and its cationic replacement with <b>DPPC</b> or <b>DSPC</b> lipid, pelleted upon centrifugation	<b>131</b>
Figure 3.14	SDS-PAGE analysis upon OVA protein adsorption at 1 mg/ml for the cationic replacement of DDA-TDB with <b>DSPC</b>	<b>131</b>
Figure 3.15	Particle size, polydispersity and zeta potential upon substitution of DDA-TDB with <b>DPPC</b> or <b>DSPC</b> and adsorption of OVA at 1 mg/ml	<b>133</b>

Figure 3.16	Quantification of non-adsorbed OVA protein in the supernatants of DDA-TDB and its substitution with <b>DPPC</b> or <b>DSPC</b> lipid, pelleted upon centrifugation	<b>134</b>
Figure 3.17	SDS-PAGE analysis upon OVA protein adsorption at 1 mg/ml for DDA-TDB and its substitution with <b>DPPC</b>	<b>134</b>
Figure 3.18	Particle size, polydispersity, zeta potential and images of DDA-TDB, DDA- <b>DSPC</b> -TDB (100/150/50 $\mu\text{g}/\text{dose}$ ), the reduced weight ratio of DDA-TDB at 2:1 (100/50 $\mu\text{g}/\text{dose}$ ) and <b>DSPC</b> -TDB, before and after OVA adsorption at 1 mg/ml	<b>139</b>
Figure 3.19	Quantification of non-adsorbed OVA protein in the supernatants of DDA-TDB, DDA- <b>DSPC</b> -TDB (100/150/50 $\mu\text{g}/\text{dose}$ ), the reduced weight ratio of DDA-TDB at 2:1 (100/50 $\mu\text{g}/\text{dose}$ ) and <b>DSPC</b> -TDB, pelleted upon OVA adsorption at 1 mg/ml	<b>140</b>
<b>Chapter 4</b>	<b>Thermodynamic analysis of the gel-to-liquid phase transition of DDA-TDB based liposomes</b>	
Figure 4.1	A typical DSC thermogram of a liposomal dispersion	<b>145</b>
Figure 4.2	Schematic representation of phospholipid acyl chain arrangements from a gel-to-liquid crystalline state	<b>146</b>
Figure 4.3	DSC thermograms and corresponding thermodynamic parameters of the gel-to-liquid phase transition of DDA and DDA-TDB vesicles	<b>148</b>
Figure 4.4	Nano DSC thermogram of the gel-to-liquid phase transition of a DDA-TDB liposomal dispersion	<b>151</b>
Figure 4.5	DSC thermograms and associated thermodynamic parameters of the gel-to-liquid phase transition of DDA-DPPC-TDB liposomes	<b>154</b>
Figure 4.6	DSC thermogram summary and corresponding parameters of the main gel-to-liquid phase transition of DDA-DSPC-TDB liposomes	<b>157</b>
Figure 4.7	DSC thermogram summary and corresponding thermodynamic parameters measured for the main phase gel-to-liquid transition of DDA-TDB liposome dispersions substituted with 25, 50 or 75 mol% DPPC	<b>159</b>
Figure 4.8	DSC thermogram summary and corresponding thermodynamic	<b>161</b>

parameters measured for the main phase gel-to-liquid transition of DDA-TDB liposome dispersions substituted with 25, 50 or 75 mol% DSPC

<b>Chapter 5</b>	<b>Liposomal immunoadjuvants and their ability to activate macrophages <i>in vitro</i></b>	
Figure 5.1	Calibration of BALB/c cell proliferation	<b>169</b>
Figure 5.2	Effect of sample concentration on the cell viability of DDA-TDB vs. DSPC-TDB	<b>170</b>
Figure 5.3	Cell viability for DDA-TDB and the replacement of DDA with (A) DPPC or (B) DSPC	<b>173</b>
Figure 5.4	Cell viability of DDA-TDB substituted with (A) DPPC or (B) DSPC lipid	<b>175</b>
Figure 5.5	Effect of DDA-TDB sample concentration on NAG activation	<b>177</b>
Figure 5.6a	Stimulation of NAG activation upon replacement of DDA within DDA-TDB	<b>180</b>
Figure 5.6b	NAG activation induced by DDA-TDB and its substitution with DPPC or DSPC	<b>181</b>
Figure 5.7	Determination of macrophage activation using an enzyme linked immunosorbent assay (ELISA) in the evaluation of the effect of DDA-TDB sample concentration on TNF- $\alpha$ secretion	<b>183</b>
Figure 5.8	Quantification of TNF- $\alpha$ secretion indicative of macrophage activation using an enzyme-linked immunosorbent assay (ELISA) in response to DDA-TDB and its cationic replacement with DPPC or DSPC lipid.	<b>184</b>
Figure 5.9	Tumour necrosis factor alpha (TNF- $\alpha$ ) enzyme-linked immunosorbent assay (ELISA) results for DDA-TDB substituted with DPPC or DSPC	<b>185</b>
Figure 5.10	Cell viability (A) NAG activation (B) and TNF- $\alpha$ secretion (C) upon further replacement of DDA within the DDA-TDB adjuvant system	<b>188</b>

<b>Chapter 6</b>	<b>Characterisation and immunological analysis of liposomal TB vaccine delivery systems</b>	
Figure 6.1	The post exposure H56 vaccine candidate which combines the fusion protein Ag85B-ESAT-6 with Rv2660 antigen	<b>192</b>
Figure 6.2	The effect of cell number and ConA concentration upon the proliferation of splenocyte cells	<b>196</b>
Figure 6.3	The effect of pulsing activity and incubation time upon the proliferation of splenocyte cells	<b>197</b>
Figure 6.4	Mean serum H56 specific antibody titres generated by DDA-TDB and its cationic replacement with DSPC for A: IgG, B: IgG1 and C: IgG2b subsets	<b>203</b>
Figure 6.5	Mean serum H56 specific antibody titres generated by DDA-TDB and its substitution with DSPC at 25-75 mol% for A: IgG, B: IgG1 and C: IgG2b subsets	<b>205</b>
Figure 6.6	Spleen cell proliferation in response to stimulation/re-stimulation with H56 antigen upon replacement of cationic content within DDA-TDB	<b>209</b>
Figure 6.7	Spleen cell proliferation in response to stimulation/re-stimulation with H56 antigen upon substitution of DDA-TDB with DSPC	<b>210</b>
Figure 6.8	Spleen cell cytokine production after re-stimulation with H56 antigen at 0, 0.5 and 5 µg/ml, quantified for A: IFN-γ, B: IL-2, C: IL-6, D: IL-5 and E: IL-10, upon DDA replacement in DDA-TDB with DSPC	<b>216</b>
Figure 6.9	Spleen cell cytokine production after re-stimulation with H56 antigen at 0, 0.5 and 5 µg/ml, quantified for A: IFN-γ, B: IL-2, C: IL-6, D: IL-5 and E: IL-10, upon DDA-TDB substitution with DSPC	<b>220</b>

**Chapter 7    The potential of liposomes as systems for pulmonary vaccine delivery**

Figure 7.1	Effect of ethanol upon the particle size, polydispersity and zeta potential of A: DDA-TDB, B: DDA-DPPC-TDB (150-100-50 µg/dose) and C: DDA-TDB-50%DPPC liposomes over time	<b>229</b>
Figure 7.2	A process map summarising the experiment conducted to directly compare the effect of Tris buffer vs. ethanol on the cationic liposomes adsorbed with OVA protein	<b>231</b>
Figure 7.3	TEM micrographs of cationic liposomes with OVA in Tris buffer vs. ethanol exposure	<b>234</b>
Figure 7.4	Comparison of 1 mg/ml OVA in Tris buffer vs. ethanol	<b>236</b>

## List of Tables

<b>Chapter 1</b>	<b>General Introduction</b>	<b>Page</b>
Table 1.1	The categorisation of the main types of vaccines into live, inactivated and subunit form	<b>26</b>
Table 1.2	Examples of currently available vaccines categorised into order of priority	<b>28</b>
Table 1.3	Functional elements critical to inducing immunity	<b>36</b>
Table 1.4	Examples of tested vaccine adjuvants within the broadly classified adjuvant groups of delivery systems and immunostimulatory adjuvants	<b>38</b>
Table 1.5	Examples of commercialised liposome-based drugs on the market	<b>49</b>
Table 1.6	The versatility of DDA-TDB: a cationic liposomal adjuvant delivery system capable of providing immunity against a variety of disease targets	<b>54</b>
Table 1.7	DDA, TDB, DPPC and DSPC lipids used in the liposomal formulations and tested as novel adjuvants for TB subunit vaccine delivery	<b>55</b>
Table 1.8	Future vaccination strategies against tuberculosis	<b>64</b>
<b>Chapter 2</b>	<b>Materials &amp; Methods</b>	
Table 2.1	Incorporation of lipids for the substitution of DDA-TDB	<b>69</b>
<b>Chapter 3</b>	<b>Characterisation of the effect of introducing supplementary lipids to DDA-TDB based liposomes</b>	
Table 3.1	The replacement of DDA within DDA-TDB with DPPC or DSPC lipid	<b>103</b>
Table 3.2	Further DDA-TDB based formulations proposed to test whether responses were due to DDA replacement or a reduced DDA presence within the system	<b>137</b>

<b>Chapter 5</b>	<b>Liposomal immunoadjuvants and their ability to activate macrophages in vitro</b>	
Table 5.1	DDA-TDB based formulations in which the main liposomal adjuvant was either substituted or replaced, prior to the evaluation of induced phagocytic activity and macrophage activation	<b>178</b>
<b>Chapter 6</b>	<b>Characterisation and immunological analysis of liposomal TB vaccine delivery systems</b>	
Table 6.1	Tested cell numbers in the optimisation of their effect upon splenocyte proliferation	<b>194</b>
Table 6.2	Immunisation study: vaccine groups tested for immunological analysis with the novel TB vaccine candidate, H56 antigen	<b>199</b>
Table 6.3	Particle size, polydispersity and zeta potential of the liposomal vaccine groups characterised before and after H56 antigen adsorption, applied for the three immunisations of mice during the 7 week <i>in vivo</i> study	<b>201</b>
<b>Chapter 7</b>	<b>The potential of liposomes as systems for pulmonary vaccine delivery</b>	
Table 7.1	Particle size, polydispersity and zeta potential of liposomes adsorbed with OVA at 1 mg/ml in Tris buffer or exposed to ethanol and redispersed back into Tris buffer	<b>233</b>
Table 7.2	Levels of OVA/I <sup>125</sup> retention to DDA liposomes before and after exposure to ethanol	<b>237</b>

## Abbreviations

<b>AbISCO</b>	AbISCO-100
<b>ABTS</b>	2,2'-azino-bis(3-ethylbenzthiazoline-6-sulfonic acid)
<b>Ag85B</b>	Antigen 85B
<b>AIDS</b>	acquired immune deficiency syndrome
<b>ANOVA</b>	analysis of variance
<b>APC</b>	antigen presenting cell
<b>B cell</b>	bone-marrow derived lymphocyte cell
<b>BALB</b>	Bagg albino
<b>BCA</b>	bicinchoninic acid protein
<b>BCG</b>	Bacille Calmette-Guérin
<b>CAF01</b>	cationic adjuvant formulation 01
<b>CD4</b>	cluster of differentiation 4
<b>CD8</b>	cluster of differentiation 8
<b>CE</b>	cellulose ester
<b>Chol</b>	cholesterol
<b>CMI</b>	cell mediated immunity
<b>CO<sub>2</sub></b>	carbon dioxide
<b>ConA</b>	concanavalin A
<b>C<sub>p</sub></b>	heat capacity
<b>CPS</b>	counts per second
<b>CTH1</b>	Chlamydia subunit vaccine
<b>CTL</b>	cytotoxic T lymphocytes
<b>Cu</b>	copper
<b>DAMP</b>	damage associated molecular pattern
<b>DC</b>	dendritic cell
<b>ddH<sub>2</sub>O</b>	double distilled water
<b>DDA</b>	dimethyldioctadecyl ammonium
<b>DMEM</b>	Dulbecco's Modified Eagle Medium
<b>Delta H (ΔH)</b>	change in enthalpy
<b>DNA</b>	deoxyribose nucleic acid
<b>DODA</b>	didodecyldimethylammonium bromide
<b>DOPE</b>	dioleoylphosphatidylethanolamine

<b>DOTAP</b>	dioleoyl-trimethyl-ammonium-propane
<b>DPI</b>	dry powder inhalers
<b>DPPC</b>	1,2-dipalmitoyl- <i>sn</i> -glycero-3-phosphocholine
<b>DSC</b>	differential scanning calorimetry
<b>DSPC</b>	1,2-distearoyl- <i>sn</i> -glycero-3-phosphocholine
<b>DLPC</b>	dilauroyl phosphatidylcholine
<b>DLS</b>	dynamic light scattering
<b>DMPC</b>	dimyristoyl phosphatidylcholine
<b>DT</b>	diphtheria-tetanus
<b>ECACC</b>	European collection of cell cultures
<b>ELISA</b>	enzyme linked immunosorbent assay
<b>EMEA</b>	European Medicines Agency
<b>ESAT-6</b>	6 kDa early secretory antigenic target
<b>FBS</b>	fetal bovine serum
<b>FCS</b>	fetal calf serum
<b>FDA</b>	Food and Drug Administration
<b>G-75</b>	sephadex gel fractionation range (3-80 kDa)
<b>g-force</b>	gravitational force
<b>GLURP</b>	glutamate rich protein
<b>H1</b>	Hybrid-1 antigen (Ag85B-ESAT-6)
<b>H56</b>	Hybrid-56 antigen (Ag85B-ESAT-6-Rv2660)
<b>H<sub>2</sub>O<sub>2</sub></b>	hydrogen peroxide
<b>H<sub>2</sub>SO<sub>4</sub></b>	sulphuric acid
<b>HAV</b>	hepatitis A virus
<b>HBV</b>	hepatitis B virus
<b>HDL</b>	high density lipoproteins
<b>HFA</b>	hydro-fluoroalkane
<b>HIR</b>	humoral immune response
<b>HIV</b>	human immunodeficiency virus
<b>HRP</b>	horseradish peroxidase
<b>I.M.</b>	intramuscular
<b>IFN-<math>\gamma</math></b>	interferon-gamma
<b>Ig</b>	immunoglobulin

<b>IL</b>	interleukin
<b>IRIV</b>	immunopotentiating reconstituted influenza virosomes
<b>ISCOM</b>	immune stimulating complex
<b>J/g</b>	joules per gram
<b>kBq</b>	kilobecquerel
<b>KCl</b>	potassium chloride
<b>kDa</b>	kilodalton
<b>KH<sub>2</sub>PO<sub>4</sub></b>	Potassium dihydrogen phosphate
<b>kV</b>	kilovolts
<b>LaB6</b>	lanthanum hexaboride B6 filament
<b>LDH</b>	lactate dehydrogenase
<b>log</b>	logarithm
<b>LTBI</b>	latent tuberculosis infection
<b>LUV</b>	large unilamellar vesicle
<b>MAP</b>	mitogen-activated protein
<b>MBq</b>	megabecquerel
<b>MDI</b>	metered-dose inhaler
<b>MDP</b>	muramyl dipeptide
<b>MDR</b>	multi-drug resistant
<b>mg</b>	milligram
<b>MHC</b>	major histocompatibility complex
<b>min</b>	minute
<b>mJ</b>	millijoules
<b>ml</b>	millilitre
<b>MLV</b>	multilamellar vesicle
<b>mM</b>	millimolar
<b>MMR</b>	measles, mumps and rubella
<b>MP</b>	1-monopalmitoyl glycerol
<b>MPS</b>	mononuclear phagocytic system
<b>Mol</b>	mole
<b>MPL</b>	monophosphoryl lipid A
<b>MSP1</b>	Merozoite surface protein 1
<b>MTB</b>	Mycobacterium tuberculosis

<b>mV</b>	millivolts
<b>MW</b>	molecular weight
<b>MWCO</b>	molecular weight cut off
<b>NaCl</b>	sodium chloride
<b>NAG</b>	N-Acetylglucosaminidase
<b>NF<math>\kappa</math>B</b>	Nuclear factor kappa-light-chain-enhancer of activated B cells
<b>Na<sub>2</sub>HPO<sub>4</sub></b>	Sodium dihydrogen phosphate
<b>ng</b>	nanogram
<b>nm</b>	nanometre
<b>NP-GlcNAc</b>	4-Nitrophenyl-N-acetyl- $\beta$ -D-glucosaminide
<b>O/W</b>	oil in water
<b>OH</b>	hydroxyl group
<b>OVA</b>	ovalbumin
<b>p.d.</b>	polydispersity
<b>pI</b>	isoelectric point
<b>pMDI</b>	pressurised metered dose inhaler
<b>P-Value</b>	probability value
<b>PAMP</b>	pathogen associated molecular pattern
<b>PBS</b>	phosphate buffered saline
<b>PBST</b>	phosphate buffered saline/tween
<b>PC</b>	phosphatidyl choline
<b>PCS</b>	photon correlation spectroscopy
<b>pg</b>	picogram
<b>pH</b>	potential Hydrogen
<b>pI</b>	isoelectric point
<b>PLG</b>	polylactide-co-glycolide
<b>pMDI</b>	pressurised metered-dose inhaler
<b>PMS</b>	phenazine methosulfate
<b>PRR</b>	pattern recognition receptor
<b>PSG</b>	Penicillin/Streptomycin/L-Glutamine
<b>QELS</b>	quasi elastic light scattering
<b>R<sup>2</sup></b>	regression squared
<b>RPM</b>	revolutions per minute

<b>RT</b>	room temperature
<b>SD</b>	standard deviation
<b>SDS-PAGE</b>	sodium dodecyl sulfate polyacrylamide gel electrophoresis
<b>SMIPs</b>	small-molecule immune potentiators
<b>SMPC</b>	stearylmyristoyl-sn-phosphatidylcholine
<b>SSI</b>	Statens Serum Institut
<b>SUV</b>	small unilamellar vesicle
<b>TB</b>	Tuberculosis
<b>T Cell</b>	thymus-derived lymphocyte
<b>T<sub>c</sub></b>	crystallisation temperature
<b>TDB</b>	trehalose dibehenate
<b>TDM</b>	trehalose dimycolate
<b>TEM</b>	transmission electron microscopy
<b>Th1</b>	T-helper type 1 cell
<b>Th2</b>	T-helper type 2 cell
<b>TLR</b>	toll-like receptor
<b>T<sub>m</sub></b>	melting temperature
<b>TMB</b>	tetramethylbenzidine
<b>TNF-<math>\alpha</math></b>	tumour necrosis factor-alpha
<b>Tris</b>	tris(hydroxymethyl)aminomethane
<b>UK</b>	United Kingdom
<b>UNICEF</b>	United Nations International Children's Emergency Fund
<b>UN</b>	United Nations
<b>VLP</b>	virus-like particles
<b>WHO</b>	World Health Organisation
<b>XDR</b>	extensively drug-resistant
<b>ZP</b>	zeta potential
<b><math>\alpha</math></b>	alpha
<b><math>\beta</math></b>	beta
<b><math>^{\circ}\text{C}</math></b>	degrees Celsius
<b><math>^{\circ}\text{C/h}</math></b>	degrees Celsius per hour
<b>[<math>^3\text{H}</math>]thymidine</b>	tritiated thymidine
<b>I<sup>125</sup></b>	Iodine <sup>125</sup>

<b><math>\mu\text{Ci}</math></b>	microcurie
<b><math>\mu\text{g}</math></b>	microgram
<b><math>\mu\text{l}</math></b>	microlitre
<b><math>\mu\text{m}</math></b>	micrometre
<b><math>\mu\text{mol}</math></b>	micromole

# **Chapter 1**

## **General Introduction**

## ***1.1. Vaccines***

### *1.1.1. Vaccines for the prevention of disease*

The scientific foundation that shaped the concept of vaccination was fashioned by Edward Jenner in the eighteenth century when he recognised that patients with smallpox could be protected when vaccinated with the related cowpox virus. This led to the development of an effective vaccine which ultimately led to the abolition of smallpox by the end of the twentieth century, whilst also inspiring the intention of providing protection against exposure to contagious diseases (Seder & Hill, 2000; Plotkin, 2005).

Indeed, vaccination as a deliberate endeavour was initiated by Louis Pasteur when he discovered attenuation upon inadvertently inoculating an aged chicken cholera culture into chickens, exemplifying his belief that “*chance favours the prepared mind*” (Plotkin, 2005). Subsequent work conducted by Pasteur, when developing vaccines against anthrax and rabies, verified the hypothesis that the attenuation of pathogens could be affected by environmental factors such as extreme temperature, oxygen and chemicals. Another major breakthrough in the field of vaccination can be attributed to the recognition of antibody and cellular responses of the adaptive immune system, pioneered by Paul Ehrlich and Ilya Mechnikov, who were both acknowledged for their work on immunity when receiving the prestigious accolade of a Noble Prize early in the twentieth century. Such a discovery prompted vaccinologists to focus on eliciting adaptive immune responses (Plotkin, 2005).

As we have entered the 21<sup>st</sup> century, vaccines can be regarded as an efficient and essential means of health care and their impact is evident, particularly in the

developing world (O'Hagan *et al*, 2001). Moreover, they provide the ultimate biomedical guarantee of disease prevention, and although universal eradication of disease is not feasible, control of disease is, and this can only be managed if vaccination coverage is sustained. Moreover, vaccination provides various benefits to individuals, families, employers, governments and societies. Indeed, the importance of vaccination is widely endorsed by the specialised United Nations (UN) agency of the World Health Organisation (WHO), and the World Bank suggests that immunisation must be one of the main public health initiatives that governments should invest in (Taylor *et al*, 2009).

The basic principle of vaccination allows an individual to attain immunity against an infectious agent without enduring an initial infection, which is essential as the first or innate response to a natural infection is not fast enough to deter the onset of major symptoms. In contrast, memory cells of an adaptive immune response can induce rapid and robust protective reactions when exposed to an infectious agent for the second time (Perrie, 2006). The innate and adaptive immune responses will be discussed in further detail in section 1.2.

### *1.1.2. Types of vaccines*

Vaccines can be categorised into three main types; live, inactivated and subunit, as summarised in Table 1.1. The most widely used vaccines are of an inactivated nature as they can advantageously obliterate infected areas whilst maintaining present immunogenicity against certain infectious diseases. However, in comparison to vaccines of a live, attenuated form, although its administration is safe, the use of inactivated vaccines has many associated disadvantages as it is less potent, largely

limited to a humoral immune response, requires additional dosages and incurs undesirable host reactions and reversion to virulence (Black *et al*, 2010).

**Table 1.1. The categorisation of the main types of vaccines into live, inactivated and subunit form.** In addition, experimental DNA vaccines, therapeutic cancer vaccines and toxoid vaccines using detoxified exotoxins have also been created (O’Hagan *et al*, 2001; Perrie, 2006).



Live vaccines have an adjuvant capacity based upon the developed capability of the immune system to detect signs of potentially hazardous microbes, contributing immensely to disease control. Despite drawbacks of certain live vaccines for example, mutations of the polio virus and virus perseverance, its application continues to markedly reduce the effects of associated diseases (Minor, 2002; Oxman *et al*, 2005). A further example of a live, attenuated vaccine is Bacille Calmette-Guérin (BCG)

which is economical to process and dispense and efficacious in a variety of situations, particularly in strong and fatal instances of infant tuberculosis (Bloom & Fine, 1994). However, the unpredictable variability and lack of protection against certain diseases, for example with pulmonary tuberculosis in adults, render live vaccination unsafe, particularly to those whose immune systems are constrained (Chambers *et al*, 2003).

In general, for a vaccine to be regarded as effective it must meet certain criteria; to stimulate an adequate immune response, sustain safe administration, comply with issues of risk-benefit and be patient friendly in order to ultimately provide a safe means of health care. Upon understanding these identified desired attributes, of all vaccines currently in use, subunit vaccines have the best safety profile (Perrie *et al*, 2008). Moreover, the development of subunit vaccines containing selected purified antigens potentially reduces side effects, crucially eradicates reversion to virulence and the need for culturing harmful pathogens whilst eliciting specific immune responses, generating a safer, more immunologically defined form of vaccination (Black *et al*, 2010; Mohammed *et al*, 2010).

However, in spite of a favourable safety profile and relatively economical production costs for this next generation of vaccines containing purified recombinant proteins, compared to more traditional forms of vaccination, when administered alone, they are insufficient as the associated immunogenicity is limited. As a result, co-administration with appropriate immunostimulatory adjuvants is required to induce protective and prolonged immunity (Reed *et al*, 2008; O'Hagan & Gregorio, 2009).

In general, scientific and technological advances have provided numerous developments in the production and delivery of vaccines. Such breakthroughs have contributed to significantly minimising preventable deaths and the spread of disease worldwide. Table 1.2 shows selected examples of currently available vaccines prioritised for necessity.

**Table 1.2. Examples of currently available vaccines categorised into order of priority.** Vaccines of public health interest and those in use by UN agencies were defined and prioritised by The World Health Organisation and the United Nations International Children's Emergency Fund (UNICEF) according to the following criteria; demand within their specific markets, volume of supply and the unique associated profile of the available products (WHO, 2008).



Furthermore, infectious diseases where vaccines are still required include Malaria and human immunodeficiency virus (HIV), in which increases in infection rates are still currently being recorded. These diseases together with tuberculosis (TB) collectively form the devastating trio of “global killers” that urgently require prevention (Perrie *et al*, 2008). With conventional in-depth scientific knowledge of immunological mechanisms and host pathogen interactions, a push towards the ever-present challenge of formulating vaccines continues, as an answer to questions posed by today’s potentially fatal yet preventable diseases (Bramwell & Perrie, 2005).

## ***1.2. Stimulating the immune system***

With ever increasing knowledge of immunological processes, a more rational vaccine design aspires to induce specific, protective, and prolonged immunity upon vaccination (Lima *et al*, 2004). In general, immunity can be divided into two main responses of the innate and adaptive immune system.

### *1.2.1. Innate immunity: the first line of defence*

Although we frequently encounter microorganisms, disease is only ever caused occasionally, as the majority of organisms are rapidly identified and destroyed by non-antigen specific defence mechanisms. This initial stage of the host response upon infection forms the innate immune response which is a universal host defence stimulated upon infection. Only when an infectious agent manages to break this initial defence mechanism is an adaptive immune response triggered. Despite the innate immune system lacking the specificity of the adaptive immune system, it is capable of differentiating between self and non-self molecules and is vital to eliciting adaptive immunity (Janeway & Medzhitov, 2002; Storni *et al*, 2005).

The first line of defence initiated upon intrusion of microorganisms involves responses such as mucosal secretions, fever and phagocytic cells that fight pathogens in a non-specific manner. Antigen presenting cells (APCs) such as macrophages and dendritic cells (DCs), which are specialised phagocytes widely dispersed throughout the body, actively engulf, ingest and process potential antigens via phagocytosis, a mechanism that precedes antigen presentation and activation of T and B lymphocytes to generate an adaptive immune response. As a result, these activated cells collaborate with activated macrophages to destroy intra and extra-cellular pathogens (Gordon, 2002; Storni *et al*, 2005).

A crucial factor to the stimulation of innate immune responses is the detection of components commonly attached to the pathogen that are also foreign to the host and these components are known as pathogen-associated molecular patterns (PAMPs). After an infection, macrophages and DCs express mediating pattern recognition receptors (PRRs) such as toll-like receptors (TLRs) on their surface, bind such PAMPs and activate a signalling pathway to stimulate the host defences to respond to pathogens. Adaptive immunity is also initiated whilst activating APCs by eliciting pro-inflammatory cytokine secretion and upregulating co-stimulatory molecules (Werling & Jungi, 2003; Akira, 2003; Kawai & Akira, 2011).

TLR's can be categorised into two main groups based on their cellular localisation: TLRs 1, 2, 4-6 become expressed on the plasma membrane for the detection of bacterial components and TLRs 3, 7-9 become expressed within intracellular compartments and function as nucleic acid sensors (O'Hagan & Gregorio, 2009). Furthermore, stimulation of TLR's activate NF $\kappa$ B and mitogen-activated protein (MAP) kinases which are transcription factors that respond to produce key mediators of innate immunity such as interleukin (IL)-6 and interferon-gamma (IFN- $\gamma$ ) cytokines (Storni *et al*, 2005).

### *1.2.2. Adaptive immunity: a specific and highly specialised response*

Adaptive or acquired immunity follows the innate immune response which induces the proliferation of pathogen-specific T or B lymphocytes together with T and B cell memory, providing long-term protection against disease (Storni *et al*, 2005). In instances of viral infections, both cell mediated and humoral responses are essential to controlling infection. However, cellular immunity is crucial to mediating protection against intracellular pathogens such as mycobacterium tuberculosis (MTB).

To initiate an immune response, a vaccine formulation should trigger distinct signals of the immune system. APCs within all tissues in a non-immunostimulatory phase collect antigens from the local environment. Detection of PAMPs (stranger model) and/or damage associated molecular pattern (DAMP) molecules (which act as a danger model or non-infectious signal 0 response) induce APCs to migrate to draining lymph nodes with maturation signified by enhanced presentation of antigenic material to major histocompatibility complex (MHC) class I and class II receptor molecules that subsequently become presented to the immune system. For the activation of protective T cells, the presentation of antigen to naive T cells constitutes the first of two main signals required (Figure 1.1) (Lima *et al*, 2004; Reed *et al*, 2008).

Indeed, the presentation of antigen alone is insufficient to cause naive T cells to mature into effector T cells. As a result, an ideal vaccine should contain an immunopotentiating agent or adjuvant compound besides antigen in order to activate APCs via up-regulation of CD28 and CD80/CD86 co-stimulatory molecule expression, which constitutes signal 2 (Figure 1.1), a necessary action that ultimately prevents lymphocytes becoming anergic. Upon receiving signal 1 and 2, APCs can initiate key T cell responses to antigen such as cell survival, differentiation of naive T cells to develop into effector T cells and cytokine secretion (Rescigno *et al*, 1999; Lima *et al*, 2004; Reed *et al*, 2008).

CD4<sup>+</sup> T cells identify antigens that have been processed by APCs, for example by DCs, macrophages and B cells, that express MHC class II molecules (Figure 1.2) and upon such recognition, activation of CD4<sup>+</sup> T cells and T helper (Th) differentiation can take place into Th1 and Th2 type subsets (Seder & Hill, 2000). These two subsets

secrete a variety of cytokines and a typical Th1 type cytokine is IFN- $\gamma$  which induces phagocyte-mediated defence against infection, particularly with intracellular microbes. In contrast, Th2 type cytokines such as IL-4 and IL-5, down regulate Th1 type immune responses and activate B cells to stimulate antibody synthesis (Lima *et al*, 2004).

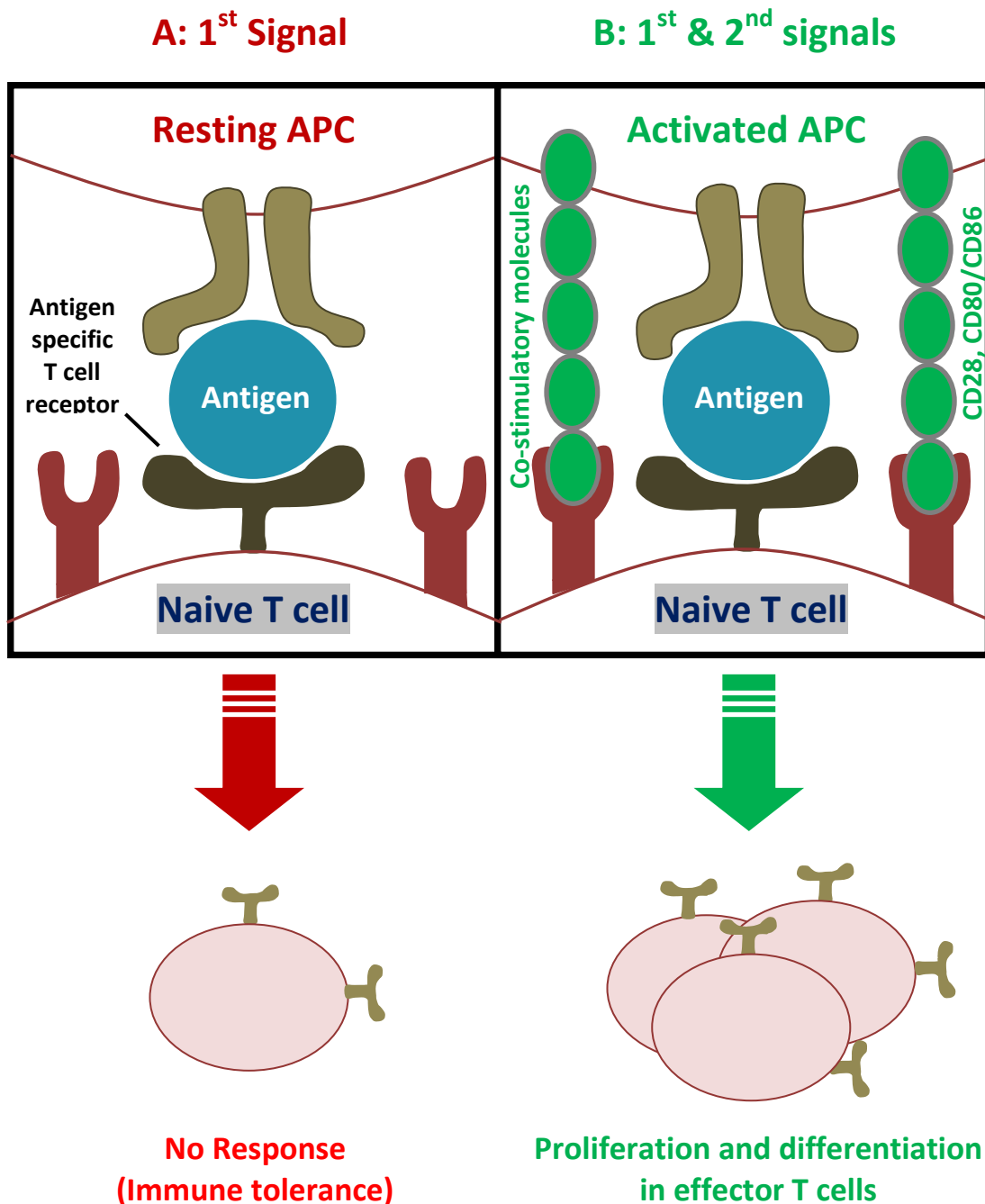


**Figure 1.1. The main signalling events required to initiate T cell activation.** Resting APCs can present antigen material to naive T cells which represents the first signal, but naive T cells do not become activated until APCs express co-stimulatory molecules (Figure adapted from Lima *et al*, 2004).

Alternatively, antigens that become processed and presented via cells that express MHC class I molecules are identified by CD8<sup>+</sup> T cells that also mediate their effector function upon cytokine secretion, of which IFN- $\gamma$  and tumour necrosis factor (TNF)- $\alpha$  is fundamental to the activation of APCs, particularly macrophages (Figure 1.2). In addition, the mechanism of cytotoxic killing is mediated by the release of granzyme and perforin granules from CD8<sup>+</sup> T cells (Seder & Hill, 2000).



**Figure 1.2. Schematic overview of T cell activation and effector function.** A: antigen processing and recognition by T cells, B: Th1 and CD8<sup>+</sup> T cell effector function (Figure from Seder & Hill, 2000).

### *1.2.3. Immunological memory*

The immune response predominantly involves the distinction between self and non-self coupled with immunological memory, which is the conceptual basis for preventative vaccination and possibly the most significant consequence of adaptive immunity. In terms of cellular memory, CD4<sup>+</sup> and CD8<sup>+</sup> memory T cells express specific cell-surface markers which signify previous activation and consequently, are more easily activated than naive T cells. Therefore, memory cells react to previously encountered pathogen or antigen, i.e. during a secondary response, in a stronger and faster manner in comparison to naive T cells, reflecting the pre-existence of clonally expanded antigen-specific lymphocytes. In addition, memory cells can be categorised into ‘resting’ and ‘effector’ cells: resting memory cells such as CD4<sup>+</sup> or CD8<sup>+</sup> T cells must be re-stimulated with antigen prior to activation, whereas the equivalent effector cells more readily secrete cytokines or directly partake in cell mediated cytotoxic activity (Seder & Hill, 2000; Storni *et al*, 2005).

### *1.2.4. The emergence of Th17*

As highlighted earlier, T helper cells are typically believed to differentiate into either Th1 or Th2 type cell subsets, with the former required to clear intracellular pathogens and the latter fundamental in clearing extracellular organisms. However, distinctive to Th1 or Th2 cells, interleukin 17 producing Th17 cells are now acknowledged as a third and separate subset (Bettelli *et al*, 2006; Hirota *et al*, 2011). Moreover, it is believed that Th17 cells are highly pro-inflammatory and may play a crucial role in mediating host defence against extracellular pathogens that are not sufficiently cleared by initiated Th1 and Th2 type immune responses (Bettelli *et al*, 2007).

In addition, Th17 cells secrete cytokines such as interleukin 21 and 22 that induce an abundance of inflammatory and anti-microbial reactions in alternative cell types, for example in myeloid and epithelial cells. Th17 type responses have been implicated in fuelling protective immune responses against bacterial and fungal pathogens and inflammatory effects of these responses may also become implicated, leading to the development of autoimmune diseases (Vautier *et al*, 2010).

In summary, defence-system mechanisms of the body that must be induced are antigen-presenting cells (APCs), thymus-derived lymphocytes (T cells), and bone-marrow derived lymphocytes (B cells). Immunopotentiators stimulate antigen presenting cells that express TLRs in order to screen the environment for pathogens and TLR activation results in enhanced recruitment of innate immune cells to the infection site together with pro-inflammatory cytokine and chemokine production, facilitating an antigen specific adaptive immune response. Furthermore, to counter undesirable efficacy levels, utilisation of adjuvant systems are established in improving the immunogenicity of vaccines by providing protection and competent antigen targeting for antigen presenting cells (Perrie *et al*, 2008; Mastelic *et al*, 2010). An overview of the components responsible for inducing an immune response is displayed in Table 1.3.

**Table 1.3. Functional elements critical to inducing immunity.** (Table adapted from O'Hagan *et al.*, 2001).

Response	Function
Antigen Presenting Cells	Engage, process and present antigens as peptides via the major histocompatibility complex class I and class II pathways.
B lymphocytes	Responsible for producing antibodies and the function of APCs.
PAMPs	Molecules that associate to pathogens for recognition by innate immune system cells.
PRRs	Expressed by innate immune system cells to recognise PAMPs.
T lymphocytes CD8 <sup>+</sup> (MHCI)	Cytotoxic T lymphocytes (CTL) that terminates infected cells.
CD4 <sup>+</sup> (MHCII)	Promotes B cell and CTL activation and differentiation.
Co-stimulatory signals	Required for proficient antigen presentation and T cell stimulation.
Adjuvants	Increases co-stimulatory molecule expression to activate APCs for effector T cell differentiation.
Th1	Secretes IFN- $\gamma$ which is pivotal to APC activation and ultimately mediates termination of intracellular pathogens.
Th2	Secretes IL-4 and IL-5 which aids antibody stimulation and down regulates Th1 responses.
Th17	Secretes IL-17, 21 and 22, forming the later discovered third subset of T helper cells key to inflammatory responses.

### ***1.3. Vaccine adjuvants***

Immunological adjuvants were principally defined by Ramon, (1924) as “*substances used in combination with a specific antigen that produced a more robust immune response than antigen alone*” and such a definition qualifies an extensive array of materials (Vogel & Powell, 1995). Indeed adjuvants must be appropriately formulated to maintain the stability of vaccine antigen and crucially help to stimulate broad and sustained immune responses, to ultimately maximise the vaccine effect (Reed *et al*, 2008; Mbow *et al*, 2010). Furthermore, adjuvants can be applied to improve immune responses to vaccine antigens in many ways such as; elevating the immunogenicity of weak antigens, modulating and prolonging stimulated immune responses, invigorating cellular immunity, increasing cost-effectiveness by minimising antigen required per vaccine dose, preventing competition between antigens when combination vaccines are administered and enhancing vaccine efficacy in infants, elderly or immunocompromised individuals (O'Hagan *et al*, 2001; Reed *et al*, 2008).

However, despite the promising potential of vaccine adjuvants, their mechanisms of action remain insufficiently understood which has delayed the progress and approval of novel adjuvant development. Furthermore, immunisation triggers an intricate cascade of responses which makes it difficult to distinguish the principle effects of the adjuvant *in vivo* (O'Hagan *et al*, 2001; O'Hagan & Gregorio, 2009).

Indeed, numerous adjuvants have been developed previously but have failed to attain acceptance for routine vaccination due to issues of safety, such as acute toxicity and potentially delayed adverse effects. As a result, the benefits of vaccine adjuvants ought to be considered against the risk of any associated adverse reactions, which the European Medicines Agency (EMA) when evaluating medicines for human use have

outlined, stating that safety is favoured above efficacy when a vaccine is being designed for a healthy population and increased toxicity is only ever acceptable when targeting protection against high risk patients and if there is considerable benefit from the vaccine (EMA, 2005).

In spite of these concerns, adequate data on adjuvants is now emerging, particularly in regards to their immunostimulatory impact and associated safety profile. Such information demonstrates the capability of next generation adjuvants in being safely administered to diverse human populations and allow for many vaccines combined with innovative adjuvants to attain licensure (O'Hagan & Gregorio, 2009).

Adjuvants may be largely classified into two main groups based on their key mechanisms of action: delivery systems, which deliver antigens to immune cells and immunostimulatory adjuvants, which directly affect immune cells, generating their activation (O'Hagan & Valiante, 2003; Reed *et al*, 2008). Table 1.4 highlights some examples of approved vaccine adjuvants tested in each category.

**Table 1.4. Examples of tested vaccine adjuvants within the broadly classified adjuvant groups of delivery systems and immunostimulatory adjuvants.**

Adjuvant Type	Vaccine Adjuvant
Delivery systems	Nano and microparticles, emulsions, immune stimulating complexes, virus-like particles, mineral salts.
Immunostimulatory adjuvants	MPL and its synthetic derivatives, DDA, TDM, TDB.

### *1.3.1. Delivery systems*

Delivery systems are predominantly particulate in nature and in general, increase cellular infiltration at the site of injection which facilitates and enhances antigen uptake into antigen presenting cells or directly transports antigen to the lymph nodes. Consequently, fundamental antigen presenting cells such as DCs migrate to the lymph nodes and present antigen to naive T cells for their activation (O'Hagan *et al*, 2001).

#### *1.3.1.1. Nano and microparticles*

Small solid particles such as nanoparticles (10-1000 nm) and microparticles (1-100 µm) are formed from a variety of biocompatible and biodegradable polymers and can provide a lasting depot-effect, proficient targeting and is ideal for single dose multi-release vaccines (Cox & Coulter, 1997). Antigen uptake by APCs can be increased upon antigen association with polymeric microparticles and also by polymers or proteins that self-assemble into particles. Biodegradable and biocompatible polyesters such as polylactide-co-glycolides (PLG) are suitable for micro particulate development as adjuvants and have been used in humans as sustained release drug delivery systems, with their adjuvant effect a result of uptake into APCs and local lymph nodes upon intramuscular injection (O'Hagan *et al*, 2001).

Lipid nanoparticles, of which the most widely used are liposomes, demonstrate great potential as particulate delivery systems. The selected liposomal composition affects resultant interactions with immune systems cells and therefore, can be designed to elicit desired biological responses (Bramwell & Perrie, 2006), as liposomal adjuvants are capable of stimulating enhanced and diverse immune responses (Perrie *et al*, 2008). The use of liposomes as delivery systems will be discussed in greater detail in section 1.4.

#### *1.3.1.2. Oil and water emulsions*

Emulsion adjuvants have been successfully formulated as delivery systems with the licensed MF59 oil in water emulsion (O/W) adjuvant used in Europe since the late nineties, forming part of a safe and potent vaccine that provides protection against the influenza virus (O'Hagan, 2007). MF59 comprises an oil (squalene)-in-water nano-emulsion and is understood to act via a depot-effect to induce cytokine secretion by monocytes, macrophages and granulocytes. MF59 administered with other antigens can induce higher, more balanced levels of antibody titres than Alum, however like Alum, MF59 is predominantly a Th2 inducer and fails to elicit increased CD4<sup>+</sup> Th1 type immune responses (Reed *et al*, 2008).

#### *1.3.1.3. Immune stimulating complexes*

Immune stimulating complexes (ISCOMs) were initially described by Morein *et al*, (1984) as novel structures that facilitated antigenic presentation of membrane proteins and to date, have been widely applied as adjuvants in veterinary vaccines (Reed *et al*, 2008). ISCOMs are cage-like particles approximately 40 nm in size that entrap protein antigen through hydrophobic interactions and due to their particulate nature, ISCOMs entice more efficient uptake from APCs through the process of endocytosis (Reed *et al*, 2008). Furthermore, when immunogen are integrated into ISCOMs, they can effectively elicit Th1 and Th2 type immunity, provide proficient targeting and presentation and strong cytotoxic T-lymphocyte (CTL) responses (Cox & Coulter, 1997).

#### *1.3.1.4. VLP and IRIV*

Viruses like particles (VLPs) are self-assembling particles consisting of at least one viral protein, forming nanoparticles of approximately 20-100 nm. VLP vaccines for hepatitis B virus (HBV) and HPV have been produced for commercial use (Reed *et al*, 2008) and immunopotentiating reconstituted influenza virosomes (IRIVs), which are proteoliposomes made from phospholipids, influenza hemagglutinin and selected antigen, become processed by APCs upon delivery by hemagglutinin receptor-mediated endocytosis (Reed *et al*, 2008). Moreover, IRIVs are registered in Europe, Asia and South America as part of the Hepatitis A vaccine as during clinical development, it stimulated faster immunity and fewer adverse reactions upon injection in comparison to conventional Alum-containing vaccines (Holzer *et al*, 1996). Both VLPs and IRIVs promote uptake by APCs via receptor mediated endocytosis and are capable of inducing cellular and humoral immune responses (Gluck *et al*, 2004).

#### *1.3.2. Immunostimulatory adjuvants and their combination with delivery systems*

Although particulate adjuvant delivery systems may promote antigen uptake and presentation, this may not necessarily elicit an immune response and as highlighted earlier, the presence of antigen alone simply initiates “signal 1” leading to “immunological tolerance”. In order to stimulate an immune response, “signal 2” must be triggered, in which co-stimulatory molecules and cytokines, that are usually provided by APCs, prime T helper cells to initiate antigen specific protection via B cell proliferation and antibody production, whilst also assisting cytotoxic T lymphocyte responses (O'Hagan *et al*, 2001).

This broad adjuvant group of immunostimulatory adjuvants originate from pathogens such as bacterial cell wall components, which upon delivery, are capable of directly increasing responses to antigens, initiate signalling mechanisms upon induction of cytokine release or co-stimulatory molecules on APCs, and can be interpreted by the host as a threat of infection by the innate immune system. Indeed, such agents correspond to pathogen associated molecular patterns which interact with pattern recognition receptors expressed by phagocytes to activate pro-inflammatory pathways and mediate the onset of an adaptive immune response (O'Hagan *et al*, 2001; Reed *et al*, 2008).

Conventional aluminium based mineral salts (generically referred to as 'Alum') as delivery systems are the most widely used vaccine adjuvants granted approval for human administration. Indeed, due to an acceptable safety record, Alum are components of many licensed vaccines, providing protection against diphtheria-tetanus (DT), hepatitis A virus (HAV), hepatitis B virus (HBV) and the human papilloma virus (Reed *et al*, 2008; Mbow *et al*, 2010).

In general, alum absorption enhances the uptake of antigen at the site of injection and can induce local pro-inflammatory reactions which elevate the immunogenic effect (Mbow *et al*, 2010). However, in comparison to other adjuvants, limitations in the use of Alum are their inability to stimulate cell-mediated Th1 or CTL responses and coupled with relatively weak antibody initiation to protein subunits, they are inadequate in providing the type of immunity necessary to control the majority of intracellular pathogens responsible for major diseases such as tuberculosis, HIV and malaria (Gupta *et al*, 1998; Relyveld *et al*, 1998; Reed *et al*, 2008).

For potentially fatal infections such as tuberculosis, protective efficacy is only possible with a targeted approach whereby cellular responses are enthused. Therefore, novel adjuvants are required with the capacity to induce intricate immunological reactions that carry potent antigen specific T cell stimulation and antibody production (Agger *et al*, 2008). The current generation of vaccines increasingly consist of highly purified recombinant proteins but such antigens are often poorly immunogenic and thus, require co-administration with adjuvants to enable them to become potent vaccines (O'Hagan & Gregorio, 2009). Immunostimulatory adjuvants can be combined with particulate delivery systems in order to intensify responses, initiate a particular desired pathway, for example the induction of Th1 or Th2 type immunity, or acquire a mixture of such immunological responses (Cox & Coulter, 1997; O'Hagan *et al*, 2001).

The combination of delivery systems and immunostimulatory agents to create adjuvant delivery systems provides a great challenge when producing vaccines that can combat pathogens that progress into chronic infections such as tuberculosis, HIV and Malaria, in which cell mediated immunity is required (O'Hagan *et al*, 2001). Thus, creations of innovative adjuvants that can promote vast targeted immune responses are highly advantageous and a necessity worldwide. As highlighted by Christensen *et al* (2007a), individually, antigens are not adequately immunogenic and in order to establish precise immune responses, co-administration of a successful adjuvant is vital. An essential function of vaccine adjuvants is to stimulate the activation of APCs and boost the differentiation of effector T and B cells. A focal point of modern adjuvant research is not just the initiation of potent immune responses but exclusively targeting APCs and associated receptors to achieve such a response, whilst being as non-toxic as possible. A promising example of such a combinational strategy of an immunoadjuvant delivery

system that can be utilised as a means of potent vaccine delivery are the use of cationic liposomes, which will be discussed in section 1.4.

*1.3.2.1. The use of Monophosphoryl Lipid A as an immunostimulatory adjuvant*

Monophosphoryl Lipid A (MPL), which is a non-toxic derivative of a bacterial lipopolysaccharide (LPS) of *Salmonella* Minnesota, is a strong inducer of Th1 type immune responses. The structure of LPS provides two major functions with its hydrophilic polysaccharide portion enhancing solubility and the hydrophobic lipid moiety, known as lipid A, responsible for the resultant endotoxic activity. Vaccines incorporating MPL have attained licensure in Europe as an allergy treatment due to its effectiveness in down-modulating Th2 responses to allergens and MPL is regarded as a safe, well-tolerated and potent vaccine adjuvant component (Reed *et al*, 2008).

*1.3.2.2. The future of adjuvants and the success of AS04: a combined vaccine adjuvant*

Many issues such as unacceptable adverse effects and associated toxicity of adjuvants have stalled the progress in the production of novel candidate adjuvants, with regulatory standards for adjuvant approval considerably higher since Alum was first approved. However, recent discoveries into the manner in which immune responses become activated have rejuvenated the invention of new and improved vaccine adjuvants (Reed *et al*, 2008).

Fast moving and continual progress in molecular immunology is accommodating the screening process for new kinds of small-molecule immune potentiators (SMIPs). As a result, it is possible to foresee that in the coming years a variety of new molecules with the ability of inducing distinct immune responses will emerge and comprise new vaccine adjuvants against different types of pathogens (O'Hagan & Gregorio, 2009).

The PRRs that have been strongly linked to vaccines are TLRs that are expressed by immune cells such as DCs, macrophages and B cells and the future development of SMIPs that target TLRs shows great promise (O'Hagan & Gregorio, 2009), particularly as pathogenic actions may be replicated upon TLR activation, potentially facilitating adaptive immune responses. Indeed the first TLR targeting adjuvant that attained licensure for human use was MPL, which alongside aluminium hydroxide forms a vaccine adjuvant combination known as AS04, produced by GlaxoSmithKline (GSK), and is used in a licensed vaccine against hepatitis B, whilst also part of a human papillomavirus vaccine (Mastelic *et al*, 2010).

The pharmaceutical industry has an established record in constantly providing safe and efficacious vaccines for developed and developing countries worldwide (Taylor *et al* 2009), and it is feasible that new combinations of current adjuvants and innovative adjuvants targeting emerging molecular targets can enhance the efficacy of new preventive vaccines against infectious diseases (Mbow *et al*, 2010). When designing novel vaccine adjuvants, an optimal formulation would ideally be safe, stable before administration, be capable of eliciting antigen specific immunity and be well-defined chemically and physically in order to assure reproducible manufacturing and activity (Reed *et al*, 2008). Indeed, such attributes have been demonstrated upon the application of liposomal vaccine adjuvant delivery systems, whilst potentially providing protective efficacy against a variety of diseases.

#### ***1.4. Liposomes: an effective vehicle for drug delivery***

Liposomes were initially discovered in the 1960s by Bangham and Horne upon investigation of “bag-like” phospholipid configurations in water using an electron microscope and more specifically, liposomes are spherical vesicles comprising of one or more phospholipid bilayers encompassing an aqueous cavity (Rongen, 1997). Indeed, when phospholipids are placed in water, they arrange themselves in such a manner that protects the hydrophobic tails of the phospholipid molecule from water, whilst the hydrophilic heads are attracted to water and thus, aggregate into a dual or bilayer vesicular structure (Figure 1.3).

Based on their sizes and according to associated physical structures, liposomes can be categorised into multi, large and small unilamellar vesicles (Figure 1.3). Large unilamellar vesicles (LUVs) and multilamellar vesicles (MLVs) approximately range from a few hundred nanometres to several micrometres in size and upon further treatment via sonication, small unilamellar vesicles (SUVs) are generated, typically less than 100 nm in size (Jones, 1995).

The structural arrangement of liposomes makes them incredibly adaptable as vehicles for drug delivery as molecules can be associated to liposomes in many ways including encapsulation into the inner aqueous core, partitioning within lipid bilayer tails and electrostatic interaction with polar lipid head-groups. Hydrophilic molecules such as enzymes, DNA, vaccines and pharmaceutical compounds can be encapsulated into the inner core, and the bilayer structure can extend the longevity of encapsulated material by protecting them from destructive entities upon delivery, whilst drug release can be controlled, minimising any associated cytotoxic effects (Edwards & Baeumner 2006b).

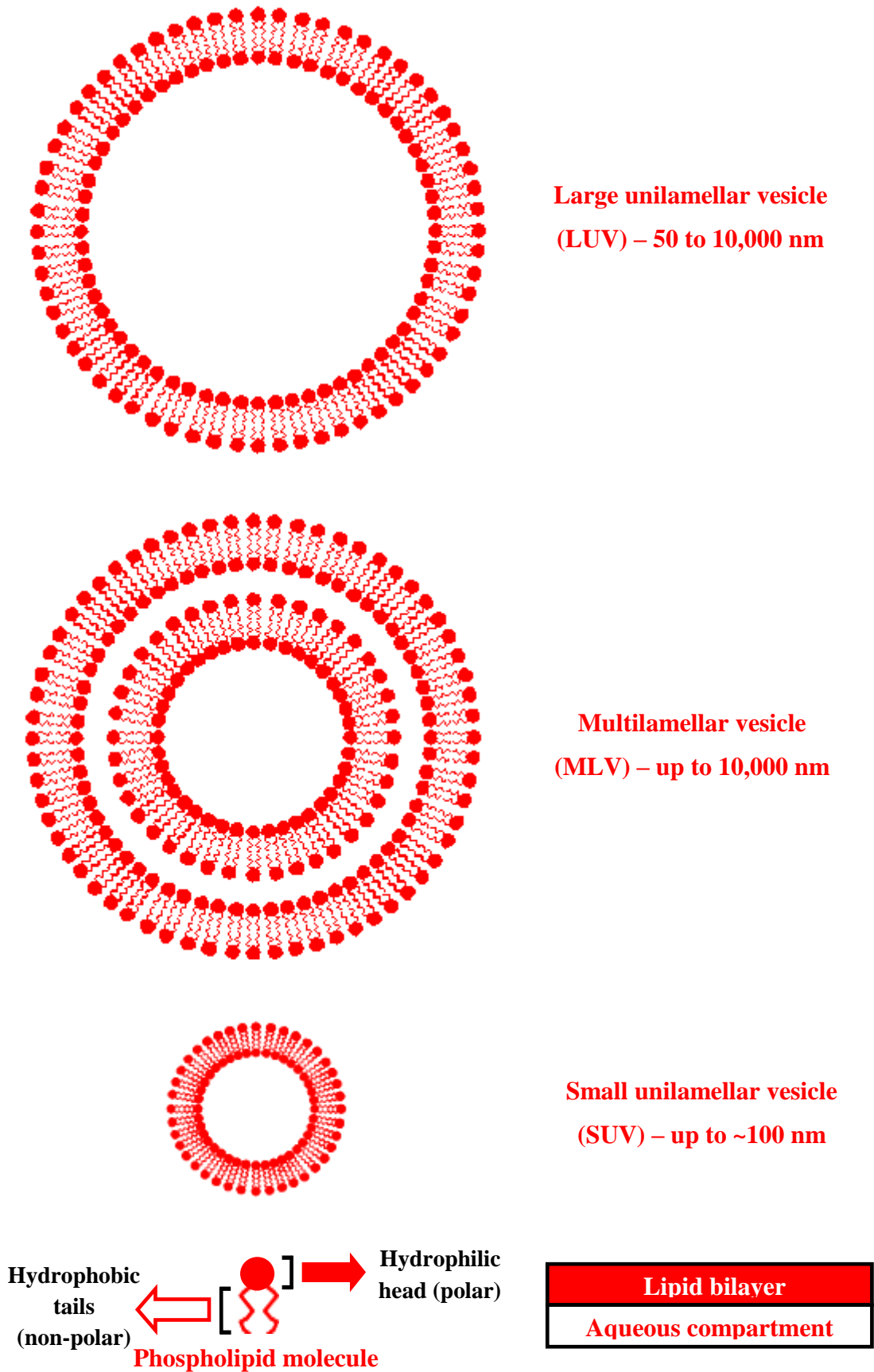


**Figure 1.3. The classification of liposomes characterised by size and physical structure.** Liposomes are flexible drug delivery vehicles as both lipid and water soluble molecules can become associated to the liposomal bilayer or aqueous compartment respectively (Figure adapted from Jones, 1995).

Physicochemical properties of lipids that form liposomes for example, surface charge, membrane fluidity and permeability can influence the nature and degree of liposome-cell interactions upon administration and thus, liposomal composition has a great affect on the intracellular delivery of drugs (Sharma & Sharma, 1997). Indeed, liposomes can be prepared to attain a neutral, cationic or anionic surface charge and when used as immunostimulatory adjuvant delivery systems, can facilitate the association of a variety of proteins and particulate antigens whilst inducing potent immune responses specific to the delivered antigen. Furthermore, phospholipids with various polar head groups and hydrophobic regions of varying chain length and saturation can be selected to desirably modify the resultant liposomal properties (Edwards & Baeumner, 2006b), which makes liposomes extremely versatile structures that can be utilised for research, therapeutic and analytical applications (Edwards & Baeumner, 2006a).

Initial work bringing liposomes into prominence as vehicles for drug delivery was conducted by Gregory Gregoriadis in the 1970s and their use as vaccine adjuvants was first described by Alison & Gregoriadis, (1974), demonstrating that entrapment of diphtheria toxoid in liposomes enhanced antibody responses. Since then, advances in liposomal technology and the understanding of *in vivo* liposomal behaviour both experimentally and clinically has prompted the design and approval of formulations to treat microbial infections and cancers, together with liposome based vaccines licensed for use in humans (Gregoriadis, 1991; Gregoriadis, 2000). In fact, ground breaking research has generated approval and licensure for the administration of liposomal-based products against a variety of diseases, with some examples summarised in Table 1.5.

**Table 1.5. Examples of commercialised liposome-based drugs on the market.** The variety of diseases treatable illustrates the flexibility of liposomal systems.

Marketed Product	Company	Target Disease	Drug/therapeutic agent	Formulation	Route
Caelyx™ or Doxil™	Schering Plough (Caelyx) Ortho Biotech (Doxil)	Kaposi's sarcoma (KS), breast and ovarian cancer	Doxorubicin	80-100 nm liposomes composed of HSPC:Chol:PEG 2000-DSPE (56:39:5 molar ratio).	Intravenous
Myocet	Zeneus Pharma	Metastatic breast cancer	Doxorubicin	HCl complexed with citrate encapsulated within 150 nm liposomes composed of PC:Chol (55:45 molar ratio).	Intravenous
Epaxal	Berna Biotech	Hepatitis A	Inactivated hepatitis A virus	150 nm immunopotentiating reconstituted influenza virosoes (IRIV) composed of DOPC/DOPE (75:25 molar ratio).	Intramuscular
AmBisome	Gilead Sciences	Fungal infection	Amphotericin B	< 100 nm sized Liposomes composed of HSPC, DSPG, cholesterol and amphotericin B (2.0:0.8:1.0:0.4 molar ratio).	Intravenous
Visudyne	Novartis	Age-related macular degeneration	Vereporfin	Liposomes composed of BPD-MA:EPG:DMPC (1:3:5 molar ratio).	Intravenous

#### *1.4.1. Liposomes as vaccine delivery systems*

When defending against the onset of microbial infection, vaccines are a favoured alternative to treatment with a great ability of saving millions of lives (Gregoriadis *et al*, 2002). Proficient efficacy can be achieved by replicating natural infections without disease, with the objective of stimulating defence mechanisms involved in generating a consistent immune response. Despite the innovation of aluminium based adjuvants in the 20<sup>th</sup> century, liposomes remain one of the few immunological adjuvants approved for human administration and liposome based vaccine delivery systems have been extensively recognised as potent stimulators of immunity (Bramwell & Perrie, 2005).

Furthermore, the next generation of adjuvants was triggered by the innovation and application of muramyl dipeptide (MDP), which in the mid 70s, was recognised as a diminutive water soluble element of the mycobacterial cell wall that could potentially attenuate adjuvant like behaviour by stimulating immunity (Ellouz *et al*, 1974). Consequently, it was appreciated that the effectiveness of such mycobacterial constituents could not be maximised until they were attached to current adjuvants such as those derived from liposomes (Siddiqui *et al*, 1978).

The versatility in the structural properties of liposomes coupled with their ability to accommodate a variety of drugs has facilitated the production of safe subunit vaccines. However, such vaccines are weakly or non-immunogenic and thus require co-administration with immunological adjuvants in order to be effective. The use of liposomes provides a safe, versatile, universal adjuvant capable of eliciting humoral and cellular immune responses to antigens upon parenteral or enteral administration (Gregoriadis, 1990; Gregoriadis, 1991).

#### *1.4.2. Cationic liposomal vaccine delivery systems*

Cationic liposomes are lipid-bilayer vesicles formed from positively charged amphiphilic lipid molecules (Lonez *et al*, 2008) yielding a net positive surface charge. Such systems have received great attention due to their biocompatibility and versatility, demonstrating potential for delivery of protein and DNA vaccines (Bramwell & Perrie, 2006). Moreover, DNA vaccines entrapped inside cationic liposomes protect DNA from nuclease degradation and are a viable system that can accommodate the delivery of DNA to APCs. Upon local injection, DNA containing liposomes become rapidly endocytosed by APCs that penetrate the site of injection or the draining lymph nodes (Perrie *et al*, 2001). Due to its convenience and efficacy, the use of cationic lipid mediated gene delivery to target cells or tissues *in vivo*, provides a viable means of gene therapy (Chrai *et al*, 2002; Liang & Chou, 2009).

In addition, studies have demonstrated that co-administration of antigen with liposomes of a cationic nature elicit stronger antigen specific immunity in comparison to their anionic or neutral counterparts (Nakanishi *et al*, 1997; Perrie *et al*, 2001). It is understood that positively charged liposomes protect antigens from clearance within the body, whilst incorporating immune potentiators to enhance and modulate a desired response and delivering associated antigens to APCs and thus, are proficient vaccine delivery systems for specific disease targets (Christensen *et al*, 2007b).

#### *1.4.3. The promising potential of DDA-TDB as a liposomal adjuvant delivery system*

The cationic synthetic amphiphile of dimethyldioctadecylammonium (DDA) was first discovered as an immunostimulatory adjuvant in the 1960s by Gall, (1966) and the versatile adjuvanticity of DDA was recognised by Hilgers & Snippe (1992),

establishing its ability as a reasonable Th2 inducer and a powerful Th1 inducer. The primary adjuvant mechanism of DDA-based liposomes is to transport associated antigen to APCs, enhance antigen uptake and subsequent presentation of antigen material to T cells (Korsholm *et al*, 2007), as DDA can not only deliver associated antigen but also potentiate the immune response, acting as a combination of a vaccine delivery system and an immunostimulatory adjuvant. Moreover, the mechanism of action that provides DDA with immunopotentiating activity is due to its cationic surface charge and ability to incorporate antigens (Hilgers *et al*, 1985). Indeed, DDA consists of a positively charged hydrophilic polar dimethylammonium head group and two hydrophobic 18-carbon-long alkyl chains (Table 1.7) and in an aqueous environment, forms liposomal bilayer structures when heated beyond its main phase transition temperature (Carmona-Ribeiro & Chaimovich, 1983).

TDB is a synthetic analogue of trehalose 6,6'-dimycolate (TDM), also known as cord factor, which is an immunostimulant found within the mycobacterial cell wall (Pimm *et al*, 1979; Lemaire *et al*, 1986). Due to its structure being composed of smaller fatty acid chains (Table 1.7) compared to its TDM counterpart, TDB yields a decreased level of toxicity (Pimm *et al*, 1979; Olds *et al*, 1980). However, due to its lipidic properties, TDB cannot be administered alone and therefore, integration into a delivery system is required (Vangala *et al*, 2007). Over the last decade, liposomes have been utilised as complex immunoadjuvant delivery systems for experimental subunit vaccines and the combination of DDA with TDB as a liposomal adjuvant system for subunit vaccine delivery was first considered by Holten-Andersen *et al*, (2004). TDB has been shown to provide a stabilising effect, alleviating the issue of physical instability associated with DDA vesicles whilst potentiating the immune response of

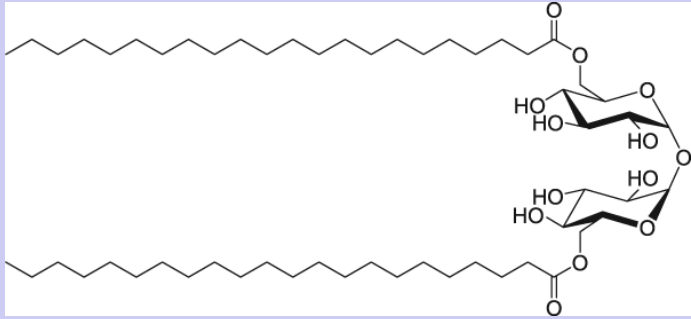
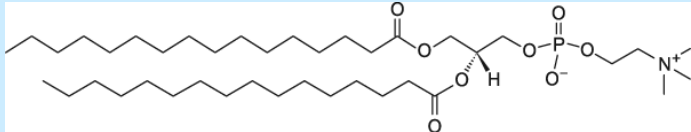
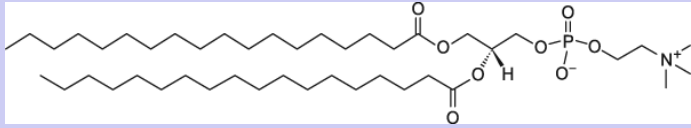
DDA, inducing cell mediated immune responses upon immunisation of mice with a TB vaccine antigen candidate, Ag85B–ESAT-6 (H1), characterised by elevated levels of the T-cell enhancing cytokine, IFN- $\gamma$  (Davidsen *et al*, 2005). In addition, the DDA-TDB immunoadjuvant delivery system (also referred to as cationic adjuvant formulation 01 or CAF01) has been shown to be a potentially viable adjuvant for a variety of diseases eliciting either cellular or humoral immunity or even a combination of such immune responses when providing protection against infectious diseases (Table 1.6).

The DDA to TDB weight ratio of 5:1, previously optimised by Davidsen *et al*, (2005), provides the foundation of formulations to be tested in the present study as adjuvant subunit vaccine delivery systems, whilst also incorporating additional lipids of 1,2-dipalmitoyl-sn-glycero-3-phosphocholine (DPPC) or 1,2-distearoyl-sn-glycero-3-phosphocholine (DSPC), with the objective of applying the DPPC based systems for pulmonary vaccine delivery and the DSPC systems for immunological analysis in a mouse model. Phospholipids form the main constituent of the absorptive surfaces deep into the lung, for example in surfactants at the surface of pulmonary alveoli and within alveolar cell membranes (McAlister *et al*, 1996), and the phospholipid that predominantly comprises pulmonary surfactant is DPPC, which can facilitate the absorption of compatible liposomal systems (Wright, 1990). The long DSPC fatty acyl chains result in a higher transition temperature, possibly enhancing the structural rigidity of DDA-TDB upon incorporation, with the possibility of favourably reducing the overall toxicity of the formulation. Table 1.7 summarises further details on these additional lipids to be incorporated into DDA-TDB based liposomes as adjuvant formulations to be tested in this study, for delivery of a novel subunit vaccine against tuberculosis.

**Table 1.6. The versatility of DDA-TDB: a cationic liposomal adjuvant delivery system capable of providing immunity against a variety of disease targets.**

Disease	Desired protective immune response	Vaccine Antigen	Results/findings	Reference
Tuberculosis	Cell mediated immunity	Ag85B–ESAT-6 (H1)	Immunisation with DDA/TDB at a 5:1 weight ratio generated elevated levels of IFN- $\gamma$ and low levels of IL-5, together with substantial IgG1 and IgG2 antibody titres.	Daidsen <i>et al</i> , (2005)
Malaria	Humoral immunity	Merozoite surface protein 1 (MSP1) and glutamate rich protein (GLURP)	Strong antigen specific IgG1 and IgG2 antibody and IFN- $\gamma$ cytokine responses and a Th2 humoral response characterised by MSP1 and GLURP specific IgG1 and IgG2 antibody titres (upon incorporation of a non-ionic surfactant and cholesterol).	Agger <i>et al</i> , (2008) + Vangala <i>et al</i> , (2006)
Influenza	Cell mediated + humoral immunity	Vaxigrip influenza split vaccine	Elevated cellular and humoral immune responses, eliciting significantly higher IFN- $\gamma$ and IgG antibodies compared to administration without the adjuvant.	Christensen <i>et al</i> , (2010)
Chlamydia	Cell mediated + humoral immunity	Major outer membrane protein (MOMP)	Elevated levels of IgG1 and IgG2 antibody isotype titres, IFN- $\gamma$ and TNF- $\alpha$ cytokines and a significantly reduced vaginal chlamydial load upon challenge when compared to naive control mice.	Agger <i>et al</i> , (2008)
Hepatitis B	Cell mediated immunity	Hepatitis B surface antigen (HBsAg)	Strong antigen specific IL-2 and IFN- $\gamma$ cytokine production and elevated IgG, IgG1 and IgG2a antibody isotype titres.	Vangala <i>et al</i> , (2007)

**Table 1.7. DDA, TDB, DPPC and DSPC lipids used in the liposomal formulations and tested as novel adjuvants for TB subunit vaccine delivery.** (Structures were obtained from [www.avantilipids.com](http://www.avantilipids.com), 2011).

Lipid	Structure	Molecular formula	Molecular weight	Transition temperature
Dimethyl-dioctadecylammonium (DDA)		$C_{38}H_{80}NBr$	630.95 g/mol	47 °C
Trehalose 6,6-dibehenate (TDB)		$C_{56}H_{106}O_{13}$	987.433 g/mol	/
1,2-dipalmitoyl-sn-glycero-3-phosphocholine (DPPC)		$C_{40}H_{80}NO_8P$	734.039 g/mol	41 °C
1,2-distearoyl-sn-glycero-3-phosphocholine (DSPC)		$C_{44}H_{88}NO_8P$	790.14 g/mol	55 °C

### ***1.5. Vaccination for protection against tuberculosis***

Evidence of tubercular decay can be linked to ancient Egyptian times and was also prominent during the periods of ancient Greece and Imperial Rome (National Institute of Allergy and Infectious Diseases, 2008). Furthermore, TB has plagued humanity for centuries, attaining an epidemic status in Europe and North America in the 18<sup>th</sup> and 19<sup>th</sup> century, with such an overwhelming outbreak of the infection prompting a reputation of being a “*captain among these men of death.*” (Daniel, 2006). However, understanding the pathogenesis of TB was further developed by Jean-Antoine Villemin who demonstrated the contagious effect of the mycobacterium tuberculosis infection in 1865, prior to Robert Koch recognising tubercle bacilli as the main causative agent in 1882. Early in the 20<sup>th</sup> century, Clemens von Pirquet created the tuberculin skin test and subsequently used it to exhibit the latent TB infection in healthy infant carriers.

Tuberculosis is an infectious and airborne disease that results in approximately 2 million deaths each year from the mycobacterium tuberculosis infection (WHO, 2010a). Despite potentially curative pharmacotherapies being readily available for many decades, tuberculosis is still the primary cause of preventable deaths worldwide (Sosnik *et al*, 2010). In addition, with as many as 2 billion people potentially carrying the disease, such an incredibly high frequency of the latent infection facilitates the prevalence of TB in its active form, with inhalation of just a minute quantity of TB bacilli sufficient to incur infection (Gupta *et al*, 2007; WHO, 2010a). Although the number of TB related deaths has decreased by 35% since 1990, in 2009, almost 10 million new cases of TB were reported, with an immense majority of deaths occurring in the poorer developing countries, particularly within the African region (Figure 1.4) (WHO, 2010b; Sosnik *et al*, 2010).



**Figure 1.4. Estimated cases of tuberculosis reported in 2009 by country.** A vast majority of global TB incidence is attributed to the developing world, particularly in Africa, where HIV is also prevalent. (Figure from WHO, 2010c).

Following HIV/AIDS, TB is the second highest fatally infectious disease (Frieden & Driver, 2003) with HIV and TB forming a deadly combination, each accelerating the other's progress, resulting in TB becoming the primary cause of death amongst HIV-positive infected individuals (WHO, 2010a). In 1993, the World Health Organisation declared TB as an international emergency (WHO, 1993), with the latest global targets outlined by the WHO Stop TB partnership aiming to save five million lives between 2011 and 2015, whilst stating that the objective to half global TB mortalities by 2015 compared to 1990 remains successfully on course (WHO, 2010b). Although the occurrence of new TB cases declined in the 60s and 70s, this predicament was aggravated further by the onset of multi-drug resistant TB (MDR-TB), defined as resistance to first-line TB treatments of isoniazid and rifampicin and in extreme cases, extensively drug-resistant TB (XDR-TB) which is also resistant to fluoroquinolone and, as a minimum, one second-line injectable TB treatment (WHO, 2010c). Due to

the extent of TB prevalence, the necessity for a new vaccine strategy to combat the disease has been recognised as a global research priority (Anderson & Doherty, 2005).

If left untreated, every actively infected person may transmit the disease to 10-15 people each year. However, people infected with MTB do not necessarily have the active TB disease as a healthy patient can carry the TB infection in its latent form, yet fail to attain sterile eradication of the pathogen. Such latent carriers are susceptible to develop the active form of TB in their later life and represent approximately one third of the world's population. The vast scale of TB incidence is evident as a TB bacillus infects a new individual every second (Kaufmann, 2010), with such alarming figures resultant of a deadly cycle of TB (Figure 1.5).



**Figure 1.5. The deadly cycle of tuberculosis.** This figure portrays the estimated global levels of MTB and latent MTB incidence, new TB cases and TB related mortalities, forming a vicious cycle that amplifies the onset of infection (Figure from Kaufmann, 2010).

### *1.5.1. Tuberculosis infection*

The TB infection is activated upon inhalation of the mycobacterium into the respiratory system via aerosol particles. Subsequently, bacteria become non-specifically phagocytosed by alveolar macrophages which lead to bacterial antigen presentation to T lymphocytes, prior to rapid proliferation of the pathogens by terminating host cells and spreading towards local lymph nodes within the lungs via lymphatic circulation. As a result, TB bacilli spread from the lungs to the central nervous system and other organs of the body such as the liver, kidneys etc (Smith, 2003).

Recent studies have indicated the potential influence of IL17-producing Th17 cells which draw in monocytes to where MTB replication takes place. This eventually generates a solid granuloma containing mononuclear phagocytes and T cells and such a formation restrains MTB but does not eliminate the infection, with this balanced coexistence symptomatic of the latent tuberculosis infection (LTBI). The active form of TB results from immune weakening which liquefies the granuloma as MTB multiplies and spreads to other organs, with patients enduring the extremely contagious active form of TB, which can ultimately lead to death (Parida & Kaufmann, 2010).

It is understood that protection against TB is dependent on Th1 type CD4 T cells, whilst principle effector functions of T cells during an immune response to MTB are the secretion of cytokines, in particular IFN- $\gamma$  and TNF- $\alpha$ , which are significant in mediating control of the infection (Quesniaux *et al*, 2010; Meraviglia *et al*, 2011). Where CD4 T cells are crucial to controlling the infection in the acute phase, CD8 T cell responses are essential to the latent phase of MTB (SSI, 2010). Indeed CD8+ T

cells also provide protection by secreting similar cytokines and by generating perforin and granulysin, substances that aid the termination of macrophages containing MTB, whilst also directly targeting the pathogen (Parida & Kaufmann, 2010).

In summary, the main events that contribute to MTB infection can be categorised into a series of stages. The acute phase, whereby bacteria divide and multiply within organs until an immune response is strengthened, the latent phase, in which bacterial levels are stabilised from an active to dormant form of MTB, and a reactivation phase, which involves the recommencement of bacterial proliferation (SSI, 2010).

#### *1.5.2. Protection against TB: past, present and future promise*

Prior to establishing vaccination against TB, initial treatments were relatively basic. George Bodington and Hermann Brehmer were physicians that proposed the curative effects of dry and fresh air, which led to early medical facilities for TB being situated in alpine regions. Moreover, in conjunction with rest and a nutritious diet, TB infected individuals did respond favourably, yet such treatment methods probably contributed more to controlling the spread of infection by isolating patients (Campbell, 2005).

Currently, the vaccine of choice against TB is the BCG vaccine which was commonly used after the first world war (Daniel, 2006) and to date, has been received by 4 billion people due to the protection it provides, particularly against TB in infants (Parida & Kaufmann, 2010). However, growing concerns over its safety, waning sensitivity and a highly variable protective efficacy (0-80%) against adult pulmonary TB have invigorated a push for a more potent vaccine alternative (Fine, 1995; Chambers *et al*, 2003; Anderson & Doherty, 2005).

In addition, adverse effects of BCG vaccination are apparent upon alterations in resultant immune responses which can lead to the onset of autophagy, causing cell degradation and defence mechanisms to inhibit the protective action of BCG (Gutierrez *et al*, 2004). Furthermore, variations of numerous strains from the original BCG vaccine of 1921 add confusion to the consideration of an optimal strain of choice (Behr, 2002). For all such reasons, the use of BCG is widely alleged as being ineffective and coupled with its diminishing effect over time, the production of new and enhanced vaccines for TB is of great necessity.

Vaccine development has been significantly advanced by determining genomic information via “reverse vaccinology”, which can generate novel and alternative solutions to vaccines that could not previously be developed, whilst evading the time consuming, conventional approach of pathogen cultivation (Rappuoli, 2001). Great efforts have been made to identify protective mycobacterial substances and it is understood that MTB carries and secretes numerous proteins that are potentially viable as components for a novel MTB vaccine (Brandt *et al*, 2000). Indeed, publication of the entire genome sequence for the greatest characterised MTB strain revealed approximately 4000 associated genes with the potential to encode as many proteins (Cole, 1998), providing a fundamental breakthrough that has facilitated the identification of revolutionary protein vaccine candidates and revitalised interest in TB vaccine research (Sable *et al*, 2007b). With the acknowledgment of a model vaccine candidate being able to provide protective efficacy in a variety of ethnic populations, multicomponent subunit vaccines combining defined MTB antigens is a desired approach for future development (Sable *et al*, 2007b).

TB is renowned as the principle cause of preventable deaths worldwide, yet attempts to surmount the infection by developing innovative treatments has hit many stumbling blocks along the way, for example poor aqueous solubility and stability, restricted bioavailability and minimal patient compliance (Sosnik *et al*, 2010). Exploration of novel vaccine candidates has predominantly focused on proteins secreted from dividing bacteria. A notable fusion protein that has shown the ability to stimulate a protective immune response against TB is Ag85B fused with ESAT-6 (Brandt *et al*, 2000). Due to the intracellular nature of mycobacterium bacillus, cell mediated immunity is required in order to be effective. As highlighted earlier, the use of cationic liposomal adjuvants as part of a subunit vaccine delivery system facilitates protein antigen delivery whilst enhancing immunity. Moreover, the combination of DDA liposomes with the TDB glycolipid as a stable aqueous liposomal adjuvant system has been proven to induce cell mediated immunity upon immunisation of mice with a TB vaccine antigen candidate, Ag85B–ESAT-6 (H1), characterised by elevated levels of the T-cell enhancing cytokine, IFN- $\gamma$  (Davidsen *et al*, 2005).

The fusion of early secreted TB antigens Ag85B and ESAT-6 (forming H1 antigen) has been shown to be a competitive alternative to the current BCG vaccine, and as a booster, to enhance the protective efficacy of the currently available live TB vaccine. However, a post exposure vaccine that can provide protection against the late persistent stage of infection is still of high priority (Moreno-Mendieta *et al*, 2010). Thus, a vaccine comprising of antigens expressed by bacteria of the first growth phase and during the latent stage of TB could enhance long-term immunity when applied as a preventative vaccine. Such a multiphase vaccine can be efficient as a therapeutic

vaccine, particularly for those in developing countries who may already be latently infected prior to receiving a future TB vaccine (SSI, 2010).

Numerous proteins harbour the potential capability to act as late antigens (recognised during latent infection) as they are predominantly expressed long after infection, in which the immune system has already elicited an initial adaptive defence, producing a hostile environment for mycobacteria to survive. Furthermore, *in vitro* hypoxic culture conditions that mimic an oxygen deprived atmosphere has been considered relevant to analysis of gene expression alterations, and Rv2660c has been identified as an antigen that is stimulated or upregulated in such an environment (Betts, 2002; SSI, 2010).

The TB vaccine research group at the Statens Serum Institut (SSI) has implemented an antigen discovery program, screening over 250 TB vaccine mycobacterial antigen candidates, with the most promising preventative antigens being part of the Ag85 and ESAT-6 family (SSI, 2010). However, recently a multi-stage TB vaccine that combines the early secreted TB antigens that form the H1 vaccine with the later expressed Rv2660c antigen forming the H56 vaccine, has successfully protected against TB before and after exposure, managing reactivation and reducing the bacterial load in mice (Aagaard *et al*, 2011). In addition, the H56 vaccine was capable of controlling bacterial growth on par with BCG, whilst exceeding the vaccine performance of BCG and H1 at later time points upon challenge, eliciting elevated IFN- $\gamma$  levels specific to all three vaccine components (Aagaard *et al*, 2011). With new and upcoming preclinical advances in TB vaccination coupled with the global priority of reducing TB incidence, Kaufmann (2010) reviewed key medium to long term vaccination strategies against TB and summarised them into three main stages (Table 1.8), which if applied, could contribute towards crucially eradicating the pathogen.

**Table 1.8. Future vaccination strategies against tuberculosis.** The three main stages of a TB vaccine strategy is summarising information reviewed by Kaufmann, (2010).



### ***1.6. Aims & Objectives***

The aim of this work was to investigate the physicochemical characteristics of DDA-TDB based cationic liposomes as adjuvant delivery systems for subunit antigen, upon incorporation of DPPC, for potential pulmonary vaccine delivery or DSPC, for immunological analysis upon delivery of H56 vaccine, a novel subunit TB vaccine antigen. Moreover, the role of DDA within the formulation was assessed by incrementally replacing cationic content with DPPC or DSPC lipid, alongside the substitution of DDA-TDB to ascertain the effect of DDA-TDB concentration, whilst evaluating the potential of such systems to activate antigen presenting cells *in vitro*, using a macrophage cell line as a general model to observe the viability of the proposed liposomal formulations for administration *in vivo*. In order to accomplish these aims the objectives were to:

- Physicochemically characterise the outlined systems, upon incorporation of DPPC or DSPC into DDA-TDB, for particle size, zeta potential, short term stability, surface morphology, antigen retention/release and interactions with serum proteins.
- Conduct thermodynamic analysis to attain the main phase transition temperature, whilst determining the interdigitation of the multiple lipid formulation components.
- Determine the associated cytotoxicity of the proposed liposomal immunoadjuvants upon macrophages and their ability to stimulate phagocytic activity and the activation of macrophages *in vitro*.
- Characterise the performance of the liposomal adjuvants as vaccine delivery systems *in vivo*, in order to fully appreciate the resultant immunological effect of DDA and TDB adjustment and additional lipid incorporation into DDA-TDB.
- Assess the suitability of the DPPC based cationic systems for pulmonary delivery.

## **Chapter 2**

### **Materials & Methods**

### **2.1. Materials**

Tris (Ultra Pure) was purchased from ICN Biomedicals (Aurora, OH). Phosphate buffered saline (PBS) tablets and D-glucose (glucose monohydrate) were purchased from Sigma-Aldrich Co. Ltd. (Dorset, UK). Methanol (extra pure), chloroform (extra pure) and hydrochloric acid (used to adjust the pH of Tris buffer), were purchased from Fisher (UK). Dimethyl dioctadecylammonium bromide (DDA),  $\alpha,\alpha'$ -trehalose 6,6'-dibehenate (TDB), 1,2-dipalmitoyl-*sn*-glycero-3-phosphocholine (DPPC) and 1,2-distearoyl-*sn*-glycero-3-phosphocholine (DSPC) were obtained from Avanti Polar Lipids (Alabaster, AL). The purity of all compounds used was > 99%, determined by HPLC. SDS-PAGE 12% Tris-glycine gels (1.0 mm X 12 well) and the protein molecular weight standard (broad range – 11 polypeptides, MW 6500-205,000 Daltons) were purchased from Invitrogen (Paisley, UK). The bicinchoninic acid protein assay kit including reagents, bicinchoninic acid solution and copper sulphate solution and the  $\beta$ -N-Acetylglucosaminidase (NAG) assay kit was obtained from Sigma-Aldrich Co. Ltd. (Dorset, UK). The cell titer 96<sup>®</sup> AQueous non-radioactive cell proliferation (MTS) assay was purchased from Promega (UK). A mouse TNF- $\alpha$  ELISA development kit was obtained from R&D Systems Europe Ltd. (Abingdon, UK). Fetal bovine serum (FBS) was obtained from Biosera (East Sussex, UK). For the radioactive studies, IODO-GEN<sup>®</sup> pre-coated iodination tubes were purchased from Pierce Biotechnology (Rockford, IL). Sephadex<sup>®</sup> G-75 was purchased from Sigma-Aldrich Co. Ltd. (Dorset, UK).  $I^{125}$  (NaI in NaOH solution), [ $^3$ H] thymidine and ultima gold scintillation fluid were obtained from Perkin Elmer (Waltham, MA). Dialysis cellulose ester (CE) membrane tubing (Molecular weight cut off (MWCO): 100,000) was purchased from Spectra/Por<sup>®</sup> Biotech (Breda, Netherlands). Ag85B-ESAT-6-Rv2660 (H56 antigen) was supplied by Statens Serum Institut (SSI),

(Copenhagen, Denmark) at a concentration of 0.7 mg/ml. All other reagents used were of analytical grade.

## **2.2. Methods**

### *2.2.1. Production of liposomes via lipid hydration*

DDA-TDB based liposome formulations were prepared by the method of lipid hydration based on studies by Bangham *et al*, (1965) and modified as described by Davidsen *et al*, (2005). Firstly, weighed amounts of powdered lipids were dissolved in a chloroform:methanol solvent mixture (9:1, v/v) and pipetted into a round bottomed flask, fixed to a final concentration of 1.25 mg DDA and 0.25 mg TDB per ml. Removal of the solvent was achieved via rotary evaporation of the mixture contained in the round bottomed flask together with subsequent nitrogen streaming which produces a fine lipid layer at the base of the flask. Multilamellar vesicles were produced by hydrating the remaining lipid film in 10 mM Tris buffer (pH 7.4). The lipid film was hydrated for twenty minutes with intermittent vortexing, in conditions 10 °C above the main phase transition temperature for the lipids used, providing total hydration (Davidsen *et al*, 2005). Independent batches of the vesicle systems were prepared and hydrated in either Tris buffer (10 mM, pH 7.4), dextrose (5% w/v) or phosphate buffered saline. Figure 2.1 summarises the technique of lipid hydration.

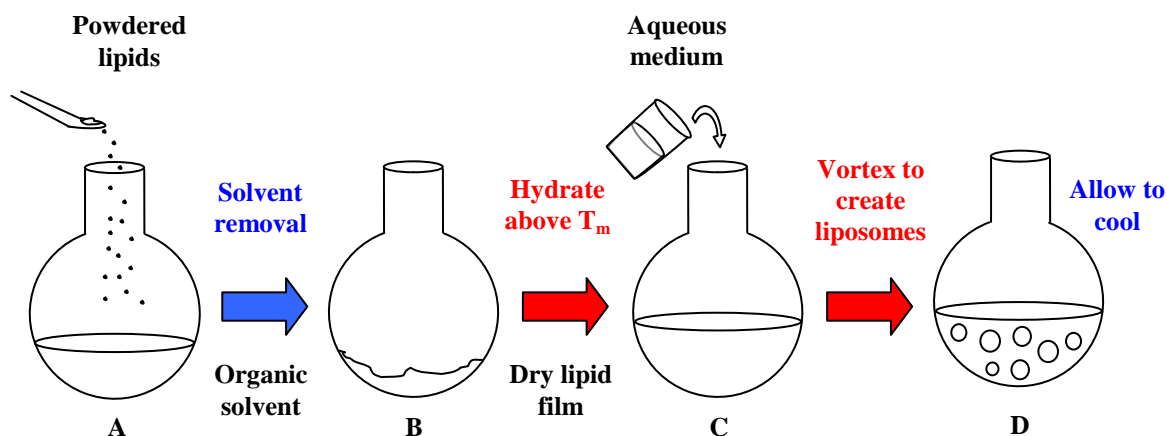


**Figure 2.1. The production of liposomes via lipid hydration.** Upon the addition of powdered lipids (A) in chloroform:methanol (9:1, v/v), the solvent was removed yielding a dry lipid film (B) before rehydration in an aqueous medium (C) producing liposomes upon cooling (D).

The incorporation of increasing amounts of DPPC or DSPC to DDA-TDB at various molar % ratios from 0 to 75% were investigated (Table 2.1) (All lipids were dissolved in chloroform:methanol solutions - 9:1 v:v ratio).

**Table 2.1. Incorporation of lipids for the substitution of DDA-TDB.** Values of weight or moles upon the addition of DPPC or DSPC to the DDA-TDB adjuvant system are represented to the final volume of 1 ml.

DDA-TDB based Formulation (mol%)	DDA Weight (mg) /Moles	TDB Weight (mg) /Moles	Lipid Weight (mg) /Moles
0%	1.25 / $1.98 \times 10^{-6}$	0.25 / $2.53 \times 10^{-7}$	0 / 0
+ 25% DPPC	0.94 / $1.49 \times 10^{-6}$	0.18 / $1.78 \times 10^{-7}$	0.41 / $5.58 \times 10^{-7}$
+ 50% DPPC	0.62 / $9.81 \times 10^{-7}$	0.13 / $1.34 \times 10^{-7}$	0.82 / $1.12 \times 10^{-6}$
+ 75% DPPC	0.31 / $4.91 \times 10^{-7}$	0.07 / $6.69 \times 10^{-8}$	1.23 / $1.67 \times 10^{-6}$
+ 25% DSPC	0.94 / $1.49 \times 10^{-6}$	0.18 / $1.78 \times 10^{-7}$	0.44 / $5.58 \times 10^{-7}$
+ 50% DSPC	0.62 / $9.81 \times 10^{-7}$	0.13 / $1.34 \times 10^{-7}$	0.88 / $1.12 \times 10^{-6}$
+ 75% DSPC	0.31 / $4.91 \times 10^{-7}$	0.07 / $6.69 \times 10^{-8}$	1.32 / $1.67 \times 10^{-6}$

### ***2.3. Dynamic light scattering: characterisation of liposome systems***

#### *2.3.1. Determination of particle size*

The particle size of all liposome systems was measured using a ZetaPlus instrument (Brookhaven Instrument Corporation, Worcestershire, UK) via dynamic light scattering, which is a simple, efficient technique that can accurately measure particle sizes in the range of 2 to 3000 nm. For samples that are of sub-micron particle size, dynamic light scattering (DLS), also known by the techniques of photon correlation spectroscopy (PCS) and quasi elastic light scattering (QELS), is the most suitable instrumentation.

Based on the principle of Brownian motion, when particles are suspended in an aqueous medium, the rate of particle diffusion is relative to their size with small particles diffusing faster than larger particles. The time disparity of subsequent scattered intensity is detected by studying their auto-correlation, thus ascertaining a diffusion coefficient from which particle size can be measured. The instrument passes a laser through the liposome sample which is scattered by the particles in multiple directions and is subsequently measured by a photomultiplier tube. A unique auto-correlation function is processed and this function, exclusive to the sample population, ultimately gives an accurate calculation of particle size. The PCS technique calculates scattered light intensity that varies over time intervals. Thus, intensity autocorrelation function is produced upon calculating an average of the intensity products within dispersions as a function of time. Therefore, the scattered diffusion rate represents the particle size (Brookhaven Instruments Corporation, 2004).

### 2.3.2. Determination of zeta potential

Zeta potential is the difference in electrical potential, measured in millivolts (mV), present between the stern plane of counter ions encompassing a colloidal particle and its dispersion medium. At the particle surface, the net charge impacts ion dispersal in the adjacent area, in turn increasing the volume of counter ions at the surface. This forms an electrical double layer at the particle-liquid interface (Figure 2.2). This liquid layer that encompasses the particle is split into two sections, an inner region, the stern plane, containing strongly associated ions, and an outer diffuse layer, with less firmly bound ions, with the zeta potential measured at the boundary of the shear plane (Kaszuba *et al*, 2010) (Figure 2.2). Thus, zeta potential can indirectly signify the surface charge of a particle, which is significant to the characterisation and management of colloidal stability, an imperative factor to be controlled when optimising physically stable delivery systems (Brookhaven Instruments Corporation, 2004).

The measured electrical charges greatly affect the interactions between particles in the dispersed phase and the resultant physical stability of the systems, especially of those in the size range of colloidal particles. For dispersed systems utilised as vehicles of drug delivery, such as liposomes for example, the *in vivo* fate, and thus the resultant protective efficacy, is considerably influenced by surface charge (Li & Tian, 2006).

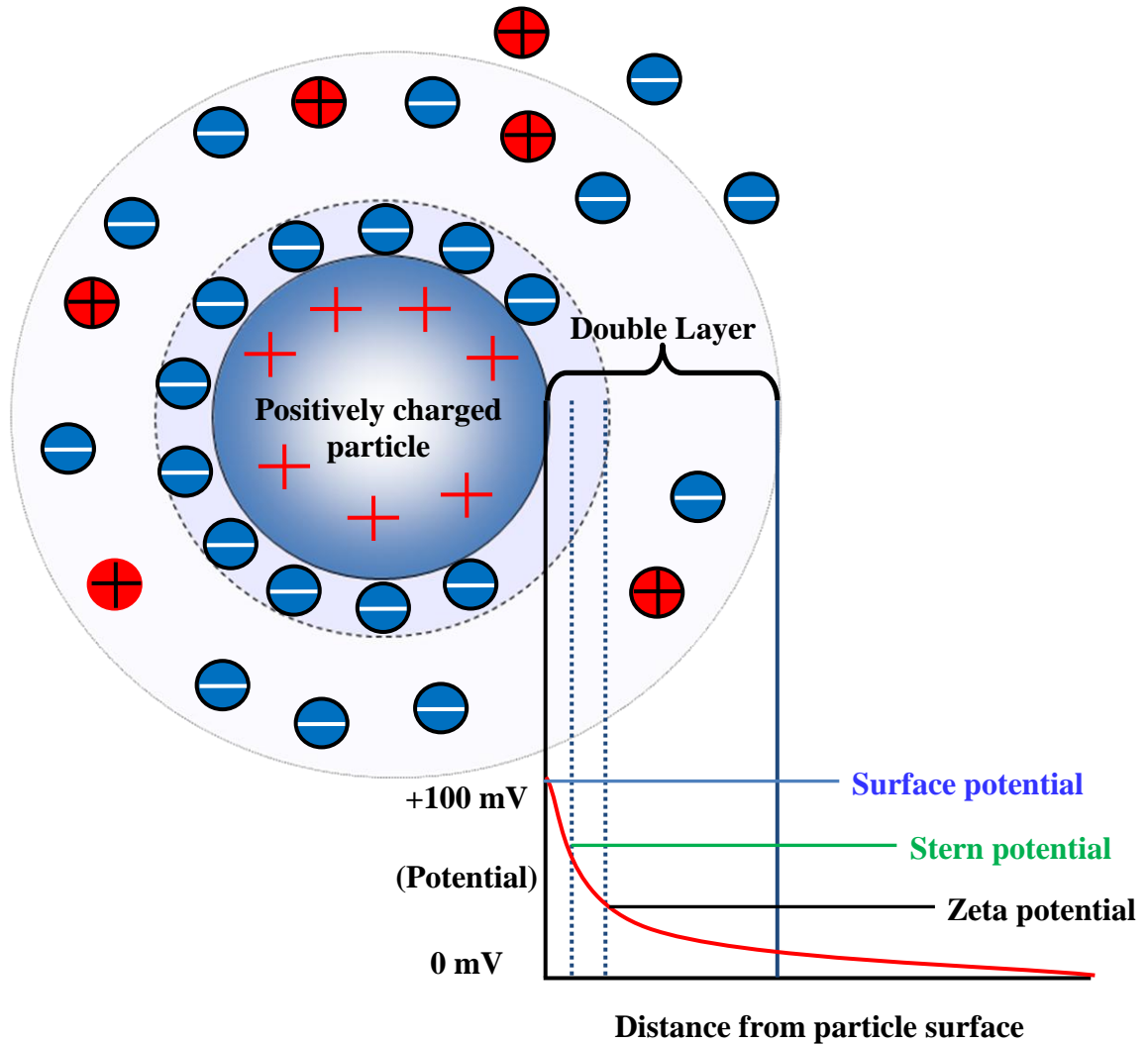


**Figure 2.2.** A schematic illustration of the zeta potential of a particle. The electrical double layer that surrounds a particle with a net surface charge (in this instance a positive charge) and the electrical potentials encompassing the particle provides the zeta potential, which is measured at the surface of the shear plane.

Overall, through the use of dynamic light scattering, the average diameter and zeta potential of the liposomal formulations were measured using a ZetaPlus analyser (Brookhaven Instrument Corporation). Particle sizes were averaged for their mean after three minutes, with three measurements averaged across one minute intervals. When measuring the particle size and zeta potential, approximately 100  $\mu\text{l}$  of sample was suspended in 2 ml of the corresponding 1/10 diluted buffer solution (e.g. 1 mM Tris buffer, pH 7.4) with readings taken at room temperature. The zeta potential results

were mean averages taken from ten readings made for each formulation in triplicate. Standard control readings were taken regularly and recorded for particle size (499 nm +/- 5 nm; Brookhaven) and zeta potential (-68 mV +/-6.8 mV; Malvern).

#### ***2.4. Differential Scanning Calorimetry (DSC) of liposomal dispersions***

The gel-to-liquid phase transition temperatures were attained for the liposomal dispersions via DSC and thermograms were acquired using a Pyris Diamond DSC (Perkin Elmer Instruments LLC, USA). A scan rate in the range of 2-20 °C/min is generally utilised for liposome samples. In this study, with a greater resolution associated to slower scan rates, a scan rate of 10 °C/min (600 °C/h) was applied, for a balance between enhanced sensitivity and resolution (Taylor & Craig, 2003), over the range of 25 °C to 75 °C. All scans were carried out in triplicate, as it is a standard approach to run at least two additional DSC scans to verify reproducibility (Feitosa *et al*, 2006).

The conditions and settings were adjusted accordingly to optimise the application of differential scanning calorimetry of fluid liposomal dispersions. Suspensions were contained in air tight pans which were sealed immediately upon loading to reduce the effect of evaporation, with a sample load weight of approximately 10 mg. A reference pan filled with an equal volume of either water or buffer is beneficial compared to empty pans, with the corresponding buffer used as a reference. This yielded an improved baseline, achievable through a comparable thermal composition with the sample. Pyris software, version 5.00.02 (Perkin Elmer Instruments LLC, USA) was used for all data analysis.

## ***2.5. Protein loading studies***

### *2.5.1. Separation of liposome associated and non-associated protein*

To separate the liposome associated antigen from the free, non-associated antigen, liposomes were centrifuged at 125000 g (45000 RPM) for sixty minutes at room temperature (RT) to pellet the liposomes. The supernatants were then collected and the pellets were re-suspended back into their original volume, using the corresponding buffer.

### *2.5.2. Sodium dodecyl sulphate polyacrylamide gel electrophoresis*

Gel electrophoresis occurs when a charged particle moves through an electrical field. Sodium dodecyl sulphate polyacrylamide gel electrophoresis (SDS-PAGE) is utilised to ascertain the molecular weight for specific polypeptide chains. Initially, native proteins are denatured into individual polypeptides through the addition of the detergent sodium dodecyl sulphate, which breaks down hydrophobic bonds. Further breakage into disulfide bonds is achieved upon the application of mercaptoethanol. In this induced environment, polypeptide chains are generated by proteins that transform into inadvertent coils which attach to an abundance of SDS at a constant weight ratio of SDS detergent per gram of polypeptide. As a result, the charges of the polypeptides become redundant in comparison to the negative charges of the SDS, generating a consistent negative charge for the polypeptides. Therefore, with an identical charge/mass ratio, each SDS-protein complex has an equal electrophoretic mobility. When such complexes undergo electrophoresis on a polyacrylamide gel, a sieving motion aids sample separation and protein mobility can take place based on their respective molecular weights. The larger molecules take longer to migrate down the gel and, alongside a known standard marker, unknown proteins can be established for an approximate molecular weight (Stenesh, 1998).

Upon centrifugation, as highlighted earlier, which is conducted to separate the liposome associated protein from the non-associated protein, the resultant samples in an equal volume of SDS sample buffer were heated at 90 °C for three minutes in order to denature the proteins to their individual polypeptides. Subsequently, 10 µl of pellet and supernatant samples from each formulation were analysed via SDS-PAGE for semi-quantification of the protein concentrations present.

### *2.5.3. Bicinchoninic acid (BCA) assay: quantification of non-adsorbed protein*

Determination of protein can be pivotal to biochemical research and the BCA assay allows for protein recognition, achieved by the development of a  $\text{Cu}^{2+}$  protein complex in an alkaline environment, prior to  $\text{Cu}^{2+}$  reduction to  $\text{Cu}^{1+}$ . Furthermore, the volume of this reduction reaction is directly proportional to any protein present. The formation of a purple-blue complex is resultant from BCA that binds with  $\text{Cu}^{1+}$  in alkaline conditions. Consequently, protein determination can occur and the colour change reaction provides a means of observing the reduction of alkaline  $\text{Cu}^{2+}$  from proteins. Indeed, the BCA assay holds numerous advantages over alternative protein determination assays including:

- Ease of application,
- Stability of colour complexes formed,
- Can be applied to an array of protein concentrations.

The BCA assay has a working range of 0.5 to 30 µg/ml of protein, with triplicate 25 µl supernatant solutions (from liposome samples adsorbed with OVA at 1 mg/ml) added to 200 µl of BCA reagent per well, tested to ascertain the level of non-adsorbed protein from the proposed liposomal formulations. Overall, unknown OVA protein

concentrations present within the supernatants were quantified by the BCA protein assay in accordance with the associated protocol (Sigma-Aldrich Co. Ltd. Dorset, UK).

A protein standard concentration curve for OVA from 0-1 mg/ml (Figure 2.3) was formed and plotted to establish the equation of the line, upon which the percentage of free protein within the sample supernatants could be determined from the known concentrations. Indeed, upon reduction of  $\text{Cu}^{2+}$  to  $\text{Cu}^{1+}$  from proteins in the alkaline solution, the presence of bicinchoninic acid yields blue or violet complexes. This in turn allows for quantification of total protein from sensitive colorimetric detection, with mean absorbance values measured at the wavelength of  $\sim 560$  nm (Pierce Biotechnology Inc, 2005).

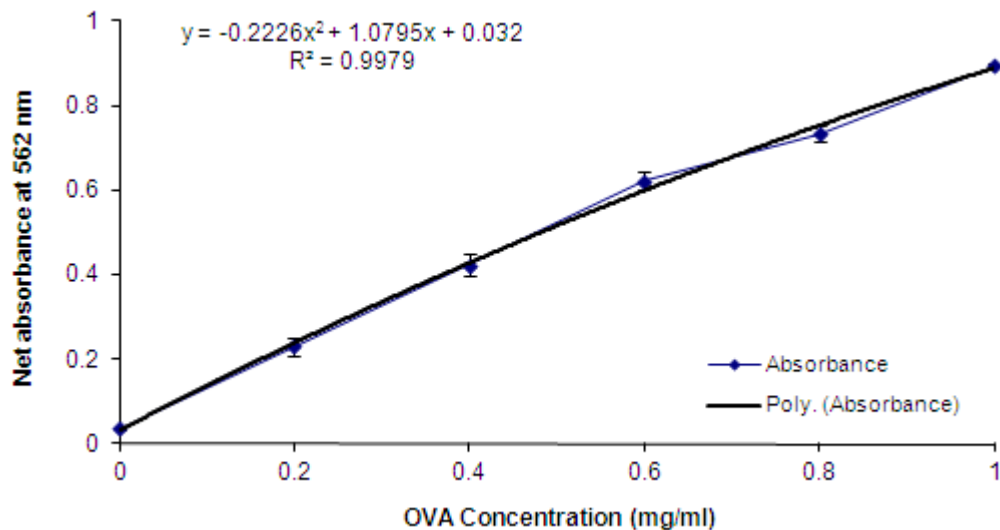


**Figure 2.3.** An example OVA protein standard curve for the BCA assay. Results represent the mean average from three readings for each concentration upon the net absorbance read at the wavelength of  $\sim 560$  nm.

## ***2.6. Quantification of adsorbed OVA protein via radiolabelling***

### ***2.6.1. Radiolabelling OVA***

For the studies of antigen retention and release over time, OVA protein was radiolabelled with iodine 125 ( $I^{125}$ ). OVA and  $I^{125}$  was added to a pre-coated iodination tube and allowed to bind for up to one hour, with swirling taking place at regular intervals. In order to generate an approximate 1-2 ml stock of radiolabelled OVA/ $I^{125}$ , 100  $\mu$ l OVA (1 mg/ml) was mixed with 2 MBq  $I^{125}$ . Sephadex G-75 (fractionation range for globular proteins of 3-80,000 MW) gel filtration media in water was formed in a 10 ml column and hydrated with Tris buffer. The radiolabel-OVA mixture was passed through the column, maintained with a stable flow rate of Tris buffer, for the collection of  $I^{125}$  in 80 samples of 0.5 ml.

Upon sample collection, the extent of activity per iodine sample was measured using an auto-gamma counter for counts per second (CPS) and plotted (Figure 2.4), with confirmation of radiolabelled OVA determined by the BCA assay, whereby a colour change indicated the presence of protein (Figure 2.5). The samples that correlated to the uppermost gamma counts with a corresponding indication of protein presence were pooled together. This stock was subsequently diluted accordingly with Tris buffer in order to adsorb radiolabelled OVA to the liposome samples at the desired concentration.

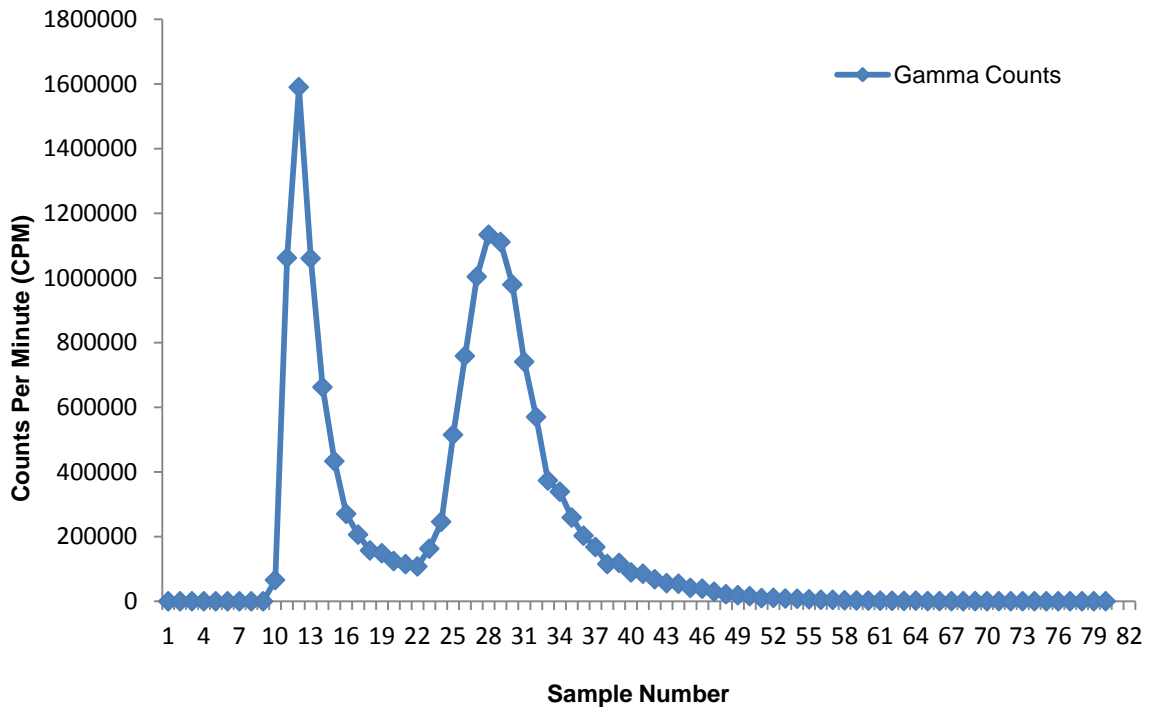


**Figure 2.4. Determination of  $\gamma$ -radiation activity for iodine labelled OVA samples eluted through a sephadex column.** Each sample contained a volume of ~0.5 ml as 80 samples were passed through a 10 ml column. OVA antigen was found to be associated to samples 11, 12 and 13, later confirmed with the BCA assay. The second visible peak is typical of free iodine, not associated to any protein.

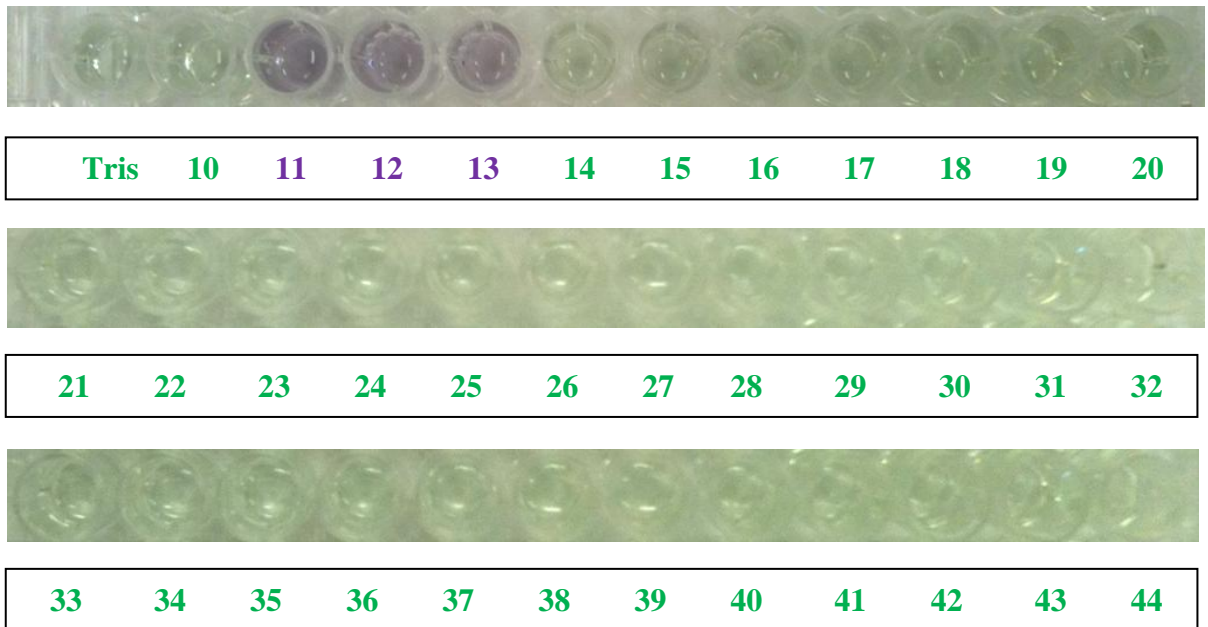


**Figure 2.5. Confirmatory BCA assay results for suspected protein labelled samples.** A colour change from green to purple, indicative of protein presence corresponded to the 1<sup>st</sup> peak of gamma counts associated to OVA/ $I^{125}$  samples of 11-13. A lack of protein was also confirmed in samples of the 2<sup>nd</sup> free iodine peak.

### 2.6.2. Determination of *in vitro* release via dialysis of liposomes adsorbed with OVA/I<sup>125</sup>

Prior to the adsorption of radiolabelled OVA to the DDA-TDB based liposome systems, the release of radiolabelled OVA was assessed via dialysis experiments. This was firstly validated by ascertaining whether OVA alone would pass through the pores of the dialysis tubing in the absence of the liposomes. Such an experiment was conducted over a 72 hour time period with the tubing clipped and closed at either end with dialysis clips, prior to being immersed in 30 ml of Tris buffer or FBS/Tris in falcon tubes, at 37 °C in a shaking water bath.

At regular intervals, 1 ml of sample was removed and measured for its iodine activity using an auto-gamma counter, giving results in counts per second. This allowed for the extent of radiolabelled OVA release at each designated time point to be calculated over time, from an initial measured total sample. Upon removal of a 1 ml sample, the media was changed with an identical volume of either Tris buffer or FBS/Tris as the same, original dialysis tubing was placed in a new falcon tube to be returned to the shaking water bath. After the final time point was measured, the remainder of I<sup>125</sup> activity from within the dialysis tubing was then measured for gamma counts. This dialysis procedure was subsequently followed when applying the liposome/OVA/I<sup>125</sup> samples to the tubing, to ascertain the release profiles over time for the various DDA-TDB based liposomal formulations.

### 2.7. Serum stability studies: interaction of serum proteins with liposomes

All of the proposed DDA-TDB based liposome systems were immersed in Tris buffer and/or in FBS, in a 50% v/v mixture with Tris buffer, in order to mimic *in vivo*

conditions. Measurements of particle size and zeta potential of the systems was carried out via dynamic light scattering using a ZetaPlus analyser (Brookhaven Instrument Corporation) as previously conducted. Upon the addition of each liposome batch in Tris buffer to an equal volume of FBS/Tris (50% v/v), samples were incubated in a water bath at 37 °C over 24 hours. At various intervals across this time period, the samples were centrifuged (Beckman Coulter - 125,000×g, 4 °C, 45 mins) to remove any unbound proteins, prior to measurements of particle size and zeta potential as previously conducted.

### ***2.8. Transmission electron microscopy (TEM)***

Transmission electron microscopy is one the main techniques of choice for the micro-structural characterisation of materials. Conventional TEM consists of an array of advanced instrumentation including vacuum science technology, electronic and mechanical stability, electron sources and highly sensitive digital imaging, amongst many other processes (Zhang & Zhang, 2001).

The transmission electron microscope directs a specialised beam of electrons (as opposed to light used in a light microscope), in conjunction with magnetic coils onto a specimen, with the chosen sample suspended within a vacuum. Electron interaction occurs as the specialised beam enters the specimen, forming a representative image. Contrast can be established through the use of heavy-metal stains that engage or diffract electrons, removing them from the electron beam as it enters the sample material. Such a powerful analytical tool is recognised in the potential resolution achievable with magnification as high as  $X1 \times 10^6$ . In addition, for biological

specimens, a transmission electron microscope possesses the resolving power to distinguish features down to a mere 2 nm (Alberts, 2004).

In the current study, morphological examination was conducted using a “Jeol 1200EX” transmission electron microscope fixed with a LaB6 filament within an operating voltage range of 40 to x 120 kV. 10 µl of the liposome sample was positioned on a polymer filmed copper grid and was left to rest for two minutes. Surplus sample was removed using filter paper with subsequent application of uranyl acetate (10 µl). The copper grid was once more left for two minutes prior to cleaning with distilled water and air drying, producing a thin film. Upon sample preparation into a film, observation took place at 70 kV.

### ***2.9. Cell culture/in vitro studies***

A macrophage “J774” BALB/c mice cell line (Source: ECACC - European collection of cell cultures) was grown in Dulbecco’s modified eagle medium (DMEM) supplemented with 1% Penicillin/Streptomycin/L-Glutamine (PSG) and 10% (v/v) Foetal bovine serum. Incubation took place in sterile conditions at 37 °C, in humid conditions of 5% CO<sub>2</sub>.

### ***2.10. CellTiter 96 aqueous non-radioactive cell proliferation assay (MTS assay)***

The non-radioactive cell proliferation assay is a colorimetric technique that establishes the quantity of live, viable cells. The assay contains solutions of a tetrazolium compound; 3-(4,5-dimethylthiazol-2-yl)-5-(3-carboxymethoxyphenyl)-2-(4-sulfophenyl)-2Htetrazolium, inner salt; (MTS) with an electron coupling reagent, phenazine methosulfate (PMS). The bio-reduction of MTS by cells yields formazan

product, soluble within the tissue culture medium. Further processing is not required as complete absorbance of formazan at 490 nm is read directly from the plate. All metabolically functional cells contain dehydrogenase enzymes responsible for converting MTS into the soluble form of formazan (Figure 2.6). Therefore, the level of absorbance determined from the presence of formazan product is directly proportional to the volume of live cells in culture (Promega, 2007).



**Figure 2.6. The structure and conversion of MTS into formazan.** MTS is converted by dehydrogenase enzymes present in active cells, responsible for the breakdown of MTS tetrazolium salt into the resultant formazan product (Promega, 2007).

The MTS assay is required to understand the levels of cell proliferation possible with the outlined DDA-TDB based systems. As discussed by Lappalainen *et al*, (1994) when comparing cell proliferation assays using cationic liposomes, the necessity to ascertain cell proliferation and cytotoxicity is vital when formulating drug delivery systems. Although results obtained *in vitro* do not exactly correlate to the possible behaviour *in vivo*, such applications can indicate the functions and survival potential of components at a cellular level, within physiological conditions. The MTS and MTT (3-(4,5-dimethylthiazol-2-yl)-2,5-diphenyltetrazolium bromide) assays were applied to the cationic samples by Lappalainen *et al*, (1994), and proved to be almost identical in

results. However, as well as being convenient in use, non-radioactive and flexible, the use of the MTS assay is justified as it has favourable advantages over the MTT assay including;

- Efficiency - No washing or harvesting of cells together with solubilisation steps (used in the MTT assay) are required for this assay.
- Safe - To solubilise the formazan product, which is quantitatively, a directly proportional indication of viable cells in culture, volatile organic solvents are not required (necessary for the MTT assay).
- Flexible - The 96 well plates used to read and quantify the absorbance of remaining formazan product can be re-incubated for additional development of the reaction and measurement, as measuring absorbance is non-destructive (Promega, 2007).

Cytotoxicity upon macrophages was determined by the MTS cell proliferation assay in conjunction with the DDA-TDB based systems. More specifically, the commercially available “CellTiter 96<sup>®</sup> AQueous One Solution Cell Proliferation Assay” (Promega, USA) was applied to the DDA-TDB formulations at 5.0 µg/ml (concentration calculated for the cationic component, DDA: total concentration = 6 µg/ml) on 96 well plates with 8x10<sup>4</sup> cells/ml (8x10<sup>3</sup> cells/well). The cell number and viability was determined accordingly to the desired concentration and plated out for each formulation, together with positive and negative controls (macrophage cells or DMEM respectively) in triplicate wells. The total volume per well was 100 µl.

Upon 24 hours incubation at 37 °C in a humidified atmosphere of 5% CO<sub>2</sub>, ensuring adherent cells, the DDA-TDB liposomes were applied at the set concentrations (serum

free DMEM was used as serum binds to the cationic components in the formulation). The following day, upon incubation of the cells and sample, 20  $\mu\text{l}$  of CellTiter 96<sup>®</sup> AQueous One solution reagent per 100  $\mu\text{l}$  was pipetted to each well and the plate was incubated at 37 °C, 5% CO<sub>2</sub>. Absorbance was read after one hour using a 96-well protein assay micro plate reader, recorded at the wavelength of 490 nm as displayed in the schematic in Figure 2.7.

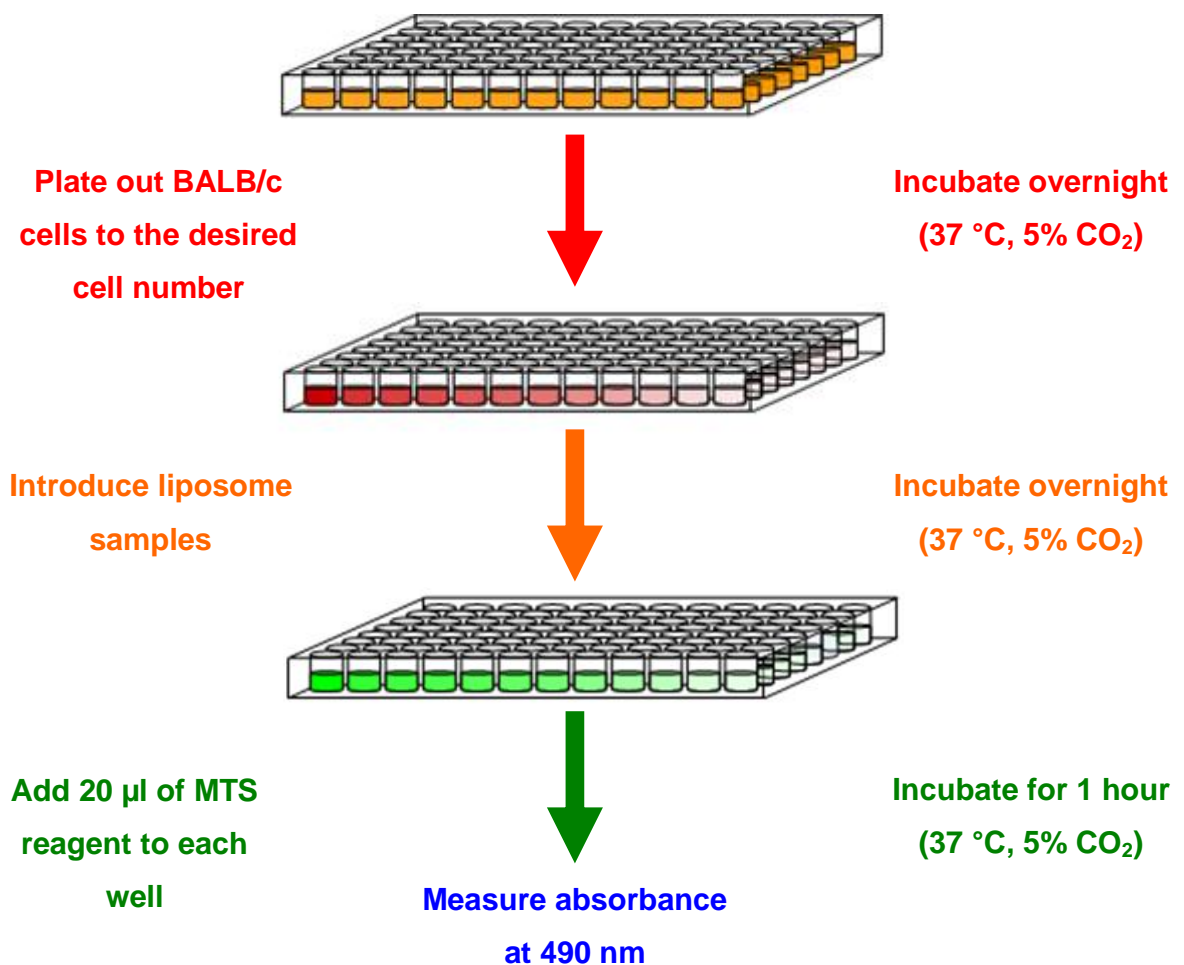


**Figure 2.7. Schematic diagram summarising the main steps of the MTS cell proliferation assay.** Initially, BALB/c cells were plated out to a set cell number and incubated overnight at the set humidified conditions. Upon sample preparation, adjustment to the desired sample concentration and a further night of incubation, the MTS reagent was added before determining absorbance at the set wavelength of 490 nm.

### 2.11. $\beta$ -N-Acetylglucosaminidase assay

N-acetyl- $\beta$ -D-glucosaminidase (NAG) is a lysosomal enzyme of mammalian cells that contributes to the intracellular degradation of glycolipids and glycoproteins (Legler *et al*, 1991). The NAG assay occurs due to the hydrolysis of the NAG substrate, 4-Nitrophenyl N-acetyl- $\beta$ -D-glucosaminide (NP-GlcNAc), by the lysosomal enzyme. Such enzymatic hydrolysis of the NAG substrate emancipates *p*-nitrophenol ions (Figure 2.8). After ionisation, the product reactant can be colourimetrically determined using a micro plate reader, (Bio-Rad, Herts, UK) set to the wavelength of 405 nm (Sigma, 2009).



**Figure 2.8. The enzymatic hydrolysis of NAG substrate.** Hydrolysis liberates *p*-nitrophenol with subsequent introduction of stop solution resulting in the formation of yellow *p*-nitrophenylate ions, measured at the wavelength of 405 nm (Sigma, 2009).

A  $\beta$ -N-Acetylglucosaminidase assay kit (Sigma-Aldrich Co. Ltd., Dorset, UK) was conducted according to manufacturer's instructions using 96 well cell culture plates with a BALB/c cell number of  $8 \times 10^4$ /ml, as fixed previously for the MTS assay. With the desired cell number correctly determined, plated and incubated overnight at 37 °C in a humidified atmosphere of 5% CO<sub>2</sub>, liposomal DDA-TDB based formulations at a 5 µg/ml sample concentration were introduced in triplicate, mirroring the first two stages of the MTS assay, as displayed previously in Figure 2.7.

After a second overnight incubation of cells and liposome samples, at identical conditions (37 °C, 5% CO<sub>2</sub>), 10 µl from each well was transferred to a new plate with the addition of 90 µl of substrate solution (1 mg/ml of 4-Nitrophenyl-N-acetyl- $\beta$ -D-

glucosaminide (NP-GlcNAc) in 0.09 M citrate buffer). A blank control (100 µl of substrate solution), a standard control (300 µl of standard solution) and a positive control (98 µl of substrate solution + 2 µl of NAG control enzyme) were included in triplicate to the new 96 well plate. This plate was then incubated at 37 °C, 5% CO<sub>2</sub> as previously conducted for 10 minutes. Following incubation, the reaction was stopped by adding 200 µl of stop solution per well, except the wells containing standard solution. The plate was then read on a micro plate reader at 405 nm.

### ***2.12. Determination of tumour necrosis factor-alpha (TNF-α) cytokine release***

Immunoassays consist of experiments that utilise antibodies as reagents and more specifically, enzyme immunoassays employ enzymes bound to a reactant that ultimately yields quantification, possible from a colour change reaction that materialises upon the introduction of substrate. In general, ELISAs consist of a stepwise introduction and subsequent reaction of reagents to a solid-phase bound substance, via incubation and separation of bound and unbound reagents upon washing. An enzyme labelled reactant causes a characteristic colour change that allows for quantification of the reaction to take place (Crowder, 2001).

Macrophage activation was detected by the application of a mouse TNF-α ELISA development kit (R&D Systems Europe Ltd., Abingdon, UK). The general enzyme-linked immunosorbent assay (ELISA) protocol and subsequent analysis was conducted in accordance with the manufacturer's recommendations.

Initially for plate preparation, capture antibody was diluted to a working concentration of 0.8 µg/ml and was used to coat a 96 well plate prior to incubation overnight at room temperature (RT). Subsequent washing and blocking rendered the plate ready for sample addition after a repeated wash stage. 100 µl cell culture supernatants of the DDA-TDB based formulations and standards were added, and after 2 hours incubation at RT and a further wash stage, the introduction of 100 µl detection antibody (200 ng/ml) allowed for the TNF- $\alpha$  cytokine to be detected. After 2 hours incubation at RT and a further wash stage, an enzyme marker, Streptavidin-HRP (horseradish peroxidase) was added prior to incubation at RT for 20 minutes (plates were covered to avoid exposure to light). After washing and introducing 100 µl of substrate solution, the plates were covered and incubated for a further 20 minutes. 50 µl of stop solution was then added to each well and the plates were gently tapped, to ensure thorough mixing and inhibit any further reaction.

After all experimental steps were followed to develop and stop the reaction, the optical density was read immediately using a micro plate reader (Bio-Rad, Herts, UK). Absorbance readings were made at the wavelength of 450 nm for each well, including the seven point standards to produce a corresponding standard curve for mouse TNF- $\alpha$  concentration (pg/ml) against the optical density. The enzyme-linked immunosorbent assay (ELISA) process and all the protocol steps conducted are summarised in Figure 2.9.

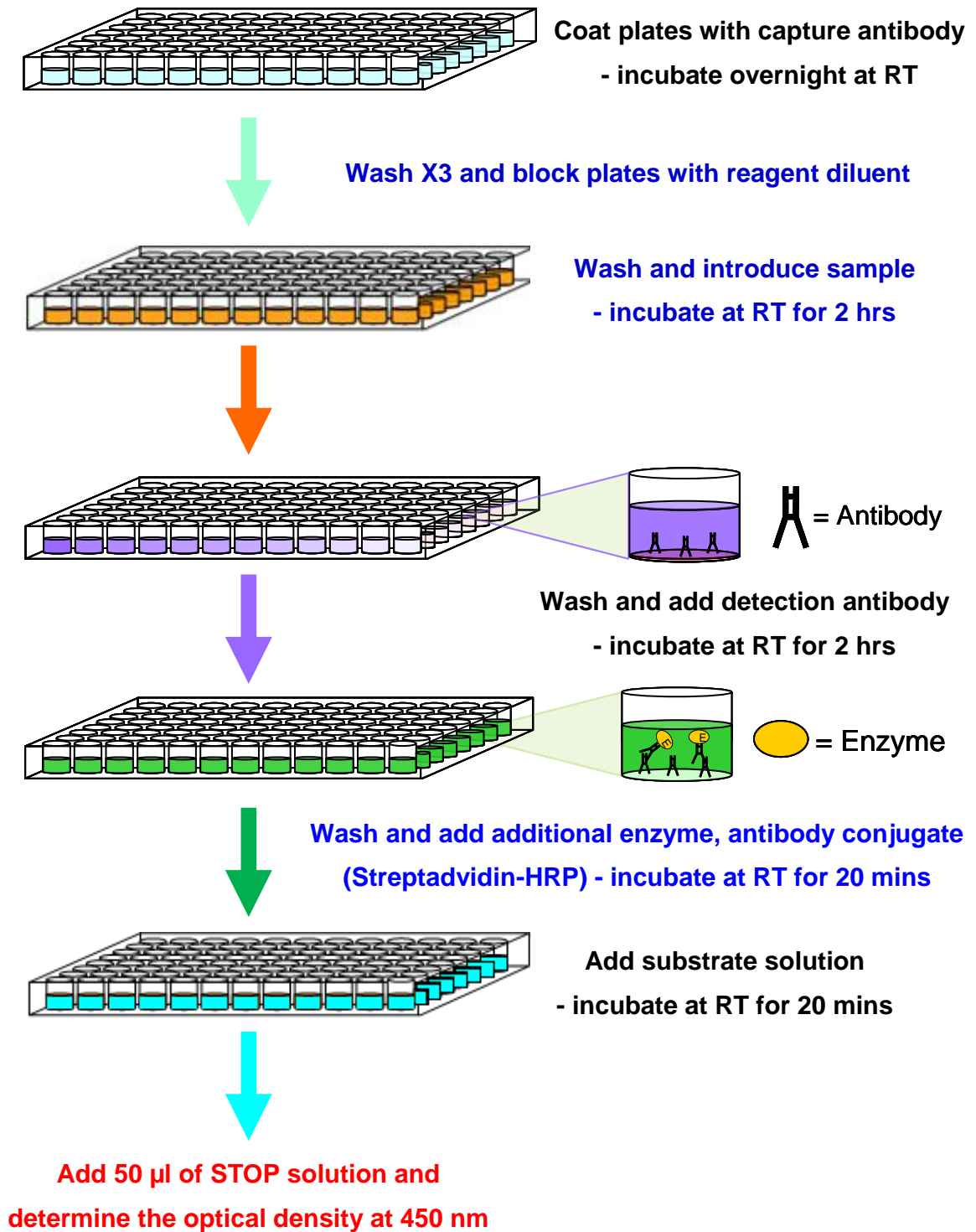


**Figure 2.9. Schematic summary of the mouse TNF- $\alpha$  enzyme-linked immunosorbent assay (ELISA) development kit.** ELISA plates were coated with capture antibody prior to numerous wash stages (with 0.05% Tween 20 in PBS as wash buffer) and blocking with reagent diluent. Washing prior to each stage of introducing sample, detection antibody and additional antibody conjugate for bound antibody recognition took place with incubation at room temperature. Addition of the activating substrate with further incubation and subsequent addition of stop solution completed the experiment, prior to reading absorbance at 450 nm.

### ***2.13. In vivo studies: immunological analysis of DDA-TDB based liposomes***

All experimentation strictly adhered to the 1986 Scientific Procedures Act (UK) and was conducted in a designated establishment. For the main immunisation study, female C57BL/6 mice, 6-8 weeks old (acquired from Charles River, UK) were split into 11 groups of 5.

#### *2.13.1. Immunisation of mice*

Vaccine preparations were made with DDA-TDB based liposomes incorporating Ag85B-ESAT-6-Rv2660 (Hybrid56) antigen to a final concentration of 0.1 mg/ml (5 µg/vaccine dose). All mice, with the exception of the naive group, were immunised intramuscularly (i.m.) with the proposed vaccines (0.05 ml/dose) three times, with two week intervals between each immunisation.

Blood samples were taken at regular intervals throughout the seven week study, prior to termination. Blood was drawn from the tail vein upon a small incision, obtaining 50 µl with micropipette capillary tubes lightly coated in heparin solution (0.1% w/v in PBS). The blood was subsequently added to 450 µl PBS (giving a final dilution of 1/10) and centrifuged using a micro centrifuge at 13,000 RPM for 5 minutes. The supernatants of each mouse sample was collected and transferred to a fresh eppendorf prior to storage at -20 °C for future analysis. As a result, assuming that the haematocrit or packed cell volume is approximately 50%, sera obtained from each mouse consisted of a final 20-fold dilution.

### 2.13.2. Splenocyte proliferation

Upon experiment termination, mice were humanly culled prior to aseptic spleen removal and placement in ice-cold, sterile PBS. Spleen cell suspensions were produced upon light grinding through a fine wire mesh into 10 ml RPMI 1640 cell culture medium (W/O Glutamine) supplemented with 10% (v/v) FBS and 1% (v/v) PSG (BioSera, East Sussex, UK). The cell suspension was left for 5 minutes to settle before transferring the suspension to sterile falcon tubes, ensuring that the cellular debris was not disrupted. The cell suspension was then centrifuged at 1000 RPM for 10 minutes at 15 °C. The resultant supernatant was then removed with the remaining pellet resuspended in 10 ml of fresh RPMI media, prior to further centrifugation at 1000 RPM for 10 minutes at 15 °C. The supernatant was removed and the pellet was resuspended in 5 ml of fresh RPMI media. The single cell suspensions were subsequently used to evaluate splenocyte proliferation and antigen specific cytokine responses.

For the analysis of splenocyte proliferation, H56 antigen was added to sterile 96 well cell culture plates (Greiner Bio-One Ltd, Gloucestershire, UK) at the concentrations of 0, 0.05, 0.5, 5.0 and 25 µg/ml (adjusted to the desired concentration using supplemented RPMI) alongside a positive control of concanavalin A at 2 µg/ml. 100 µl of the splenocyte cell suspensions were subsequently added to each well prior to incubation at 37 °C, 5% CO<sub>2</sub>. Upon 72 hours incubation, 40 µl of [<sup>3</sup>H] thymidine at 0.5 microcurie (µCi) in supplemented RPMI media was added to each well before incubation for 24 hours (37 °C, 5% CO<sub>2</sub>). All well contents were harvested on to quartz filter mats (Skatron/Molecular Devices, Berkshire, UK) using a cell harvester (Titertek Instruments, Alabama, USA). Individual discs representative of each well per

plate was passed through to 20 ml scintillation vials (Sarstedt, Leciester, UK) containing 5 ml of liquid scintillation cocktail (Ultima Gold, PerkinElmer, Cambridgeshire, UK). Incorporation of [<sup>3</sup>H] thymidine in the cultured cells was measured using a Tri-carb 3100TR liquid scintillation analyzer (Packard BioScience Co., Meriden, CT, USA), according to standard operating procedures.

### *2.13.3. Evaluation of H56 antigen specific antibody isotypes*

Serum samples collected at regular time intervals over the seven week immunisation study were assessed for levels of IgG, IgG1 and IgG2b antibodies by applying an enzyme-linked immunosorbent assay (ELISA). The ELISA plates (96 well, flat bottomed, high binding, Greiner Bio-One Ltd, Gloucestershire, UK) were firstly coated with 60 µl/well of H56 antigen at 3 µg/ml in PBS, prior to overnight incubation at 4 °C. All plates were washed three times with PBST wash buffer (40 g NaCl, 1 g KCl, 1 g KH<sub>2</sub>PO<sub>4</sub>, 7.2 g Na<sub>2</sub>HPO<sub>4</sub>, (2H<sub>2</sub>O) per 5 litres of ddH<sub>2</sub>O, incorporating ~0.4 ml of Tween 20) using a plate washer (Microplate washer, MTX Lab Systems, INC., Virginia, USA) with subsequent blotting onto paper towels to remove any unbound antigen. In order to eradicate any non-specific antigen binding, the plates were blocked by coating each well with 100 µl of Marvel in PBS (dried skimmed milk powder, 4% w/v, Premier Foods, Hertfordshire, UK) and incubated for one hour at 37 °C before the plates were washed again three times with PBST buffer. 140 µl of serum sample was serially diluted in PBS (70 µl sequentially across the plate) in dilution plates, added to the washed ELISA plates and then incubated for one hour at 37 °C. The plates were then washed five times with PBST buffer before the addition of 60 µl/well of horseradish peroxidase (HRP) conjugated anti-mouse isotype specific immunoglobulins of IgG, IgG1 and IgG2b (AbD serotec, Oxfordshire, UK) upon

adjustment in PBS to the suggested dilutions of 1/750, 1/4000 and 1/4000, to identify anti-H56 antibodies. The plates were washed a further five times with PBST buffer prior to the addition of 60 µl/well substrate solution (colouring agent: 6x 10 mg tablets of 2,2'-azino-bis (3-ethylbenzthiazoline-6-sulfonic acid) (ABTS; Sigma, Dorset, UK) in citrate buffer (0.92g Citric Acid + 1.956g  $\text{Na}_2\text{HPO}_4$  per 100 ml) incorporating 10 µl of hydrogen peroxide (30%  $\text{H}_2\text{O}_2$ /100 ml) before incubation for 30 minutes at 37 °C. The absorbance was then read at the wavelength of 405 nm using a microplate reader (Bio-Rad Laboratories, model 680, Hertfordshire, UK). A known positive serum and pooled naive mice sera were used as a positive and negative control respectively.

#### *2.13.4. Quantification of cytokines via the ELISA (sandwich ELISA)*

The isolation of splenocyte cell suspensions and plating onto 96 well cell culture plates was conducted as summarised in section 2.13.2. The cells were subsequently incubated for 48 hours at 37 °C (5%  $\text{CO}_2$ ), prior to removal of supernatants and storage at -70 °C for future analysis. Quantification of the cytokines, IL-2, IL-5, IL-6, IL-10 and IFN- $\gamma$  within cell culture supernatants took place using each specific DuoSet ELISA development kit (R&D Systems, Oxfordshire, UK). The plates were firstly coated with 100 µl capture antibody per well (diluted in PBS to 1.0 µg/ml for IL-2 and IL-5, to 2.0 µg/ml for IL-6 and to 4.0 µg/ml for IL-10 and IFN- $\gamma$ ) and incubated at room temperature overnight. The plates were then washed three times with PBST buffer before blocking with blocking agent (reagent diluent). The plates were subsequently incubated at room temperature for a minimum of one hour before washing a further three times with PBST buffer. 100 µl/well of sample or standards were then added to the plates which were covered with an adhesive strip and incubated for two hours at

room temperature. The plates were washed again three times with PBST buffer before adding 100  $\mu$ l of detection antibody for the particular cytokine per well (diluted in reagent diluent to 100 ng/ml for IL-5 and IFN- $\gamma$ , to 200 ng/ml for IL-6 and 400 ng/ml for IL-2 and IL-10) and incubating for two hours at room temperature. Upon washing three times with PBST buffer, 100  $\mu$ l of Streptavidin-horseradish peroxidase (HRP) was added to each well at the working dilution of 1/200. The plates were covered to protect from direct light and then incubated at room temperature for 20 minutes. The plates were then washed a further three times in PBST buffer before the addition of 100  $\mu$ l substrate solution to each well (1:1 mixture of colour reagent A and B: stabilised hydrogen peroxide and stabilised tetramethylbenzidine (TMB) respectively). The plates were again covered to avoid exposure to direct light and then incubated at room temperature for 20 minutes. The experimental reaction was halted through the addition of 50  $\mu$ l stop solution (2N H<sub>2</sub>SO<sub>4</sub>) to each well. The optical density of each well was immediately determined using a microplate reader at the wavelength of 450 nm (Bio-Rad Laboratories, model 680, Hertfordshire, UK).

#### ***2.14. Statistical analysis***

Data was tested using one-way analysis of variance (ANOVA) followed by the Tukey test in order to compare the mean values of different groups. Differences were considered to be statistically significant at  $p < 0.05$ ,  $p < 0.01$  or  $p < 0.001$  in all studies. Each value was obtained from triplicate samples from each case and expressed as the mean  $\pm$  standard deviation (SD), unless stated otherwise.

## **Chapter 3**

### **Characterisation of the effect of introducing supplementary lipids to DDA-TDB liposomes**

### ***3.1. Introduction: characterisation of liposomal delivery systems***

Liposomes have been widely shown to be effective vaccine delivery systems (e.g. Alison & Gregoriadis (1974); Kersten & Crommelin, 1995), in particular DDA-TDB, which as a vaccine adjuvant, has the ability to stimulate cell mediated immunity when combined with a novel mycobacterial fusion protein antigen for TB (Davidsen *et al*, 2005). However, the mechanisms of action in correlation with the systems characteristics have yet to be fully investigated. Therefore, the aim of this study was to further characterise DDA-TDB liposomes and also consider modifications of the systems by incorporating additional lipids of DPPC or DSPC given that it has previously been reported that cationic agents are toxic to cells due to induced cell membrane interactions, which can lead to the inhibition of cellular regulation and modification (Farhood *et al*, 1992; Fischer *et al*, 2003). Consequently, in the current study, the cationic lipid presence within DDA-TDB was investigated upon replacement of DDA content, whilst in another set of formulations, the DDA:TDB ratio remained fixed at the ratio previously optimised for effective vaccine adjuvanticity (Davidsen *et al*, 2005), with their combined level reduced in concentration upon substitution with additional lipids.

Liposomes are formed upon the introduction of lipids to an aqueous environment. However, when producing such vesicles, numerous variables must be taken into account and controlled. Hence, the characteristics of the formulations and any such variations that may affect the biological performance of these systems must be identified. The significance of managing key physicochemical properties for liposomal products has been acknowledged by the Food and Drug Administration (FDA), of which factors such as particle size, liposome structure, drug-lipid ratios, stability, extent of drug loading, in vitro

release rate, and phase transition temperatures, were highlighted as pivotal characterisation parameters for liposomal drug delivery systems (Janoff, 1999).

To be exploited as effective subunit vaccine delivery systems, the physicochemical characteristics of liposomes must be studied in detail and correlated with their effectiveness *in vivo*, in an attempt to elucidate key aspects controlling their efficacy. There are a range of widely used methods that can be employed to study and characterise liposomes and within this study the following characteristics were considered:

- Dynamic light scattering was used to determine particle size and zeta potential, as these are major factors that can greatly influence the ability of liposomal carrier systems and their capacity to bind antigen.
- Morphological analysis was undertaken by transmission electron microscopy.
- Antigen adsorption was assessed via the BCA assay for the quantification of non-adsorbed protein, together with SDS-PAGE analysis, which allowed for visual evaluation and quantification of liposome associated protein.
- Interactions of the liposomal systems with serum proteins and the modelling of release rates in physiological conditions were examined, to ascertain the potential of the proposed formulations as immunoadjuvants.

The main adjuvant formulation consisted of DDA liposomes that incorporated TDB at 11 mol%, remaining locked at a 8:1 molar ratio for DDA:TDB (equivalent to a 5:1 weight ratio), as previous studies by Davidsen *et al* (2005), have shown that this ratio is most

beneficial to DDA liposomes in terms of alleviating their physical instability, whilst also eliciting strong Th1 type antibody and cytokine responses.

### ***3.2. Characterisation of liposomes composed of DDA and TDB***

To consider the characteristics of DDA-TDB liposomes a range of parameters were investigated and the effect of their formulation was considered.

#### *3.2.1. The effect of buffers on the cationic liposome characteristics*

Buffer solutions are expansively utilised in the field of drug delivery to control the pH of aqueous solutions and attain the greatest stability required to optimise physiological performance. The pH of blood is sustained at approximately 7.4 by primary and secondary buffer constituents located in the plasma and erythrocytes respectively (Florence & Attwood, 1998). Initial studies were conducted to examine the effect of buffer used to hydrate the lipid film in the production of DDA-TDB liposomes. Tris buffer (10 mM) was selected as it is commonly used as a pH buffer, due to easily dissolving in water and remaining stable in solution for many months (Leonard, 2010). However, Tris buffer is non-isotonic and therefore, isotonic solutions of Dextrose (5% w/v in water) and phosphate buffered saline (PBS) were also investigated for their effect upon rehydration of the dry lipid films, with the resultant liposomes characterised for their particle size and zeta potential.

DDA-TDB liposomes formulated in either Tris buffer or 5% Dextrose were approximately 500 nm, displaying no significant difference between one another (Figure 3.1). However, for DDA-TDB prepared in PBS, significantly larger vesicles ( $P < 0.01$ ) were produced, in

the region of three micrometres, with typically heterogeneous liposomal populations expressed for all the systems as the polydispersity ranged between 0.31-0.43 (Figure 3.1). No significant differences between the zeta potentials of the systems prepared in Tris buffer, Dextrose or PBS were observed, with a recorded zeta potential of 45-50 mV (Figure 3.1). The observed particle sizes also generally correlated to the visual appearance of the systems which were comparably clear for DDA-TDB prepared in Tris or 5% Dextrose buffer, whilst hydration of the lipid film in PBS produced a cloudy, turbid appearance (Figure 3.1).

Although the use of 5% Dextrose buffer resulted in the production of sub-micrometre sized liposomes, this buffer was disregarded for its future use due to the weak long term stability of sugars in solution. In addition, vesicles prepared in PBS were subject to salt induced aggregation, as saline based buffers contain neutralising counter ions that ultimately minimise the repulsion forces between neighbouring particles (Yan & Huang, 2009). This effect has been shown to be immunologically beneficial, as a cationic liposomal vaccine delivery system was enhanced in terms of Th1 and Th2 type immunity, with such a salt-induced effect interfering with the electrostatic interaction between the cationic carrier system and the protein antigen, promoting antigen release and the activation of APCs (Yan & Huang, 2009). However, with the importance of long term stability of the pharmaceutical product, the immediate physical instability displayed in the liposomal system prepared in PBS prevents the use of this buffer. Therefore, Tris buffer was selected as the hydration medium for future preparations of the immunoadjuvants, and will require adjustment to make the buffer isotonic for future liposomal application *in vivo*.

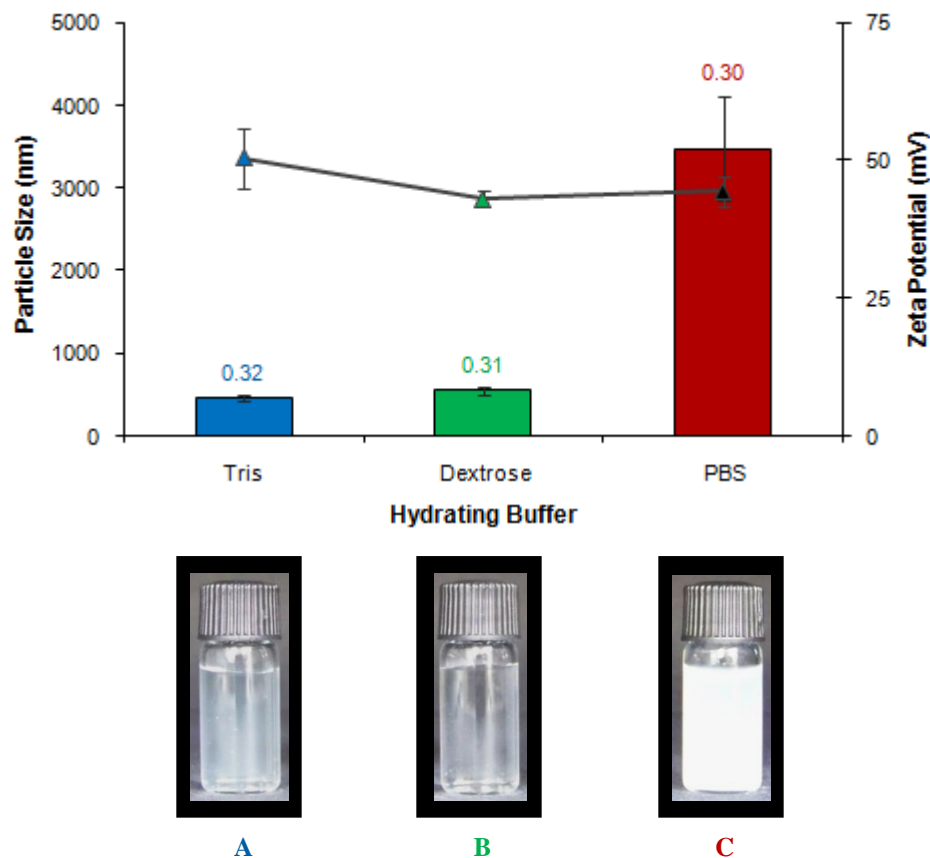


**Figure 3.1.** The effect of hydrating medium during liposome production characterised for particle size, polydispersity and zeta potential, together with visual observations of liposomes prepared in **A: Tris buffer**, **B: 5% Dextrose** and **C: PBS**. Samples were suspended in a 1/10 dilution of the corresponding buffer for the DLS measurements. Results represent the mean average and standard deviation from at least three independent experiments.

### 3.2.2. The effect of buffer concentration upon the measured zeta potential

Prior to further characterisation of the proposed systems in the selected buffer, the effect of Tris buffer and PBS concentration on the zeta potential of DDA-TDB vesicles was measured. Studies by Perrie & Gregoriadis, (2000) had previously established a working dilution of 1 in 10 for measuring the zeta potential of cationic liposomes. This was due to the equipment available at such time being unable to analyse the zeta potential of samples in undiluted PBS. However, to investigate the effect of buffer concentration on the zeta potential of DDA-TDB vesicles measured with the Brookhaven ZetaPlus instrument, and

to decide upon an appropriate dilution for the suspension of liposome samples when taking future measurements, Tris buffer and PBS was serially diluted to a range of concentrations for measurements of zeta potential. This took place in ddH<sub>2</sub>O (0), pure buffer and buffer diluted to the ratios of 1/10, 1/100, 1/1000 and 1/10,000, with all dilutions (v/v) made with ddH<sub>2</sub>O.

The measured zeta potential of DDA-TDB liposomes suspended in ddH<sub>2</sub>O was 33.1 mV (+/- 2.7) with DDA-TDB suspended in Tris buffer dilutions of 1/10,000 (0.001 mM), 1/1000 (0.01 mM) and 1/100 (0.1 mM) significantly ( $P < 0.05$ ) increasing the zeta potential to within the region of 40 mV (Figure 3.2 A). Furthermore, the zeta potential of the liposomes in 1/10 Tris (1 mM) and pure Tris buffer (10 mM) was significantly ( $P < 0.001$ ) increased further to 54.6 mV (+/- 4.4) and 56.0 mV (+/- 5.3) respectively, showing no significant difference between one another (Figure 3.2 A). The general trend apparent was that as the electrolyte concentration in the media in which the liposome sample was suspended in became more concentrated, closer to Tris buffer in its pure form, the resulting zeta potential measurements increased (Figure 3.2 A). Indeed, an increased zeta potential infers electrostatic stability of the colloidal suspension, resulting in mobile and charged particles, and as the zeta potential is determined from mobility (Brookhaven Instruments Corporation, 2010a), the rise in the zeta potential measured in the present study upon increased Tris buffer concentrations suggests an increased sample mobility, with elevated electrostatic repulsion forces present between the charged particles.

Contrastingly, dilutions of PBS demonstrated an opposing influence on the zeta potential of DDA-TDB, with the zeta potential decreasing when measured in stronger

concentrations of PBS (Figure 3.2 B). This was apparent as the recorded zeta potentials in ddH<sub>2</sub>O, 1/10,000, 1/1000 and 1/100 PBS generated a strong cationic zeta potential for DDA-TDB of between 50-60 mV (Figure 3.2 B). However, at a 1/10 dilution of PBS (1 mM), the measured zeta potential of DDA-TDB was significantly ( $P < 0.05$ ) reduced to 45.5 mV (+/- 2.6), followed by a further significant ( $P < 0.05$ ) reduction to 28.7 mV (+/- 2.5) when suspended in PBS (10 mM) (Figure 3.2 B), which was approximately half of the recorded zeta potential of DDA-TDB measured in ddH<sub>2</sub>O. The higher concentrations of PBS in turn increases the salt concentration of the liposomal suspension, with such conditions known to reduce the measured zeta potential (Brookhaven Instruments Corporation, 2010b), and the increased presence of phosphate ions may possibly be masking the determined zeta potential, reducing the electrostatic repulsion forces and mobility present between particles of the suspensions measured at the lower PBS concentrations.

With the variability displayed in the resultant zeta potential of DDA-TDB vesicles suspended in different buffer concentrations, there was a necessity to standardise the concentration in which DDA-TDB based liposomes were suspended in for subsequent characterisation. With Tris being the buffer of choice at 10 mM when rehydrating DDA-TDB vesicles and with no apparent difference between measurements made in pure Tris buffer (10 mM) and in the 1/10 dilution of Tris buffer (1 mM), for the future characterisation of particle size and zeta potential of the proposed DDA-TDB based systems, 1 mM Tris buffer was chosen as the concentration to suspend the liposome samples in for the DLS measurements using the Brookhaven ZetaPlus instrument.

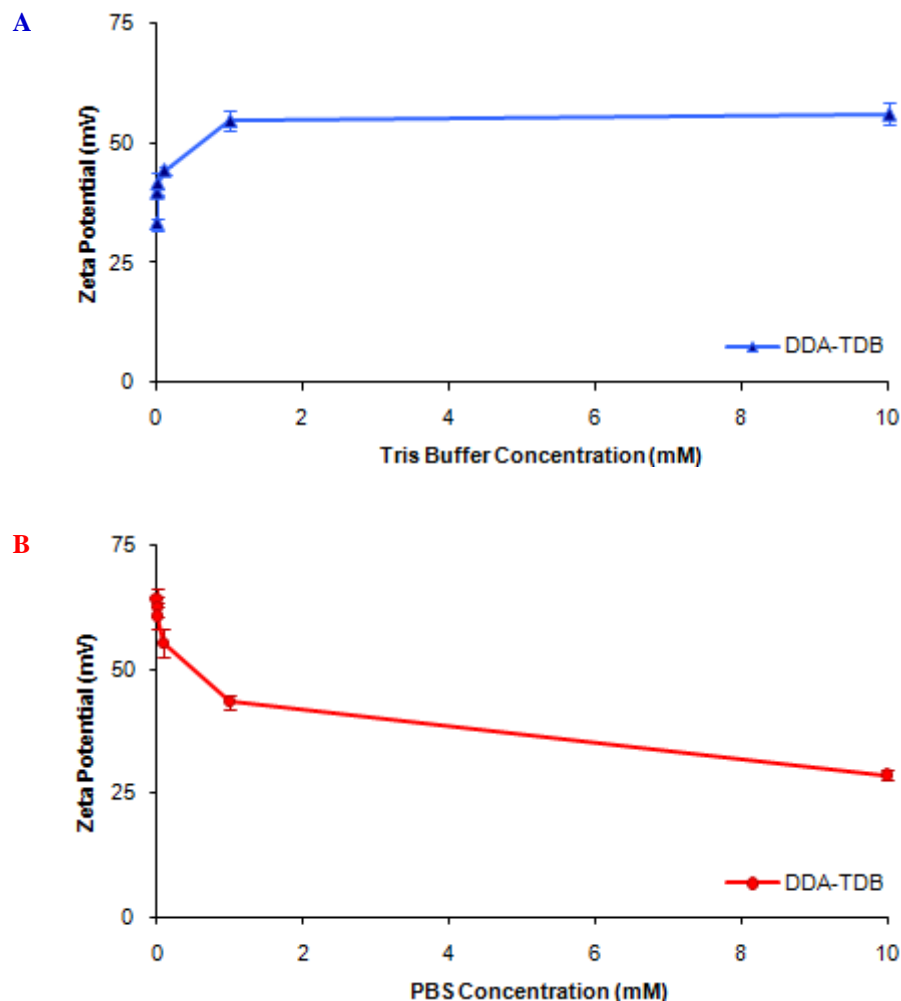


**Figure 3.2. The effect of Tris buffer or PBS concentration on the measurement of zeta potential for DDA-TDB liposomes.** All vesicles were prepared in their corresponding buffer and serially diluted in **A: Tris buffer** or **B: PBS**. Dilutions were made with ddH<sub>2</sub>O and samples were tested in undiluted buffer and buffer diluted to 1/10, 1/100, 1/1,000 and 1/10,000 respectively. Results displayed are the mean average of at least three independent experiments, with error bars representing the standard deviation from the mean.

### 3.3. Replacement of DDA within DDA-TDB with DPPC or DSPC lipid

To investigate the role of the cationic component within DDA-TDB, previously shown to be an effective adjuvant system (Davidsen *et al*, 2005; Agger *et al*, 2008; Christensen *et al*, 2010), a series of formulations were prepared in which DDA was proportionally replaced with either DPPC or DSPC lipid, with the volume of TDB remaining fixed within the formulation (Table 3.1).

**Table 3.1. The replacement of DDA within DDA-TDB with DPPC or DSPC lipid.** The volume of TDB remained fixed at 50 µg per dose in all proposed formulations. The values of weight (µg) for DDA, DPPC or DSPC lipid and TDB for each formulation are stated as per dose (200 µl Tris buffer).

Formulation	DDA (µg/dose)	DPPC or DSPC (µg/dose)	TDB (µg/dose)
DDA-TDB	250	0	50
DDA/LIPID/TDB	150	100	50
DDA/LIPID/TDB	50	200	50
DDA/LIPID/TDB	25	225	50
DPPC-TDB or DSPC-TDB	0	250	50

These proposed systems in which DDA was replaced within DDA-TDB were firstly characterised for their particle size and zeta potential. DDA-TDB displayed an average particle size of ~500 nm, a polydispersity in the region of 0.3 and a cationic zeta potential of 50 mV (Figure 3.3), which was in good agreement with previous characterisation data (Davidsen *et al*, 2005; Christensen *et al*, 2007a; Henriksen-Lacey *et al*, 2010b).

Cationic replacement of DDA-TDB, with either DPPC or DSPC lipid, generated 500-600 nm sized vesicles when DDA was still present within the formulation (Figure 3.3). In contrast, upon complete DDA replacement, DPPC-TDB and DSPC-TDB liposomes were significantly ( $P < 0.05$ ) larger in size than the DDA based systems, in the region of two micrometres (Figure 3.3). The polydispersity of all of the empty vesicle systems was

consistently in the proximity of 0.3, suggesting a characteristic heterogeneous liposomal population (Vangala *et al*, 2007).

The measured zeta potential was approximately 50 mV for all of the formulations that contained DDA, coinciding with a sub-micrometre particle size (Figure 3.3). However, DPPC-TDB and DSPC-TDB liposomes were significantly ( $P < 0.05$ ) reduced to a slightly neutral to anionic zeta potential in the region of -20 mV (Figure 3.3). Additionally, no significant difference was apparent between the formulations when either DPPC or DSPC lipid was used as the replacing lipid within DDA-TDB.

In addition, coinciding with the particle size data attained, notable turbidity of the larger DPPC-TDB and DSPC-TDB liposomes was evident. This was particularly observed in comparison to the significantly smaller sized and comparatively clearer systems in which DDA was still present within the formulation (Figure 3.3).

The impact of DDA upon the zeta potential was evident as removal of the cationic component ultimately diminished the positive charge of the formulation, which is vital to facilitating the surface adsorption of many anionic subunit proteins. Surface properties have an immense effect upon the rate, degree, and the mechanism of protein adsorption, with a net negative charge of proteins having an increased tendency to adsorb to cationic surfaces (Brash & Horbett, 1995).

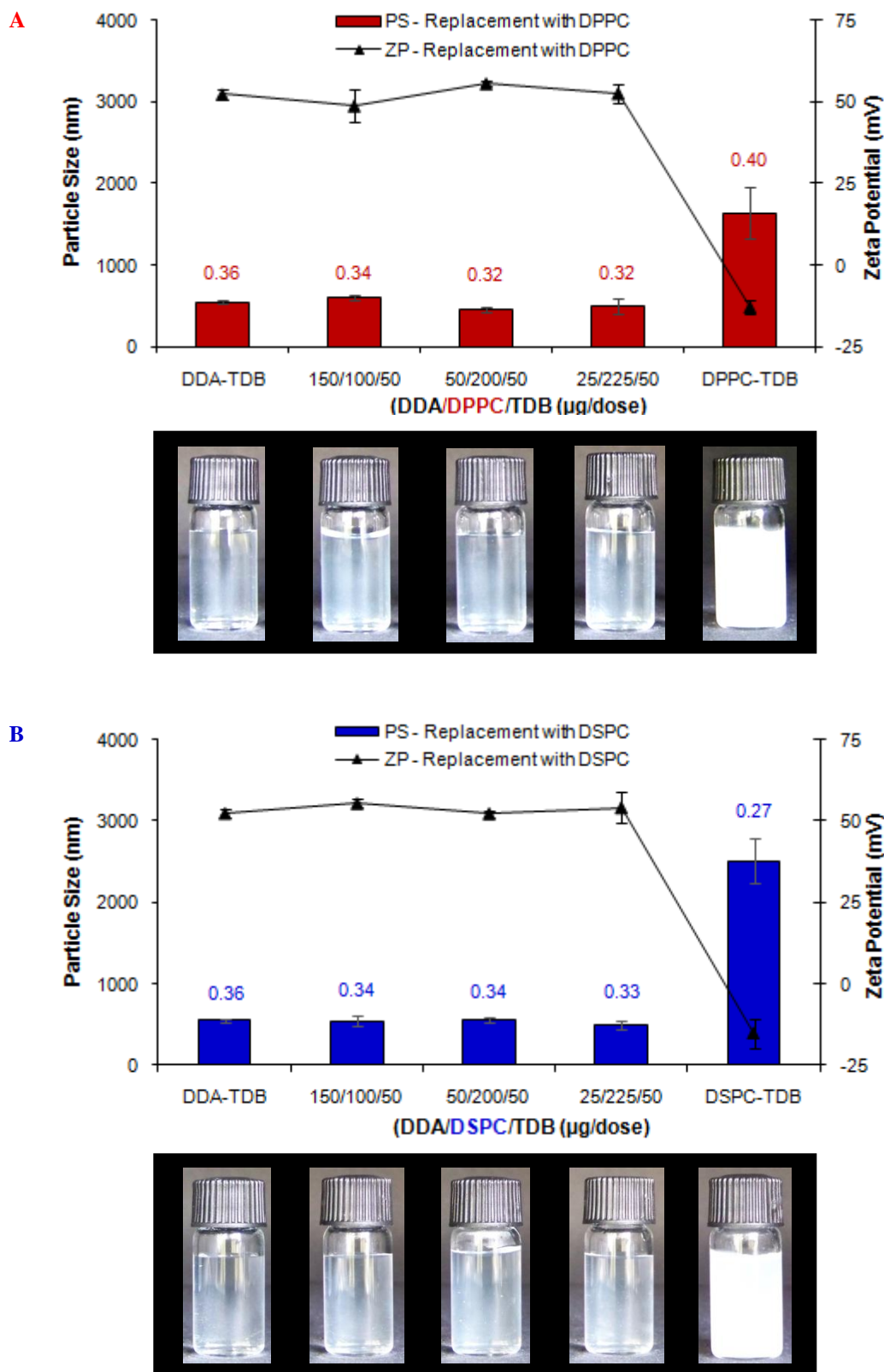


Figure 3.3. Replacement of DDA within DDA-TDB characterised for particle size, polydispersity and zeta potential, together with visual observations with **A: DPPC** or **B: DSPC**. Vesicles were produced by lipid hydration in Tris buffer (10 mM, pH 7.4). Results represent the mean  $\pm$  SE from three experiments.

Previous studies by Filion & Phillips, (1997) employed a similar experimental approach with the incorporation of DPPC lipid to a cationic dioleoylphosphatidylethanolamine-dioleoyldiacyltrimethylammonium propane (DOPE-DOTAP) system, taking place in the replacement of DOPE content. DOTAP provided a net cationic charge to the system and in terms of the measured zeta potential, increased incorporation of DPPC to the cationic liposomes prepared in 0.85% w/v sodium chloride (NaCl), retained a cationic zeta potential of over 40 mV. This trend of increasing the introduction of a neutral lipid to a cationic liposomal formulation, whilst maintaining the cationic properties of the multi-lipid system, coincides with the consequent findings for the measured zeta potential in this present study. Indeed as DDA content within the main DDA-TDB formulation was reduced, no significant change in the measured zeta potential was observed, until complete cationic replacement occurred with DPPC or DSPC lipid.

The incorporation of zwitterionic lipids in the replacement of DDA demonstrates potential in favourably reducing the toxicity of the DDA-TDB liposomes. This may be conducted whilst maintaining the ability to electrostatically surface adsorb protein antigen, and induce antigen specific immune responses, upon administration of the proposed adjuvants.

#### ***3.4. Substituting DDA-TDB with DPPC or DSPC lipid***

Alongside the assessment of replacing cationic content within DDA-TDB, to further understand the role of DDA and TDB within the adjuvant system, another set of formulations were assessed. More specifically, formulations substituting DDA-TDB with DPPC or DSPC lipid, at the ratios of 25, 50 and 75 mol%, were prepared and characterised.

### *3.4.1. The effect of buffer upon DDA-TDB substituted with additional lipids*

Initial tests were conducted to investigate the effect of buffer upon the formation of DDA-TDB based liposomes. Incorporation of DDA-TDB with DPPC or DSPC lipid at 25, 50 and 75 mol% took place with Tris buffer or PBS used as the hydrating medium. These systems were directly compared to one another in terms of particle size and zeta potential, to establish whether the incorporation of zwitterionic lipids could stabilise the formulations and possibly prevent the aggregating effect seen previously when PBS was used as the hydrating medium in the preparation of DDA-TDB.

The particle size of DDA-TDB in Tris buffer prior to substitution was ~500 nm as previously characterised in this study. Substitution of DDA-TDB in Tris buffer with either DPPC or DSPC at 25, 50 and 75 mol%, whilst retaining a mean sub-micrometre particle size, generated a significant ( $P < 0.05$ ) increase in vesicle size from DDA-TDB, measured between to 650-800 nm (Figure 3.4). However, substitution with DPPC or DSPC at 25-75 mol% displayed no significant change in the resultant zeta potential of the DDA-TDB based liposomes, remaining strongly cationic in the region of 50 mV when prepared in Tris buffer (Figure 3.4).

In contrast, all equivalent DDA-TDB systems incorporating 25-75 mol% DPPC or DSPC in PBS demonstrated a significant ( $P < 0.001$ ) increase in mean vesicle size from a sub-micrometre size range in Tris buffer to 2-3000 nm when prepared in PBS (Figure 3.4). Upon incorporation of DPPC or DSPC at 25-75 mol%, no significant difference in the zeta potential was apparent between all of the systems regardless of the substituting lipid used, ranging between 45-55 mV, which was comparable to the equivalent systems in Tris

buffer (Figure 3.4 A and B). The polydispersity expressed for all systems was in the proximity of 0.3, regardless of the hydrating medium or the level of DDA-TDB substitution (Figure 3.4 A and B).

The introduction of additional lipids, at a variety of mol% ratios, failed to prevent an instantaneous increase in vesicle size, as observed with DDA-TDB liposomes in PBS. The differences between the two tested buffers, particularly in terms of particle size, is evident when visually comparing the formulations upon incorporation of DPPC or DSPC, with turbidity visible in all formulations prepared in PBS, opposing the clarity of the equivalent Tris buffer samples (Figures 3.4 A and B). Although a strong cationic zeta potential was observed, the significantly larger vesicle sizes indicate possible aggregation and instantaneous physical instability upon formation in PBS, resulting in the selection of Tris buffer as the hydration medium of choice, to be used for the production of all subsequent liposomal formulations. Indeed, the impact on particle size observed upon preparation of vesicles in PBS may be attributed to salt induced aggregation, as with cationic liposome suspensions, aggregation may arise upon a reduction in electrostatic repulsions between particles as a result of neutralising counterions associating to charged lipid surfaces, with resultant clustered populations dictated by the ionic strength (Bordi & Cametti, 2002).

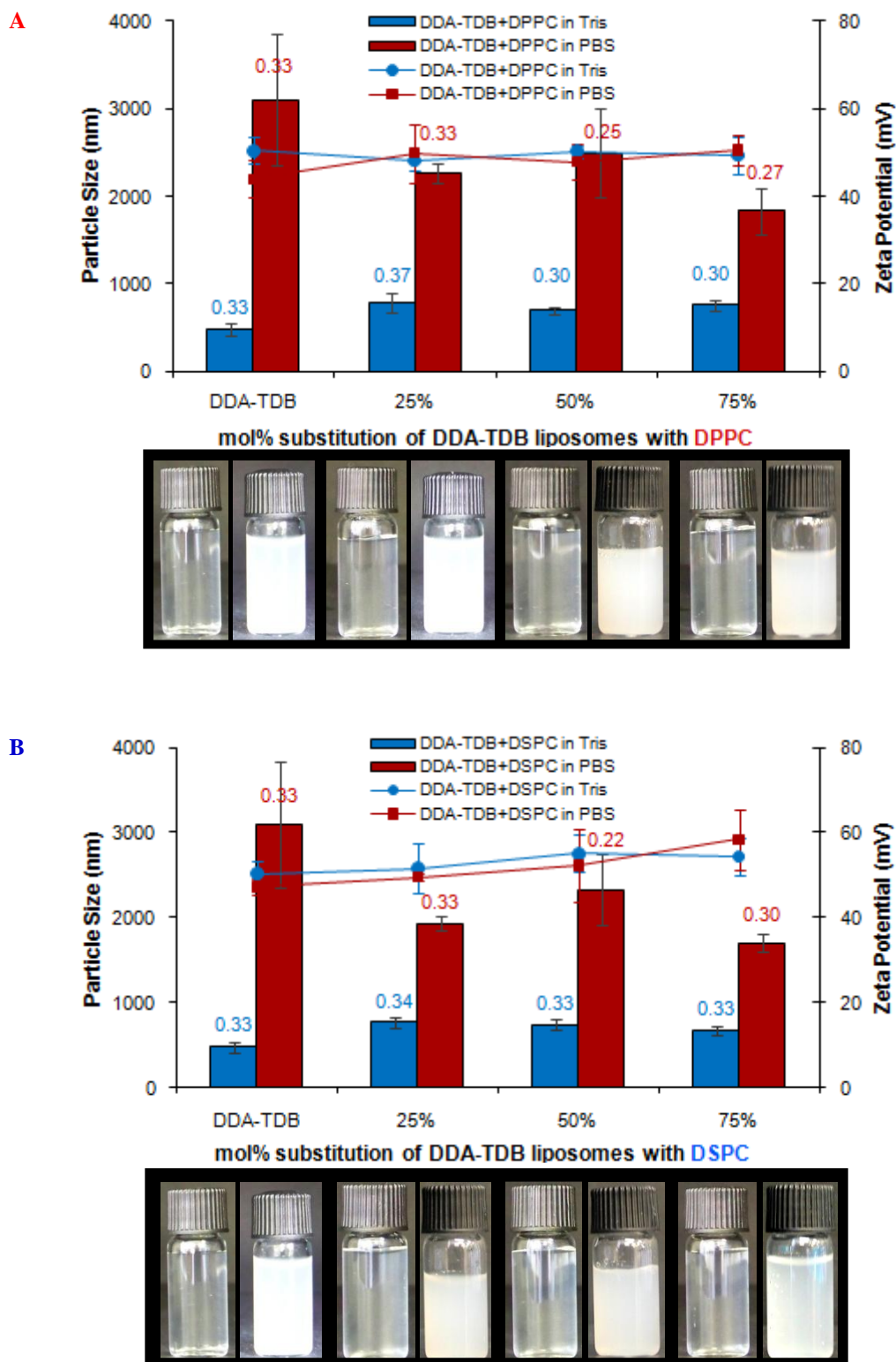


Figure 3.4. The effect of Tris buffer vs. PBS (10 mM, pH 7.4) in the hydration of DDA-TDB substituted with **A: DPPC** or **B: DSPC** and characterised for particle size, polydispersity and zeta potential with corresponding sample images. Each photo on the left was prepared in Tris buffer with liposomes prepared in PBS on the right hand side. Results represent the mean  $\pm$  SD of three experiments.

### 3.4.2. Stability of DDA-TDB liposomes substituted with additional lipids

#### 3.4.2.1. DDA-TDB based formulations incorporating DPPC

Whilst DDA-TDB liposomes provide a cationic charge ideal for antigen absorption, there may be issues of long term stability with such a combination (Davidsen *et al*, 2005). Furthermore, with a vast array of literature highlighting the potential of liposomal drug delivery, a lack of liposome based vaccines currently available could possibly be due to their weak physical stability in solution (Mohammed *et al*, 2010). The addition of zwitterionic lipids such as DPPC or DSPC may retain the stability of DDA-TDB whilst being biocompatible and desirably less toxic. As a result, DDA-TDB substituted with 0-75 mol% DPPC or DSPC was measured over 28 days, at the storage temperatures of 4 °C and 25 °C.

DDA-TDB liposomes in Tris buffer were ~500 nm in particle size with a cationic zeta potential of approximately 65 mV, which was sustained over 28 days in both storage conditions (Figure 3.5). Upon DPPC incorporation at a 25, 50 and 75 mol% ratio to DDA-TDB, the average vesicle size had risen significantly ( $P < 0.05$ ) on day 0 to 650-800 nm, however no significant difference to DDA-TDB was observed in the measured zeta potential, as a strong cationic charge was consistently maintained, inferring a stable vesicle formulation (Figure 3.5). This remained the case for the duration of the 28 days, with no significant difference observed between all of the various substituted ratios analysed at 4 °C and 25 °C (Figure 3.5). The polydispersity for all of the tested systems remained in the region of 0.3.

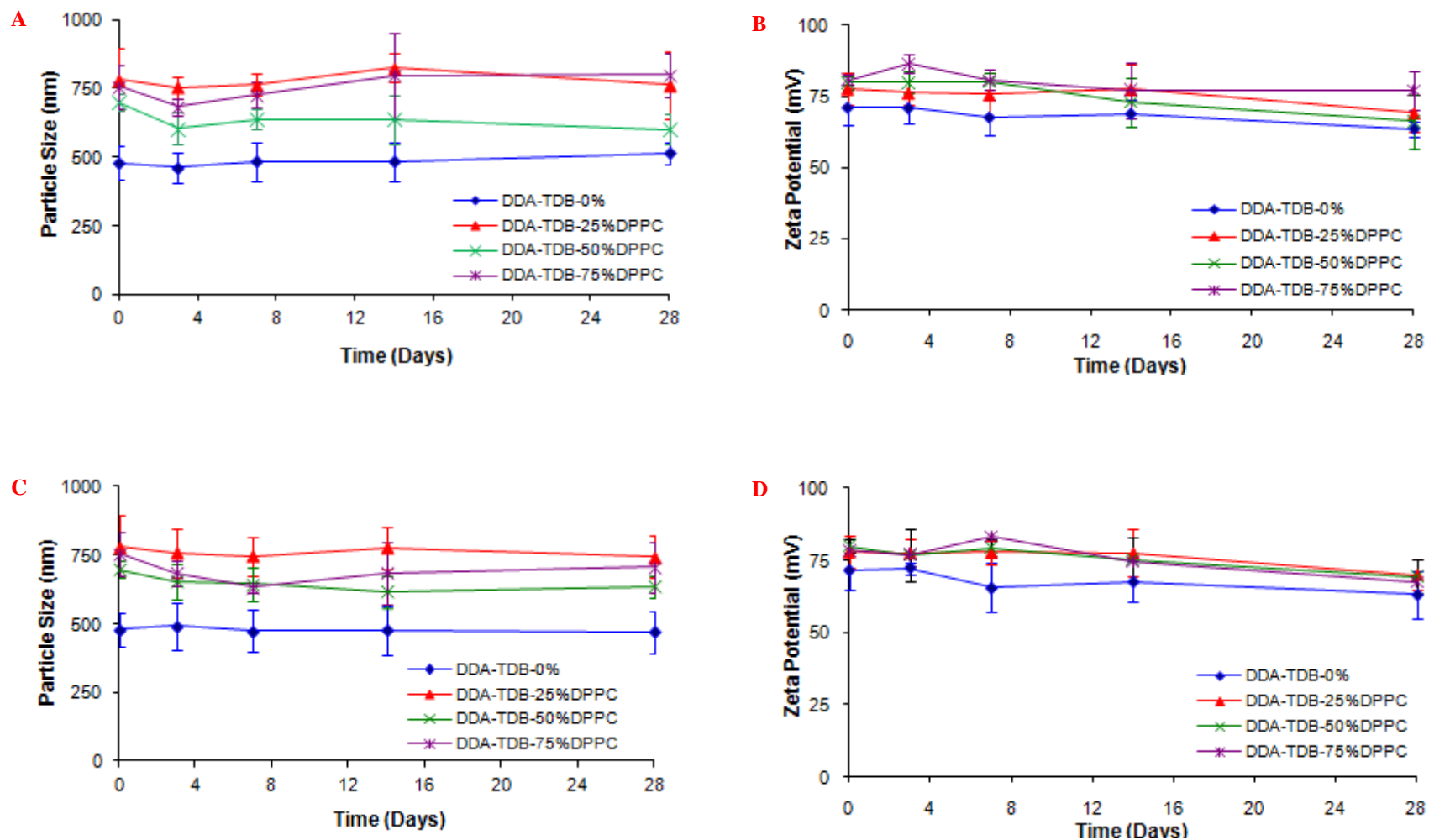


Figure 3.5. Time development of particle size and zeta potential for DDA-TDB and its substitution with 25-75 mol% DPPC stored at 4 °C (A & B) and at 25 °C (C & D). All formulations were produced by lipid hydration in Tris buffer (10 mM, pH 7.4). Results shown are the mean and standard deviation of three independent experiments.

#### 3.4.2.2. DDA-TDB based formulations incorporating DSPC

Upon substitution with DSPC at 25-75 mol%, the resultant liposomes were 650-800 nm, which represented a significant increase ( $P < 0.05$ ) from DDA-TDB, yet generated a comparably strong cationic zeta potential of ~65 mV and a polydispersity in the region of 0.3, which was maintained throughout the study, displaying no significant difference between the varying levels of DSPC incorporation over 28 days at 4 °C and 25 °C (Figure 3.6). Figure 3.7 visually demonstrates the clarity in all the tested formulations, with no apparent difference between samples at day 0 or day 28 when kept at 25 °C (with no observed difference to the corresponding samples stored at 4 °C).

Overall, DDA-TDB remained stable over 28 days, as shown by Davidsen *et al*, (2005), and such stability was also retained in the present study for both sets of formulations in which DPPC or DSPC was substituted into DDA-TDB, with no significant difference displayed between these systems. The consistently retained strong cationic charge when either lipid was incorporated into DDA-TDB confers stability of the systems, as it is understood that with a higher zeta potential, a suspension is more likely to remain stable as the charged particles possess greater repulsion forces against one another, ultimately overcoming a natural propensity to aggregate (Brookhaven Instruments Corporation, 2004). Furthermore, as no difference was observed between DDA-TDB and its substitution with either lipid, the stabilising effect of TDB can be seen to be maintained, with trehalose possibly acting as a steric barrier inhibiting fusion between vesicles (Spargo *et al*, 1991), preventing particle aggregation. The retention of physical stability reiterates the use of TDB in the proposed adjuvants and the lack of difference between DDA-TDB and its substitution suggests that DPPC or DSPC slots into the liposomal system.

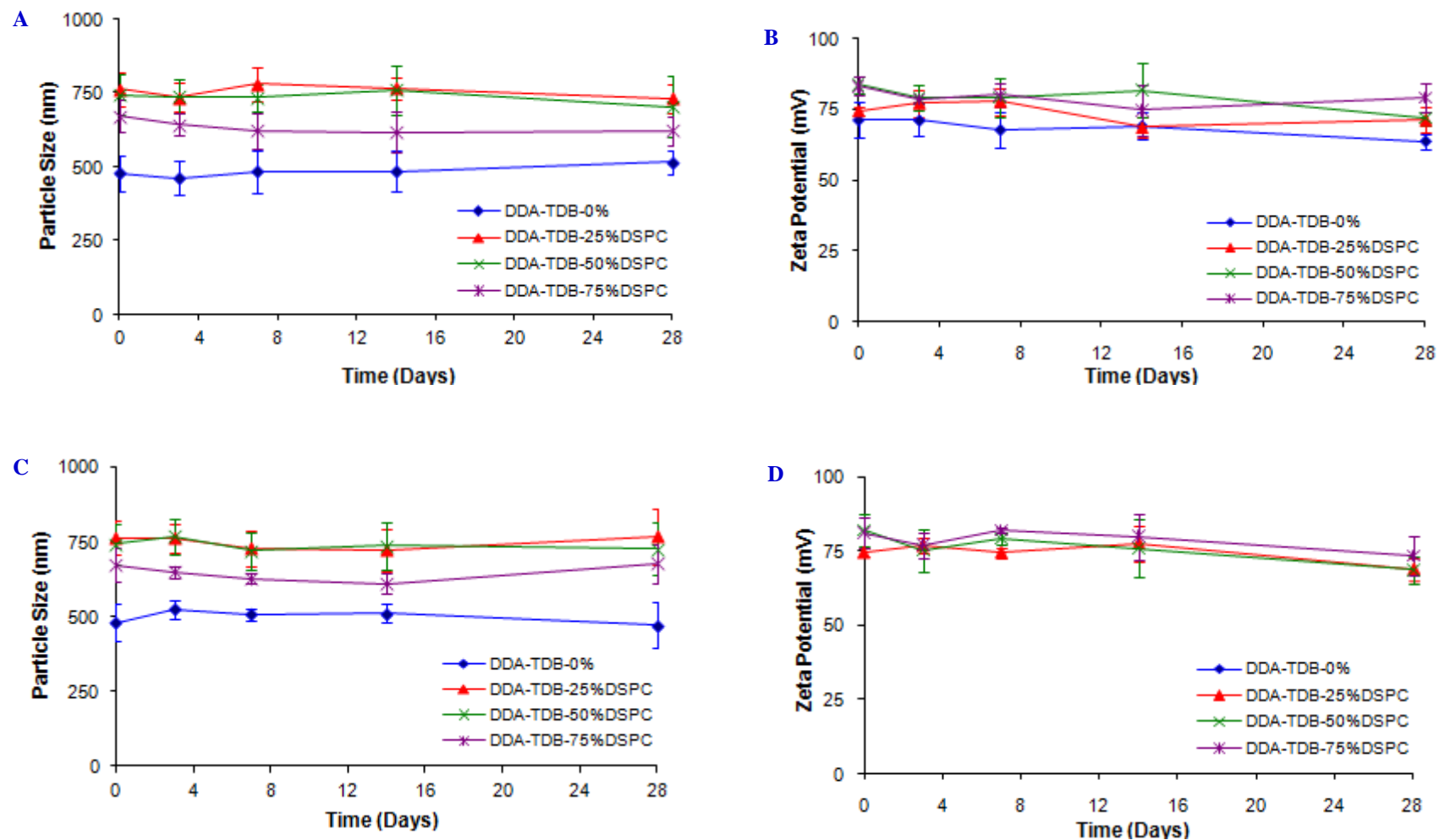


Figure 3.6. Time development of particle size and zeta potential for DDA-TDB and its substitution with 25-75 mol% DSPC stored at 4 °C (A & B) and at 25 °C (C & D). All formulations were produced by lipid hydration in Tris buffer (10 mM, pH 7.4). Results shown are the mean and standard deviation of three independent experiments.

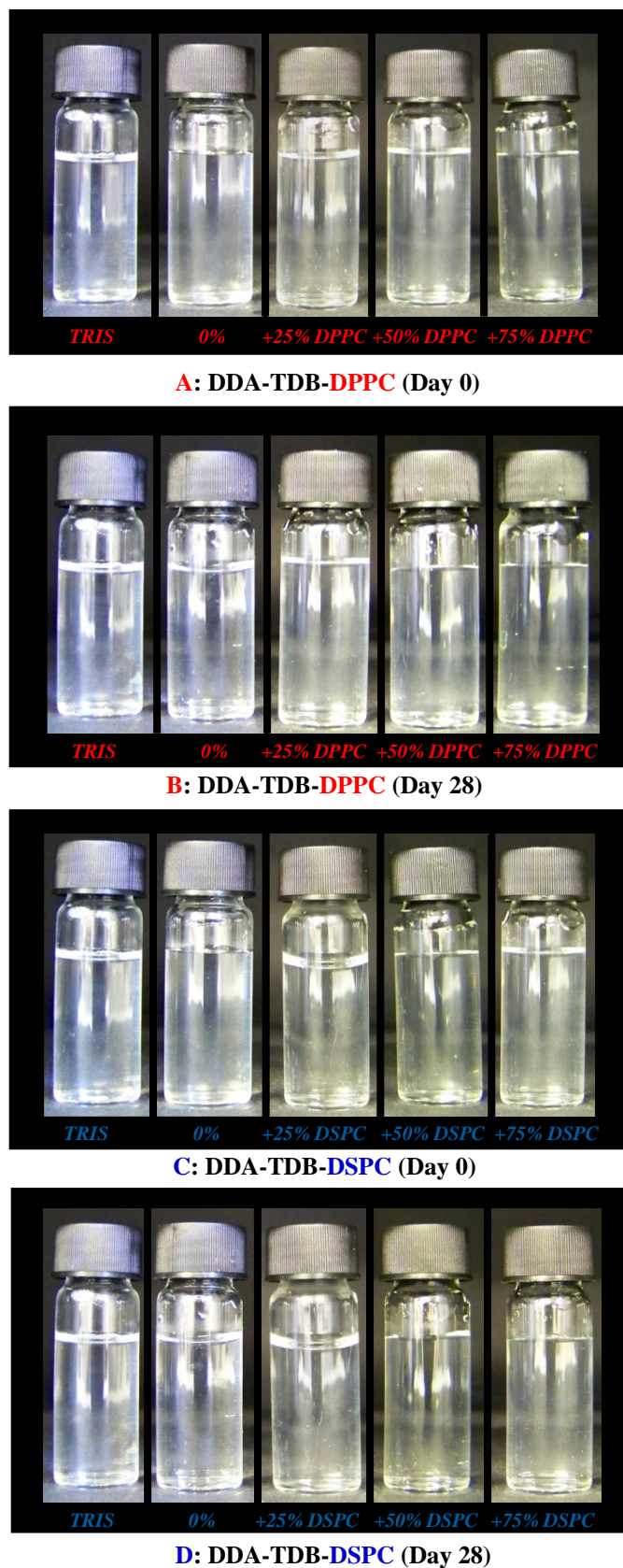


Figure 3.7. Images of DDA-TDB in Tris buffer and its substitution at 25-75 mol% with **DPPC** at **A**: day 0 and **B**: day 28 or with **DSPC** at **C**: day 0 and **D**: day 28, stored at 25 °C.

### ***3.5. Morphological analysis of DDA-TDB based liposomes***

Microscopic analysis was conducted via TEM in order to examine the general structures of the liposomal systems. As there can be a possible over dependence on physicochemical analytical techniques such as particle sizing via laser diffraction, the application of microscopic imaging analysis can confirm the structural integrity of the liposomes produced, a process often disregarded during characterisation (Bibi *et al*, 2011).

#### *3.5.1. TEM of DDA-TDB upon cationic replacement with additional lipids*

Initial analysis was conducted upon DDA-TDB partially replaced with DPPC or DSPC at 150/100/50 µg/dose, or completely replaced producing DPPC-TDB and DSPC-TDB liposomes. It was observed that upon partial DDA replacement with either lipid, minimal differences between the two sets of formulations were apparent, producing spherical vesicles within a broad size range (Figure 3.8 A & B). With DDA still present in the lipid mixture of these selected formulations, the imaged vesicles corroborated with the characterisation data previously attained for the liposomes via DLS, with populations predominantly under a micrometre in particle size (Figure 3.8 A & B).

Contrastingly, DPPC-TDB and DSPC-TDB liposomes were substantially larger than the systems containing DDA (Figure 3.8 C & D). Although spherical structures indicative of liposome formation was evident, these vesicles were beyond a micrometre in particle size, in good agreement with corresponding analysis determined via DLS. Additionally, these liposomes, characterised in the present study for attaining a slightly anionic zeta potential, were less isolated than the other cationic formulations, remaining in closer proximity to one another, suggesting a susceptibility to aggregate (Figure 3.8 C & D).

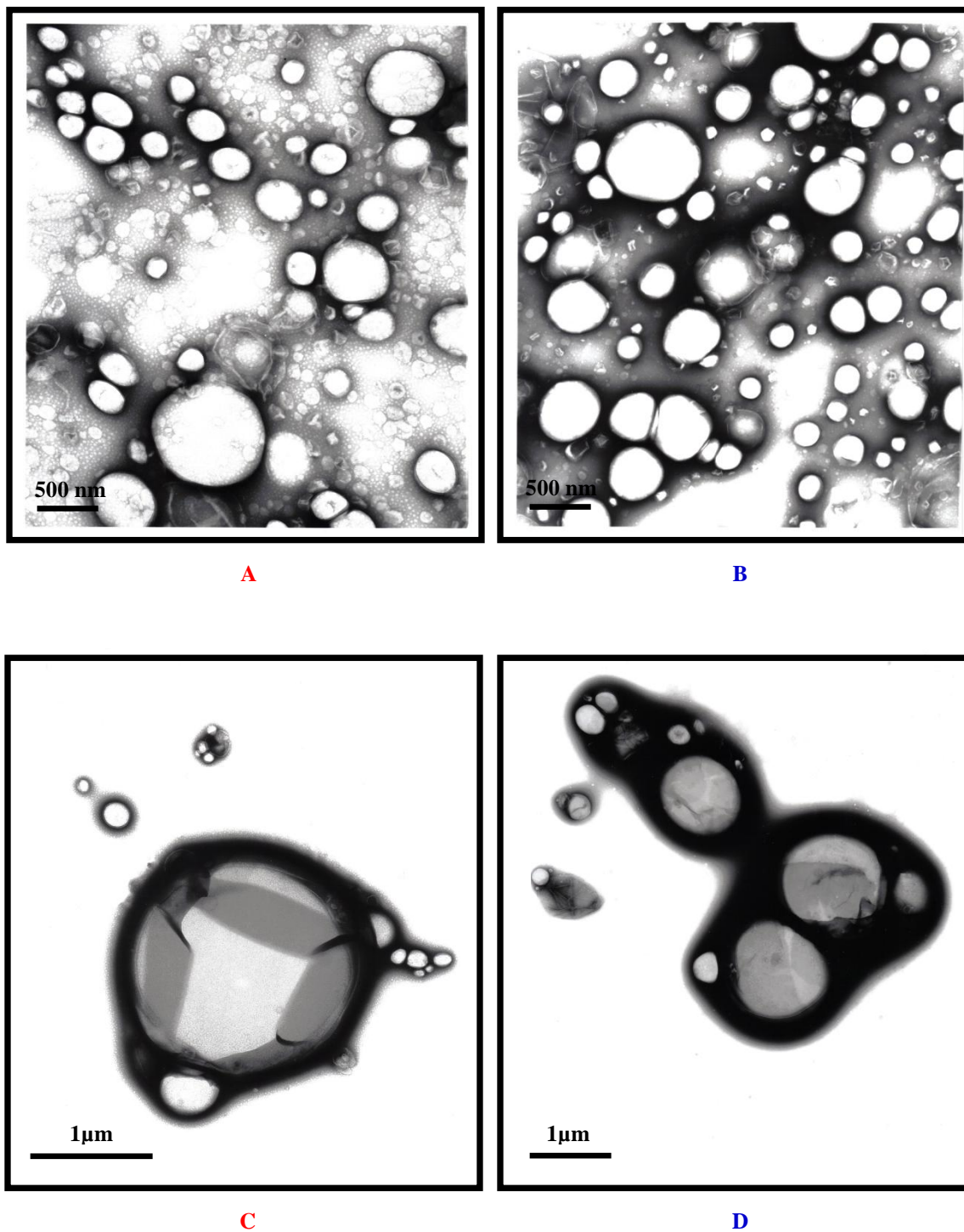


**Figure 3.8.** TEM micrographs of DDA-TDB replaced with either **DPPC** or **DSPC** lipid. Images represent the replacement of DDA within DDA-TDB liposomes that occurred partially with **A**: DDA-**DPPC**-TDB and **B**: DDA-**DSPC**-TDB (at 150/100/50 μg/dose) or totally with **C**: **DPPC**-TDB and **D**: **DSPC**-TDB. All formulations were prepared in Tris buffer and produced by the method of lipid hydration.

### 3.5.2. TEM of DDA-TDB and its substitution with additional lipids

DDA-TDB liposomes and its substitution with either DPPC or DSPC lipid at 50 mol% was also analysed (Figure 3.9 A-C). DDA-TDB was found to generate consistent formations of spherical vesicles with no apparent aggregation observed (Figure 3.9 A). It can be presumed that the larger hydrophilic trehalose head group of TDB escalates net hydration at the surface, which acts to minimise dehydration of the DDA head groups, thus reducing the effect of aggregation (Davidsen *et al*, 2005). The morphological features observed for DDA-TDB (Figure 3.9 A) are comparable to TEM imaging previously conducted for this cationic liposomal immunoadjuvant system (Davidsen *et al*, 2005; Vangala *et al*, 2007).

Upon substitution of the DDA-TDB formulation with either DPPC or DSPC, the additional lipids appeared to be successfully incorporated and were similar in vesicular appearance to that of DDA-TDB, with abundant formations of a spherical nature and minimal aggregation. The morphological analysis conducted also coincided with the previously determined particle size findings, displaying a polydisperse population of liposomes with the majority of vesicles remaining within a sub micrometre particle size range (Figure 3.9 B & C).

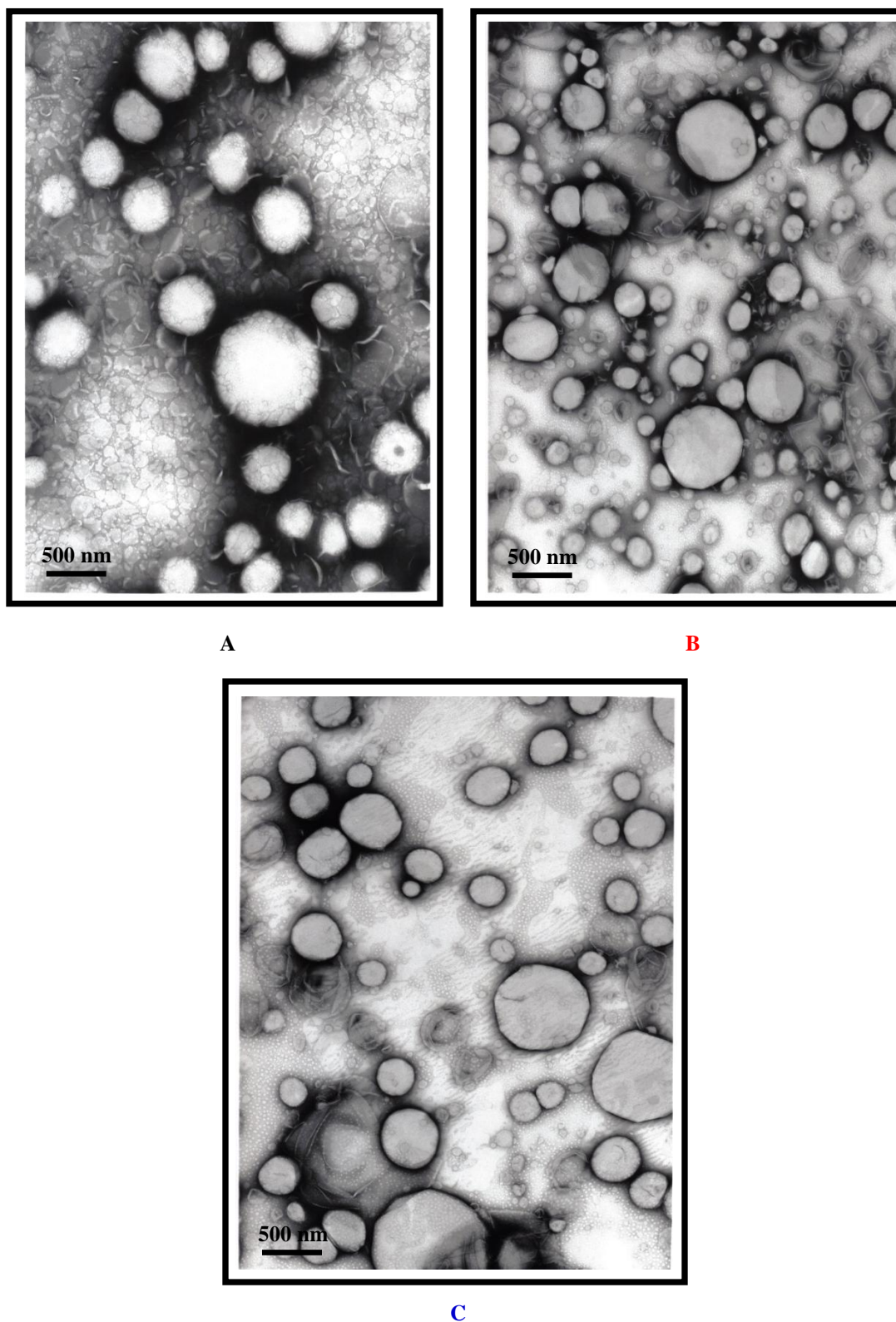


**Figure 3.9.** TEM micrographs of **A: DDA-TDB**, **B: DDA-TDB-50% DPPC** and **C: DDA-TDB-50% DSPC**. All formulations were prepared in Tris buffer and produced by the method of lipid hydration.

### ***3.6. Protein adsorption studies***

The ability of the proposed liposomal adjuvant systems to adsorb antigen was measured using ovalbumin (OVA) protein. OVA has a molecular weight of 45 kilodaltons (kDa) and an isoelectric point (pI) of 4.5, therefore carrying a net anionic charge at pH 7.4, facilitating electrostatic adsorption to the surfaces of cationic liposomes. Due to the great availability and low cost of OVA, it has been extensively utilised as a protein standard in an array of immunological studies (Huntington & Stein, 2001). Proficient liposomal delivery can be determined by the ability of the delivered protein to associate with liposomes, for example via surface adsorption. As a result, OVA was used to determine the loading characteristics of selected liposomal systems in Tris buffer, providing a protein model with a comparable molecular weight to the candidate antigen to be used in future immunological studies.

Furthermore, OVA was added to the liposomes at a wide range of concentrations, from 10 µg/ml to 1 mg/ml, potentially saturating the systems, to investigate the effect of protein adsorption upon the physicochemical properties of the liposomes. The selected liposomal systems, which represented cationic replacement and substitution of the DDA-TDB adjuvant, were measured for particle size, zeta potential and levels of protein adsorption. Subsequently, the interaction of the carrier systems with serum proteins was also assessed, whilst the potential *in vivo* preparations were examined for antigen retention/release over time in replicated physiological conditions, by dialysis of the liposomes adsorbed with radiolabelled OVA.

### ***3.6.1. Physicochemical characterisation of liposomal systems in dosage form***

#### *3.6.1.1. Liposomal interactions with serum proteins and OVA-I<sup>125</sup> release over time*

Upon administration, a delivery system will encounter an abundance of blood components such as blood cells and an array of serum proteins. Such interactions with particulate delivery systems, such as liposomal adjuvants, can affect their deposition (Opanasopit *et al*, 2002). Following on from the characterisation of the proposed DDA-TDB based carriers systems, these formulations, prepared by lipid hydration in Tris buffer, were suspended in the mediums of Tris buffer or 50% foetal bovine serum (FBS) and assessed for their stability and serum interactions in terms of particle size and zeta potential over 24 hours, and radiolabelled antigen retention/release over 72 hours via dialysis, all at 37 °C. The FBS media consisted of 50% FBS and 50% Tris buffer (v/v) as blood plasma represents ~50% of total blood volume, thus mimicking the physiological conditions that the liposomal immunoadjuvants may encounter upon injection.

Prior to the dialysis of the liposomal systems upon electrostatic adsorption of OVA-I<sup>125</sup>, as a control experiment, the release of OVA-I<sup>125</sup> alone was tested in Tris buffer and FBS/Tris over 72 hours, and the dialysis tubing was appropriately selected for OVA due to its well defined pore size (50-100,000 MW). The majority of OVA-I<sup>125</sup> was released as an initial burst with ~80% release, quantified by measured gamma counts in relation to the total, in both Tris buffer and FBS/Tris. Almost all of the OVA-I<sup>125</sup> was released after 4 hours in the absence of liposomes, with total clearance taking place at 72 hours (Figure 3.10). Additionally, minimal counts of the remaining sample in the dialysis tubing at the end of the experiment correlated to the total counts introduced at the beginning. These findings

validated the approach for subsequent experiments into the extent of radiolabelled antigen adsorption and retention over time.

Alongside the assessment of serum interactions, the liposomal systems were physicochemically characterised in Tris buffer upon antigen adsorption at 10 µg/ml. Liposomes of DDA-TDB, substitution with 50 mol% DPPC or DSPC and partial DDA replacement with DSPC at 150/100/50 µg/dose generated a sub micrometre particle size and a cationic zeta potential of 50 mV, whilst DSPC-TDB was 2 to 3 micrometres with an anionic zeta potential of approximately -20 mV (Figures 3.11: A, C, E, G and I). The addition of OVA at 10 µg/ml was not significantly different to the equivalent empty systems characterised earlier (see Figures 3.3 and 3.4). Furthermore, no fluctuations in particle size or zeta potential were apparent for each of the systems over 24 hours when placed in Tris buffer (Figures 3.11: A, C, E, G and I).

However, DDA-TDB exposed to FBS produced a particle size of ~2000 nm after 3 minutes (0.05 hours) and remained at 2-3 micrometres in the serum-induced environment over 24 hours, which was significantly ( $P < 0.01$ ) greater than DDA-TDB in Tris buffer. This indicated instantaneous serum binding to the cationic liposomes, coinciding with a significantly ( $P < 0.001$ ) reduced zeta potential, from a strongly cationic charge in Tris to approximately -25 mV in FBS (Figure 3.11 A). Corresponding antigen release was calculated using OVA radiolabelled with  $I^{125}$  and adsorbed to each liposomal formulation at 10 µg/ml. A vast majority of OVA- $I^{125}$  adsorbed to DDA-TDB remained associated to the vesicles in both Tris buffer and FBS/Tris, with OVA retention consistently maintained over the 72 hour time period (Figure 3.11 B). Calculated antigen release was ~5% after 3

minutes in Tris buffer and FBS/Tris, and this high level of antigen retention was sustained with an approximate 10% loss at 24 hours. Minor further losses were observed in the following 48 hours as antigen retention was ~85%, with no difference apparent between OVA release in the Tris and FBS/Tris environments (Figure 3.11 B).

Upon incorporation of DPPC or DSPC to DDA-TDB, at either 50 mol% substitution or partial DDA replacement with DSPC at 150/100/50 µg/dose, and exposure to FBS, no significant change in particle size took place until the first few hours, whereby a substantial rise in vesicle size occurred to beyond a micrometre (Figures 3.11: C, E and G). The elevated vesicle size was maintained over time with a further significant ( $P < 0.01$ ) increase to beyond 2 micrometres observed for the substituted DDA-TDB systems between 4 and 24 hours (Figures 3.11: C, E and G). All of the cationic systems in FBS were significantly ( $P < 0.01$ ) larger in particle size after 24 hours compared to the Tris buffer counterparts, with an instantaneous and significantly ( $P < 0.001$ ) reduced zeta potential of -25 mV (Figures 3.11: C, E and G), as the initial cationic charge was masked upon interaction with serum proteins of the FBS environment.

These particular formulations containing additional zwitterionic lipids by either substitution or replacement showed antigen retention at a lower range to that of DDA-TDB, with release profiles comparable to one another (Figures 3.11 D, F, and H). These cationic adjuvants released 10-15% OVA-I<sup>125</sup> in both Tris buffer and FBS/Tris after three minutes, with the majority of antigen release occurring within the first 1-2 hours of incubation. This period coincided with the point at which the particle size increased upon serum interaction, as DPPC or DSPC incorporation slightly delayed the observed increase

in particle size in comparison to the instantaneous aggregating effect seen on DDA-TDB. Furthermore, at 24 hours, a 20-30% antigen loss was observed with minor further losses as approximately 70% OVA-I<sup>125</sup> was retained at 72 hours (Figures 3.11 D, F and H).

DSPC-TDB liposomes demonstrated no significant difference in terms of particle size and zeta potential, regardless of the medium used, as the liposomes remained in the proximity of 2-3 micrometres, whilst consistently attaining a zeta potential in the region of -20 mV over 24 hours in Tris buffer or FBS (Figure 3.11 I). The slightly anionic DSPC-TDB liposomes appeared to interact with the plasma proteins of FBS in a different manner to that of the cationic liposomes with minimal association to the serum proteins, as no significant affect on the vesicle size and zeta potential characteristics were observed. The lack of cationic charge in DSPC-TDB was reflected in the inability to electrostatically adsorb antigen, as OVA-I<sup>125</sup> was rapidly released (Figure 3.11 J). More than half of the total antigen associated to DSPC-TDB was released within the first hour, and this high level of antigen release continued, leading to a substantial calculated antigen loss of ~85% after 72 hours. Such findings are in complete contrast to the cationic systems tested, as the anionic liposomes failed to retain antigen in both Tris buffer and the simulated *in vivo* conditions of FBS (Figure 3.11 J).

As highlighted earlier, incorporation of TDB alleviates the physical instability of DDA liposomes (Davidsen *et al*, 2005), however, when placed in FBS, the particle size and zeta potential was still greatly affected as DDA-TDB aggregated upon binding to plasma proteins. Incorporation of DPPC or DSPC lipid, in the substitution or partial replacement of DDA-TDB, also failed to prevent the eventual aggregation of the cationic liposomes.

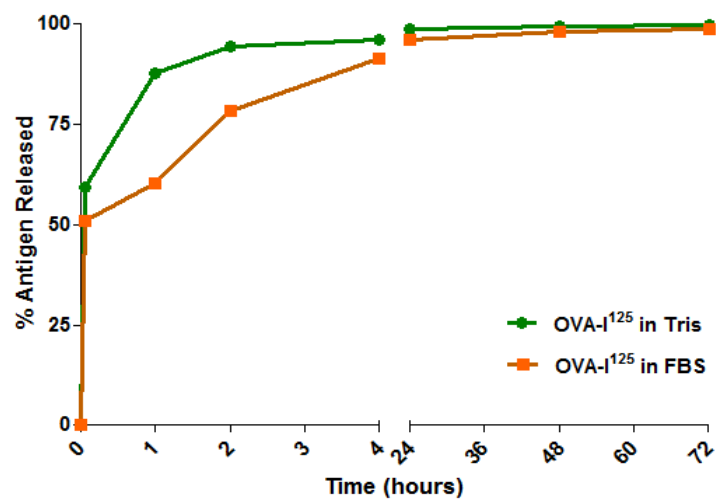
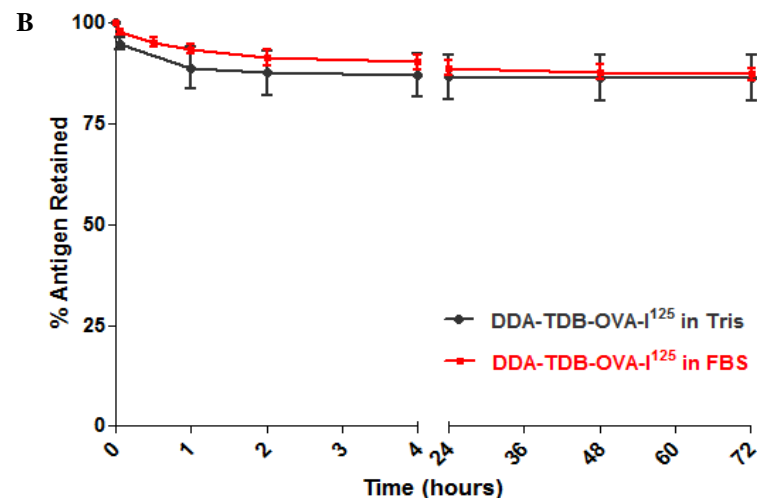
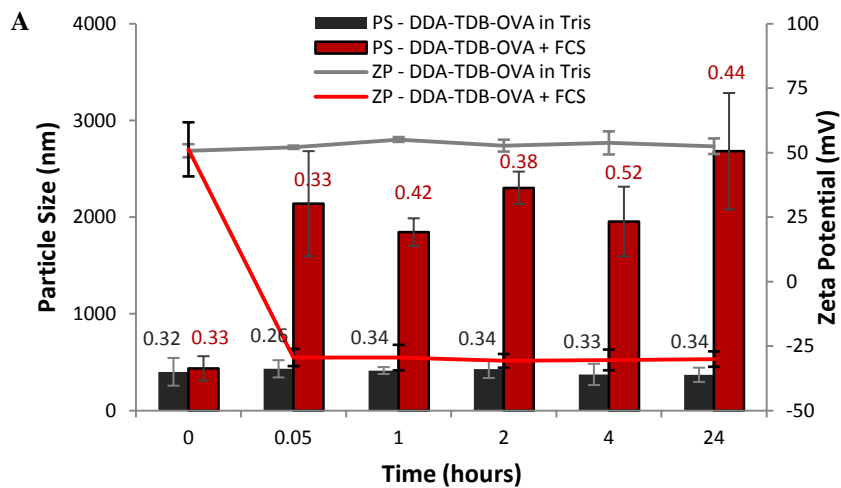
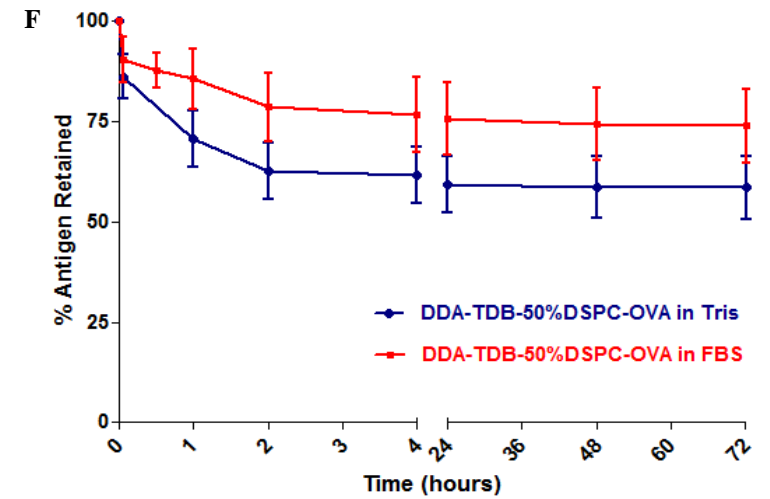
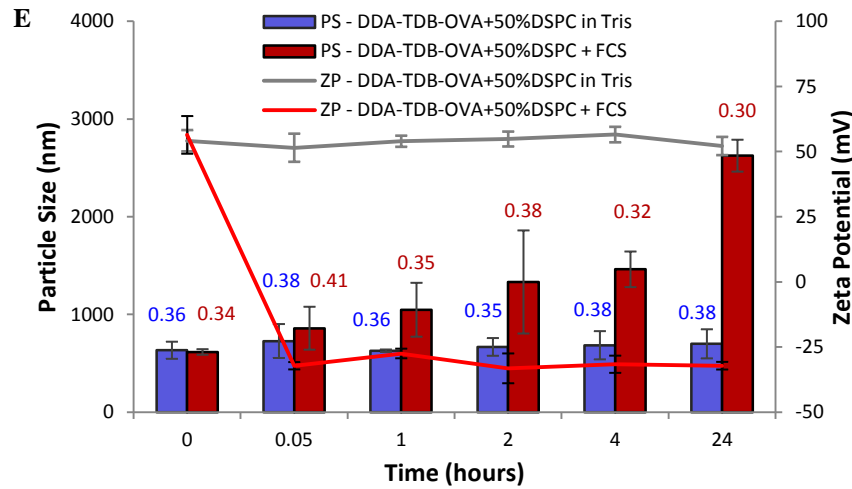
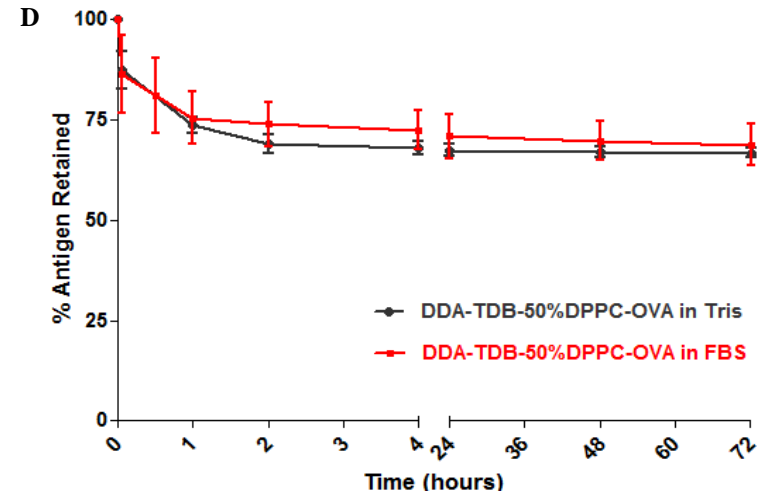
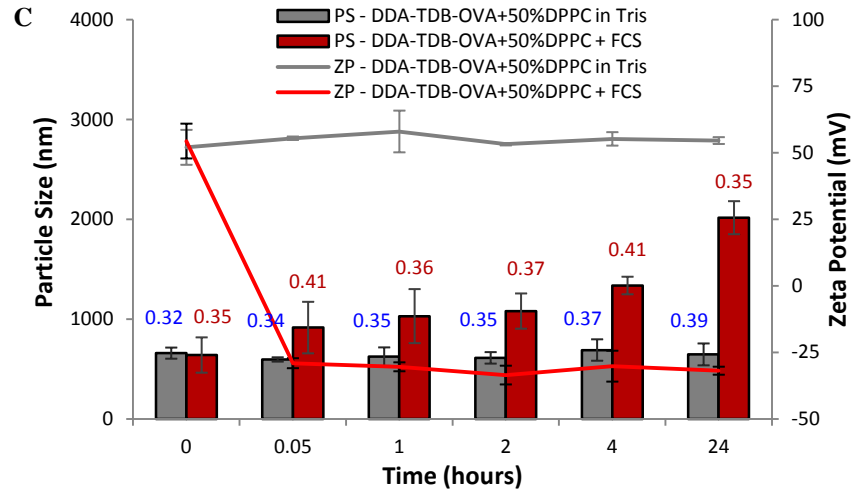
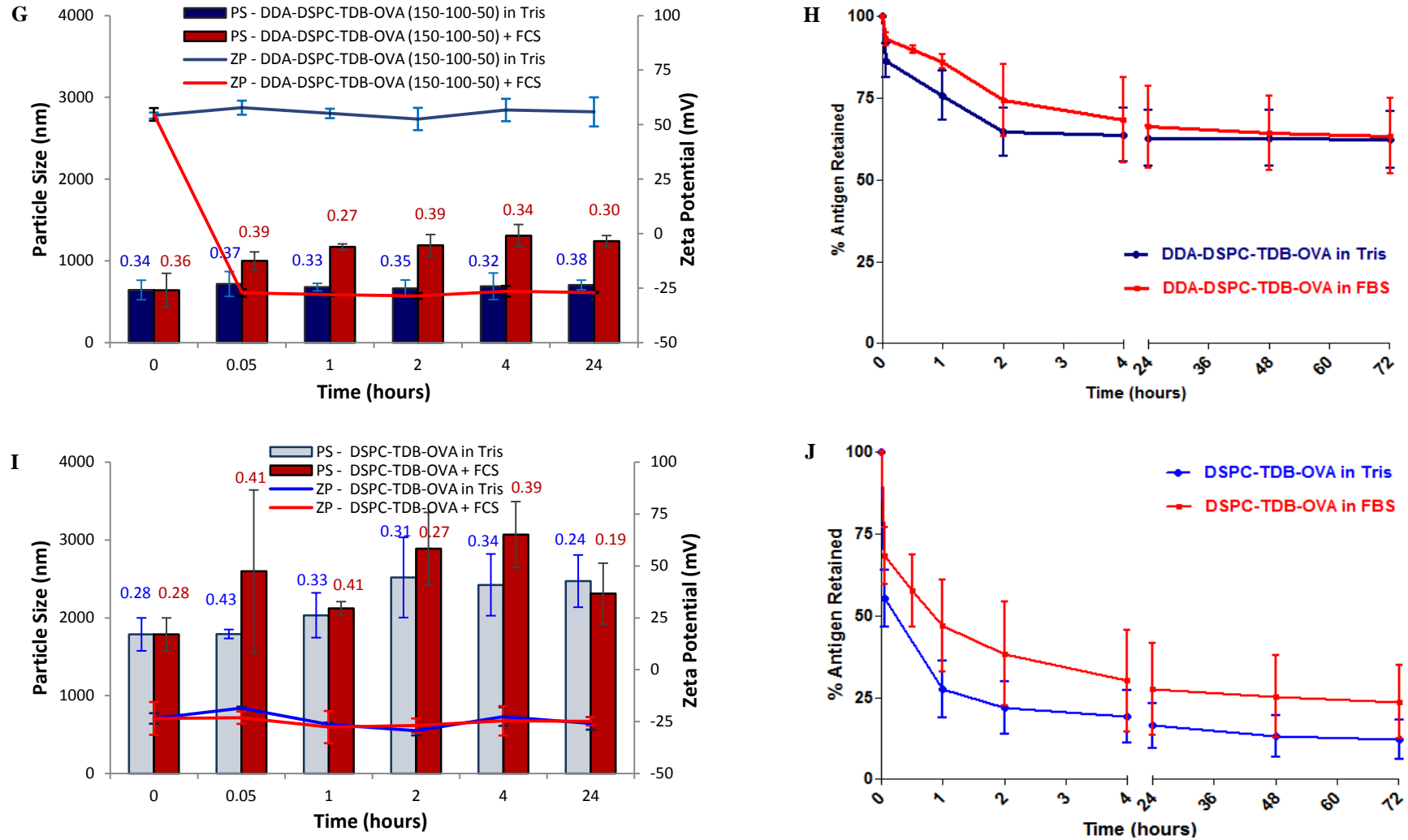


Figure 3.10. OVA/I<sup>125</sup> release profile in Tris buffer or FBS. All of the I<sup>125</sup>-labelled OVA was released over the tested 72 hour time period.







**Figure 3.11. Vesicle size, zeta potential and antigen release of liposomes adsorbed with 10 µg/ml OVA in Tris or FBS.** The size/zp and antigen retention profiles are for A&B: DDA-TDB, C&D: +50% DPPC, E&F: +50% DSPC, G&H: DDA-DSPC-TDB (150/100/50 µg/d) and I&J: DSPC-TDB, with the mean average displayed (n=3 ± SD).

Cationic liposomal systems of DDA and DDA-TDB have been previously studied for their interactions with serum proteins, in which the visual appearance of aggregating particles was apparent and confirmed by particle sizes measured at 2  $\mu\text{m}$  over 24 hours (Henriksen-Lacey *et al*, 2010a). The zeta potentials observed in this study upon exposure to serum proteins are also in good agreement with the literature for such cationic liposomal systems, with DDA and DDA-TDB adjuvants found to decrease considerably to a negative zeta potential in the region of -30 mV (Henriksen-Lacey *et al*, 2010a). In addition, the instantaneous serum effect upon liposomes has also been shown to alter the zeta potential of cationic liposomal systems made of DOTAP lipid for DNA delivery, attaining an anionic zeta potential upon introduction to a serum induced environment (McNeil & Perrie, 2006).

The effect of vesicle stability as a result of serum interactions has been previously studied (Ostro, 1983; Gregoriadis, 1988), whereby interactions of plasma proteins with liposomes were considered to be a charge dependent reaction, as highlighted in this current study with the cationic DDA-TDB based systems aggregating and attaining an anionic zeta potential upon exposure to FBS. These findings also correlate to studies by Foradada *et al*, (1997), in which cationic stearylamine containing liposomes were susceptible to aggregation when fused with serum, evident from an immediate increase in vesicle size, determined by photon correlation spectroscopy. Adsorption of serum proteins to cationic vesicle surfaces take place via electrostatic interactions, which conceals the surface charge and ultimately facilitates particle aggregation. The cationic charge dependent effect generating vesicle aggregation supports the results of this current study, as FBS had no effect upon the negatively charged DPPC-TDB or DSPC-

TDB liposomes, as an anionic zeta potential was maintained after being subjected to FBS.

Serum proteins can induce either liposomal breakdown or adsorb to the liposomal surface. Taking into account that the zeta potential represents the magnitude of potential at the hydrostatic plane of shear, the resultant serum induced net negative zeta potential of the proposed adjuvants can indicate liposomes coated in protein, as opposed to disrupted vesicles (Foradada *et al*, 1997).

### ***3.6.2. Physicochemical characterisation of liposomes adsorbed with OVA at 1 mg/ml***

#### ***3.6.2.1. Vesicle size, zeta potential and protein adsorption upon DDA replacement***

DDA-TDB liposomes and its partial DDA replacement, in conjunction with varying levels of either DPPC or DSPC incorporation, were in the region of 2000 nm when adsorbed with OVA at 1 mg/ml (Figure 3.12), which in comparison to the equivalent empty systems and upon OVA adsorption at 10 µg/ml (see Figures 3.3 and 3.11), were significantly ( $P < 0.01$ ) larger in vesicle size. Furthermore, the previously attained strong cationic zeta potential of the systems was significantly ( $P < 0.05$ ) reduced to a zeta potential of between 0 and -30 mV (Figure 3.12). Contrastingly, DPPC-TDB and DSPC-TDB liposomes were not significantly affected upon OVA loading at 1 mg/ml, in comparison to the equivalent systems prior to OVA adsorption, with a recorded vesicle size of 1-2 micrometres and an anionic zeta potential in the region of -25 mV (Figure 3.12), and was therefore not saturated with OVA at this elevated level of protein addition. Corresponding values of polydispersity for the systems was within a wider range of 0.2-0.6, which still represented a heterogeneous sample population

(Figure 3.12), with no differences apparent between the systems when DPPC or DSPC or DSPC was used to replace the cationic content in DDA-TDB.

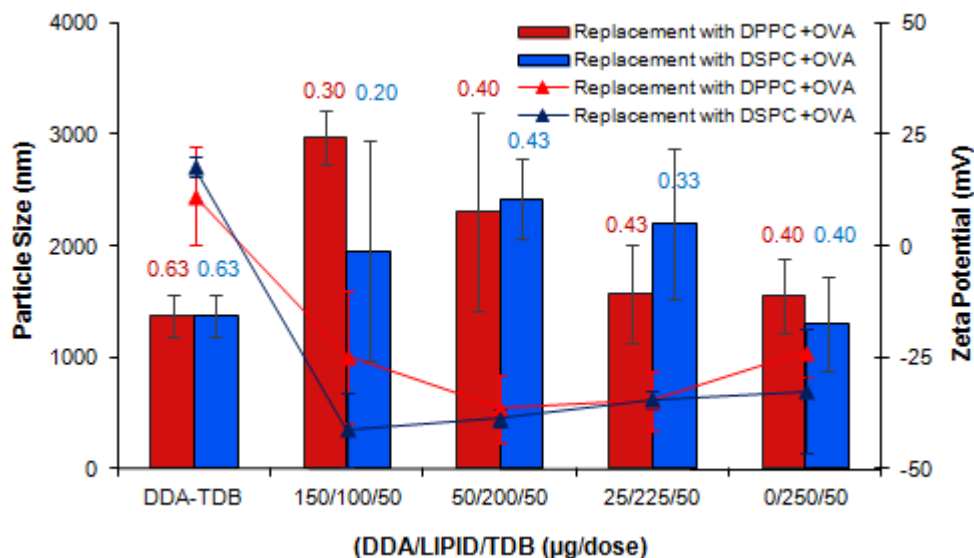


**Figure 3.12.** Particle size, polydispersity and zeta potential upon replacement of DDA in DDA-TDB with DPPC or DSPC and adsorption of OVA at 1 mg/ml. Results represent the mean average  $\pm$  standard deviation of three independent experiments.

The BCA assay was subsequently carried out on the DDA-TDB based formulations adsorbed with OVA at 1 mg/ml to quantify the level of non adsorbed protein, free in the supernatant of the liposomes pelleted upon centrifugation. It was observed that upon increased replacement of DDA with DPPC or DSPC lipid, the percentage of quantified non-associated OVA also increased, as more protein failed to bind to the liposomal systems (Figure 3.13). This was expected as electrostatic adsorption of the protein to the liposomes is dependent on the presence of DDA, providing the net cationic properties of the liposomal system from its positively charged head groups.

Indeed for DDA-TDB liposomes, low levels of non-associated OVA were found as approximately 5% protein was quantified within the supernatant (Figure 3.13). Upon partial DDA replacement with either lipid at 150/100/50 µg/dose, the volume of free

OVA significantly ( $P < 0.01$ ) increased to within the region of 35% (Figure 3.13). Further replacement of DDA content at 50/200/50 and 25/225/50  $\mu\text{g}/\text{dose}$ , generated a further significant ( $P < 0.01$ ) increase in non-associated protein, quantified at ~80% (Figure 3.13). Additionally, DPPC-TDB and DSPC-TDB liposomes were unable to retain antigen as ~95% of OVA was found free within the supernatant solution (Figure 3.13), with the vast quantity of unbound protein resultant of a diminished cationic zeta potential. Additionally, as previously observed, no differences were apparent between the systems when either DPPC or DSPC was used as the replacing lipid.

Following on from protein quantification via the BCA assay, upon centrifugation, the pellet and supernatant samples of the various liposomal systems surface adsorbed with OVA at 1 mg/ml were assessed by SDS-PAGE. It was observed that the presence of non-adsorbed OVA increased as DDA was continually replaced with either DPPC or DSPC lipid, signified by an increased intensity of banding in the gel for the supernatants of each formulation, as displayed in Figure 3.14 for DDA replacement within DDA-TDB with DSPC. Furthermore, no apparent differences were observed in the retention properties of the systems when either DPPC or DSPC was used to replace DDA-TDB, and such findings confirmed the trends observed in the BCA assay data for the corresponding formulations.

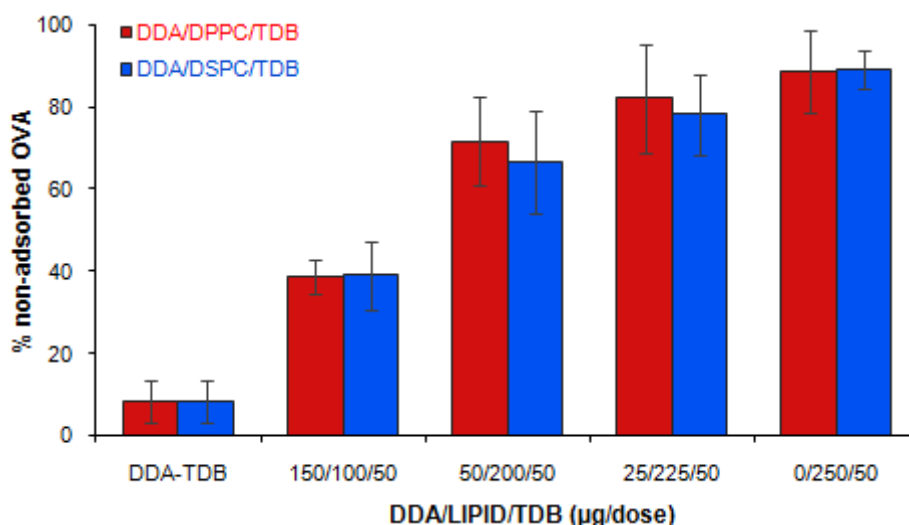


**Figure 3.13.** Quantification of non-adsorbed OVA protein in the supernatants of DDA-TDB and its cationic replacement with **DPPC** or **DSPC** lipid, pelleted upon centrifugation. Results are based on triplicate readings from at least three independent experiments with error bars representative of the standard deviation from the mean average.

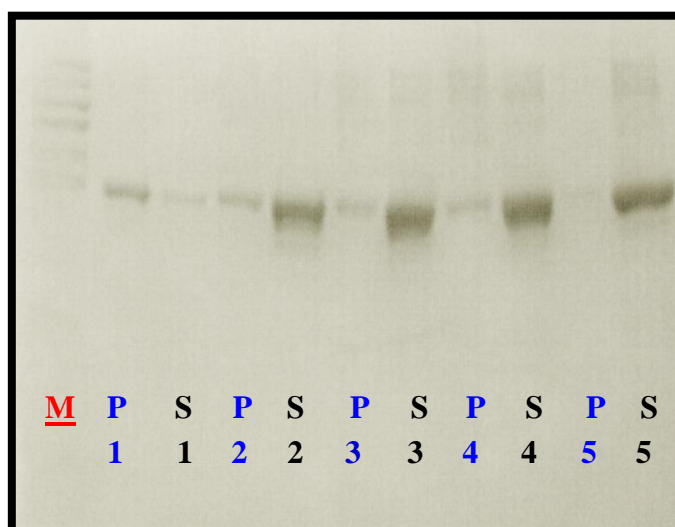


**Figure 3.14.** SDS-PAGE analysis upon OVA protein adsorption at 1 mg/ml for the cationic replacement of DDA-TDB with **DSPC**. The allocated lanes represent the protein standard marker (**M**), the pellet (**P**) and supernatant (**S**) samples for 1: DDA-TDB, 2: DDA/DSPC/TDB at 150/100/50 µg/dose, 3: 50/200/50 µg/dose, 4: 25/225/50 µg/dose and 5: DSPC-TDB.

The level of unbound OVA quantified for DDA-TDB was similar to the findings of previously related studies by Korsholm *et al*, (2007), in which protein adsorption at 1 mg/ml to DDA liposomes, which also have a comparably strong cationic zeta potential, resulted in a vast majority of protein binding, quantified as high as 90%. Furthermore, it is evident that DDA is required to provide the net cationic charge essential in facilitating the adsorption and retention of anionic protein antigen, and although previous characterisation data in the present study displayed no significant difference in the cationic zeta potentials of the partially replaced formulations, the variation in antigen adsorption was dependent upon DDA presence.

#### *3.6.2.2. Vesicle size, zeta potential and protein adsorption upon DDA-TDB substitution*

Substitution of DDA-TDB with 25, 50 and 75 mol% DPPC or DSPC and adsorption of OVA at 1 mg/ml produced a mean particle size in the region of 2000 nm, and a neutral to anionic zeta potential (Figure 3.15). This significant change in particle size and zeta potential reflected the saturation of the substituted systems with OVA, resulting in liposomal aggregation, as antigen addition at 1 mg/ml was close to the total lipid weight of the cationic DDA-TDB based systems. The polydispersity of all formulations was recorded between 0.3-0.6 (Figure 3.15).

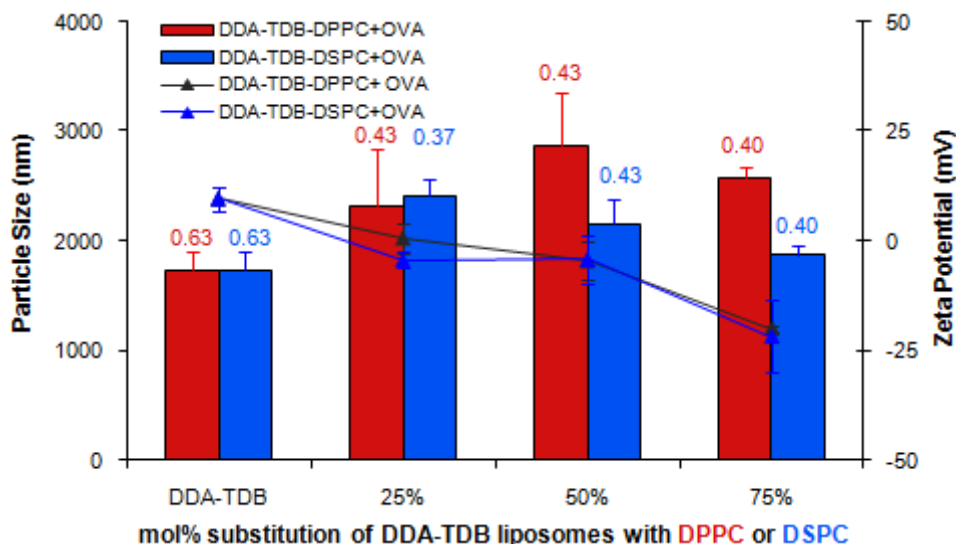


**Figure 3.15.** Particle size, polydispersity and zeta potential upon substitution of DDA-TDB with **DPPC** or **DSPC** and adsorption of OVA at 1 mg/ml. Results represent the mean average  $\pm$  standard deviation of three independent experiments.

The incorporation of DPPC or DSPC at 25, 50 and 75 mol% to DDA-TDB liposomes demonstrated that upon increased substitution, a higher level of non-adsorbed OVA was quantified by the BCA assay (Figure 3.16). With DDA-TDB representing the peak of assumed antigen retention, substitution with 25 and 50 mol% DPPC or DSPC generated a significantly ( $P < 0.01$ ) higher level of free OVA antigen, quantified at ~35% (Figure 3.16). Further substitution, with either DPPC or DSPC at 75 mol%, generated 50%-60% non-adsorbed OVA, which was an approximate 10-fold increase in the volume of unbound antigen when compared to the levels observed from DDA-TDB (Figure 3.16).

Subsequent SDS-PAGE analysis displayed a trend of an increased intensity of banding for the supernatant samples as DDA-TDB was continually substituted with DPPC or DSPC at 25, 50 and 75 mol%, displayed in Figure 3.17, for systems substituted with DPPC (similar banding was also observed with the equivalent DSPC systems). Such

behaviour mirrors the results achieved when DDA was continually replaced, whilst coinciding with the trend demonstrated upon quantification via the BCA assay.

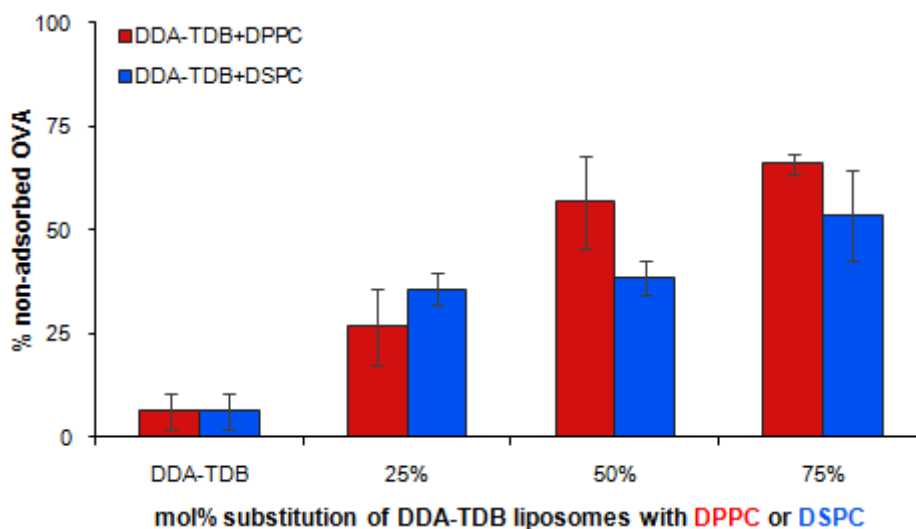


**Figure 3.16. Quantification of non-adsorbed OVA protein in the supernatants of DDA-TDB and its substitution with DPPC or DSPC lipid, pelleted upon centrifugation.** Results are based on triplicate readings from three independent experiments with error bars of the standard deviation from the mean average.

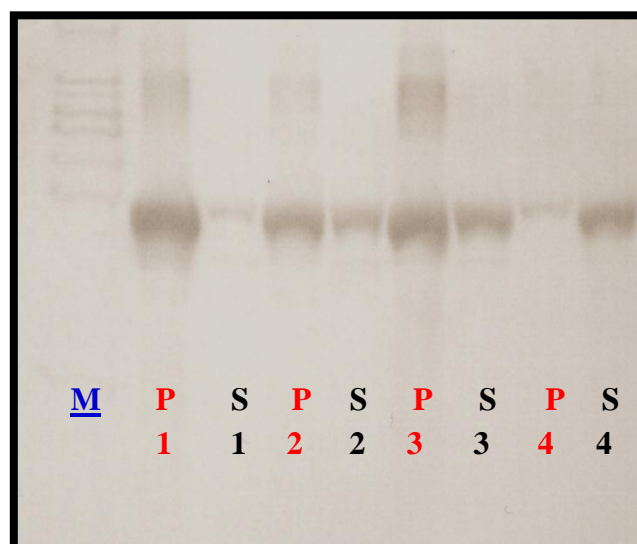


**Figure 3.17. SDS-PAGE analysis upon OVA protein adsorption at 1 mg/ml for DDA-TDB and its substitution with DPPC.** The allocated lanes represent the protein standard marker (M), the pellet (P) and supernatant (S) samples for 1: DDA-TDB, 2: DDA-TDB-25% DPPC, 3: DDA-TDB-50% DPPC and 4: DDA-TDB-75% DPPC.

Protein aggregation can either be beneficial or detrimental to a vaccine delivery system, depending on the processes involved for a particular type of response required. The manner in which antigen presentation occurs to the immune system is crucial to accomplish functional immunity. It has been shown that an antigen is capable of improved immunity when administration takes place as an aggregated, colloidal form, for example as a protein micelle (Morein *et al*, 1978), whilst it is also believed that most adjuvants utilised till the mid 90s, activated an enhanced inflammatory response at the site of injection, essentially providing a depot effect in order to induce stronger antigen specific immunity (Badiee *et al*, 2007).

Contrastingly, competent antigen deposition has also been achievable at the site of injection upon administration with non aggregated, cationic DDA based liposomal delivery systems (Henriksen-Lacey *et al*, 2010a), and with a greater understanding of Th1 and Th2 type immune responses, it is apparent that each vaccine requires a specific adjuvant to maximise a desired immune response (Campos-Neto, 2002). Thus, aggregation is not always necessary if an appropriate adjuvant-antigen complex is employed, as seen with the application of the promising TB fusion antigens of Ag85B–ESAT-6 or Ag85B–ESAT-6-Rv2660, providing antigen specific antibody and cellular immune responses upon delivery of DDA-TDB adjuvant liposomes adsorbed with the TB fusion proteins, at 10 and 100 µg/ml respectively (Davidsen *et al*, 2005; Aagaard *et al*, 2011).

### ***3.7. Further replacement of DDA within DDA-TDB***

#### *3.7.1. Physicochemical characterisation upon further DDA replacement*

An additional set of experiments was carried out to test the level of DDA content within DDA-TDB upon further cationic replacement. This was conducted to ascertain whether the characterised responses were due to a decreased level of DDA presence, or from the increased incorporation of further lipids. DDA-TDB was assessed upon further cationic replacement with DDA-DSPC-TDB at 100/150/50 µg/dose, alongside DDA-TDB at a reduced DDA:TDB weight ratio of 2:1 (Table 3.2), which represented additional varying levels of DDA or DSPC content, to possibly aid the understanding of the role of DDA within the TDB enriched liposomal immunoadjuvant system.

DSPC was selected as the replacing lipid as no difference was apparent between the introduction of DPPC or DSPC throughout the previous characterisation studies completed to date. DDA-TDB and DSPC-TDB (both at a 5:1 weight ratio) was also assessed in conjunction with these additional formulations for comparison, with all systems initially characterised for their particle size and zeta potential before and after antigen loading at 1 mg/ml OVA, followed by the quantification of non-associated protein via the BCA assay, allowing for comparisons to be made with the related DDA-TDB replacement formulations of this study.

**Table 3.2. Further DDA-TDB based formulations proposed to test whether responses were due to DDA replacement or a reduced DDA presence within the system.** The weight ratios of 5:1 and 2:1 for DDA-TDB, alongside partial and total DDA replacement with DSPC was tested as the volume of TDB remained fixed throughout all of the formulations.

Formulation	Volume of DDA (µg/dose)	Volume of DSPC (µg/dose)	Volume of TDB (µg/dose)
DDA-TDB (5:1)	250	0	50
DDA-DSPC-TDB (Further replaced)	100	150	50
DDA-TDB (2:1)	100	0	50

DDA-TDB was characteristically 500 nm in particle size with a zeta potential of 50 mV, which was not significantly different to DDA-TDB at the reduced weight ratio of 2:1 (Figure 3.18). Further replacement of DDA with DDA-DSPC-TDB at 100/150/50 µg/dose produced a significantly ( $P < 0.05$ ) larger vesicle size compared to DDA-TDB, measured at ~700 nm, yet the zeta potential remained unchanged from DDA-TDB at both weight ratios, at 50 mV (Figure 3.18). This increased size and sustained cationic zeta potential was comparable to the related DDA replacement formulation at 150/100/50 µg/dose measured earlier, which incorporated a slightly elevated level of DSPC in replacement of DDA. As previously observed, DSPC-TDB was ~2 µm in size with a zeta potential of -20 mV, and the polydispersity of all empty systems was in the proximity of 0.3 (Figure 3.18).

Upon surface adsorption of OVA at 1 mg/ml, DDA-TDB together with DDA-DSPC-TDB at 100/150/50 µg/dose and DDA-TDB at a 2:1 weight ratio had changed significantly ( $P < 0.01$ ) in mean particle size to 2-3 micrometres and to a neutral to

anionic zeta potential (Figure 3.18). The exception to this trend was the lack of change observed with DSPC-TDB, as a particle size of 2 micrometres and an anionic zeta potential was sustained upon OVA addition, with all systems expressing a polydispersity of around 0.4-0.6 (Figure 3.18).

OVA adsorption at 1 mg/ml induced liposomal aggregation in the cationic formulations, as previously seen in this study for the other related DDA-TDB based systems, as when compared to their empty counterparts, larger particles with a diminished cationic charge were produced. The strong cationic zeta potential recorded for these outlined further DDA replaced formulations prior to protein addition, inevitably facilitated OVA adsorption and retention, and due to their cationic nature, such liposomes are able to electrostatically bind the anionic protein (Korsholm *et al*, 2007).

Indeed, the saturated concentration of OVA protein resulted in a neutralised zeta potential and an increased particle size for the cationic systems, indicative of particle aggregation. This was also visibly reflected in the formulations as the aggregated samples upon protein adsorption appeared to be more turbid than the equivalent empty systems, with the exception of DSPC-TDB, which displayed no observable effect upon OVA adsorption at 1 mg/ml (Figure 3.18).

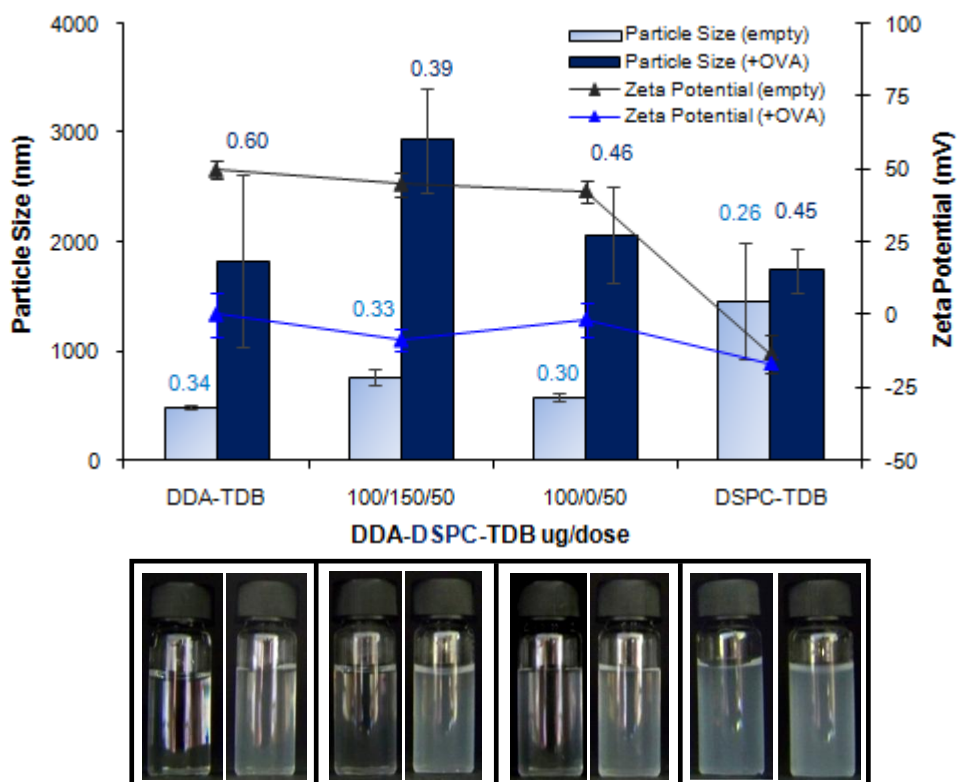
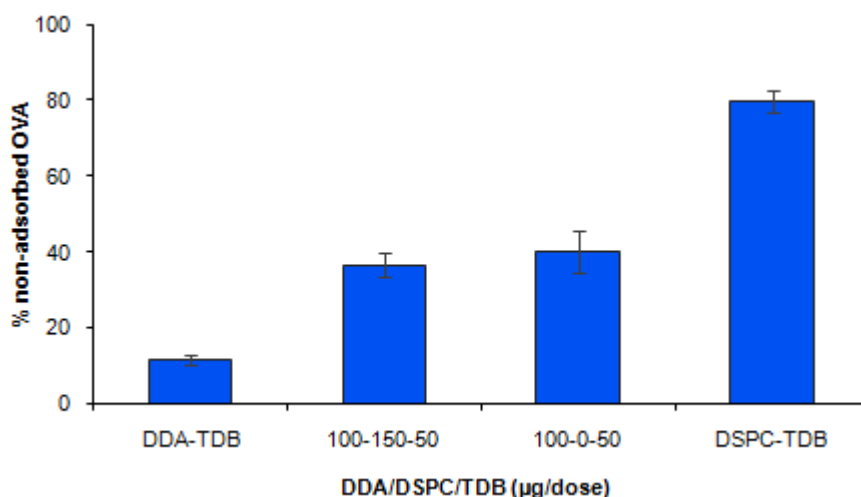


Figure 3.18. Particle size, polydispersity, zeta potential and images of DDA-TDB, DDA-DSPC-TDB (100/150/50 µg/dose), the reduced weight ratio of DDA-TDB at 2:1 (100/50 µg/dose) and DSPC-TDB, before and after OVA adsorption at 1 mg/ml. Results represent the mean  $\pm$  SD from three experiments.

The BCA assay was subsequently applied to quantify the volume of non-adsorbed protein in the supernatants of the additional DDA replacement formulations, pelleted upon OVA adsorption at 1 mg/ml. This was conducted as the level of antigen to be delivered and its association to the vesicles, via surface adsorption for example, indicates the potential efficiency of a liposomal delivery system (Korsholm *et al*, 2007), and these experiments also provided a further point of comparison with the previously characterised DDA-TDB based formulations in which DDA content was replaced.

DDA-TDB (5:1) generated the lowest level of non-associated OVA at ~10% (Figure 3.19) and as DDA content decreased within the formulation, more antigen became free, as compared to the DDA-TDB liposomes, DDA-DSPC-TDB at 100/150/50 µg/dose and the reduced weight ratio of DDA-TDB (2:1) generated significantly ( $P <$

0.01) higher levels of non-adsorbed antigen at 30-40%, which was half the level attained in the supernatants of DSPC-TDB, in which ~80% of quantified OVA was non-associated from the slightly anionic system (Figure 3.19). Additionally, no significant difference was exhibited between these two additional replacement systems tested. Overall, the further replaced formulations appear to have comparable characteristics to DDA-TDB and its partial DDA replacement, with these outlined systems to be further characterised and immunologically assessed, in order to fully appreciate the role of the cationic lipid DDA vs. DSPC content within the proposed TDB based liposomal adjuvants.



**Figure 3.19.** Quantification of non-adsorbed OVA protein in the supernatants of DDA-TDB, DDA-DSPC-TDB (100/150/50 µg/dose), the reduced weight ratio of DDA-TDB at 2:1 (100/50 µg/dose) and DSPC-TDB, pelleted upon OVA adsorption at 1 mg/ml. Results are based on triplicate readings of three independent experiments, with error bars representative of the standard deviation from the mean average.

### 3.8. Conclusions

Upon initial studies into the effect of buffer on the hydration of the lipid film, Tris was selected as the most suitable medium, with DLS measurements made with samples suspended in 1 mM Tris buffer. The liposomes characterised upon incorporation of DPPC or DSPC, by cationic replacement or substitution of DDA-TDB, produced vesicles in a sub-micrometre size range with a cationic zeta potential. The exceptions

were observed with DPPC-TDB and DSPC-TDB, which were significantly larger with an anionic zeta potential. Furthermore, the substituted systems were physically stable over 28 days as no fluctuations in mean particle size or zeta potential was apparent, with TEM demonstrating heterogeneous populations of vesicles whilst corroborating with the particle size analysis.

A DDA dependent effect upon the levels of liposome associated and non-associated antigen was observed with DDA-TDB, followed by its partial replacement or substitution retaining the highest levels of antigen coupled with relatively low OVA release in the replicated physiological conditions, whilst demonstrating interactions with serum proteins. The necessity of DDA was further demonstrated with the lack of OVA retained in the DSPC-TDB liposomes, coinciding with rapid and continual antigen release.

With the aim of investigating the physicochemical characteristics of the liposomal adjuvants used to deliver antigens, these outlined formulations may be developed into potential vaccine delivery systems, as the characterised attributes displayed upon partially incorporating or replacing DDA content have been encouragingly comparable to the recognised DDA-TDB adjuvant. The findings reported in this chapter for the multi-component liposomal formulations can be further assessed for their thermodynamic properties to confirm lipid interdigitation, with further *in vitro* evaluation into associated cytotoxicity and activation of macrophages, prior to immunological characterisation in response to a novel vaccine antigen, to determine whether the main DDA-TDB formulation can possibly be enhanced, whilst fully appreciating the role of DDA and the effect of additional lipid incorporation in the proposed liposomal immunoadjuvants.

## **Chapter 4**

### **Thermodynamic analysis of the gel-to-liquid phase transition of DDA-TDB based liposomes**

## **4.1. Introduction**

### *4.1.1. Differential scanning calorimetry for thermodynamic analysis*

Differential scanning calorimetry (DSC) is a widely used method of thermal analysis that has been applied to investigate and characterise a range of pharmaceutical systems (Giron, 2002). The thermal examination of materials can give a range of thermal properties including phase transitions and heat capacity changes, which are key factors of the drug delivery formulation process, allowing indications of system stability at various temperature conditions. DSC is commonly applied for such investigations due to its ease of use, speed of application and for laboratory analysis, its relatively low costs (Demetzos, 2008). Differential scanning calorimetry measures the heat flow that enters or exits a material at a given heating or cooling rate from which the heat capacity ( $C_p$ ) at a continuous pressure can be determined. The heat capacity is representative of the quantity of heat input necessary to increase the temperature of a sample by one degree Celsius at a constant pressure (Demetzos, 2008).

As a function of time and temperature, DSC is a technique capable of measuring the heat flow and temperature of a given sample. Thermal transitions such as the melting of crystalline materials, crystallisation of melts, glass transitions of amorphous materials and phase transitions from a crystalline to a liquid crystalline form can be detected and quantified using DSC (Gill *et al.*, 1993). All thermal transitions are influenced by the chemical structure and physical nature of the material, making the application of DSC a useful tool, for example in the thermal characterisation of liposomal dispersions. Quality control in liposome production can also be achieved, particularly in multicomponent systems when determining the effect of additional components to main phase transitions, leading to an improved understanding of the

thermodynamic behaviour of lipids used in liposomal formulations (Biltonen & Lichtenberg, 1993).

#### *4.1.2. Thermal characteristics of liposomes*

Thermal transitions of vesicular systems such as liposomal dispersions can be obtained for characterisation via DSC. The features that define a typical melting transition in a thermogram for a liposomal dispersion are shown in Figure 4.1. One of the major features of interest is the main phase transition temperature ( $T_m$ ), representing the peak melting temperature, which is the uppermost, maximum point of the endothermic peak. The energy of the main melting point is taken from the area under the peak in J/g. This area is proportional to the energy associated to the main phase transition (Chapman & Urbina, 1974).

For the analysis of lipid dispersions, in the studies within this chapter, a heat, cool, re-heat method was applied to remove any thermal history and ascertain the main melting point of the proposed systems. The endothermic event of melting to a liquid phase, whereby energy is absorbed, is characterised by a single, upward deviation from the baseline (heat flow displayed as endo up on the Pyris Diamond DSC system, Perkin Elmer Instruments LLC, USA). Contrastingly, an exothermic event such as crystallisation, in which energy is released, is displayed as an inverse of a  $T_m$  peak when cooling (Figure 4.1), as the system returns to a gel phase after attaining fluidity, prior to a final re-heating stage (PerkinElmer, 2010).

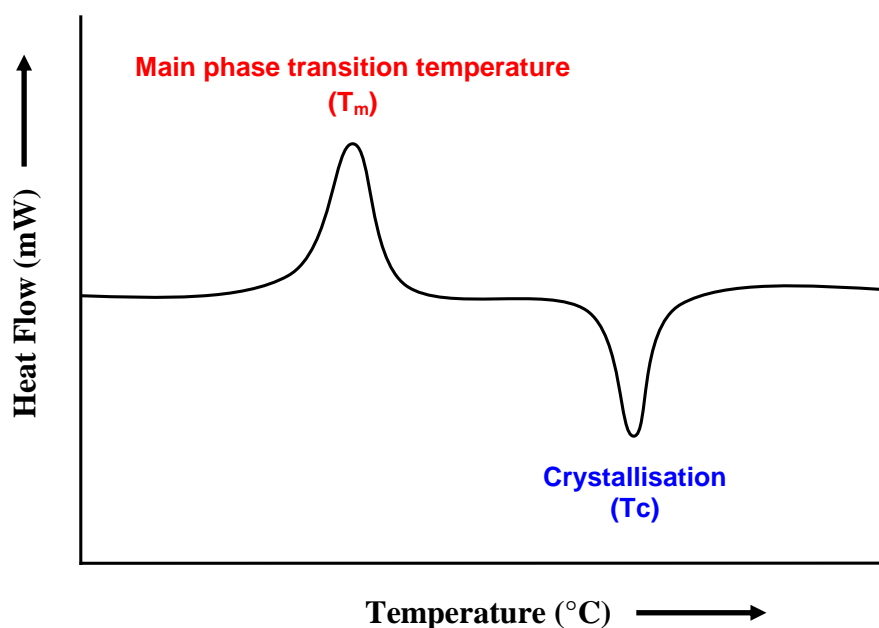


**Figure 4.1. A typical DSC thermogram of a liposomal dispersion.** An endothermic main melting event indicative of a main transition from a gel-to-liquid crystalline state and an exothermic crystallisation is evident in the opposing deviations from the baseline (Figure adapted from Taylor & Craig, 2003).

Upon the addition of thermal energy to lipid bilayers (e.g. to multilamellar liposomes), the major change in state that takes place is the gel-to-liquid crystalline phase transition, which is effectively a melting transition, from a crystalline to a liquid crystalline state (Figure 4.2). The transition of lipid bilayers is influenced by the level of Van der Waal interactions between the hydrocarbon chains of adjacent lipid molecules. These interactions are determined by the length of lipid chains, with longer chain lipids having an increased area in which to interact, in turn strengthening this interaction and ultimately resulting in decreased lipid mobility. Therefore, shorter tailed lipids are more fluid than their longer tailed counterparts (Rawicz *et al*, 2000).

The amphiphilic structure of a lipid molecule, consisting of a polar head group and two attached non-polar tails, together with the phase transition behaviour of hydrated lipids is displayed in Figure 4.2. It is understood that longer chain phosphatidylcholines remain in a consistently, well ordered gel state with extended acyl chains and

predominantly motionless head groups at the water interface (Fuldner, 1981). However, upon heating (towards a liquid crystalline state), a cooperative melting of the acyl chains results in a disordered hydrocarbon arrangement as the mobility of the acyl chains is increased (Koyama *et al*, 1999; El Maghraby *et al*, 2005).



**Figure 4.2. Schematic representation of phospholipid acyl chain arrangements from a gel-to-liquid crystalline state.** A lipid molecule (A), e.g. the saturated DPPC lipid, produces a well-ordered bilayer of molecules when in a gel state (B), which later becomes altered upon heating to a liquid crystalline state (C) (Demetzos, 2008).

Therefore, depending on the structural attributes of the lipids forming the liposomal suspension, its bilayers may be in a rigid, gel state or a fluid, liquid crystalline state at a given temperature. Liposomes are in a liquid crystalline phase when the vesicle suspension is at a temperature above its main phase transition temperature, and in a rigid state when at a temperature below the crystalline transition temperature.

Indeed the greatest modification to vesicle bilayers takes place in the main phase transition from a gel-to-liquid crystalline state (Lentz *et al*, 1976). Hence, the choice of phospholipids and introduction of additional lipids can affect the main phase transition

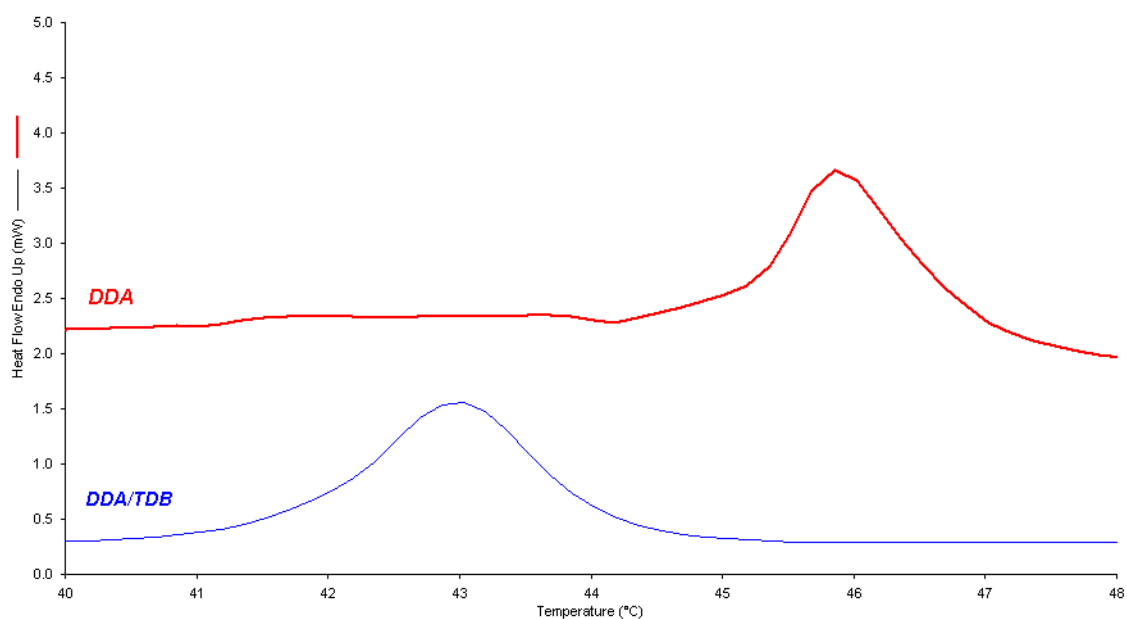
and in turn, vesicle bilayer fluidity. This can favourably influence the system by increasing the overall transition temperature of the lipid bilayer, decreasing bilayer fluidity and consequently preventing leakage of encapsulated components at physiological temperature (Sharma & Sharma, 1997).

The crystalline state of lipid bilayers, i.e. their bilayer fluidity, is a key influencing factor upon the *in vivo* behaviour of liposomes. Early work by Senior & Gregoriadis, (1982) demonstrated that drug retention in liposomes *in vivo* was dependent on the phase transition temperature of the lipids used. Lipids with various chain lengths and resultant phase transitions were tested such as, dilauroyl phosphatidylcholine (DLPC) (C<sub>12</sub>, T<sub>m</sub> of -1 °C), dimyristoyl phosphatidylcholine (DMPC) (C<sub>14</sub>, T<sub>m</sub> of 23 °C), and DPPC (C<sub>16</sub>, T<sub>m</sub> of 41 °C), quickly released entrapped drug, whereas DSPC liposomes, which possesses a longer fatty acid chain and thus a higher T<sub>m</sub>, (C<sub>18</sub>, T<sub>m</sub> of 55 °C), were shown to retain increased amounts of entrapped drug (carboxyfluorescein) (Senior & Gregoriadis, 1982).

In the present study, the aim of this chapter was to investigate the effect of incorporating varying levels of DPPC or DSPC lipid to DDA-TDB based liposomal systems. This was achieved by identifying particular structural phases and determining lipid miscibility via DSC, indicated by the temperature at which the main phase transition from a gel-to-liquid crystalline state occurs for the proposed multicomponent adjuvants. Cationic replacement or substitution with the further lipids took place upon the main DDA-TDB liposomal formulation, previously shown to be an effective adjuvant (Davidsen *et al*, 2005).

#### 4.2. DSC of DDA and the effect of TDB on the gel-to-liquid phase transition

DSC was initially carried out on DDA and DDA-TDB liposome dispersions in order to establish a method for analysis and characterise the main gel-to-liquid phase transition temperature of these systems. The thermograms and thermodynamic parameters characterised for both DDA and DDA-TDB are summarised in Figure 4.3. An endothermic event for the main thermal transition can be seen with DDA dispersions in the region of 47 °C within the heat capacity curve. Upon 11 mol% TDB addition (5:1 weight ratio) to the DDA liposome formulation, the onset of  $T_m$  is lowered by approximately 5 °C with a noticeable broadening of the peak.



Liposome	Onset (°C)	Peak Max (°C)	Delta H (J/g)
DDA	46.1 ± 0.6	47.1 ± 0.6	1.9 ± 0.2
DDA-TDB	41.6 ± 0.4	42.8 ± 0.6	1.3 ± 0.8

**Figure 4.3. DSC thermograms and corresponding thermodynamic parameters of the gel-to-liquid phase transition of DDA and DDA-TDB vesicles.** Liposomes were produced via lipid hydration in 10 mM Tris buffer (pH 7.4). DSC Thermograms were made at 10 °C/min (600 °C/h) over the tested temperature range of 25-75 °C. One of three thermograms for each vesicle system is shown with the results representative of the mean ± the standard deviation of three independent liposome batches.

These results are in line with previous studies (Davidsen *et al*, 2005) in which the  $T_m$  for DDA was detected at 47 °C, and the integration of the TDB glycolipid acyl chains into the hydrophobic region of DDA bilayers changed the lipid chain arrangements, signified by a broader, highly significantly down shifted  $T_m$  ( $P < 0.01$ ) to ~42 °C, also in good agreement with previous studies (Christensen *et al*, 2007a). With TDB substituted into DDA, a broadened DSC peak at the main phase transition demonstrates the concept of multiple cooperative heat transitions hypothesised by Davidsen *et al*, (2005). This is possibly resulting from alterations to the local lipid bilayer configuration as the 22-carbon acyl chains of TDB are accommodated within the hydrophobic core of DDA bilayers, affecting the lipid chain packing characteristics (Davidsen *et al*, 2005).

#### **4.3. Investigations using Nano DSC**

DDA-TDB liposomes were also tested for their main phase transition using a new Nano DSC (TA Instruments). This system is described as being able to precisely control the temperature of the sample and provide higher sensitivity and reproducibility of data with greater baseline stability than conventional DSC (TA Instruments, 2011). Such attributes allow for samples at lower concentrations to be used, with DDA-TDB scans prepared in dosage form (1.25/0.25 mg/ml) as opposed to the higher concentrations used to maximise the thermal events for the other equivalent scans of this study via DSC. Furthermore, the Nano DSC scans were made at a scan rate of 2 °C/min, providing a good balance between signal to noise ratio and resolution, maximising the thermal event and hence a more prominent  $T_m$ .

The heat-cool-reheat conditions for DSC can offer valuable characterisation information of the thermodynamic behaviour for a given sample. This is achieved as cooling and subsequent reheating removes the original thermal history of a sample, replacing it with a solid, more controlled thermal history, allowing increased sensitivity, highlighting any thermal events that may not be apparent during the first heat (Sichina, 2000).

The DDA-TDB liposomal sample was firstly heated and cooled which displayed a pre-transition in the region of 30 °C and a subsequent main transition, of a large magnitude, split into two domains beyond 40 °C. However, upon cooling, a single crystallisation peak was observed, suggesting a more homogenous sample. Subsequently, the same sample was reheated to examine the reproducibility of the transition and confirm the main melting point of the lipid dispersion. This first reheat displayed a pre-transition prior to a two domain main transition (Figure 4.4), as characterised in the first heat. However, a further heat (second repeated heat), with a new thermal history, showed no pre-transition and a prominent, single domain, main phase transition (Figure 4.4). This single transition peak of the repeated heat, positioned between the previously observed twin domain, displays homogeneity within the sample.

Reproducibility of phase transitions was achievable in both heating and cooling of the sample and once initially melted and cooled, subsequent melting and re-crystallisation was identical in behaviour, characterised for the main melting point of the DDA-TDB liposomal dispersions. The magnitude of the main phase transition was large and prominent for the sample scans and as the area associated to the transition was not

significantly altered (found to be consistently in the region of 23.5 mJ) between each repeated scan (additional repeated scans not shown), no physical or chemical degradation of the liposome system was apparent, as a function of repeated heating, in the tested temperature range.

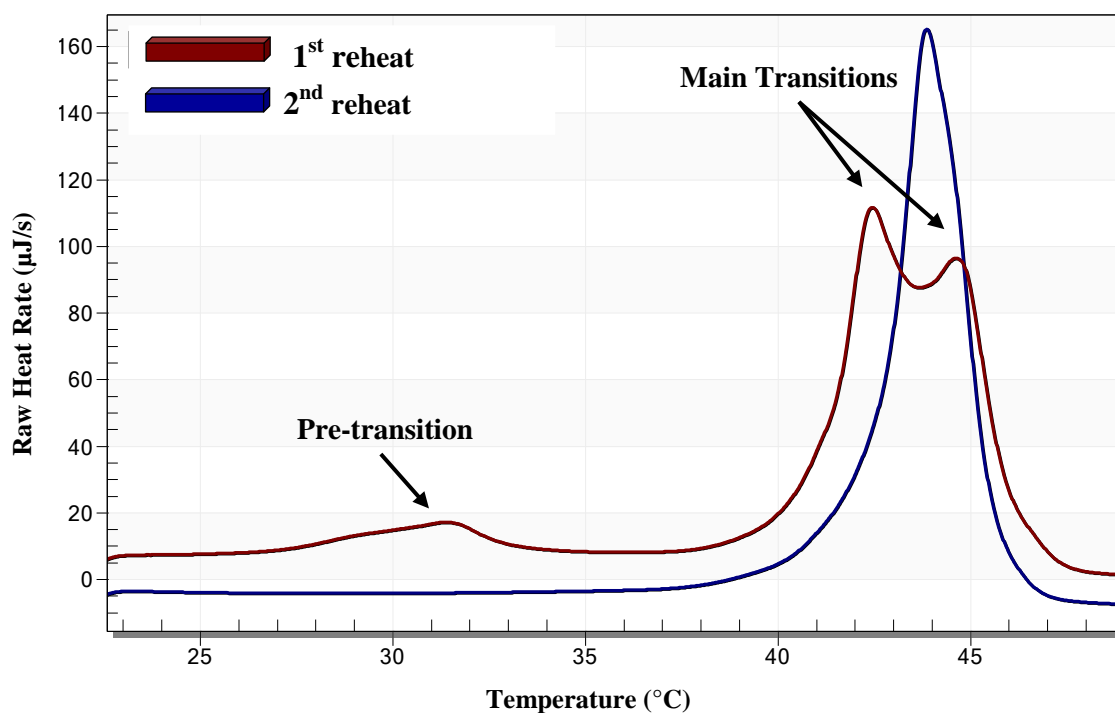


**Figure 4.4. Nano DSC thermogram of the gel-to-liquid phase transition of a DDA-TDB liposomal dispersion.** The liposomes were produced via lipid hydration in Tris buffer (10 mM, pH 7.4) with the scans made at 2 °C/min (120 °C/h) over the tested temperature range of 20-70 °C.

From the successful reproduction of these highlighted results, the DSC method applied for liposomal dispersions in this study was validated. The heat, cool, re-heat instrumental approach removed any thermal history allowing for the main phase transition to be successfully characterised. Further confirmation of the main melting point of DDA-TDB determined via Nano DSC also corroborated with the findings of conventional DSC instrumentation. The analysis of DDA and DDA-TDB thus effectively acted as a control for subsequent thermodynamic studies of the novel

formulations in this study, which included a variety of phospholipid combinations incorporating DPPC or DSPC lipid.

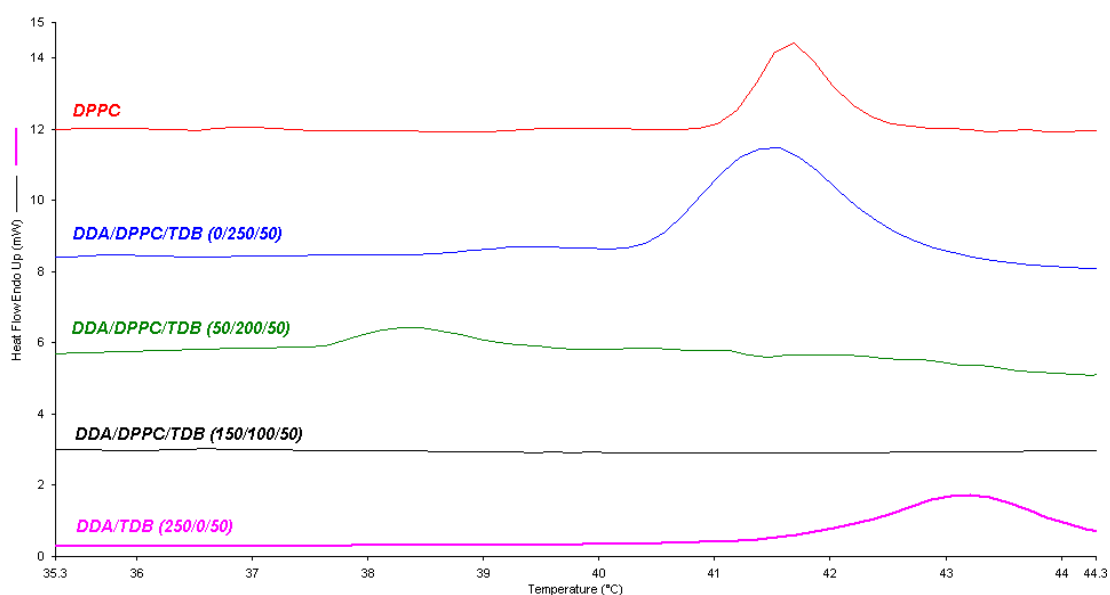
#### ***4.4. DSC of DDA-TDB based liposomes replacing DDA with DPPC or DSPC lipid***

DSC was conducted upon the DDA replacement formulations, previously characterised for vesicle size, zeta potential, antigen retention and release (see Chapter 3), in order to ascertain the temperature point at which the main transition from a gel-to-liquid phase occurred for the DDA-TDB based lipid mixtures. With a fixed weight of TDB present within the formulation, the cationic DDA component within the DDA:TDB 5:1 weight ratio was replaced with DPPC or DSPC lipid. These lipids are from the phospholipid family of saturated phosphatidylcholines, and only differ by the number of carbon atoms within their acyl chains: DPPC and DSPC lipids contain two 16 and 18-carbon alkyl chains respectively (see Chapter 1, Table 1.7 for schematic structures of DPPC and DSPC).

DSC thermograms were attained across a temperature range of 25-75 °C at a scan rate of 10 °C/min to characterise the main gel-to-liquid crystalline phase transition ( $T_m$ ) (Figure 4.5). The main melting point attained for pure DPPC liposome dispersions was 42.3 °C  $\pm$  0.2 °C (Figure 4.5). When DPPC completely replaced DDA in the liposomes (DPPC-TDB; 250/50  $\mu$ g/dose), the main melting point was not significantly different in comparison to pure DPPC lipid, remaining in the region of 42 °C. When DDA was introduced alongside DPPC and TDB at 50/200/50  $\mu$ g/dose, the measured peak maximum temperature for the main phase transition dropped significantly ( $P < 0.01$ ) by approximately 4 °C, as the liposomal system incorporated multiple phospholipid components, coinciding with an evident broadening of the peak. Interestingly, for the

phospholipid mixture of DDA-DPPC-TDB at the weight ratio of 150/100/50  $\mu\text{g}/\text{dose}$ , no endothermic peak indicative of a main phase transition was detected in the tested temperature range (Figure 4.5).

Results for liposome suspensions prepared from pure DPPC dispersions correspond with previously conducted DSC studies into such liposomes (McMullen *et al*, 1995; Biruss *et al*, 2007; Bolean *et al*, 2010), noting the main phase transition for DPPC at 42 °C. Hoyrup *et al*, (2001) analysed phospholipid mixtures composed involving DPPC and stearylmyristoyl-sn-phosphatidylcholine (SMPC), adjusting the SMPC concentrations to examine bilayer interactions via DSC. SMPC is an asymmetrical phospholipid as it consists of two chains of unequal carbon lengths (C18/C14). Such lipids are common in biological membranes and interestingly, miscibility with symmetrical phospholipids is possible, whilst raising the main melting point. Furthermore, with the presence of DPPC lipid, all tested ratios yielded a maximum  $T_m$  beyond 40 °C, where pure DPPC liposome dispersions were expected to generate a highly cooperative phase transition. As DPPC was increasingly introduced within the SMPC-DPPC phospholipid mixture, the corresponding phase transitions of the systems were measured at higher temperatures (Hoyrup *et al*, 2001). For this current study, the general trend apparent was that with an increased incorporation of DPPC lipid in the replacement of DDA, the resultant main phase transition temperatures became closer to DPPC lipid in its pure form. In all instances, the main phase transition did not exceed that of DPPC alone which was characterised at approximately 42 °C (Figure 4.5).



DDA-DPPC-TDB ( $\mu\text{g}/\text{dose}$ )	Onset ( $^{\circ}\text{C}$ )	Peak Max ( $^{\circ}\text{C}$ )	Delta H (J/g)
DPPC	$41.4 \pm 0.3$	$42.3 \pm 0.2$	$2.8 \pm 1.4$
0/250/50	$40.8 \pm 0.1$	$41.6 \pm 0.1$	$1.8 \pm 0.5$
50/200/50	$36.8 \pm 0.8$	$37.4 \pm 0.8$	$0.8 \pm 0.4$
150/100/50	$0.0 \pm 0.0$	$0.0 \pm 0.0$	$0.0 \pm 0.0$
250/0/50	$41.6 \pm 0.4$	$42.8 \pm 0.6$	$1.3 \pm 0.8$

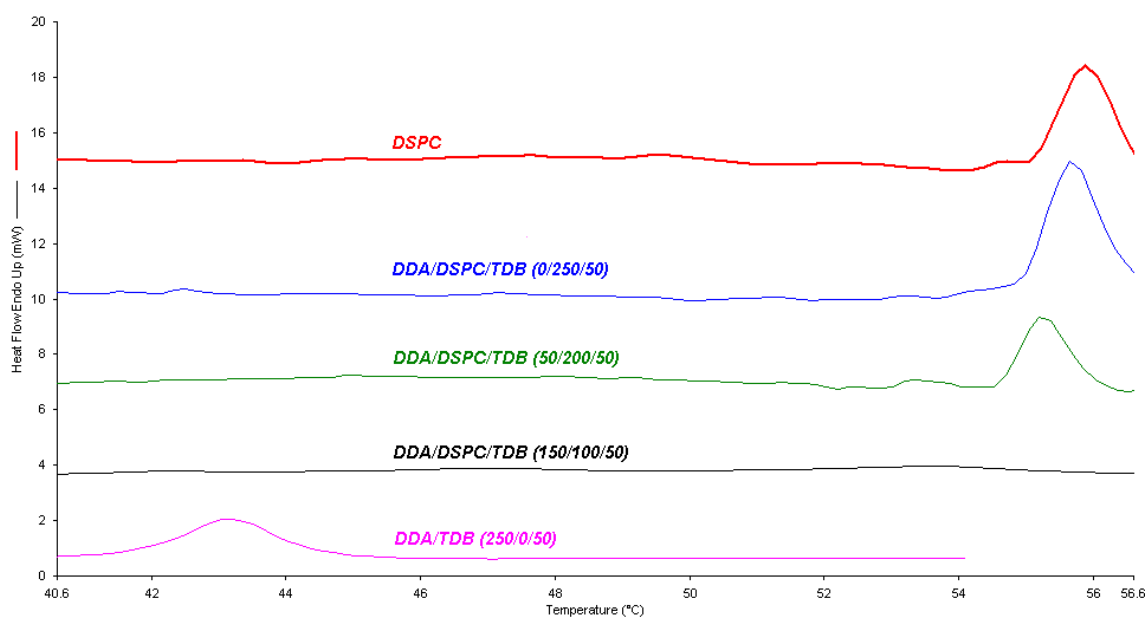
**Figure 4.5. DSC thermograms and associated thermodynamic parameters of the gel-to-liquid phase transition of DDA-DPPC-TDB liposomes.** Liposomes were made by lipid hydration and rehydrated in 10 mM Tris buffer (pH 7.4). DSC thermograms were taken at 10  $^{\circ}\text{C}/\text{min}$  (600  $^{\circ}\text{C}/\text{h}$ ) over the temperature range of 25-75  $^{\circ}\text{C}$ . One of three thermograms per formulation is shown with results representative of the mean  $\pm$  the standard deviation of three independent batches.

When phospholipids are blended together, main phase transitions are known to occur over a wider range as opposed to phospholipids in their pure form (Taylor & Craig, 2003). All lipid components that made up the mixtures in this study contained chains of equal length, comprising of an even number of carbon atoms. The single, well defined peaks represented a more stable system for the multi saturated lipid mixture, suggesting miscibility of all the components. Alternatively, DSC thermograms characterised by several endothermic peaks indicate liposomal instability in multiple lipid formulations, derived from potential heterogeneity in the molecular arrangement within the bilayer (Giatrellis *et al*, 2009).

In the present study, similar experiments were also carried out with DDA replacement in DDA-TDB with DSPC lipid, with such liposome dispersions prepared in Tris buffer as previously conducted. The main phase transition of pure DSPC dispersions was characterised at  $56\text{ }^{\circ}\text{C} \pm 0.2\text{ }^{\circ}\text{C}$  (Figure 4.6), in accordance with findings previously reported in the literature (Koyama *et al*, 1999). When TDB was mixed into the DSPC liposome formulation (DSPC-TDB; 250/50  $\mu\text{g}/\text{dose}$ ) no significant difference in the main melting points was observed ( $56.0\text{ }^{\circ}\text{C} \pm 0.2\text{ }^{\circ}\text{C}$  vs.  $55.1\text{ }^{\circ}\text{C} \pm 0.6\text{ }^{\circ}\text{C}$ , respectively, Figure 4.6). In the multicomponent liposome systems containing DDA, DSPC and TDB at a ratio of 50/200/50  $\mu\text{g}/\text{dose}$  again, the measured  $T_m$  was not significantly different from the DSPC-TDB formulation (Figure 4.6). However, when the amount of DDA increased to 150  $\mu\text{g}/\text{dose}$  (total DDA-DSPC-TDB ratio of 150/100/50  $\mu\text{g}/\text{dose}$ ) no transition was measured within the tested temperature range (Figure 4.6). The absence of a thermal event replicates a stabilising cholesterol effect on the system, as a main phase transition is reported to be abolished upon bilayer incorporation of cholesterol (Chapman & Urbina, 1974), enhancing the orientational order of hydrocarbon chains in the liquid crystalline state and reducing the passive permeability

of lipid bilayers beyond the gel-to-liquid phase transition (McMullen & McElhaney, 1996), evident upon increased integration of cholesterol concentrations up to 50% (Moghaddam *et al*, 2011). The broadening and eventual  $T_m$  elimination upon cholesterol incorporation organises membrane lipids into a state between a solid ordered gel phase and a liquid crystalline phase, producing an intermediate liquid-ordered phase (Mannock *et al*, 2010).

As highlighted earlier, when phospholipids are blended together, a characteristic singular, broader peak is observed, or indeed removed as in the case of DDA replacement with DPPC or DSPC at 150/100/50  $\mu\text{g}/\text{dose}$  (Figures 4.5 & 4.6), via DSC. Contrastingly, when two lipids fail to interdigitate with one another, two separate well defined peaks can be expected (Feitosa *et al*, 2006). For example, the phase characteristics of DDA based cationic liposome mixtures were previously examined by Feitosa *et al*, (2006). Specifically, cationic lipid mixtures of DDA and didodecyldimethylammonium bromide (DODA) were investigated via DSC for the main transition temperature from a gel-to-liquid crystalline state, whereby DDA molar fractions of 0.2-0.8 within DDA-DODA liposomes at a net 1.0 mM lipid concentration were tested. Moreover, two distinct peaks were observed with individual melting points, representing two divided populations of DDA and DODA-enriched liposomes. These separate, independent peaks signified that the two lipids had a low affinity for one another and opposed the observed lipid mixtures of this study, whereby single, broadened peaks obtained for the lipid blends tested were symptomatic of multiple lipid incorporation.



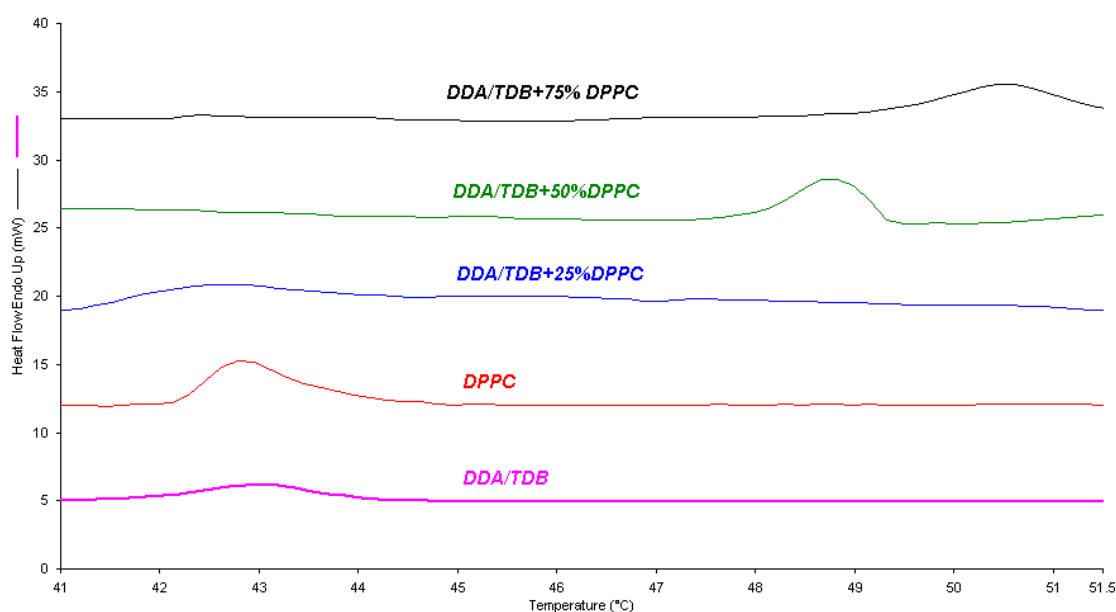
DDA-DSPC-TDB ( $\mu\text{g}/\text{dose}$ )	Onset ( $^{\circ}\text{C}$ )	Peak Max ( $^{\circ}\text{C}$ )	Delta H (J/g)
DSPC	$55.4 \pm 0.2$	$56.0 \pm 0.1$	$1.8 \pm 0.2$
0/250/50	$55.1 \pm 0.5$	$55.1 \pm 0.6$	$1.6 \pm 0.4$
50/200/50	$54.2 \pm 0.4$	$54.7 \pm 0.6$	$0.5 \pm 0.4$
150/100/50	$0.0 \pm 0.0$	$0.0 \pm 0.0$	$0.0 \pm 0.0$
250/0/50	$41.6 \pm 0.4$	$42.8 \pm 0.6$	$1.3 \pm 0.8$

**Figure 4.6. DSC thermogram summary and corresponding parameters of the main gel-to-liquid phase transition of DDA-DSPC-TDB liposomes.** Liposomes were made by lipid hydration in 10 mM Tris buffer (pH 7.4). DSC thermograms were taken at 10  $^{\circ}\text{C}/\text{min}$  (600  $^{\circ}\text{C}/\text{h}$ ) over the temperature range of 25-75  $^{\circ}\text{C}$ . One of three thermograms per formulation is shown with results representative of the mean  $\pm$  the standard deviation of three independent batches.

#### ***4.5. DSC of DDA-TDB liposomes substituted with DPPC or DSPC lipid***

Differential scanning calorimetry was also conducted using an identical experimental approach on further liposomal formulations. More specifically, DSC was used to measure the thermodynamic effect of incorporating additional lipids upon substitution of the DDA-TDB adjuvant, rather than directly replacing the DDA component, i.e. the DDA-TDB ratio remained at a 5:1 weight ratio and the addition of DPPC or DSPC at mol% ratios of 25, 50 and 75 % in substitution of DDA and TDB occurred.

In this series of formulations, liposomal dispersions with 25 mol% DPPC incorporation displayed a single, broadened peak indicative of a melting event of a phospholipid mixture (Figure 4.7). The temperature at which this main melting event occurred was not found to be significantly different to DDA-TDB alone, occurring at 43 °C (Figure 4.7). Indeed, low levels of DPPC incorporation to DDA-TDB have been noted to have no significant effect on the main phase transition from a gel-to-liquid crystalline state (Henriksen-Lacey *et al*, 2010). With DDA-TDB substitution at 50 and 75 mol%, a main melting point was determined in the region of 50 °C. Although both systems showed no significant difference to one another, these two uppermost substituted mixtures allowed for a significant ( $P < 0.05$ ) increase in the measured  $T_m$ , of almost 10 °C, compared to DDA-TDB dispersions prior to further lipid incorporation (Figure 4.7). Here, a favourable increase in the main phase transition was achieved as the systems remained in the gel phase at higher temperatures prior to the main melting event, attaining structural rigidity whilst successfully interdigitating into a single mixture. The broadened shaped endotherms detected for such formulations suggest ideal mixing of the multiple lipid formulation components used in this study (Ali *et al*, 2000).

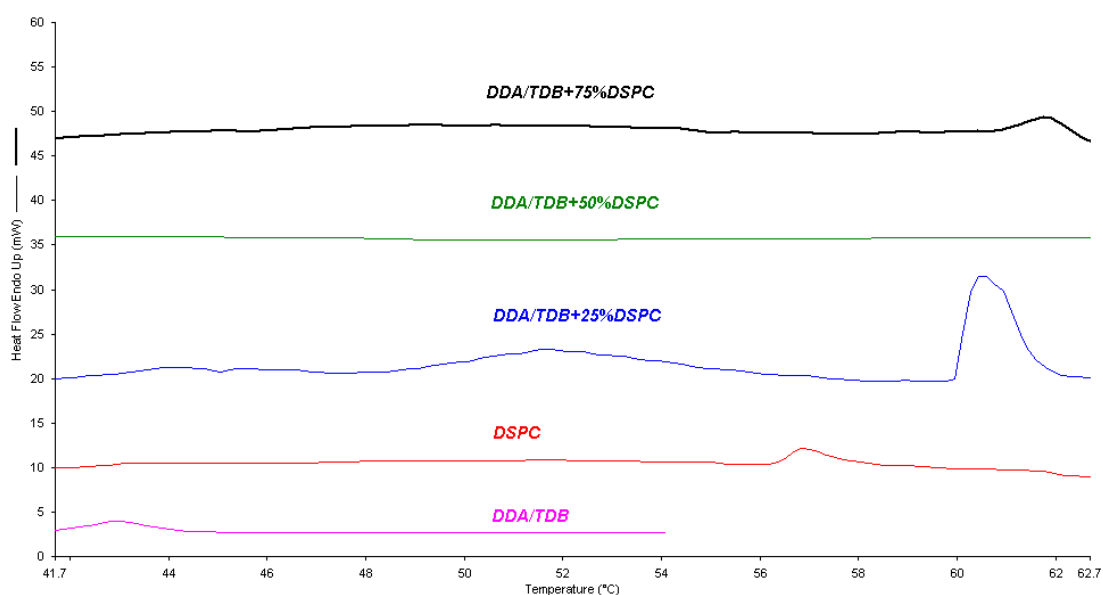


<b>DDA-TDB + mol% DPPC</b>	<b>Onset (°C)</b>	<b>Peak Max (°C)</b>	<b>Delta H (J/g)</b>
+ 25% DPPC	42.1 ± 1.3	43.4 ± 1.5	0.5 ± 0.3
+ 50% DPPC	49.0 ± 1.1	49.4 ± 1.8	0.8 ± 0.4
+ 75% DPPC	50.1 ± 0.8	51.1 ± 0.9	1.2 ± 0.3
<b>DPPC</b>	<b>41.4 ± 0.3</b>	<b>42.3 ± 0.2</b>	<b>2.8 ± 1.4</b>
<b>DDA-TDB (0 %)</b>	<b>41.6 ± 0.4</b>	<b>42.8 ± 0.6</b>	<b>1.3 ± 0.8</b>

**Figure 4.7. DSC thermogram summary and corresponding thermodynamic parameters measured for the main phase gel-to-liquid transition of DDA-TDB liposome dispersions substituted with 25, 50 or 75 mol% DPPC.** Scans of DDA-TDB and pure DPPC lipid have also been overlaid for comparison. Liposomes were produced via lipid hydration in 10 mM Tris buffer (pH 7.4) and thermograms were made at a scan rate of 10 °C/min (600 °C/h) over the tested temperature range of 25-75 °C. One of three thermograms for each formulation is displayed with results representative of the mean ± the standard deviation of three independent liposome batches.

DSC was also conducted upon DDA-TDB systems substituted with DSPC at 25, 50 and 75 mol% (Figure 4.8). Upon incorporation of 25 mol% DSPC, an endothermic peak was evident, shifting to a significantly higher ( $P < 0.05$ ) maximum temperature of  $60.2 \text{ }^{\circ}\text{C} \pm 0.7 \text{ }^{\circ}\text{C}$ , from that of DDA-TDB. This contrasted with the  $T_m$  observed for the equivalent DPPC formulation, as the incorporation of DSPC, with its longer hydrocarbon chains, led to higher temperatures required to alter its well ordered gel state. Interestingly, when DDA-TDB was substituted with 50 mol% DSPC, no main melting event was detected within the tested temperature range. For DDA-TDB-75 mol% DSPC, the main phase transition was also significantly modified ( $P < 0.05$ ) by  $20 \text{ }^{\circ}\text{C}$  from DDA-TDB, characterised at a peak of  $62 \text{ }^{\circ}\text{C}$  (Figure 4.8). This particular composition represented the uppermost incorporation of DSPC, and the main thermal event occurring over a wider temperature range suggests complete miscibility for the multicomponent adjuvant system (Taylor & Morris, 1995), with the configuration of DSPC within DDA-TDB possibly strengthening the hydrocarbon arrangement, thus requiring more energy to melt the hydrocarbon chains at the point of phase transition.

It is understood that lipids with chain length differences encourage bilayer integration in lipid bilayer mixtures (Sisk, 1990). The differences in chain lengths are apparent when observing the phospholipid mixtures formed as a result of DDA-TDB adjustment in this study, from either its cationic replacement or substitution. An increased introduction of DPPC for example, with its 16 carbon chains that represented a small chain length difference between the 18 carbons of DDA within DDA-TDB, generated noticeably broader peaks. Furthermore, substitution with the longer chained DSPC lipid led to elevated phase transition temperatures whilst also displaying multiple lipid incorporation, characterised by single defined peaks.



DDA-TDB + mol% DSPC	Onset (°C)	Peak Max (°C)	Delta H (J/g)
+ 25% DSPC	59.6 ± 0.4	60.2 ± 0.7	3.3 ± 2.8
+ 50% DSPC	0.0 ± 0.0	0.0 ± 0.0	0.0 ± 0.0
+ 75% DSPC	61.6 ± 1.0	62.5 ± 0.6	3.1 ± 0.9
DSPC	55.4 ± 0.2	56.0 ± 0.1	1.8 ± 0.2
DDA-TDB (0%)	41.6 ± 0.4	42.8 ± 0.6	1.3 ± 0.8

**Figure 4.8. DSC thermogram summary and corresponding thermodynamic parameters measured for the main phase gel-to-liquid transition of DDA-TDB liposome dispersions substituted with 25, 50 or 75 mol% DSPC.** Scans of DDA-TDB and pure DSPC have also been overlaid for comparison. Liposomes were produced via lipid hydration in 10 mM Tris buffer (pH 7.4) and thermograms were made at a scan rate of 10 °C/min (600 °C/h) over the tested temperature range of 25-75 °C. One of three thermograms for each formulation is displayed with results representative of the mean ± the standard deviation of three independent liposome batches.

The exception to all of the tested substituted systems was seen with 50 mol% DSPC substitution of DDA-TDB, with thermal events abolished beyond detection, producing a possible intermediate fluid ordered phase (Henriksen-Lacey *et al*, 2011a). A comparable effect is seen from increased cholesterol incorporation into liposomal dispersions, such as systems composed of saturated phosphatidylcholines of DPPC, whereby phase transition peaks become broader until an eventual abolition of the cooperative gel-to-liquid crystalline phase transition of the bilayers is observed (Bolean *et al*, 2010). As highlighted earlier, this abolition of a phase transition occurs when cholesterol is incorporated at concentrations of 50 mol% (McMullen *et al*, 1993), which can minimise drug leakage from formulated vesicles (Bedu-Addo & Huang, 1995).

The broadening of the peaks attained in the thermograms of this study is indicative of lipid blends, particularly with lipids of apposing hydrocarbon chain lengths, whereby a difference of two carbon atoms in the phospholipid tails represents an ideal mixture of phases. However, as the difference in hydrocarbon chains of phospholipids become greater, the level of phase mixing declines, producing regions of immiscibility in the gel phase, notably seen with chain differences as high as six carbons (Mabrey & Sturtevant, 1976). This level of immiscibility was verified by Feitosa *et al*, (2006), in which DODA-DDA mixtures represented a difference in phospholipid chain lengths of six carbon atoms. Such dispersions generated two main melting events independent of each other, opposing the singular defined peaks of the phospholipid adjuvant mixtures assessed in this study. However, as highlighted previously, the effect of TDB on the phase behaviour of DDA liposomes suggested incorporation of the 22-carbon acyl chains of TDB at 11 mol%, into the 18-carbon alkyl twin tailed DDA lipid, producing

TDB enriched domains and a resultant broadened main phase transition (Davidsen *et al.*, 2005).

#### **4.6. Conclusions**

In conclusion, liposomal dispersions of DDA, DDA-TDB and the replacement and substitution of DDA-TDB were analysed for their main phase transitions, which indicated lipid interdigitation of the proposed multicomponent delivery systems. DDA dispersions alone presented a sharp endothermic peak indicative of a main melting event, with the addition of TDB displaying incorporation within the DDA bilayers. Upon cationic replacement with an incremental increase of DPPC, the main phase transition temperature was characterised below that of DDA-TDB. In contrast, equivalent DDA replacement formulations with DSPC yielded higher phase transition events, beyond DDA-TDB upon incorporation of this longer chained phospholipid.

Additionally, as the substitution of DDA-TDB increased with DPPC or DSPC lipid, detected thermal events were generally observed at higher temperatures, beyond DDA-TDB dispersions alone and the pure substituted lipid used. All of the tested systems demonstrated thermograms typical of phospholipid mixing, with the exceptions of partial cationic replacement with either lipid (150/100/50 µg/dose) and 50 mol% substitution with DSPC, possibly enhancing the structural rigidity of the system, as the orientation of hydrocarbon chains is altered within the lipid mixture, providing a stable, fluid ordered phase, as any thermal events were undetectable in the tested temperature range.

As a result of DSC analysis, thermograms for the outlined adjuvant systems containing DDA with TDB and either DPPC or DSPC displayed single, broadened main gel-to-liquid phase transition peaks indicative of phospholipid blends, suggesting that the multicomponent liposomal dispersions interdigitated with one another. Furthermore, these liposomal systems can be prepared at lower temperatures, and may be stable beyond physiological temperature, potentially prolonging drug retention, making their application beneficial as drug delivery systems.

## **Chapter 5**

### **Liposomal immunoadjuvants and their ability to activate macrophages *in vitro***

## **5.1. Introduction**

### *5.1.1. Therapeutic applications of liposomal delivery systems*

Liposomal delivery systems have various uses in the modulation of the immune system, providing a potent means of drug delivery as they are non destructive to cell membranes, able to transfect numerous different cell types and are metabolically compatible, whilst facilitating the possibility of targeting desired tissues of interest *in vivo* (Smith *et al*, 1993). The use of liposomal adjuvants are also advantageous as they are biodegradable, relatively non-toxic and FDA approved, whilst they can be easily manufactured and tailored in order to maximise efficacy from optimising antigen-liposome complexes (Fries *et al*, 1992).

Cationic liposomal systems can be used to deliver peptides, proteins and DNA, whilst also acting as adjuvants in the enticement of immunological reactions, triggered from the effective delivery of antigens (O'Hagan & Singh, 2002). Furthermore, liposomes of a cationic nature have been utilised as potential delivery systems and immunological therapies, with the ability to function as immunomodulators in the enhancement of anti-microbial, anti-viral or anti-inflammatory treatments (Filion & Phillips, 1997).

### *5.1.2. Liposomes as immunoadjuvants*

Upon antigen delivery, activation of innate immune receptors associated to APCs, e.g. macrophages and DCs, engage with and present antigen material to T cells through pathogen recognition receptors, and are employed by APCs to identify pathogen-associated molecular patterns (Akira *et al*, 2006). Such pathogen recognition receptors activate the transportation of APCs from the site of injection for example, to the T-cell

region of the draining lymph nodes for eventual stimulation of naive T-cells, pivotal to adaptive immunity and essential to humoral and cellular immune responses (Pulendran & Ahmed, 2006).

With careful manipulation, liposomal immunoadjuvants can potentially target and associate with APCs, inducing cell mediated Th1 type immunity or a humoral Th2 type immune response in reaction to the presence of specific antigen (Gregoriadis, 1990; Galdiero *et al*, 1995). The main location in which liposomes congregate upon injection or infusion is that of the macrophages (Velinova *et al*, 1996), which can phagocytose a vast volume of antigen or liposome when presenting antigens (Filion *et al*, 1996). Key to cell mediated immunity induced from antigen delivery is the activation of macrophages and the release of cytokines, of which a major immunomodulator secreted is tumour necrosis factor alpha (TNF- $\alpha$ ). This particular cytokine receptor, primarily generated by macrophages with an anti-viral and anti-tumoural activity, improves T and B lymphocyte responses and is a significant contributory factor of inflammatory reactions (Vassalli, 1992). Such an inflammatory compound, discharged by the macrophage antigen presenting cell, therefore provides a definitive marker for macrophage activation.

Before immunological evaluation of the DDA-TDB based formulations and their ability as drug delivery systems *in vivo*, it was necessary to assess the outlined systems *in vitro*, in order to determine their potential in stimulating targeted and protective immune responses. A mouse macrophage J774 cell line was selected as the experimental model as it is one of the most sustainable cell lines to culture, justifying its widespread utilisation as an *in vitro* model (Stumpo *et al*, 2003). Therefore, the aim of this chapter was to establish associated

levels of toxicity, phagocytic activity and to quantify secreted levels of the TNF- $\alpha$  cytokine *in vitro*, verifying liposomal cytotoxicity, uptake and expression. This was conducted in response to the proposed DDA-TDB based liposomal immunoadjuvants characterised earlier in this study upon introducing additional DPPC or DSPC lipids, in which DDA was replaced or DDA-TDB was substituted whilst the DDA:TDB ratio remained locked, in order to ascertain the effect of cationic content or adjuvant concentration respectively.

### ***5.2. Cytotoxicity studies: MTS cell proliferation assay***

Given the association of DDA with toxicity, investigations into the cytotoxicity of the DDA-TDB based formulations previously characterised in Chapter 3 took place. Indeed, these liposomal systems were assessed for their effect upon macrophage cell proliferation.

#### ***5.2.1. Calibration of BALB/c cell number***

Prior to applying the MTS assay upon the DDA-TDB based formulations, the appropriate cell number to be used was determined by producing a cell calibration curve. Cell numbers ranging from 0-400,000 BALB/c cells per ml were tested to ascertain an optimum quantity of cells upon which the liposomal formulations could be introduced. As displayed in Figure 5.1, the measured absorbance, which is directly proportional to the volume of viable cells, steadily increased with a rise in cell number. The chosen number of cells to be used was deduced from where the linear range within the calibration curve started. This region can be seen to coincide with a BALB/c cell number of  $8 \times 10^4$ /ml ( $8 \times 10^3$ /well/100  $\mu$ l), and was therefore selected as a suitable cell number to be used for the subsequent *in vitro* experiments.

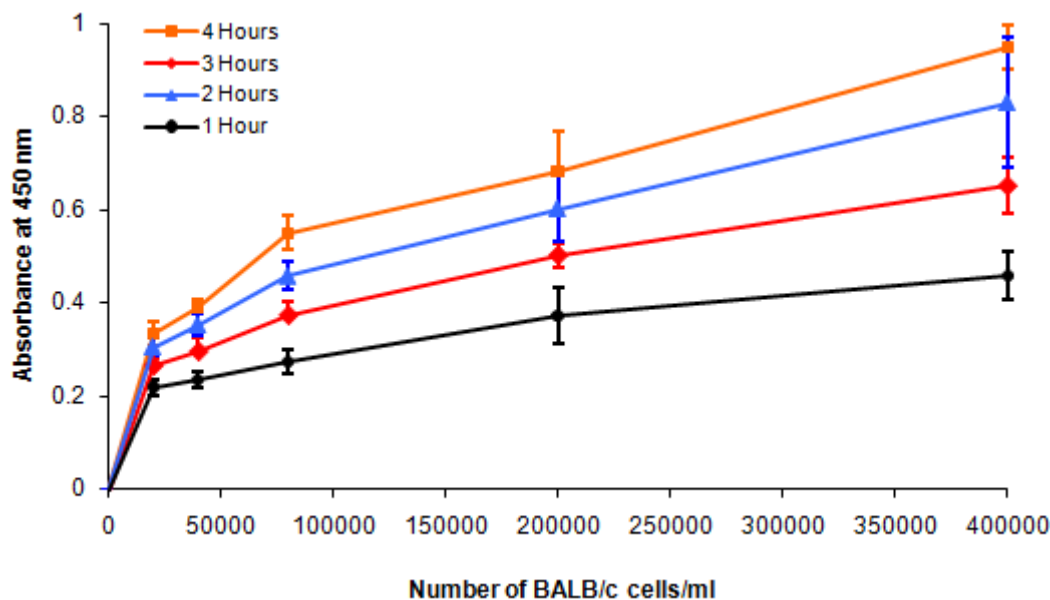


**Figure 5.1. Calibration of BALB/c cell proliferation.** MTS absorbance readings were taken over time for the BALB/c cell numbers of 0,  $2 \times 10^4$ ,  $4 \times 10^4$ ,  $8 \times 10^4$ ,  $2 \times 10^5$  and  $4 \times 10^5$ /ml. The results displayed are the mean averages and the standard deviation of triplicate wells.

### 5.2.2. Determination of liposome sample concentration

With the cell number established, the concentration of the cationic component, DDA, was analysed upon resultant macrophage cell proliferation. The selected BALB/c cell number of  $8 \times 10^4$ /ml was plated out and incubated overnight prior to the addition of DDA-TDB and DSPC-TDB liposomes, adjusted to the sample concentrations of 2.5, 5.0, 7.5, 10, and 15  $\mu\text{g}/\text{ml}$ . Subsequent incubation of the BALB/c cells and samples took place overnight before calculating the levels of cell proliferation.

Upon the addition of the MTS reagent and after one hour of incubation, which allowed for the MTS reagent to be broken down into formazan product by dehydrogenase enzymes of viable cells, the cell viability was calculated. After introducing DSPC-TDB at concentrations of 2.5 up to 15.0  $\mu\text{g}/\text{ml}$ , calculated BALB/c cell proliferation was consistently in the region of 90%, with no significant difference between the varying

sample concentrations, suggesting that this formulation had no impact on the measured cell viability in the tested concentration range (Figure 5.2). In contrast, DDA-TDB displayed a concentration dependent cytotoxic effect as DDA-TDB at a concentration of 2.5  $\mu\text{g/ml}$  generated cell viability at  $\sim 70\%$ , which was reduced to around 50-60% at concentrations of 5.0 to 7.5  $\mu\text{g/ml}$ , and finally at the highest concentration of 15  $\mu\text{g/ml}$ , little viable cells could be measured (Figure 5.2).

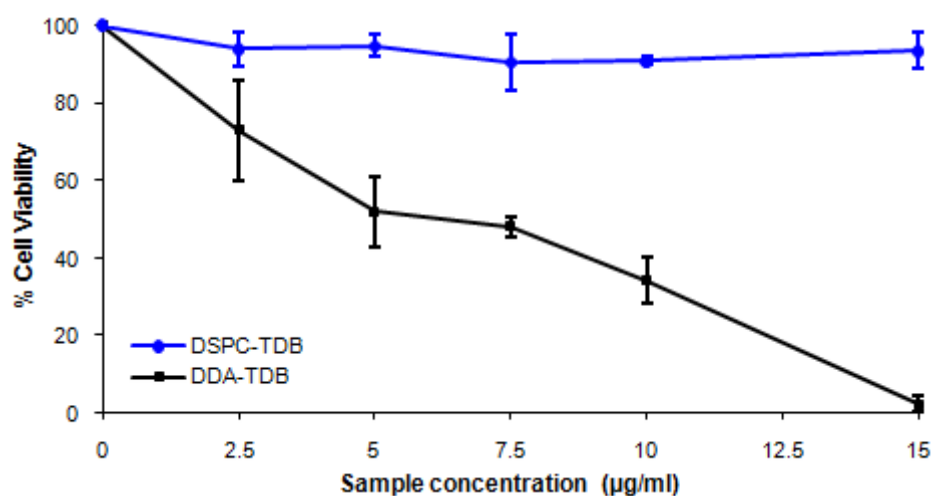


**Figure 5.2. Effect of sample concentration on the cell viability of DDA-TDB vs. DSPC-TDB.** The BALB/c cell number was adjusted to  $8 \times 10^4$  cells/ml and absorbance measurements were made for each concentration in triplicate, with error bars displaying the standard deviation from the mean average.

Cationic liposomal systems disadvantageously confer a high toxicity to cells (Romoren *et al*, 2004), resulting from electrostatic interactions with cell membranes (Fischer *et al*, 2003), and at increased concentrations, induces apoptosis of antigen presenting cells and suppresses the immune response (Ma *et al*, 2009), which unfortunately restricts their safety for clinical use (Lv *et al*, 2006). The addition of TDB to DDA vesicles not only physically stabilises DDA, it also comes with the desirable trait of being less cytotoxic due to a reduced fatty acid chain length, particularly in comparison to its

immunostimulating synthetic analogue, TDM (Pimm *et al*, 1979; Olds *et al*, 1980). Therefore, the cytotoxic effect observed in this study, upon an increased concentration of the DDA-TDB formulation, can be attributed to the cationic DDA lipid presence, opposing the DSPC based system composed of neutral lipids which generated consistently high cell proliferation levels, even at higher concentrations.

### 5.2.3. Cell toxicity studies: DDA replacement within DDA-TDB

The effect of the DDA lipid presence within DDA-TDB was assessed upon its gradual replacement with either DPPC or DSPC. DDA-TDB was used as a control formulation, with macrophage cells alone and the cell culture growth medium (DMEM), which was a negative control. Based on the preliminary studies conducted, the sample concentration was set to 5.0 µg/ml and was also compared against formulations at 10.0 µg/ml, with a BALB/c cell number of  $8 \times 10^4$ /ml applied throughout all subsequent *in vitro* assays.

As previously observed, DDA-TDB liposomes at 5.0 µg/ml produced a cell viability of 50-60%, and at a concentration of 10 µg/ml the measured viability was dramatically reduced to half the recorded level, to within the region of 30% (Figure 5.3). Upon increasing the replacement of DDA with DPPC or DSPC lipid, a rise in cell viability was observed as the presence of the cationic component decreased with, in general, no significant difference between the DPPC and DSPC based formulations at 5 µg/ml (Figure 5.3a and b), with cell viability ranging from approximately 60-90%. At the concentration of 10 µg/ml, cell viability for the DPPC based systems was significantly ( $P < 0.05$ ) lower than their DSPC equivalents ranging from ~30-60% and ~40-90% respectively, however

at this increased concentration, a similar trend was still apparent, with increased replacement of DDA content with either lipid resulting in increased cell proliferation.

Introducing zwitterionic lipids in the replacement of cationic content in the present study ultimately reduced the toxicity upon macrophages, in co-operation with previous studies by Filion & Phillips, (1997), whereby dioleoylphosphatidylethanolamine (DOPE) in conjunction with the cationic lipid of dioleoyldiacyltrimethylammonium propane (DOTAP) was replaced with DPPC. The gradual replacement of DOPE with DPPC notably diminished the toxicity upon macrophages as cell viability was enhanced, determined by lactate dehydrogenase (LDH) activity, an enzyme indicative of cell death. Although total replacement of DOPE (DPPC-DOTAP) was unable to completely eradicate the associated toxicity, the limit of toxicity was 15%, with the applied LDH assay based on murine macrophage death. Interestingly, the results of this study, which quantified the level of cell proliferation, and thus an inverse indicator of toxicity compared to the LDH assay, reached a limit of ~85% cell viability when DPPC completely replaced DDA in DDA-TDB. This corresponds to a presumed toxicity of 15% in terms of cell death, demonstrating a comparable reduction in toxicity upon introducing lipids such as DPPC.

In addition, Manosroi *et al.*, (2008), when formulating cationic liposomes for gene therapy, determined that an increased incorporation of DPPC and cholesterol to DDA vesicles reduced the toxic effect upon mouse melanoma cells. Moreover, based on the findings in this study in which an increased DDA-TDB concentration decreased cell viability, the level of cationic content can be understood to be the main factor influencing the cytotoxicity of the liposomal formulation.

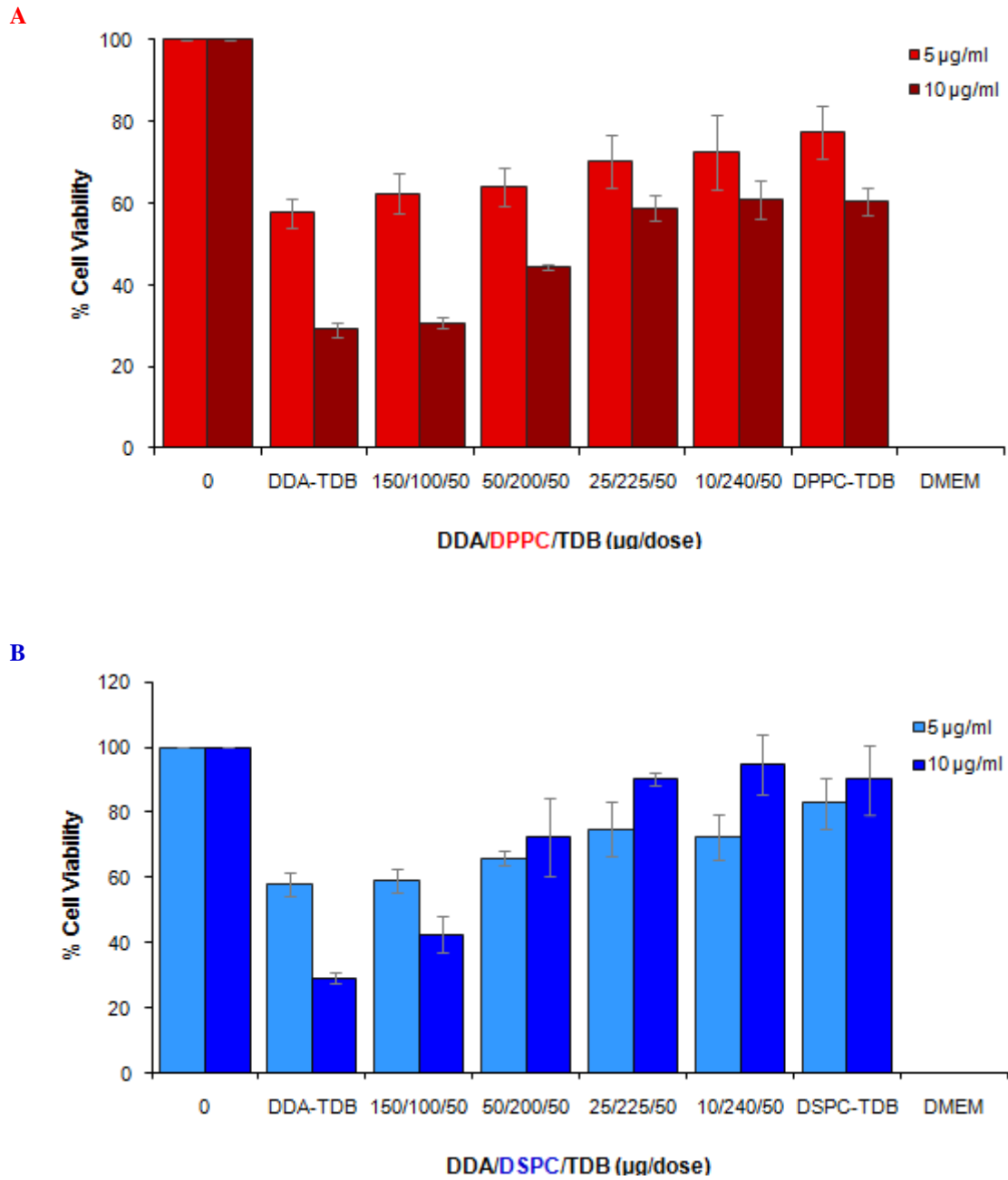


**Figure 5.3.** Cell viability for DDA-TDB and the replacement of DDA with (A) DPPC or (B) DSPC. Formulations were set to a concentration of 5.0 and 10.0 µg/ml with  $8 \times 10^4$ /ml BALB/c cells. Measurements were made on triplicate wells with results of the mean and standard error of three independent experiments.

#### 5.2.4. Cell toxicity studies: substitution of DDA-TDB

As established earlier, reducing the cationic DDA lipid content reduces the cytotoxic effect of the formulation. Subsequently, this second set of substituted systems was tested for their toxicity upon macrophage cells with the DDA:TDB ratio fixed, but upon increased substitution of the main DDA-TDB immunoadjuvant, became reduced in concentration.

As previously observed, DDA-TDB generated a cell viability within the region of 50% yet substitution with 25 mol% DPPC or DSPC significantly ( $P < 0.05$ ) elevated cell viability to within the region of 70% (Figure 5.4 A and B), which was not significantly different to the levels of macrophage cell proliferation observed upon further substitution with either additional lipid at 50 mol% (Figure 5.4 A and B). However, upon a further reduction of DDA-TDB concentration with 75 mol% incorporation of DPPC or DSPC lipid, a further significant ( $P < 0.05$ ) increase in cell viability was recorded by approximately 10% (Figure 5.4 A and B). Furthermore, no difference in the substituted systems was apparent between one another when DPPC or DSPC was substituted into DDA-TDB.

Moreover, an adjuvant concentration dependent effect upon the cytotoxicity of the formulation was apparent. Indeed, as 25, 50 and 75 mol% incorporation of either lipid indecently coincided with an approximate 25, 50 and 75% reduction in DDA content (see Chapter 2, Table 2.1), this impacted upon favourably reducing the associated cytotoxicity of DDA-TDB, whilst also corroborating with the effect of DDA previously observed when the cationic content was replaced within the formulation.

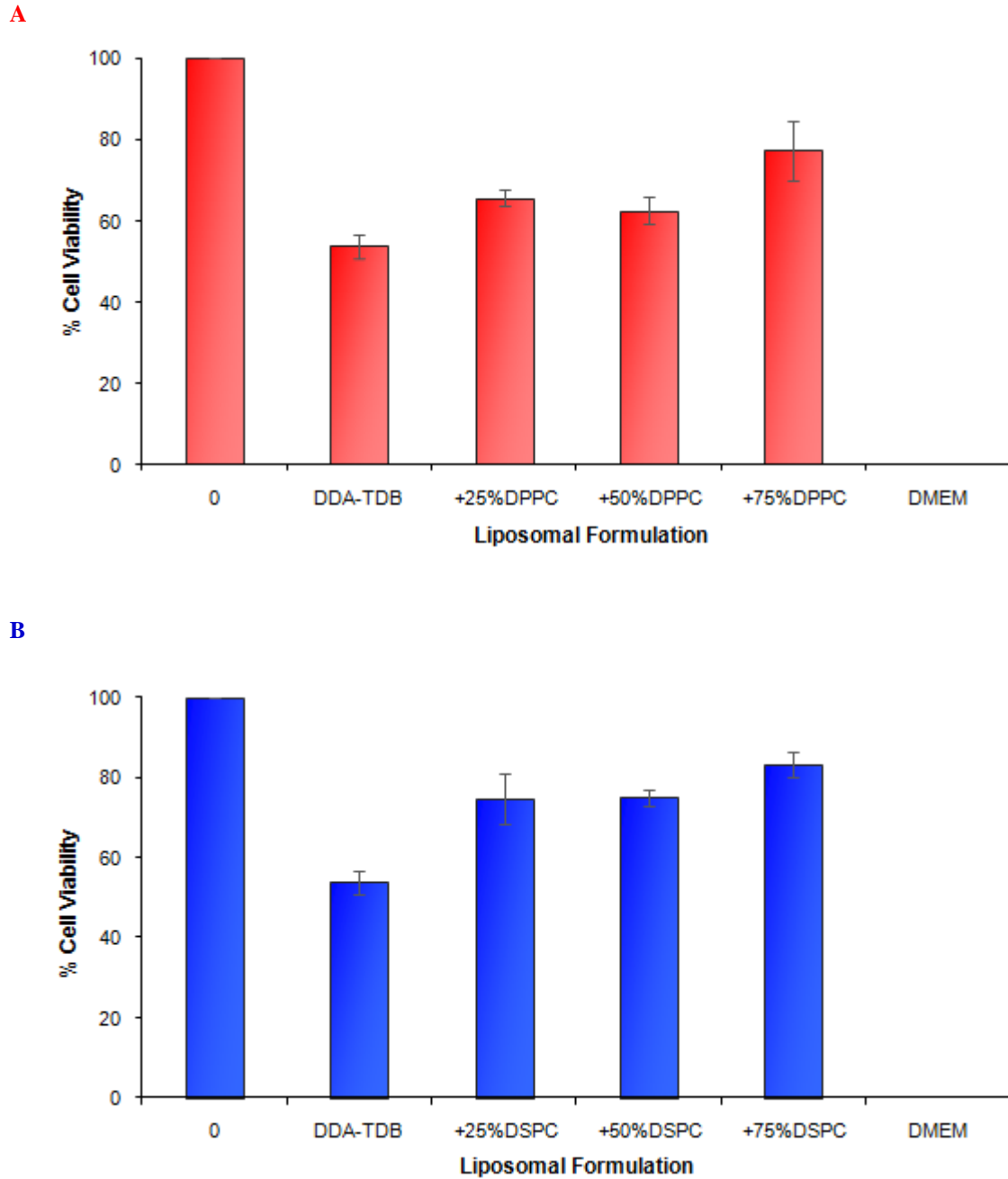


**Figure 5.4. Cell viability of DDA-TDB substituted with (A) DPPC or (B) DSPC lipid.** Formulations were set to a 5.0  $\mu\text{g/ml}$  concentration with  $8 \times 10^4/\text{ml}$  BALB/c cells. Measurements were made upon triplicate wells with results representing the mean average and standard error from three independent experiments.

### ***5.3. Determination of phagocytic activity: $\beta$ -N-Acetylglucosaminidase (NAG) assay***

It is important to understand the extent of phagocytosis induced by the proposed immunoadjuvants, primarily due to macrophages comprising an innate ability to non-specifically phagocytose an immense magnitude of particles such as liposomes, a process that T cells are unable to achieve (Adams & Hamilton, 1984). Macrophages are capable of consuming liposomal systems that carry protein antigen and subsequently present such material to T lymphocytes, advancing the initiation of an immunological response (Harding *et al*, 1991; Filion *et al*, 1996). Therefore, the NAG assay was applied to test the effect of liposomal sample concentration and the levels of phagocytic activity induced by the various DDA-TDB based formulations.

#### *5.3.1. Effect of sample concentration upon resultant NAG release*

Macrophages, also known as professional phagocytes, contain surface receptors capable of detecting foreign and dangerous particles (Robinson & Babcock, 1998; Ernst & Stendahl, 2006) and can process high quantities of material (Cannon & Swanson, 1992). The process of endocytosis, whereby cells engulf and ingest particulates, can be categorised into two main types: phagocytosis (cellular eating) of large particles, typically greater than 250 nm, and pinocytosis (cellular drinking) of smaller particles, soluble macromolecules or fluid and low molecular weight solutes, all of which are less than 200 nm in size (Silverstein *et al*, 1977; Kaisto, 2003). In order to measure the level of phagocytic activity in the present study, as all of the proposed liposomal adjuvant formulations were previously characterised to be greater than 250 nm in particle size and thus, will most likely become phagocytosed when encountered by macrophages, the release of NAG,

which is a lysosomal enzyme released by macrophages after phagocytosing particulate material (Mack *et al*, 1995), can be used as a marker of phagocytic activity.

To optimise the concentration to be used within the assay, the effect of sample concentration on stimulating NAG activation was assessed at 2.5-15 µg/ml. As previously established for the MTS assay, the BALB/c cell number of  $8 \times 10^4$ /ml was used for all NAG experiments with NAG enzyme release quantified in units per ml. DDA-TDB yielded the highest activation at 2.5 and 5.0 µg/ml, in the region of 0.8 units/ml (Figure 5.5). However, beyond a sample concentration of 5.0 µg/ml, the level of calculated activity was significantly ( $P < 0.05$ ) reduced, with DDA-TDB at 7.5, 10.0 and 15.0 µg/ml all generating NAG activity in the proximity of 0.4 units per ml, which was approximately half of the activation calculated at 2.5 and 5.0 µg/ml (Figure 5.5).

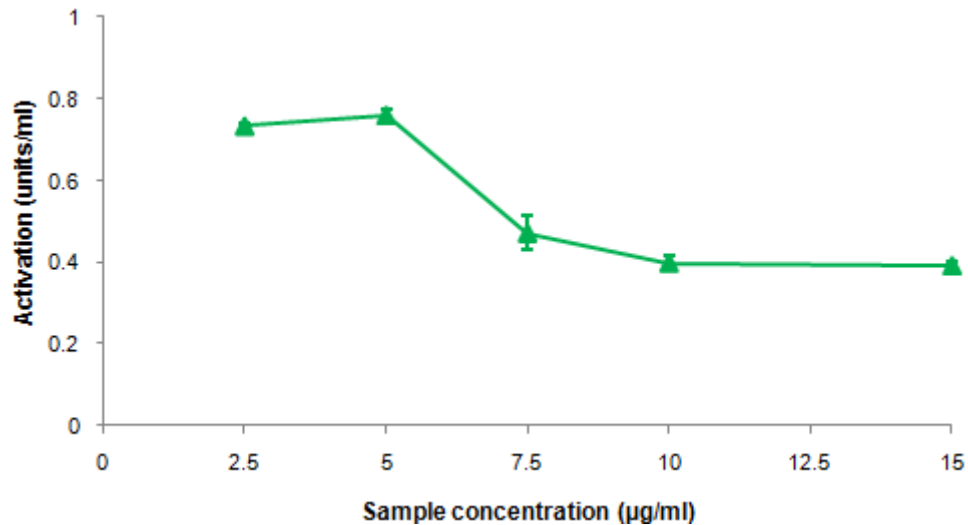


**Figure 5.5. Effect of DDA-TDB sample concentration on NAG activation.** The BALB/c cell number of  $8 \times 10^4$ /ml at DDA-TDB concentrations of 2.5-15.0 µg/ml was tested. The calculated positive and negative control values were 45.07 and 0.04 units/ml respectively. Absorbance measurements were made from each concentration in triplicate, with mean values and standard error of the calculated NAG activation displayed.

### 5.3.2. Induced phagocytic activity upon replacement of DDA or substitution of DDA-TDB

Phagocytic activity was ascertained via the NAG assay upon selected DDA-TDB replacement and substituted formulations as displayed in Table 5.1 (For a comparison of all the outlined DDA-TDB based formulations of this study, see Appendix 1). Together with DDA-TDB, partial and complete DDA replacement was tested with an intermediate level of substitution in order to cover a wide range of formulations that were physicochemically characterised previously (see Chapter 3).

**Table 5.1. DDA-TDB based formulations in which the main liposomal adjuvant was either substituted or replaced, prior to the evaluation of induced phagocytic activity and macrophage activation.**

<b>DDA-TDB Formulation</b>	<b>DDA volume (µg/dose)</b>	<b>Lipid volume (µg/dose)</b>	<b>TDB volume (µg/dose)</b>
DDA-TDB	250	0	50
DDA/DPPC/TDB	150	100	50
DDA/DSPC/TDB	150	100	50
DDA-TDB-50% DPPC	125	165	25
DDA-TDB-50% DSPC	125	175	25
DPPC-TDB	0	250	50
DSPC-TDB	0	250	50

After evaluating the effect of DDA-TDB sample concentration upon NAG activation, as previously set for the MTS assay, based on the concentration of the cationic component of DDA, the sample concentration of 5.0 µg/ml with  $8 \times 10^4$ /ml BALB/c cells was applied to

the outlined formulations in triplicate. This concentration was selected as it provided optimal detection of phagocytic activity via the NAG assay.

DDA-TDB was found to stimulate the highest level of activation, producing approximately 0.8 units/ml (Figure 5.6). Partial replacement of DDA-TDB with either DPPC or DSPC, (DDA/LIPID/TDB at 150/100/50  $\mu\text{g}/\text{dose}$ ), elicited a significantly ( $P < 0.05$ ) lower volume of NAG activation compared to DDA-TDB, at  $\sim 0.6$  units/ml (Figure 5.6a). Furthermore, complete removal of DDA, as in the case of the DPPC-TDB and DSPC-TDB liposomes, generated a further significant ( $P < 0.05$ ) reduction in the level of measured phagocytic activity, stimulating  $\sim 0.2$  units/ml (Figure 5.6a), with no significant difference apparent between the DPPC and DSPC based formulations.

Interestingly, the absence of DDA in the system did not completely eradicate NAG activation with activity remaining significantly higher ( $P < 0.05$ ) than media alone, which may be due to the presence of the immunostimulatory glycolipid TDB and/or the larger particle size of the systems. Indeed despite the variation in recorded phagocytic activity in these tested liposomal formulations, NAG activation was stimulated by all of the proposed immunoadjuvants. As highlighted earlier, vesicle size, especially particles greater than 250 nm, is a key factor influencing the onset of phagocytic activity (Kaisto, 2003) and the observed levels of NAG activation in the present study were stimulated by the proposed systems, previously characterised to be within the size range of approximately 500-2000 nm.

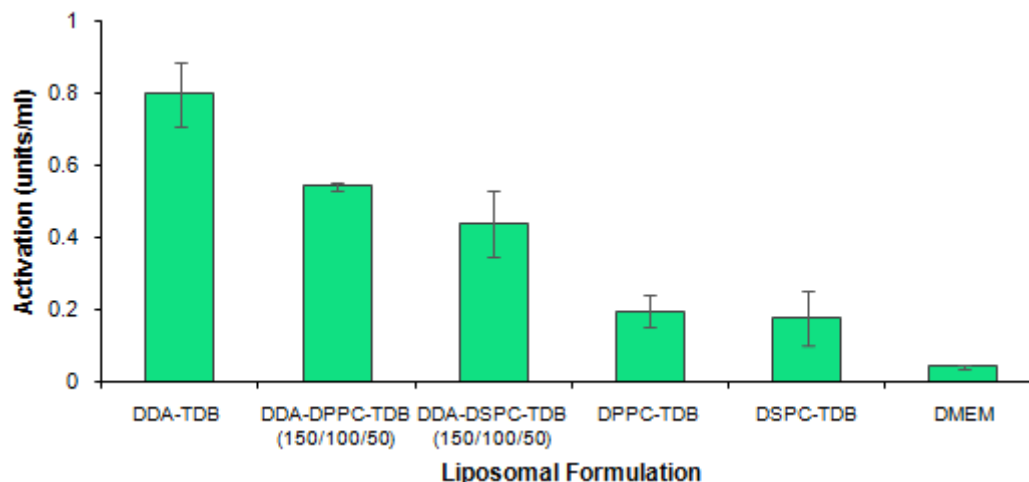


**Figure 5.6a. Stimulation of NAG activation upon replacement of DDA within DDA-TDB.** NAG activation was calculated with  $8 \times 10^4$ /ml BALB/c cells at 5.0  $\mu\text{g}/\text{ml}$ . Values represent the volume ( $\mu\text{g}$ ) of DDA, DPPC or DSPC and TDB per 200  $\mu\text{l}$  dose. The positive and negative controls generated 42.35 and 0.04 units/ml respectively. The mean and standard deviation of three independent experiments are displayed.

In consideration of vesicles where the DDA:TDB ratio was locked but reduced in concentration (Fig 5.6b), whereby both DDA and TDB concentrations were reduced (DDA/TDB + 50% DPPC or DSPC: which is equivalent to a dose of 125  $\mu\text{g}$  DDA, 25  $\mu\text{g}$  TDB and 165  $\mu\text{g}$  DPPC or 175  $\mu\text{g}$  DSPC; Table 5.1), activation levels were also significantly ( $P < 0.05$ ) reduced when compared to the DDA-TDB liposomes, to the region of 0.3 units per ml, with no significant difference apparent between the systems when either substituting lipid of DPPC or DSPC was used (Figure 5.6b).

Interestingly, this level of activation represents half the recorded level of the partially replaced DDA-LIPID-TDB systems (Figure 5.6a) which contained slightly more DDA content and twice the volume of TDB (50  $\mu\text{g}$ ), and as both these sets of formulations have been previously characterised in this study to be of a comparable particle size, the difference in response demonstrates the potentiating effect of TDB upon the formulation.

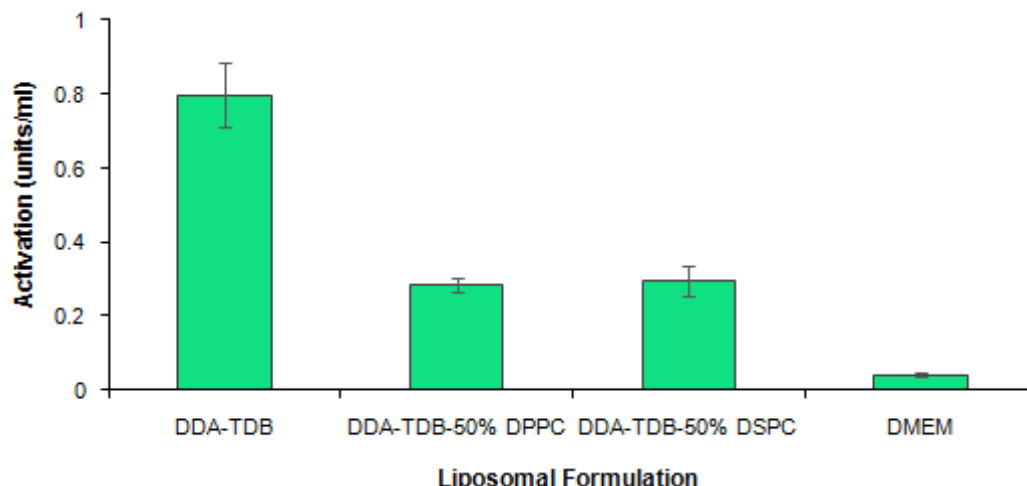


**Figure 5.6b.** NAG activation induced by DDA-TDB and its substitution with DPPC or DSPC. Phagocytic activity was indicated by NAG activation with  $8 \times 10^4$ /ml BALB/c cells at a sample concentration of 5.0  $\mu$ g/ml. Results shown are the mean average and standard deviation of three independent experiments.

#### **5.4. Determination of macrophage activation upon quantification of TNF- $\alpha$**

In the context of immunisation against TB, the TNF- $\alpha$  cytokine mediates many positive factors as it leads to formation and maintenance of granulomas to control the latent TB infection, supports apoptosis of macrophages infected with MTB and enhances the maturation of APCs, which facilitates antigen presentation to the lymph nodes to then prime T cell subsets and ultimately clear the pathogen (Wang *et al*, 2009). In addition, TNF- $\alpha$  increases macrophage function and is therefore an indicative marker of macrophage activation and for the present study, the level of TNF- $\alpha$  cytokine secretion was quantified in response to varying liposomal sample concentrations and the DDA-TDB based formulations.

##### **5.4.1. Effect of sample concentration on mouse TNF- $\alpha$ cytokine production**

The previously observed NAG activation signifies liposomal uptake via the endocytic pathway, and the onset of phagocytic activity is determined by attachment to specific

PAMPs, ultimately leading to the activation of NF- $\kappa$ B, a protein complex that acts as a primary response to harmful cellular stimuli by initiating the transcription of pro-inflammatory cytokines such as TNF- $\alpha$  (Chandel *et al*, 2000; Parham, 2005). In the present study, a mouse TNF- $\alpha$  ELISA development kit was applied to assess TNF- $\alpha$  cytokine release upon introducing the proposed liposomal adjuvants.

Prior to testing the DDA-TDB based systems, the effect of sample concentration was determined, as previously conducted for the MTS and NAG assays, with DDA-TDB set to a range of concentrations between 2.5-15.0  $\mu$ g/ml, with  $8 \times 10^4$ /ml BALB/c cells. At a sample concentration of 2.5  $\mu$ g/ml, DDA-TDB generated approximately 100 pg/ml of TNF- $\alpha$  (Figure 5.7). The peak of TNF- $\alpha$  cytokine activation produced by macrophages in the presence of DDA-TDB was induced at 5.0  $\mu$ g/ml with approximately 200 pg/ml, generating a significantly ( $P < 0.05$ ) higher level than the sample concentration of 2.5  $\mu$ g/ml (Figure 5.7). This result reinforces the selection of 5.0  $\mu$ g/ml as the desired sample concentration to proceed with and to be applied to all subsequent *in vitro* ELISA experiments involving DDA-TDB based liposomes. In addition, DDA-TDB at 7.5, 10 and 15  $\mu$ g/ml resulted in significantly ( $P < 0.05$ ) reduced levels of TNF- $\alpha$  to within the region of 100 pg/ml (Figure 5.7), which was comparable to the levels stimulated at the lowest DDA-TDB concentration initially introduced at 2.5  $\mu$ g/ml.

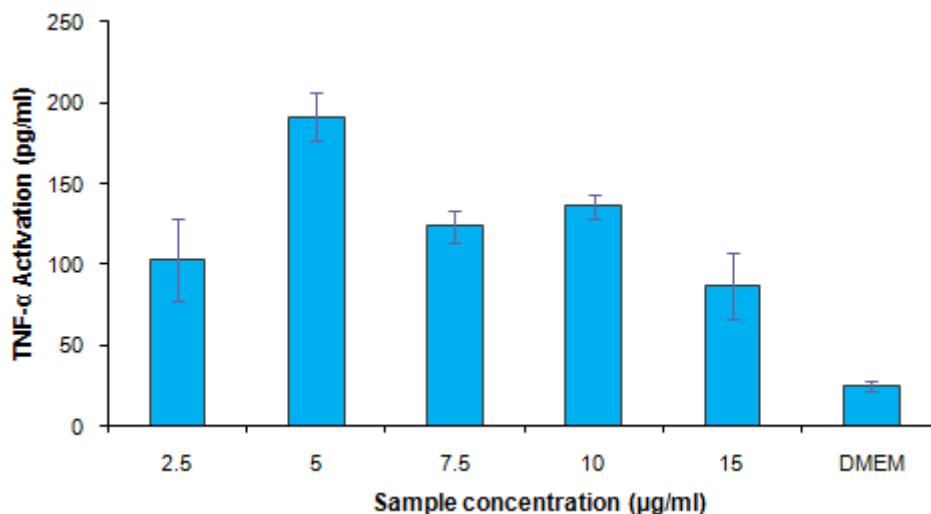


**Figure 5.7. Determination of macrophage activation using an enzyme-linked immunosorbent assay (ELISA) in the evaluation of the effect of DDA-TDB sample concentration on TNF- $\alpha$  secretion.** The calculated negative control (DMEM) generated 25 pg/ml. Results represent the mean average for each concentration in triplicate, with error bars displaying the standard deviation from the mean.

In general, after the peak of TNF- $\alpha$  release associated to DDA-TDB at 5.0  $\mu\text{g/ml}$ , a sample concentration beyond this optimum level stimulated lower levels of activation. This can possibly relate to the results of the toxicity studies, indicated by the magnitude of cell proliferation, in which fewer cells were able to survive in the DDA-TDB environment at higher concentrations. Therefore, these conditions render a diminished macrophage presence resultant from increased toxicity, consequently limiting the level of phagocytic activity and macrophage activation.

#### 5.4.2. Activation of TNF- $\alpha$ in response to DDA-TDB and its cationic replacement

Following on from the effect of sample concentration studies, the TNF- $\alpha$  ELISA kit was applied to the DDA-TDB based formulations, as previously assessed for toxicity through the MTS cell proliferation assay and phagocytic activity via the NAG assay (Table 5.1). As reported earlier, DDA-TDB induced TNF- $\alpha$  release in the region of 200 pg/ml (Figure

5.8), and further replacement of DDA content stimulated significantly ( $P < 0.05$ ) reduced TNF- $\alpha$  production in the proximity of 160 pg/ml (Figure 5.8), regardless of the replacing lipid used. DPPC-TDB and DSPC-TDB liposomes were found to generate comparable levels of macrophage activation to the partially replaced systems, quantified at ~140 pg/ml of the TNF- $\alpha$  cytokine (Figure 5.8). With DDA-TDB stimulating the peak of activity, incorporation of further lipids managed to induce comparable levels of the TNF- $\alpha$ , significantly beyond macrophage cells or the DMEM cell culture media alone, displaying the potential immunostimulatory adjuvant properties of the liposomal carrier systems.

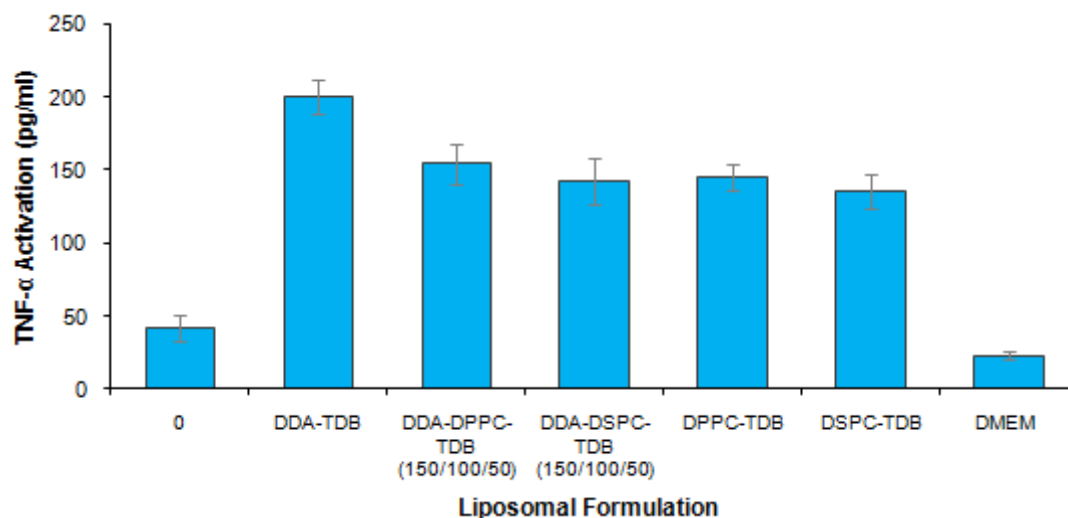


**Figure 5.8. Quantification of TNF- $\alpha$  secretion indicative of macrophage activation using an enzyme-linked immunosorbent assay (ELISA) in response to DDA-TDB and its cationic replacement with DPPC or DSPC lipid.** All samples were subjected to a BALB/c cell number of  $8 \times 10^4$ /ml at a sample concentration of 5.0  $\mu$ g/ml. The data displayed is based on the mean average of three independent experiments, with error bars displaying the standard deviation from the mean.

#### 5.4.3. TNF- $\alpha$ stimulation from DDA-TDB substituted with additional lipids

For the substituted DDA-TDB liposomes, all samples were set to 5.0  $\mu$ g/ml as previously conducted. Substitution of DDA-TDB with 50 mol% DPPC or DSPC stimulated ~170

pg/ml of TNF- $\alpha$ , which was comparable to the levels generated previously in response to the partially replaced systems and was similarly lower than the levels produced by DDA-TDB (Figure 5.9). As seen throughout all of the *in vitro* experiments conducted in this study, no significant difference in the measured outcome was observed regardless of the incorporated lipid of DPPC or DSPC to the DDA-TDB liposomes (Figure 5.9).

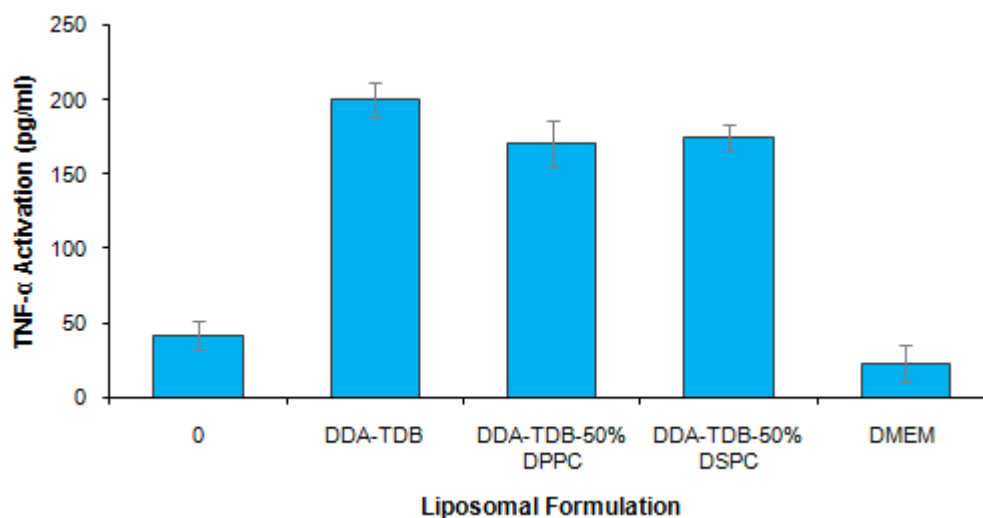


**Figure 5.9. Tumour necrosis factor alpha (TNF- $\alpha$ ) enzyme-linked immunosorbent assay (ELISA) results for DDA-TDB substituted with DPPC or DSPC.** All samples were subjected to a BALB/c cell number of  $8 \times 10^4$ /ml at a sample concentration of  $5.0 \mu\text{g/ml}$ . The calculated average was based upon the mean of three independent experiments, with error bars displaying the standard deviation from the mean.

Interestingly, all formulations stimulated macrophage activation signified by TNF- $\alpha$  levels quantified per system. This was observed in relation to the significantly ( $P < 0.05$ ) reduced cytokine levels produced by the macrophages alone and the negative control of DMEM growth media, at  $42 \text{ pg/ml}$  and  $23 \text{ pg/ml}$  respectively. One factor that all of the proposed adjuvant systems shared was the incorporation of TDB, which advantageously carries immunogenic properties that stabilise and enhance the adjuvant potency of DDA vesicles, acting as an immune potentiator for DDA response. However, due to the lipidic properties

of TDB, co-administration with an adjuvant such as DDA, recognised as a liposomal vaccine adjuvant delivery system, is required (Vangala *et al*, 2007; Davidsen *et al*, 2005).

Furthermore, DDA is crucial in providing the net cationic charge of the system, yet cationic liposomes are recognised for their cytotoxic effect as they attain a higher affinity to cell surfaces, demonstrated earlier in this study with elevated levels of macrophage cell proliferation observed upon increased cationic replacement with either DPPC or DSPC lipid. However, Korsholm *et al*, (2007) proposed that cationic DDA liposomes promote uptake via endocytosis prior to disruption or fusion with internal cellular membranes, and that the delivery of associated antigen to cells occurs upon instant contact with the cell surface through electrostatic interactions prior to active antigen uptake and presentation, which is a key mechanism behind the adjuvant properties of cationic DDA liposomes. In addition, previous studies into DDA liposomes incorporating DSPC lipid demonstrated that antigen acquisition by APCs was dependent upon DDA concentration (Korsholm *et al*, 2007), whilst in this current study, it was apparent that DDA presence was pivotal to the recorded levels of phagocytic activity and macrophage activation *in vitro*, indicative of potential uptake and expression of the proposed liposomal formulations, reiterating the necessity of a cationic constituent within the multi-component immunoadjuvant system.

##### ***5.5. Further studies into determining whether the *in vitro* cellular activity is due to DDA replacement or removal***

To consider if the above results linking DDA concentration to cellular toxicity and activity were due to the replacement of DDA with a zwitterionic lipid or the reduction of DDA concentration alone (i.e. the DSPC lipid played no role in the measured outcomes), the *in*

*in vitro* behaviour of DDA-TDB at a 5:1 (250/50 µg/dose – as previously assessed) and 2:1 (100/50 µg/dose) weight ratio, in conjunction with a further partially replaced system of DDA/DSPC/TDB at 100/150/50 µg/dose, were tested alongside DSPC-TDB, which represented complete DDA replacement. DPPC formulations were not tested as no significant difference had been observed between the incorporation of DPPC or DSPC.

As can be seen in Figure 5.10 with each of the three markers used, the presence or absence of DSPC within the formulations made no significant difference. Indeed, upon assessment of cell proliferation, there was no significant difference between DDA/DSPC/TDB at 100/150/50 µg/dose and DDA-TDB (100/50 µg/dose) with both systems showing ~70% cell viability (Figure 5.10a). Although an increased sample concentration of 10.0 µg/ml reduced the calculated cell viability to ~60%, for both of these additional systems tested, again no significant difference between the two formulations was observed (Figure 5.10a).

Subsequently, when considering induced phagocytic activity, DDA-DSPC-TDB at 100-150-50 µg/dose and DDA-TDB at 100/50 µg/dose produced levels of NAG activation which were not significantly different from one another (0.4-0.5 units/ml; Figure 5.10b). This demonstrates that the presence or absence of DSPC makes no significant difference.

Finally, when considering the level of macrophage activation induced (Figure 5.10c), TNF-α cytokine production was not significantly different between DDA-DSPC-TDB at 100-150-50 µg/dose and DDA-TDB at 100/50 µg/dose, again demonstrating that the reduced concentration of DDA in the formulation (rather than an increased DSPC concentration) is influencing the *in vitro* parameters evaluated within macrophage cells.

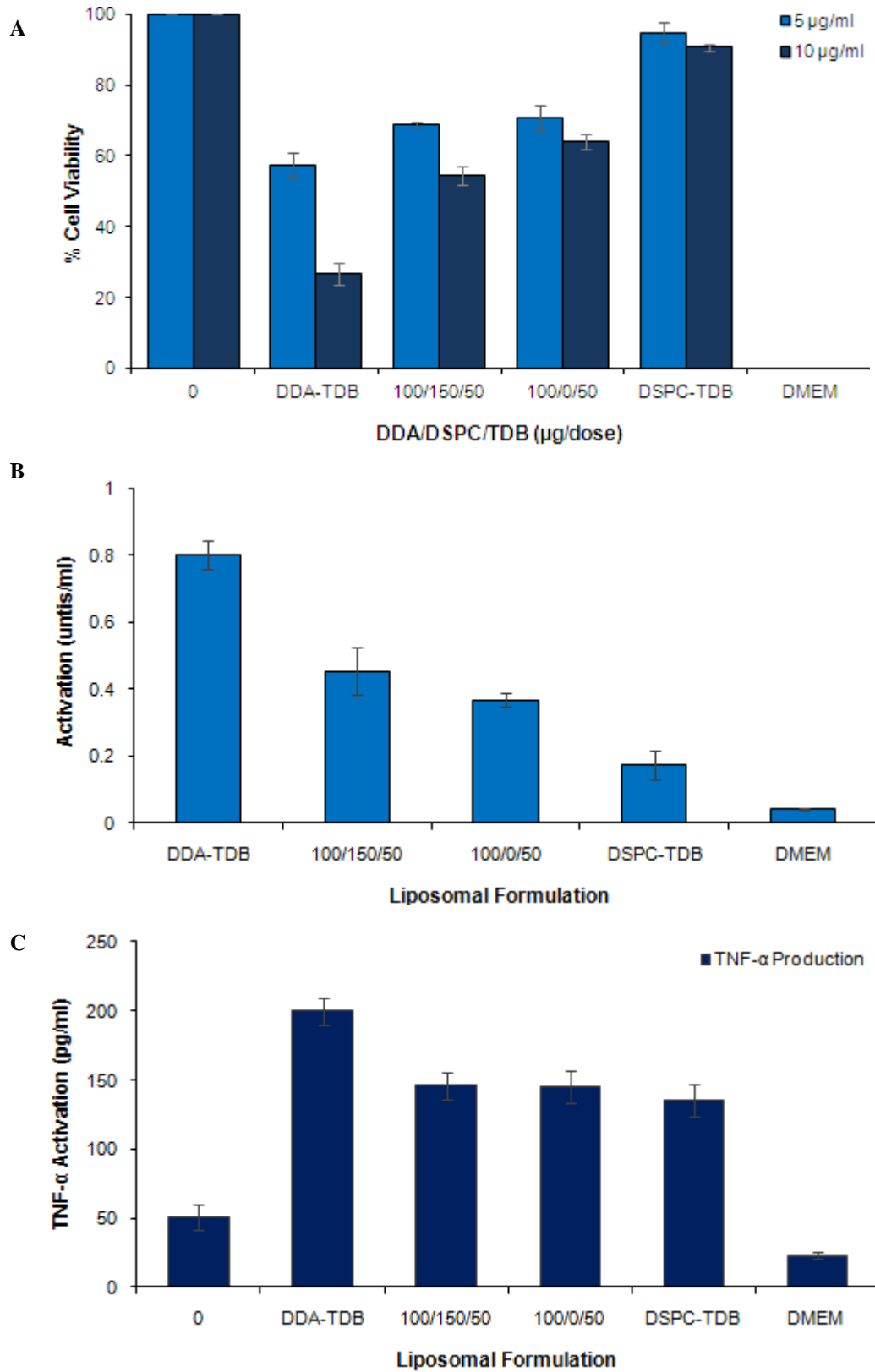


**Figure 5.10. Cell viability (A) NAG activation (B) and TNF- $\alpha$  secretion (C) upon further replacement of DDA within the DDA-TDB adjuvant system.** Formulations were set to 5.0  $\mu\text{g/ml}$  (unless otherwise stated) with  $8 \times 10^4/\text{ml}$  BALB/c cells. Calculations were made on triplicate wells per formulation ( $n=3 \pm \text{SD}$ ).

### **5.6. Conclusions**

The cytotoxic effect of DDA within the main DDA-TDB liposomal immunoadjuvant was apparent as an increased concentration of cationic content decreased the measured cell viability of BALB/c mice cells. Such a trend was demonstrated upon increased DDA replacement within DDA-TDB as complete cationic replacement with DPPC-TDB and DSPC-TDB generated elevated levels of macrophage cell proliferation. Additionally, DDA-TDB substituted with DPPC or DSPC at 25-75 mol% favourably reduced the associated toxicity of DDA-TDB, potentially providing a safer delivery system as cell viability increased by 20-30%.

The peak of phagocytic activity and macrophage activation was generated by DDA-TDB, and upon adjustment via replacement or substitution, the stimulated activity decreased. However, macrophages can be seen to recognise and trigger cellular activity in response to the liposomal carrier systems *in vitro*, demonstrated as macrophage activation signified by TNF- $\alpha$  secretion was also induced. Such cellular processes that permits invading material to be engulfed and ingested, crucially initiates the primary stages that lead to generating targeted immunity, particularly in response to the administration of a liposomal immunoadjuvant.

With previous physicochemical characterisation and stability studies, together with morphological and thermodynamic analysis, these *in vitro* experiments add to the profile produced for the replaced and substituted DDA-TDB based liposomal adjuvants, required in order to ascertain key aspects controlling their efficacy. It is understood that a cationic presence increases the associated toxicity, observed through resultant inhibition of cell

proliferation. However, from the current data, the addition of zwitterionic lipids in conjunction with TDB boosted cell proliferation levels in comparison to DDA-TDB, whilst phagocytosis and macrophage activation was also induced, readdressing a balance between adjuvant potency and safety. The effectiveness of the BALB/c cell line and its use to screen the outlined liposomal adjuvant delivery systems will be evaluated and assessed upon future *in vivo* immunological studies, which may also confirm whether the cellular processes stimulated are dependent upon a reduced DDA presence or further lipid incorporation.

To conclude, the parameters characterised to date demonstrate the potential of the proposed liposomal immunoadjuvants in stimulating an immune response and thus, suffice as proficient systems for vaccine delivery *in vivo*. Indeed, the DPPC based liposomal formulations will be considered for potential pulmonary vaccine delivery, and the DSPC based systems will be assessed in a mouse model upon intramuscular injection as part of an immunisation study involving the novel H56 vaccine for TB.

## **Chapter 6**

### **Characterisation and immunological analysis of liposomal TB vaccine delivery systems**

## 6.1. Introduction

### 6.1.1. Hybrid 56 vaccine antigen

The necessity for preventive, post exposure TB vaccines that can be administered to latently infected individuals has been recognised (SSI, 2010). Subunit vaccines based on antigens from mycobacterium TB in conjunction with an adjuvant that stimulates a strong Th1 type cellular immune response offer promising potential (Aagaard *et al*, 2011). One post exposure vaccine candidate known as Hybrid56 (H56 vaccine) is designed to prevent the reactivation of TB to those with the latent form of the TB infection. The H56 vaccine consists of the Ag85B-ESAT-6 fusion molecule with the addition of the Rv2660 latency antigen (Figure 6.1) (SSI, 2010).

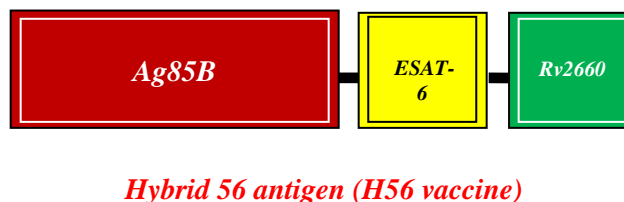


**Figure 6.1.** The post exposure H56 vaccine candidate which combines the fusion protein Ag85B-ESAT-6 with Rv2660 antigen. (Figure adapted from SSI, 2010).

Studies have shown that whole blood from individuals with the latent TB infection (LTBI) incubated with the Rv2660 mycobacterial antigen induced elevated levels of the IFN- $\gamma$  cytokine, which is indicative of macrophage activation and a key marker of cell mediated immunity, when compared with patients that developed the active form of TB. LTBI individuals were also found to preferentially recognise Rv2660 and produced an increased number of viable T cells, justifying the use of the Rv2660 latency antigen and its integration into candidate TB vaccines (Govender, 2010).

A viable approach for a post exposure vaccine is to specifically target mycobacteria in the inactive phase of infection. A vast array of potential latency antigens and numerous protein antigens have been assessed for their suitability in providing protective efficacy against TB reactivation. One such combination is the H56 vaccine against TB, in which post exposure vaccination in a mouse model of latent TB was found to proficiently control the infection. Preclinical data has indicated the potential of H56 vaccine delivery for protection against mycobacterium TB, as incorporation into the novel IC31 adjuvant capably induced T and B cell responses. As a result, the H56 vaccine is being put forward into a phase I clinical trial, scheduled for 2011, to test individuals infected with latent TB (SSI, 2010).

In the present study, the aim of this chapter was to immunologically characterise the DDA-TDB based liposomal formulations as adjuvant delivery systems for the promising H56 vaccine candidate against TB. Alongside the assessment of DDA replacement within DDA-TDB, as some toxicity was observed for the main adjuvant system, the DDA:TDB ratio remained fixed (as this has previously been shown to be an important factor) yet the total dose of DDA:TDB was reduced upon substitution with DSPC lipid. Therefore, consideration was given to whether just DDA, the ratio of DDA:TDB or both factors were crucial to the resultant adjuvanticity of the formulation.

## ***6.2. Preliminary studies – optimisation of the splenocyte proliferation assay***

### ***6.2.1. The effect of cell number and concanavalin A upon splenocyte proliferation***

To investigate the potential of the DDA-TDB based adjuvants in potentiating an immune response to the H56 antigen, prior to the immunisation studies including evaluation of

splenocyte proliferation, initial studies were conducted to optimise the protocol for this assay. Tests were conducted upon albino NMRI mice which were humanely culled before their spleens were dissected. Spleen cell numbers were adjusted to a range of concentrations from  $6.25 \times 10^5$  to  $4.0 \times 10^7$  cells per ml (Table 6.1) in order to ascertain an optimum number of cells to be cultured.

**Table 6.1. Tested cell numbers in the optimisation of their effect upon splenocyte proliferation.**

Cell number per ml	Equivalent number of cells per well (per 100 $\mu$ l)
0	0
$6.25 \times 10^5$	$6.25 \times 10^4$
$1.25 \times 10^6$	$1.25 \times 10^5$
$2.5 \times 10^6$	$2.5 \times 10^5$
$5.0 \times 10^6$	$5.0 \times 10^5$
$1.0 \times 10^7$	$1.0 \times 10^6$
$2.0 \times 10^7$	$2.0 \times 10^6$
$4.0 \times 10^7$	$4.0 \times 10^6$

Alongside the assessment of cell number, the effect of concanavalin A (ConA) concentration was also observed in order to optimise its use for the main immunisation study. ConA is widely applied in biological studies and for these particular *in vivo* experiments, ConA was used as a positive control as it is known to stimulate the proliferation of T lymphocytes. Various ConA concentrations ranging between 0-10  $\mu$ g/ml were tested upon the adjusted cell numbers and after culturing the spleen cells in triplicate

per cell number and incubating the samples for 72 hours in RPMI growth medium, all wells were pulsed with 0.5  $\mu\text{Ci}$  [ $^3\text{H}$ ]thymidine and incubated for a further 24 hours. During this incubation period, the proliferating cells incorporated various levels of [ $^3\text{H}$ ]Thymidine, depending on the number of cell divisions that took place, and thus, the measured counts for radioactivity represented the extent of stimulated cell proliferation.

For the tested cell numbers, it was observed that an increase in splenocyte cells in turn elevated the level of proliferation (Figure 6.2). This trend continued towards a maximum response at the cell number of  $5.0 \times 10^6$  cells per ml and at a ConA concentration of 2  $\mu\text{g/ml}$ . Beyond this cell number at  $1.0$ ,  $2.0$  and  $4.0 \times 10^7$  cells per ml, the increased concentration of cells decreased the level of splenocyte proliferation, as beyond the observed peak cell number, an increased presence of cells per ml had a detrimental effect.

Furthermore, with the maximum cell number for proliferation coinciding with a ConA concentration of 2  $\mu\text{g/ml}$ , ConA at 1 and 3  $\mu\text{g/ml}$  was also found to stimulate comparably high levels of splenocyte proliferation for the optimum cell number of  $5.0 \times 10^6$  cells per ml (Figure 6.2). Below and above the positive control concentration range of 1-3  $\mu\text{g/ml}$ , the level of splenocyte proliferation was significantly lower ( $P < 0.05$ ), regardless of the cell number (Figure 6.2).

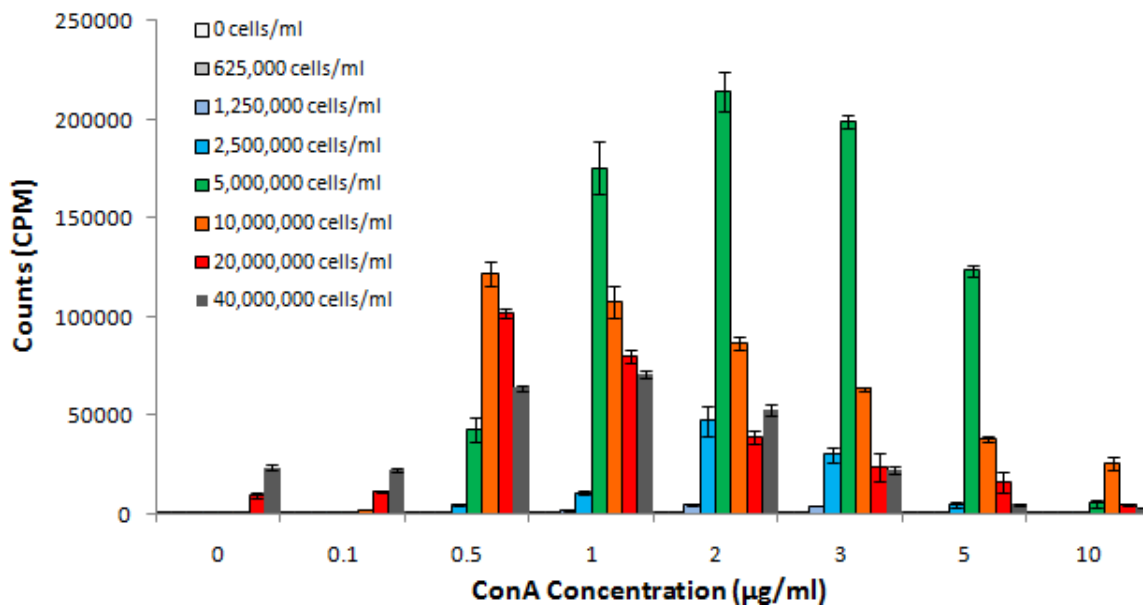


**Figure 6.2.** The effect of cell number and ConA concentration upon the proliferation of splenocyte cells. The selected cell numbers ranged from  $0-4 \times 10^7$  cells/ml at ConA concentrations of  $0-10 \mu\text{g/ml}$ . Results denote the mean and standard error from triplicate wells of naive spleens from albino NMRI mice.

### 6.2.2. The effect of pulsing activity and incubation time upon splenocyte proliferation

After establishing an optimised cell number and ConA concentration of  $5.0 \times 10^6$  cells per ml and  $2 \mu\text{g/ml}$  respectively, these parameters were fixed for all future splenocyte proliferation assays. Subsequently, the effect of pulsing activity and incubation time was analysed after culturing splenocyte cells for 72 hours. A range of [ $^3\text{H}$ ]thymidine activity levels were tested at 0, 0.25, 0.75 and  $1.0 \mu\text{Ci}$ , upon 4, 8, 16 and 24 hours of incubation.

It was observed that the lowest amount of [ $^3\text{H}$ ]Thymidine activity used ( $0.25 \mu\text{Ci}$ ) to pulse the splenocytes also coincided with the lowest levels of spleen cell proliferation (Figure 6.3). However, increasing the pulsing activity to 0.5, 0.75 and  $1.0 \mu\text{Ci}$  did increase the detection of cell proliferation, represented by higher counts per minute (Figure 6.3). This trend generally occurred in conjunction with an increased incubation time. Furthermore, great levels of variation was evident in the samples pulsed with 0.75 and  $1.0 \mu\text{Ci}$ , with no

significant difference displayed between the time points of 16 and 24 hours of incubation, particularly for 0.5  $\mu\text{Ci}$  activity and beyond (Figure 6.3). Therefore, as 0.5  $\mu\text{Ci}$  of [ $^3\text{H}$ ]thymidine activity used to pulse the splenocyte cells provided the least variation across all of the tested time points, coupled with relatively high counts indicative of splenocyte proliferation, this concentration at a time point of 24 hours was deemed the most suitable for the proliferation experiments, when characterising the immunological effect of the liposomal systems to be tested in the immunisation study.

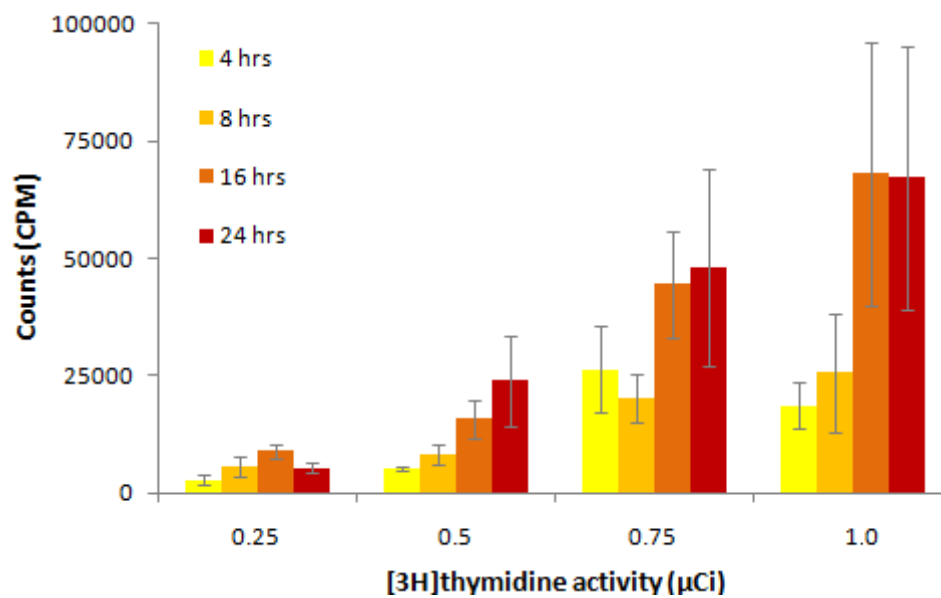


**Figure 6.3. The effect of pulsing activity and incubation time upon the proliferation of splenocyte cells.** The cell number was fixed to  $5 \times 10^6$  cells/ml with a ConA concentration of  $2 \mu\text{g/ml}$ . Results denote the mean average and standard error from triplicate wells of naive spleens from albino NMRI mice.

To summarise, based upon these preliminary studies using naive NMRI spleens, the optimised parameters for the assessment of splenocyte proliferation are as follows:

- Cell number:  $5.0 \times 10^6$  cells per ml,
- ConA positive control:  $2 \mu\text{g/ml}$ ,
- Radioactive pulsing activity of [ $^3\text{H}$ ]Thymidine:  $0.5 \mu\text{Ci}$ ,
- Incubation time: 24 hours.

### **6.3. Immunisation study: determination of immune responses to a novel TB vaccine**

#### *6.3.1. H56 vaccine groups*

Upon extensive characterisation of the DDA-TDB based systems, a range of replacement and substitution formulations were put forward to be evaluated and analysed as part of an immunisation study into the immunological efficacy of the proposed liposomal adjuvants. The extent of splenocyte proliferation, specific IgG antibody production and cytokine secretion was assessed for all of the tested groups. The study was conducted over seven weeks with five scheduled bleeds on days 0, 9, 24, 37 and 49 respectively. C57BL/6 mice were immunised three times with 5 µg of H56 antigen with injections made intramuscularly (0.05 ml/dose) on days 0, 14 & 28, maintaining two week intervals between each immunisation, as previously conducted (Christensen *et al*, 2007a; Agger *et al*, 2008).

Sera from each individual mouse were obtained in order to evaluate the antigen specific antibody production stimulated by each vaccine group. Termination of the mice took place on day 50 prior to developing spleen cell suspensions for subsequent assessment of splenocyte proliferation and antigen specific cytokine responses. A total of 55 female 6-8 week old C57BL/6 mice under a standard mouse diet were split into 11 vaccine groups (n=5 mice per group) as summarised in Table 6.2. The liposomal formulations that formed 9 of the 11 tested groups were prepared and characterised for their particle size and zeta potential before and after antigen adsorption (Table 6.3), prior to each of the three intramuscular immunisations that took place.

**Table 6.2. Immunisation study: vaccine groups tested for immunological analysis with the novel TB vaccine candidate, H56 antigen.** Female 6-8 week old C57BL/6 mice were split into 11 groups of 5. The naive and antigen groups were accompanied by nine DDA-TDB based formulations accommodating various levels of DSPC lipid. Weights stated are all in µg per dose and mg per ml of Tris buffer.

Vaccine Group	Formulation	DDA/LIPID/TDB (µg/dose)	DDA/LIPID/TDB (mg/ml)
1	Naive	/	/
2	H56 Antigen	/	/
3	DDA-TDB	250/0/50	1.25/0.00/0.25
4	DDA-DSPC-TDB	150/100/50	0.75/0.50/0.25
5	DDA-DSPC-TDB	100/150/50	0.50/0.75/0.25
6	DDA-DSPC-TDB	100/0/50	0.50/0.00/0.25
7	DDA-DSPC-TDB	50/200/50	0.25/1.00/0.25
8	DDA-DSPC-TDB	0/250/50	0.00/1.25/0.25
9	+25% DSPC	188/88/36	0.94/0.44/0.18
10	+50% DSPC	125/175/25	0.62/0.88/0.13
11	+75% DSPC	62/264/14	0.31/1.32/0.07

### 6.3.2. Characterisation of liposomes upon H56 vaccine antigen adsorption

The liposomes were produced as previously conducted via lipid hydration and rehydrated in Tris buffer. Empty DDA-TDB liposomes were characteristically found to be ~500 nm with a cationic zeta potential of 50 mV (Table 6.3). The reduced weight ratio of DDA-TDB at 2:1 (DDA-DSPC-TDB at 100/0/50 µg/dose), replacement of DDA and further replacement within this adjuvant system generated liposomes with a mean particle size of 600-800 nm, maintaining a zeta potential of 50 mV. Complete cationic replacement with the DSPC-TDB liposomes generated significantly larger vesicles ( $P < 0.05$ ) at two micrometres in particle size with a neutral to slightly anionic zeta potential, contrasting the formulations that contained DDA (Table 6.3). The systems incorporating 25-75 mol%

DSPC were also 600-800 nm in particle size coinciding with a cationic zeta potential also measured at 50 mV. The polydispersity of all the unloaded formulations were in the proximity of 0.3, suggesting a polydisperse population of liposomes (Table 6.3). Such findings for particle size and zeta potential coincide with results previously obtained in this study (Chapter 3).

For the proposed *in vivo* liposomal preparations, the main adjuvant system for example, consisted of DDA and TDB at a dose of 250 µg and 50 µg respectively (5:1 weight ratio) with H56 antigen adsorbed at 5 µg/50 µl dose. Upon surface adsorption of H56 antigen at the fixed dosage form to the cationic systems of DDA-TDB, its reduced weight ratio, the partial replacement of DDA and substitution of DDA-TDB with DSPC, the injected formulations had all risen significantly ( $P < 0.05$ ) to a mean particle size of ~1500 nm (Table 6.3). The exception to this increase in size was observed with DSPC-TDB, in which the addition of antigen produced vesicles just under two microns, displaying no significant change in particle size. The polydispersity ranged from 0.2-0.4 for all formulations (Table 6.3). Furthermore, the zeta potential of all the liposomal vaccine groups was also characterised, representing a key indicating factor into the antigen retention properties of the formulations and therefore, their potential in stimulating a particular immune response. All of the tested systems exhibited no significant change in the measured zeta potential or any difference to one another, as the positively charged DDA-TDB based liposomes remained strongly cationic at 50 mV (Table 6.3). The DSPC-TDB liposomes were also found to remain slightly anionic, showing no apparent difference to their empty counterparts upon antigen adsorption in dosage form for the immunisation of mice, as summarised in Table 6.3.

**Table 6.3. Particle size, polydispersity and zeta potential of the liposomal vaccine groups characterised before and after H56 antigen adsorption, applied for the three immunisations of mice during the 7 week *in vivo* study.** Results displayed are the mean average from three independent batches produced  $\pm$  the standard deviation. Measurements were made using one i.m. vaccine dose (50  $\mu$ l) taken from a batch used for each immunisation, per liposome formulation.

Formulation ( $\mu$ g/dose)	PS (nm) (empty)	P.D. (empty)	ZP (mV) (empty)	PS (nm) (+H56)	P.D. (+H56)	ZP (nm) (+H56)
DDA-TDB (250/50)	506.4 $\pm$ 73.4	0.32 $\pm$ 0.01	48.9 $\pm$ 3.7	1019.2 $\pm$ 327	0.36 $\pm$ 0.01	47.2 $\pm$ 3.9
DDA-DSPC-TDB (150/100/50)	813.8 $\pm$ 11.9	0.29 $\pm$ 0.05	50.8 $\pm$ 2.7	1383.3 $\pm$ 227.9	0.38 $\pm$ 0.02	49.2 $\pm$ 2.5
DDA-DSPC-TDB (100/150/50)	644.8 $\pm$ 67.3	0.32 $\pm$ 0.02	49.9 $\pm$ 3.9	1503.0 $\pm$ 303.8	0.39 $\pm$ 0.04	50.5 $\pm$ 2.5
DDA-DSPC-TDB (100/0/50)	559.6 $\pm$ 52.6	0.34 $\pm$ 0.01	43.7 $\pm$ 5.6	1391.6 $\pm$ 86.2	0.36 $\pm$ 0.11	48.4 $\pm$ 6.4
DDA-DSPC-TDB (50/200/50)	559.9 $\pm$ 90.3	0.32 $\pm$ 0.01	50.7 $\pm$ 2.8	1400.0 $\pm$ 364.9	0.43 $\pm$ 0.05	47.3 $\pm$ 0.9
DDA-TDB +25%DSPC	798.0 $\pm$ 30.3	0.34 $\pm$ 0.01	50.3 $\pm$ 3.1	1589.7 $\pm$ 159.2	0.44 $\pm$ 0.05	48.9 $\pm$ 5.4
DDA-TDB +50%DSPC	653.9 $\pm$ 49.5	0.32 $\pm$ 0.01	50.1 $\pm$ 3.6	1610.5 $\pm$ 103.2	0.39 $\pm$ 0.01	50.7 $\pm$ 2.8
DDA-TDB +75%DSPC	734.1 $\pm$ 113.7	0.33 $\pm$ 0.02	50.7 $\pm$ 3.5	1486.0 $\pm$ 183.5	0.33 $\pm$ 0.10	51.9 $\pm$ 1.9
DSPC-TDB (250/50)	1846.7 $\pm$ 115.2	0.24 $\pm$ 0.07	-8.0 $\pm$ 5.4	1730.8 $\pm$ 95.8	0.31 $\pm$ 0.05	-7.5 $\pm$ 5.2

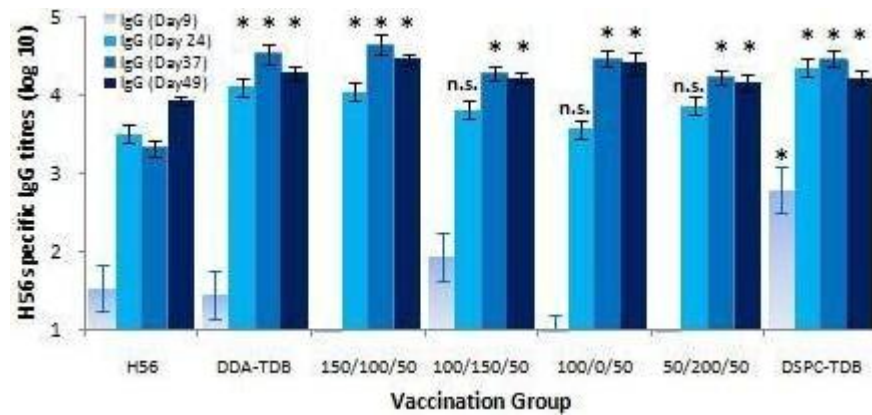
### *6.3.3. Production of anti-H56 IgG, IgG1 and IgG2b antibodies*

#### *6.3.3.1. Replacement of DDA in DDA-TDB: effect upon H56 specific antibody production*

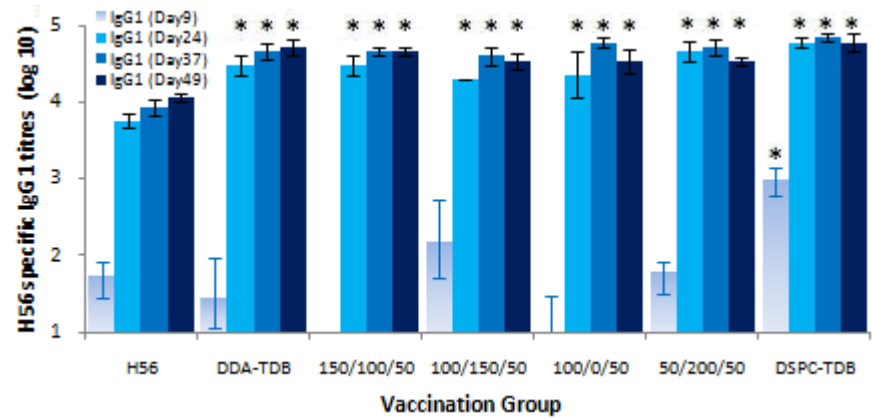
Sera collected at regular intervals throughout the vaccine immunisation study were analysed by an ELISA for antibody mediated H56 specific responses to DDA-TDB and the systemic variations of this adjuvant, as outlined in Table 6.3 (for the full immunisation schedule, see appendix 2). For IgG and IgG1 isotypes, the liposomal adjuvants stimulated comparable serum antibody levels, regardless of the cationic adjustment that took place, and were all significantly ( $P < 0.05$ ) higher than the non adjuvanted H56 antigen group, particularly by day 37 and 49, which represented the peak of antibody production (Figures 6.4 A & B). Additionally, it was observed that mice immunised with DSPC-TDB demonstrated an early response with significantly ( $P < 0.05$ ) elevated IgG and IgG1 antibody titres compared to all other vaccination groups on day 9 (Figures 6.4 A & B).

In contrast, IgG2b antibody levels showed more dependence on the level of DDA content (Figure 6.4 C), as DDA-TDB, its partial replacement with DDA-DSPC-TDB at 150/100/50  $\mu\text{g}/\text{dose}$  and its reduced concentration at 100/0/50  $\mu\text{g}/\text{dose}$ , produced the highest levels of IgG2b antibody titres, with further and complete cationic replacement of the liposomal adjuvant generating significantly (with a probability value of at least  $P < 0.01$ ) decreased levels of antibody production (Figure 6.4 C). Additionally, all liposomal adjuvants generated a significantly ( $P < 0.05$ ) higher IgG2b antibody response than the H56 antigen group, with the exception of DDA-DSPC-TDB at 50/200/50  $\mu\text{g}/\text{dose}$  and DSPC-TDB at the later stages of the study (Figure 6.4 C).

A



B



C

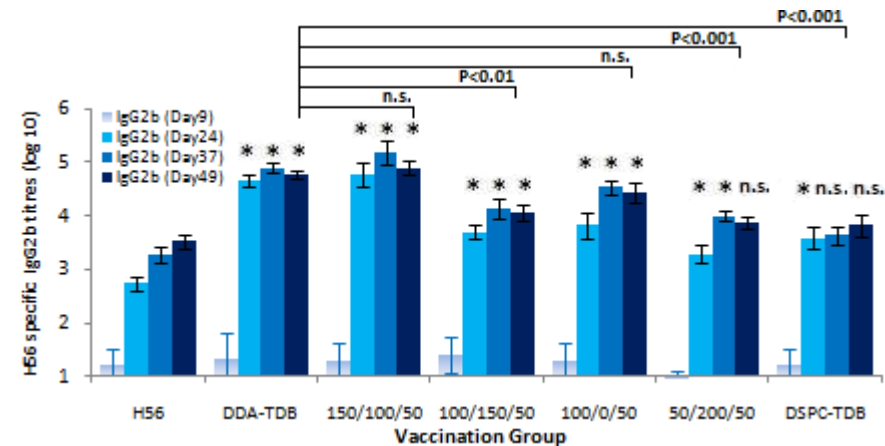


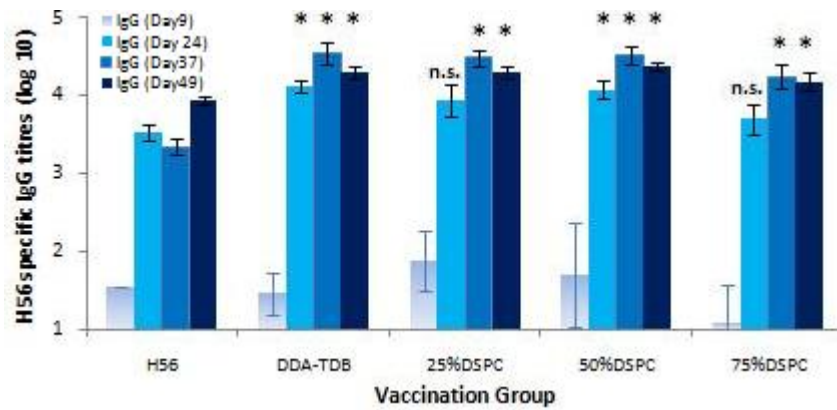
**Figure 6.4.** Mean serum H56 specific antibody titres generated by DDA-TDB and its cationic replacement with DSPC for A: IgG, B: IgG1 and C: IgG2b subsets. Values represent  $\mu\text{g}/\text{dose}$ , with sera collected before the first immunisation and on days 9, 24, 37 and 49 thereafter, prior to analysis for anti-H56 antibodies by ELISA. Results signify the positive reciprocal end point dilution ( $\log_{10}$ ) compared with untreated control sera ( $n=5 \pm \text{SE}$ ). Significance is illustrated as n.s. (not significant) or  $*p<0.05$  increase compared to H56 vaccination group, with DDA-TDB compared to equivalent IgG2b responses on day 49.

### 6.3.3.2. Substitution of DDA-TDB: effect upon H56 specific antibody production

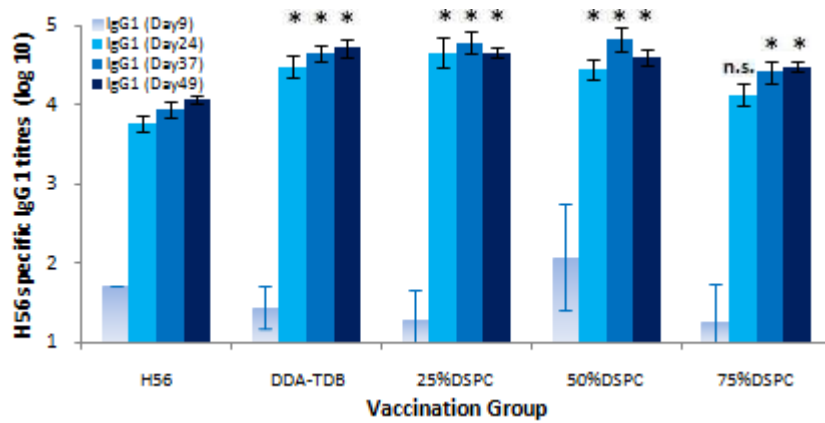
After assessing the effect of replacing DDA within DDA-TDB, substitution with DSPC represented a reduction in the total dose of DDA:TDB, rather than just a reduced DDA concentration. DDA-TDB and substitution with 25, 50 and 75 mol% of DSPC elicited comparable levels of IgG and IgG1 antibody production, with all liposomal adjuvants generating significantly ( $P < 0.05$ ) higher antibody titres than delivery of H56 antigen, particularly from day 37 onwards (Figures 6.5 A & B). Interestingly, evaluation of IgG2b antibodies showed that DDA-TDB and substitution with 25 and 50 mol% DSPC generated the highest levels, with no significant difference between these groups, whilst producing significantly more IgG2b titres than the H56 group (Figure 6.5 C). However, compared to these systems, further DDA-TDB substitution with 75 mol% DSPC generated a highly significantly ( $P < 0.001$ ) reduced level of IgG2b antibody titres, and was not significantly different to the response induced upon administration of H56 antigen alone (Figure 6.5 C), as seen previously when DDA was further reduced within the formulation (Figure 6.4 C).

From the H56 antigen specific antibody responses observed upon delivery of the proposed liposomal adjuvants, the measured levels of IgG2b titres suggest a Th1 type cell mediated immune response, induced by partial DDA replacement and substitution of DDA-TDB with DSPC and by the reduced concentration of DDA-TDB (at a 2:1 weight ratio), which may be administered without greatly compromising the immunogenic effect of DDA-TDB, recognised as a delivery vehicle capable of inducing cellular immunity vital for protection against TB (Ager *et al*, 2008). However, further spleen cell proliferation and cytokine analysis can confirm whether cellular immunity is elicited by these particular systems, and to the extent between each liposomal-H56 vaccine adjuvant group.

A



B



C

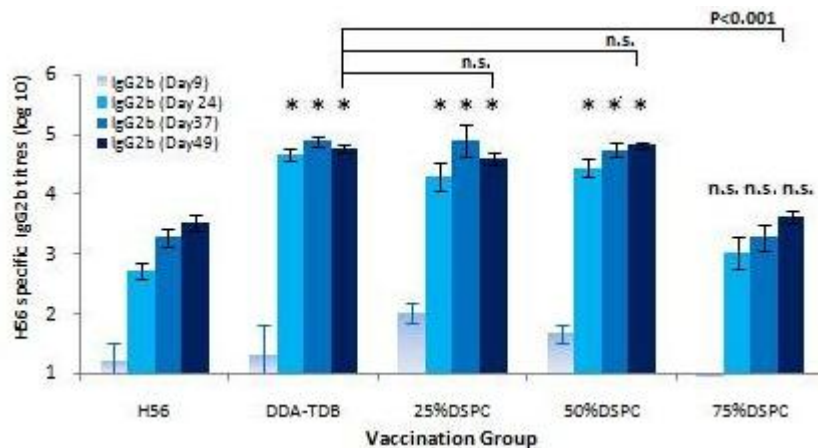


**Figure 6.5. Mean serum H56 specific antibody titres generated by DDA-TDB and its substitution with D5PC at 25-75 mol% for A: IgG, B: IgG1 and C: IgG2b subsets.** Sera was collected prior to the first immunisation and on days 9, 24, 37 and 49 respectively thereafter, prior to analysis for anti-H56 antibodies by an ELISA. Values represent the positive reciprocal end point dilution (log<sub>10</sub>) compared with untreated control sera (n=5 +/- SE). Significance is illustrated as n.s. (not significant) or \*p<0.05 increase compared to the H56 vaccination group, with DDA-TDB compared to equivalent IgG2b isotype responses on day 49.

Previous studies have assessed the effect of vesicle size on the immunoadjuvancy of DDA-TDB liposomes as experimental adjuvants for subunit TB vaccine delivery (Henriksen-Lacey *et al*, 2011b), observing that the extent of the Th1 type immune response, signified by IFN- $\gamma$  and IgG2b serum antibody levels, was not significantly affected by the wide range of DDA-TDB sizes tested. With DDA-TDB consistently stimulating cell mediated immunity, such findings indicate that the aforementioned effect upon adjuvant potency is dictated more by the immunostimulatory combination of DDA and TDB, and is less influenced by liposomal size.

Therefore, in relation to the findings of the present study, the replacement of DDA-TDB was found to generate medium sized vesicles in the nanometre range, with the exception of complete DDA replacement resulting in a larger system within the micrometre range. However, production of IgG and IgG1 antibodies were comparable across all systems regardless of the level of cationic adjustment or particle size of the adjuvants, with no apparent difference between IgG2b levels for DDA-DSPC-TDB at 50/200/50  $\mu\text{g}/\text{dose}$  and DSPC-TDB, which represented a significant difference in liposomal size, reaffirming the immunostimulatory effect of TDB due to its fixed presence in this set of formulations.

The variation in IgG2b antibody production can be attributed to the varying presence of DSPC within the liposomal adjuvants, observed upon further DDA replacement and upon substitution of DDA-TDB, as increased DSPC incorporation lowered IgG2b antibody levels and thus, the Th1 response. With elevated DDA-TDB substitution coinciding with reduced DDA and TDB content, the presence of this cationic lipid in conjunction with the immunostimulatory glycolipid plays a pivotal role in the resultant immunogenic effect.

#### *6.3.4. H56 antigen specific splenocyte proliferation*

##### *6.3.4.1. The effect of replacing DDA content within the DDA-TDB adjuvant*

The proposed DDA-TDB based adjuvants were also assessed for antigen specific spleen cell proliferation upon re-stimulation with H56 antigen at the concentrations of 0, 0.05, 0.5, 5 and 25  $\mu\text{g/ml}$ . All vaccination groups exhibited a concentration dependent trend, with DDA-TDB inducing the peak of proliferation, indicated by elevated levels of [ $^3\text{H}$ ]Thymidine (Figure 6.6). Furthermore, continual cationic replacement stimulated significantly (with a probability value of at least  $P < 0.01$ ) less splenocyte proliferation, upon re-stimulation with H56 antigen at 0.05-25  $\mu\text{g/ml}$  (Figure 6.6). More specifically, with DDA content being partially replaced out of DDA-TDB with DSPC at 150/100/50  $\mu\text{g/dose}$ , splenocyte proliferation was reduced, with another significant ( $P < 0.001$ ) reduction observed upon further replacement at 100/150/50  $\mu\text{g/dose}$  (Figure 6.6). However, the response is then seen to significantly ( $P < 0.001$ ) rise again for the lower concentration of DDA (100/0/50  $\mu\text{g/dose}$ ) and upon higher DSPC incorporation (50/200/50  $\mu\text{g/dose}$ ), with no significant difference in proliferation levels between these two systems and partial DDA replacement (Figure 6.6).

In addition, H56 antigen delivery via DSPC-TDB liposomes, representing complete replacement of DDA content, induced the lowest levels of splenocyte proliferation, and was not significantly different to the response induced upon further cationic replacement with DDA/DSPC/TDB at 100/150/50  $\mu\text{g/dose}$  at all antigen concentrations (Figure 6.6). Interestingly, comparing DDA-DSPC-TDB at 100/150/50  $\mu\text{g/dose}$  with the system of reduced DDA concentration at 100/0/50  $\mu\text{g/dose}$ , suggests that the presence of DSPC is significantly ( $P < 0.001$ ) reducing the stimulated levels of spleen cell proliferation. This

could also possibly be due to the dose of DDA, per adjuvant formulation, actually being higher in the DDA-TDB system at its reduced weight ratio of 100/0/50 µg/dose.

With TDB present in all of the tested adjuvant formulations, an immunopotentiating effect will be apparent, but the presence of DDA in the liposomal formulation may enhance the co-delivery of antigen and adjuvant, ultimately strengthening the resultant immune response. This was apparent upon previous related studies into the immunological performance of DDA-TDB compared to DSPC-TDB, whereby liposomal cationic charge and antigen retention, provided by DDA, were recognised as vital properties for eliciting cellular immunity in response to a related Ag85B-ESAT-6 TB vaccine antigen candidate (Henriksen-Lacey *et al*, 2010b). Moreover, the presence of DDA greatly affected antigen presentation *in vivo*, as administration of DDA-TDB resulted in prolonged antigen retention at the site of injection compared to DSPC-TDB, possibly providing more effective antigen presentation by APCs which resulted in stronger immunity in response to DDA-TDB, characterised by elevated IFN- $\gamma$  and IL-17 cytokine production (Henriksen-Lacey *et al*, 2010b). Thus, the reduced response of DSPC-TDB in the present study demonstrates the necessity of DDA in the liposomal adjuvant system, not only in providing the cationic charge required to retain antigen, but also to elicit the clonal expansion of spleen cells in the stimulation of antigen specific immunity.

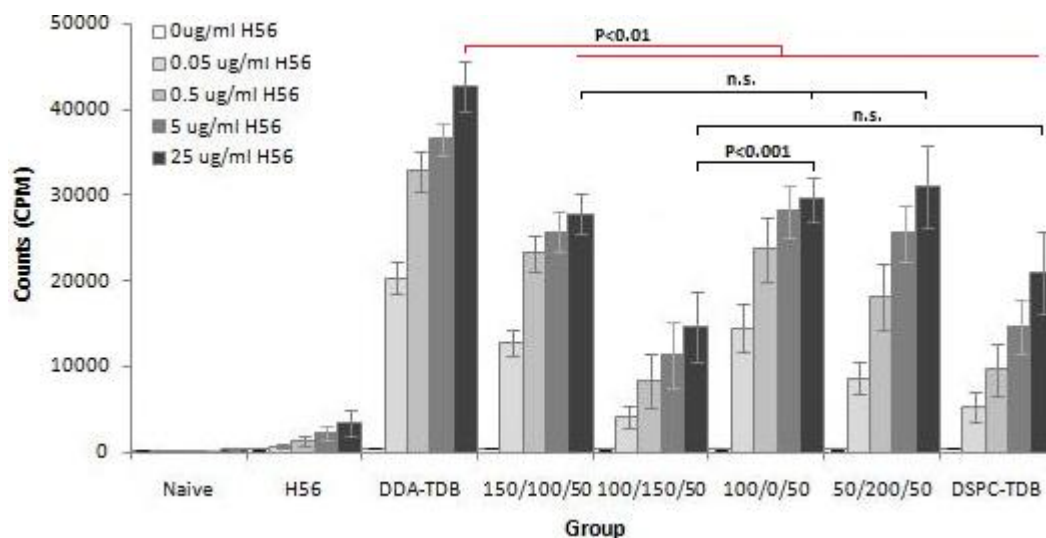


**Figure 6.6. Spleen cell proliferation in response to stimulation/re-stimulation with H56 antigen upon replacement of cationic content within DDA-TDB.** Formulation values represent µg/dose, with DDA-TDB and DSPC-TDB set to a 5:1 weight ratio (DDA/DSPC/TDB at 250/0/50 and 0/250/50 µg/dose respectively). H56 antigen specific splenocyte proliferation was indicated by the level of [<sup>3</sup>H]Thymidine incorporation into cultured splenocytes at antigen concentrations of 0-25 µg/ml. ConA was used as a positive control at 2µg/ml with all counts in the region of 100,000 CPM. The results displayed denote the mean average for each group with associated standard error at n=5. Significance is illustrated between the liposomal vaccination groups, and comparisons shown against one another are upon re-stimulation with H56 vaccine antigen at 25 µg/ml.

#### 6.3.4.2. Substitution of DDA-TDB with varying levels of DSPC lipid

To investigate if the DDA:TDB ratio was an important factor, DDA-TDB and substitution with 25-75 mol% DSPC was also evaluated for H56 specific spleen cell proliferation. DDA-TDB was found to generate the highest level of splenocyte proliferation (Figure 6.7), however, substitution with DSPC significantly ( $P < 0.05$ ) reduced the recorded levels of proliferation compared to DDA-TDB, with no significant difference in the response displayed for 25 and 50 mol% DSPC incorporation (Figure 6.7). DDA-TDB substituted with 75 mol% DSPC induced a further significant ( $P < 0.05$ ) reduction in response compared to substitution with 25 and 50 mol% DSPC, and was consistently low in terms of spleen cell proliferation, even with re-stimulation at higher concentrations of H56 antigen, as beyond 0.5 µg/ml, cell proliferation was not significantly affected (Figure 6.7).

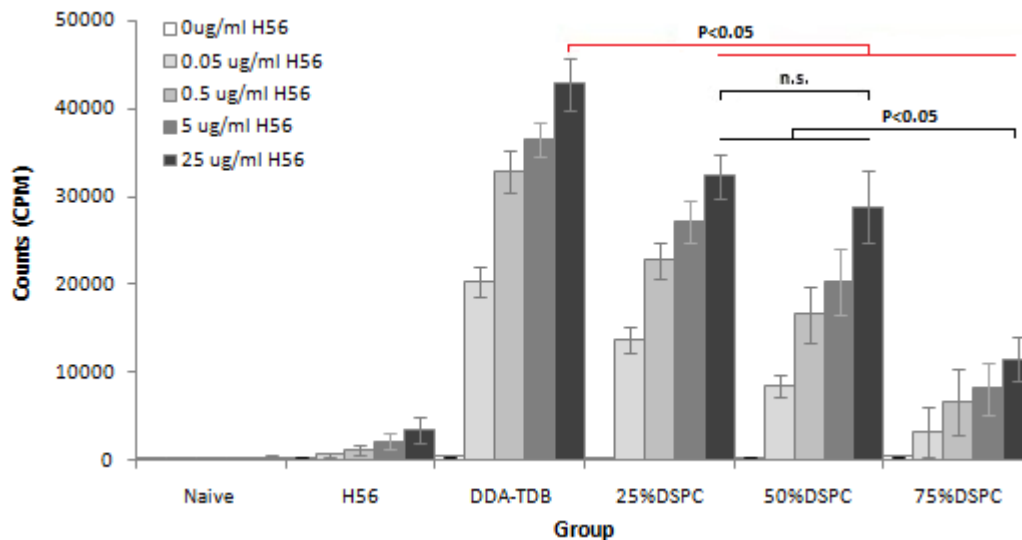


**Figure 6.7. Spleen cell proliferation in response to stimulation/re-stimulation with H56 antigen upon substitution of DDA-TDB with DSPC.** The extent of H56 antigen specific splenocyte proliferation was determined by the level of [<sup>3</sup>H]Thymidine incorporation into cultured splenocytes at antigen concentrations of 0-25 µg/ml. As a positive control, ConA was used at 2µg/ml which generated approximately 100,000 CPM. The results displayed denote the mean average for each group together with the calculated standard error at n=5. Significance is illustrated between the liposomal vaccination groups, and comparisons shown against one another are upon re-stimulation with H56 vaccine antigen at the concentration of 25 µg/ml.

Overall, the liposomal adjuvants were found to promote substantially higher responses compared to mice immunised with free H56 antigen. Moreover, DDA-TDB and its substitution with DSPC, from as low as 0.5 µg/ml re-stimulation of antigen, induced significantly higher levels of proliferation ( $P < 0.001$ ) in comparison to the non-adjuvanted H56 group. Such an antigen specific recall response being triggered at low concentrations of H56 re-stimulation could be beneficial, and in this regard, the use of a liposomal adjuvant was essential to eliciting a response.

Upon extensive examination, the DDA adjuvant has been shown to induce moderate Th2 type immunity and strong Th1 type immunity (Hilgers & Snippe, 1992), and as highlighted earlier, incorporation of TDB potentiates the immune response of DDA, eliciting stronger antigen specific Th1 type immunity (Davidsen *et al*, 2005). Furthermore,

studies into the relationship between vesicle charge and immunoadjuvancy have shown that cationic liposomes encourage further uptake by DCs, compared to their neutral counterparts (Foged *et al*, 2004). Positively charged liposomes have also demonstrated efficient uptake by macrophages, with cationic systems containing OVA found to induce higher levels of antibody and antigen-specific cytotoxic T lymphocyte responses than equivalent anionic and neutrally charged liposomes (Nakanishi *et al*, 1997). In addition, incorporation of DSPC has impacted upon the adjuvant action of liposomal delivery systems, with partial incorporation to DDA-TDB stabilised with cholesterol, reducing protective immunity (McNeil *et al*, 2011), and complete incorporation, in the substitution of DDA in DDA-TDB, also found to greatly decrease cellular immune responses upon immunisation with the H1 vaccine (Henriksen-Lacey *et al*, 2010b).

With all the substituted DDA-TDB adjuvants in the present study found to induce antigen specific spleen cell proliferation, the variation in response can be attributed to the various levels of DDA, TDB and DSPC in the proposed liposomal delivery systems. Substitution of DDA-TDB suggests that the observed splenocyte proliferation responses was affected by increased DSPC incorporation, as this in turn reduced the DDA adjuvant properties of the system and the immunopotentiating affect of TDB. Additionally, the responses exhibited were irrespective of the zeta potential of the vesicle composition, as these systems were previously characterised for attaining a comparable cationic zeta potential.

#### 6.3.5. *Quantification of cytokines*

Having characterised antigen specific spleen cell proliferation and antibody levels, in order to fully appreciate the extent and type of immunity stimulated, cytokine levels were

subsequently examined. A variety of cytokines were tested for their H56 antigen specific responses to the proposed DDA-TDB based vaccine delivery systems. Quantification of the cytokines, IL-2, IL-5, IL-6, IL-10 and IFN- $\gamma$  in the cultured splenocyte cell suspensions took place via specific sandwich ELISA experiments.

Cellular immunity is vital to mediating intracellular pathogens such as MTB, with IFN- $\gamma$  believed to be the greatest indicator of a Th1 type immune response (Sable *et al*, 2007). IL-2 is specifically generated by Th1 cells and is essential to T-cell proliferation and its consequent differentiation. In the context of *in vitro* splenocyte re-stimulation, IL-2 is indicative of cellular immunity as it is not generated by B cells (Vangala *et al*, 2007). IL-6, produced from Th2 type cells and monocytes, can act as both a pro-inflammatory and anti-inflammatory cytokine, interchangeable between Th1 and Th2 type immune responses. Contrastingly, interleukins 5 and 10 are associated with Th2 type responses. IL-5 is known to stimulate the growth and differentiation of B cells and enhance immunoglobulin secretion, whilst IL-10 down-regulates the expression of Th1 cytokines.

#### *6.3.5.1. Replacement of DDA in DDA-TDB: effect upon H56 specific cytokine production*

Upon immunisation with DDA-TDB, high levels of IFN- $\gamma$  were observed with partial replacement with DSPC (150/100/50  $\mu\text{g}/\text{dose}$ ) stimulating comparably high levels in the region of 4000 pg/ml (Figure 6.8 A). DDA-TDB at a 2:1 weight ratio also stimulated substantial levels of IFN- $\gamma$  however, further replacement within DDA-TDB coinciding with increased DSPC incorporation reduced IFN- $\gamma$  production (Figure 6.8 A). Notably, DSPC-TDB liposomes generated minimal levels of the IFN- $\gamma$  cytokine, in line with the naive and H56 vaccine groups (Figure 6.8 A). Such a trend was mirrored in the quantified

levels of IL-2, whereby DDA-TDB at a 5:1 and a 2:1 weight ratio alongside its partial replacement (150/100/50 µg/dose) represented the peak of IL-2 production, with DSPC-TDB stimulating comparatively low levels of this Th1 type cytokine (Figure 6.8 B).

For IL-6 production, reduced levels were seen across the vaccine groups (below 100 pg/ml) with the exception of DDA-TDB (at a 5:1 or 2:1 weight ratio) together with partial DDA replacement at 150/100/50 µg/dose, generating at least 200 pg/ml, with immunisation of DDA-TDB-H56 (5:1) found to generate the highest recorded levels at 400 pg/ml (Figure 6.8 C). Furthermore, quantified levels of IL-5 and IL-10, indicative of a potential Th2 type immune response, interestingly provided polarised formulation results, determined by levels of these cytokines produced when administered with the variety of DDA-TDB based vaccine adjuvants (Figure 6.8 D and E). Both sets of observed cytokine levels displayed little variation in the tested vaccine groups despite the level of cationic replacement, including the naive and H56 non-adjuvanted groups, until the highest level of DSPC was introduced to the formulation (Figure 6.8 D and E). This was evident in IL-5 and IL-10 production exhibited for DDA-DSPC-TDB at 50-200-50 µg/dose and DSPC-TDB, whereby significantly ( $P < 0.05$ ) elevated cytokine levels were detected, particularly upon re-stimulation with 5 µg/ml of H56 antigen (Figure 6.8 D and E), suggesting a Th2 bias for these DSPC enriched systems.

This polarised trend contrasted the effect of DDA-TDB against DSPC-TDB liposomes as adjuvants for the immunisation of mice with H1 antigen, whereby no significant difference in IL-5 production was apparent (Henriksen-Lacey *et al*, 2010b). Moreover, an interesting significant difference between DDA-TDB and the uppermost levels of DSPC

incorporation was observed, specifically for DDA-DSPC-TDB at 50-200-50  $\mu\text{g}/\text{dose}$ , characterised for attaining a net cationic charge yet shown to favour Th2 type immune responses, comparable to the anionic DSPC-TDB liposomes. As a result, it can be deemed that the immunological adjuvant effect was indeed influenced by the level of DDA content and replacement with DSPC and not by the zeta potential of the liposomes, corroborating previously related findings for total DDA replacement shown by Henriksen-Lacey *et al*, (2010b). Consequently, from the findings of this study, DDA-TDB based adjuvants can be produced with a comparable zeta potential, but upon further DDA adjustment, can be tailored to bias a particular desired immune response, demonstrating the flexibility of such liposomes as vaccine delivery systems.

In summary, DDA-TDB displayed a strong Th1 type immune response, characterised by elevated levels of IFN- $\gamma$  and low IL-5 cytokine production, correlating with previous studies (Holten-Andersen *et al*, 2004; Davidsen *et al*, 2005; Henriksen-Lacey *et al*, 2011b). Interestingly, partial cationic replacement produced a formulation that successfully incorporated the zwitterionic lipid of DSPC at the expense of DDA content, whilst eliciting a Th1 mediating effect comparable to levels induced by DDA-TDB, immunologically assessed and confirmed for H56 antigen specific spleen cell proliferation, IgG2b antibody production and cytokine secretion.

However, further incorporation of DSPC shifted the bias towards Th2 type immunity, indicated by specific cytokine responses and antibody levels recorded in this study. Indeed, the choice of adjuvant can greatly impact the immune response, with vaccine design intending to induce targeted, efficacious and prolonged immunity upon vaccination

(Lima *et al*, 2004). With the promising potential of the DDA-TDB adjuvant being recognised as a strong Th1 inducer, a switch to a protective Th2 type humoral immunity, upon particular levels of DSPC incorporation seen in the current study, can be of value for the treatment of other diseases. For example, delivery of Merozoite surface protein 1 (MSP1) and glutamate rich protein (GLURP) malarial antigens, using DDA and DDA-TDB adjuvants combined with a non-ionic surfactant of 1-monopalmitoyl glycerol (MP) and cholesterol, induced a Th2 type humoral response signified by proficient IgG1 antibodies, vital for protection against Malaria (Vangala *et al*, 2006). Partial incorporation of DSPC in this study provided elements of a Th1 and Th2 type response, which has been induced by other related liposomal vaccine candidates, demonstrating a required multifaceted response for protection against Chlamydia (Agger *et al*, 2008) and Influenza (Christensen *et al*, 2010).

Furthermore, adjustment of the DDA/DSPC content may be favourable for the delivery of alternative antigens, particularly for those that possess a high isoelectric point (pI) and consequently require an anionic adjuvant to associate to the carrier system via electrostatic interaction. Examples of such protein antigens include the model lysozyme antigen and the “CTH1” Chlamydia vaccine, which have a pI of 11.0 and 9.0 respectively (Henriksen-Lacey *et al*, 2010b), thus at physiological pH, attain a net cationic charge. Therefore, with careful manipulation of the liposomal adjuvant formulation, vaccine delivery can be accommodated for an array of antigens whilst generating a desired immunological effect.

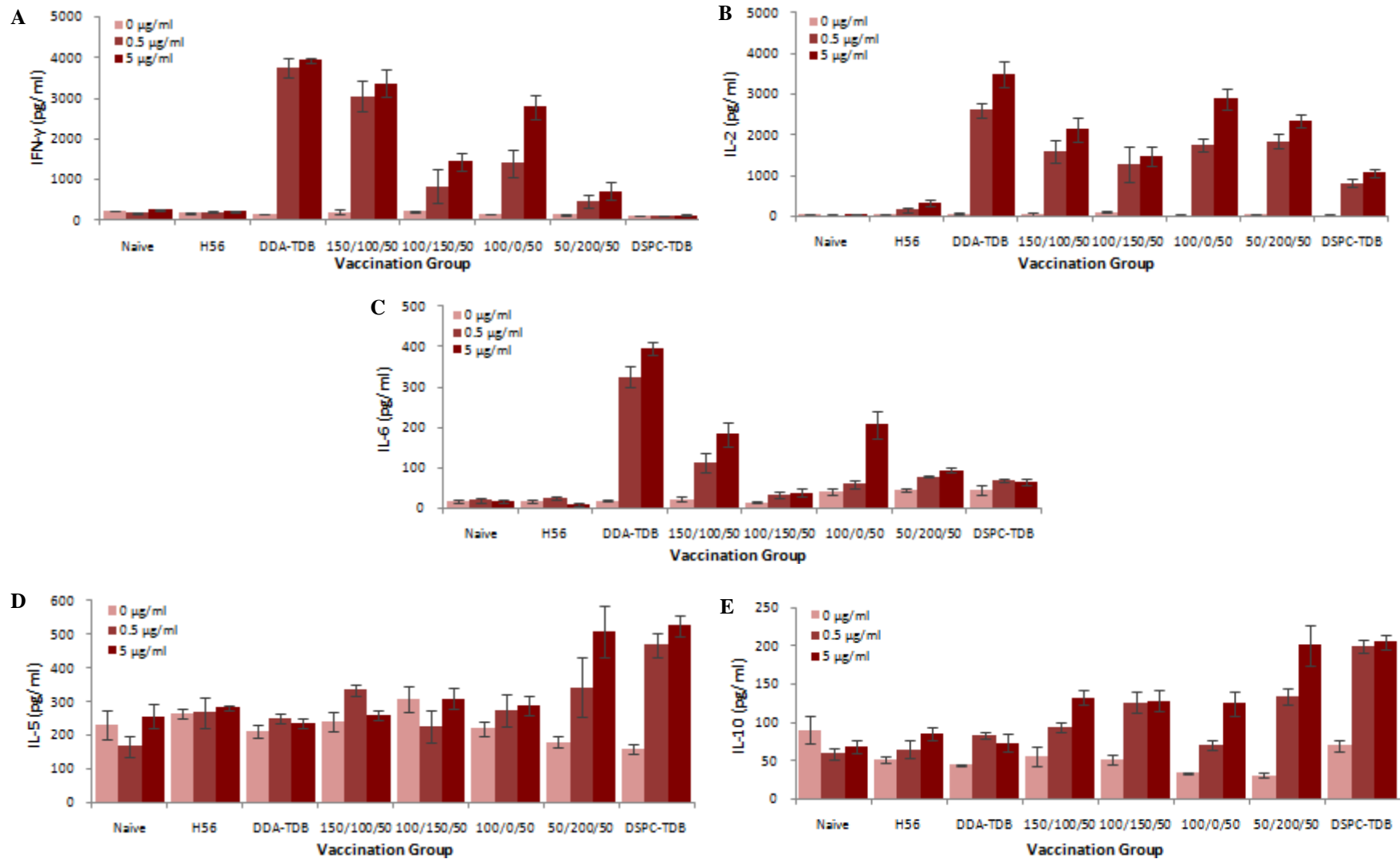


Figure 6.8. Spleen cell cytokine production after re-stimulation with H56 antigen at 0, 0.5 and 5 μg/ml, quantified for A: IFN-γ, B: IL-2, C: IL-6, D: IL-5 and E: IL-10, upon DDA replacement in DDA-TDB with DSPC. Values represent μg/dose, with results of the mean average of five spleens per group +/- SE.

Previous studies by McNeil *et al*, (2011) have also assessed the incorporation of TDB and DSPC into cationic DDA liposomes. These systems were further stabilised with cholesterol and upon immunisation with H1 antigen, good levels of IFN- $\gamma$  cytokine release were measured but were lower than levels stimulated by DDA-TDB (McNeil *et al*, 2011). Moreover, the incorporation of DDA induced more IFN- $\gamma$  than their neutral counterparts, demonstrating its necessity within the multi-component liposomal adjuvant for eliciting cellular immunity, enhanced further with TDB presence. Although the incorporation of DSPC and cholesterol decreased the level of protection provided by DDA-TDB, the neutral formulation of DSPC-Chol-TDB was found to generate protection upon MTB challenge, reiterating that liposomal surface charge was not the overriding factor behind adjuvant potency (McNeil *et al*, 2011). In general, it is understood that cationic liposomal adjuvants stimulate elevated IFN- $\gamma$  cytokine levels and in the present study, adjustment of cationic content, by reducing the level of DDA within the formulation, demonstrates that increasing DSPC content reduced IFN- $\gamma$  production (with the exception of initial DDA replacement at 150/100/50  $\mu\text{g}/\text{dose}$ ), and that the incorporation of DSPC allows for the liposomal adjuvant to be tuned with regards to the type of immunity required.

Liposomal adjuvants have previously been shown to strengthen the immunogenicity of vaccines, with DDA-TDB liposomes desirably eliciting high cellular immunity against the subunit Ag85B-ESAT-6 antigen for TB (Davidsen *et al*, 2005; Vangala *et al*, 2006). The use of DDA-TDB has also been evaluated as an adjuvant delivery system for hepatitis B surface antigen, eliciting enhanced T cell derived responses (Vangala *et al*, 2007), whilst upon immunisation, also harbouring the ability to stimulate a combination of cellular and humoral immunity required for protection against Chlamydia, demonstrating the

versatility of such an adjuvant (Agger *et al*, 2008). Additionally, for protective efficacy against Chlamydia, upon immunisation of C57BL/6 mice with Chlamydia-specific membrane proteins in various adjuvants, DDA-TDB displayed the greatest protection characterised by higher IFN- $\gamma$  and interleukin-17 cytokine responses, than the CpG oligodeoxynucleotide (CpG-ODN) adjuvant, recognised as a strong Th1 inducing agent, and the “AbISCO-100” (AbISCO) immunostimulating complex, which is known to elicit both Th1 and Th2 type immunity (Yu *et al*, 2010).

Upon the replacement of DDA with DSPC assessed in this study, for some of the tested formulations, a favoured cell mediated immune response against the promising post exposure H56 vaccine antigen was achieved to an equivalent level to that of DDA-TDB. In addition, further DSPC incorporation has been shown to reduce the cytotoxicity upon macrophages (Chapter 5), which may provide a potentially viable formulation alternative to the highly promising DDA-TDB (CAF01) liposomal adjuvant, as a subunit vaccine delivery system.

#### *6.3.5.2. Substitution of DDA-TDB: effect upon H56 specific cytokine production*

Immunisation with DDA-TDB liposomes displayed elevated levels of IFN- $\gamma$  and IL-2 and alongside this system, substitution with 25 mol% DSPC lipid induced comparable levels of these Th1 type cytokines, quantified between 3000-4000 pg/ml. Further incorporation at 50 mol% DSPC resulted in significantly reduced levels ( $P < 0.05$ ) for both cytokines with 75 mol% DSPC incorporation into DDA-TDB inducing little to no IFN- $\gamma$  or IL-2 cytokine production, similar to that observed for the non vaccinated and non adjuvanted groups (Figure 6.9 A & B).

In terms of IL-6 production, with DDA-TDB representing the highest quantified levels, DDA-TDB-25 mol% DSPC exhibited significantly ( $P < 0.05$ ) decreased production to almost half the generated level observed for DDA-TDB, with a further reduction seen upon 50 and 75 mol% substitution (Figure 6.9 C). Interestingly, for the assessment IL-5 and IL-10, the naive and H56 non adjuvanted group induced similar levels in line with all other immunisation groups displaying little variation between the liposomal adjuvants (Figure 6.9 D & E). The exception to this was observed for DDA-TDB-75 mol% DSPC producing the highest levels of IL-5, and DDA-TDB substituted with 25 and 75 mol% DSPC also representing the peak of IL-10 production (Figure 6.9 D & E).

In summary, the incorporation of 25 mol% DSPC was comparable to DDA-TDB in terms of its potential to initiate an antigen specific response in favour of cell mediated immunity. Furthermore, for the other immunological parameters characterised in this study, particularly for the presence of IgG2b antibodies and key cellular markers associated to a desired cellular immunity vital in providing protection against TB, such as IFN- $\gamma$  and IL-2, cytokine levels were also relatively as high as the optimum DDA-TDB adjuvant formulation, despite partial incorporation of DSPC lipid.

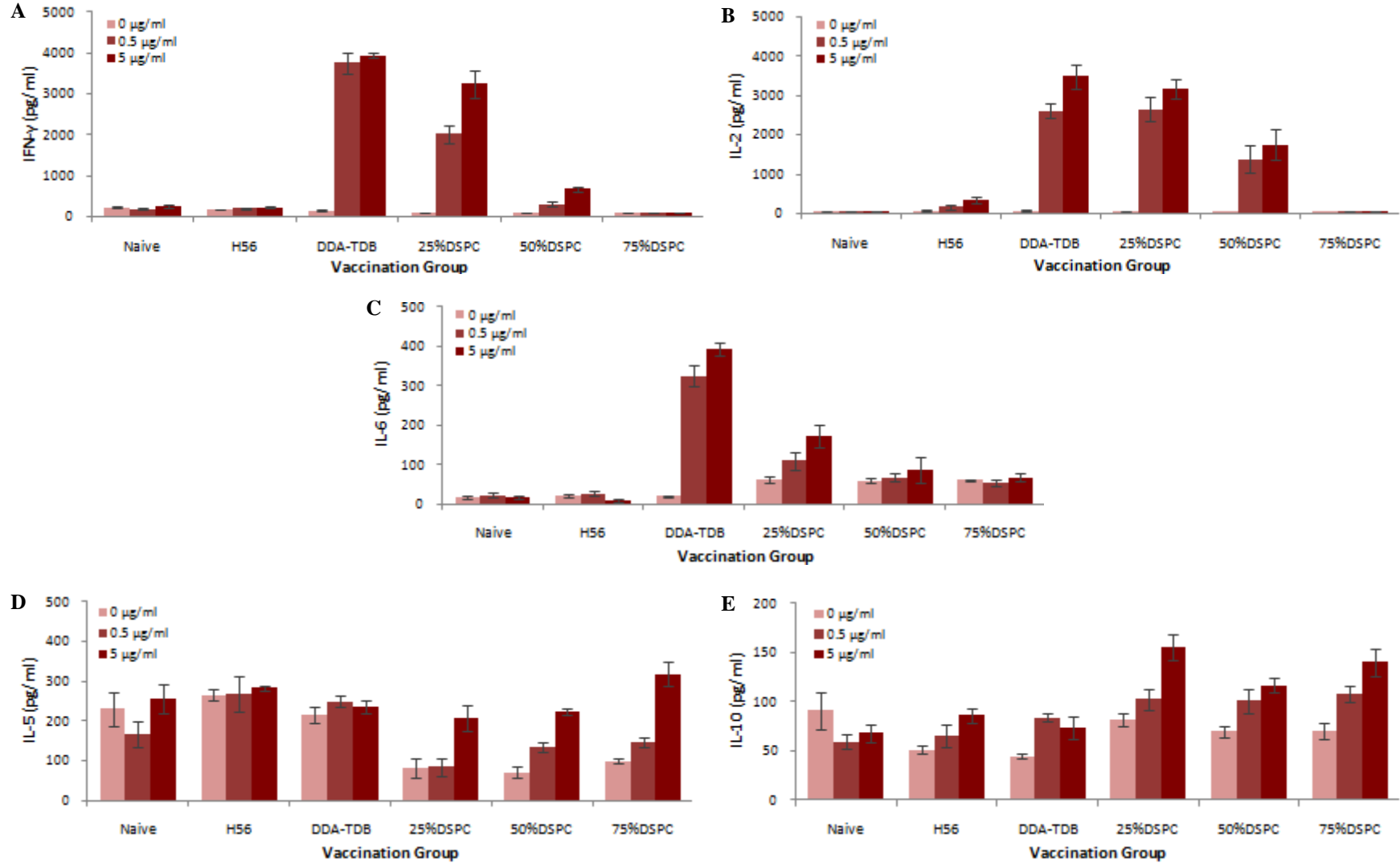


Figure 6.9. Spleen cell cytokine production after re-stimulation with H56 antigen at 0, 0.5 and 5 μg/ml, quantified for A: IFN-γ, B: IL-2, C: IL-6, D: IL-5 and E: IL-10, upon DDA-TDB substitution with DSPC. The results displayed are the mean average of five spleens per vaccination group +/- SE.

Interestingly, upon incorporation of DSPC at 75 mol%, the findings suggest a tendency towards a Th2 type immune response. With all systems found to produce equivalent levels of IgG and IgG1 antibodies, the IgG2b antibody subset together with cytokines typical of a Th1 type immune response examined in this study, provided key indications of bias towards a cell mediated immune response. With the varying levels of DSPC incorporation and the resultant immunological performance characterised, DSPC was successfully incorporated at a lower level providing a comparable formulation to that of DDA-TDB for a strong Th1 type response, whilst at higher levels of DSPC incorporation, producing a system skewed towards Th2 type activation, indicative of humoral immunity. Moreover, the cationic replacement adjuvant formulations portrayed a DDA dependent immunological effect, yet upon substitution with DSPC, in turn reducing both DDA and TDB content, the potentiating effect of TDB on the immune response of the adjuvants is demonstrated, evident as increased DDA-TDB substitution considerably altered the resultant immunological response.

As highlighted earlier, although all of the substituted systems attained a net cationic zeta potential, the strength of immune response varied with an increased level of DSPC incorporation in the substitution of DDA and TDB, particularly at 75 mol%, generating immunity skewed towards a Th2 type response. It has been reported in the literature that DDA-TDB generally stimulates reduced levels of Th2 cytokines such as IL-5 (Christensen *et al*, 2007b). Despite the comparable cationic properties of DDA-TDB substituted with 75 mol% of DSPC to that of DDA-TDB, findings in this study suggest a weak Th1 type cellular immune response upon the increased level of substitution. Therefore, the resultant Th2 type immune responses observed is stimulated by a heightened level of DSPC

incorporation and is not dependent on the zeta potential of the liposomal system, as previously demonstrated by the replacement of cationic content in this study and by Henriksen-Lacey *et al*, (2010b), whereby TDB incorporated liposomes were able to stimulate comparable levels of IL-5 cytokines, regardless of the zeta potential induced upon full incorporation of either DDA or DSPC.

It is widely recognised that live vaccines offer stronger protection against TB in comparison to killed microorganisms (Collins, 1984), providing the basis behind increased attention towards proteins secreted from live mycobacteria to attain protective antigens (Brandt *et al*, 1996). The live BCG vaccine still remains the only currently available TB vaccine, but growing concerns over its safety, waning sensitivity and a highly variable efficacy have invigorated a push for a safer, more potent vaccine alternative (Anderson & Doherty, 2005). It has been demonstrated previously in the literature that protection against TB on par with BCG is achievable via subunit vaccination of a single purified TB antigen (Brandt *et al*, 2000). In this particular instance, C57BL/6 mice immunised with purified ESAT-6 emulsified in a DDA adjuvant displayed minimal inherent immunogenicity requiring a more effective adjuvant, whilst incorporation of Ag85B induced sustained CMI, characterised by higher IFN- $\gamma$  release and a reduced bacterial load upon challenge. Although Ag85B and ESAT-6 are recognised during a natural TB infection, they both induced polarising levels of CMI when DDA liposomes were used as the adjuvant delivery system, upon which the addition of the immunostimulant MPL to DDA elicited ESAT-6-specific T-cell responses (Brandt *et al*, 2000). Therefore, the selection of a powerful immunoadjuvant is a vital influencing factor, even capable of boosting compatible molecules of previously decreased inherent immunogenicity.

Despite the development of novel TB vaccine candidates, the existing BCG vaccine is far from being replaced and with ongoing feedback from early phase clinical trials being attained, the efficacy and safety profile of proposed novel vaccine candidates can be improved (Kaufmann *et al*, 2010). H56 vaccine delivery via the established DDA-TDB (CAF01) liposomal immunoadjuvant has been shown to deter the maturation of TB to its active form, and thus provides the basis of clinical development (Aagaard *et al*, 2011).

#### **6.4. Conclusions**

The data presented demonstrates the necessity of an adjuvant system, evident from the notable levels of H56 specific splenocyte proliferation, particularly induced at low concentrations which could be a possible facet of the antigen. Furthermore, DDA presence within the adjuvant was a crucial factor as demonstrated upon partial replacement of DDA content within DDA-TDB or substitution of DDA and TDB, eliciting antigen specific cell mediated immune responses in a mouse model, signified by elevated levels of IgG2b antibodies and IFN- $\gamma$  and IL-2 cytokines, vital for providing protection against TB. In addition, as DSPC content within the adjuvant formulation increased, either by DDA replacement or reduction of DDA and TDB, the response was skewed towards Th2 type immunity, coinciding with reduced IgG2b antibody levels and elevated IL-5 and IL-10 cytokine production.

Such findings demonstrated that minor adjuvant adjustment was sufficient to influence the resultant immune response, even when the DDA-TDB ratio was maintained. Overall, the role of DDA presence against DSPC within the DDA-TDB adjuvant was appreciated, whilst strengthening the potential shown by the promising H56 vaccine against TB.

## **Chapter 7**

### **The potential of liposomes as systems for pulmonary vaccine delivery**

### ***7.1. Introduction: vaccination via the pulmonary route***

Liposomes may be regarded as a potential carrier system for subunit antigen delivery via the pulmonary route as they can be produced from phospholipids which are commonly found within the respiratory tract as a constituent of pulmonary surfactant (Mihalko *et al*, 1988). Furthermore, the use of pharmaceutical aerosols can accommodate competent drug delivery directly to the lungs (Crowder *et al*, 2001) and therapeutic liposomal aerosols have been shown to offer sustained drug release, eradicate local irritation, enhance drug potency and deliver active drugs locally (Gilbert *et al*, 1991; Parthasarathy *et al*, 1999).

Inhalational therapy provides advantages compared to other mucosal pathways for immunisation as an increased presence of mucosal antibody titres in the respiratory tract may provide immediate protection against pathogens upon targeted delivery of therapeutic agents, particularly against those that infiltrate via the lungs, for example in the case of TB (Gelperina *et al*, 2005; Sou *et al*, 2011). Also, the lungs confer advantageous features such as an immense absorptive surface area and thin alveolar epithelium (Hussain *et al*, 2004).

Indeed upon administration via this route, liposomes are engulfed by phagocytes and targeting liposome-encapsulated agents to alveolar macrophages of the lung is possible via inhalation (Myers *et al*, 1993), providing the opportunity of delivering antimicrobials and other drugs to such immune system cells intracellularly, which is of great consideration particularly for the treatment of pulmonary diseases of an intracellular nature (Thomas *et al*, 1991). *Mycobacterium tuberculosis* is a pathogenic bacteria species and is the main causative agent of TB (Ryan & Ray, 2003), with pulmonary TB constituting over 80% of TB infections worldwide. In addition, for protective efficacy against TB, subunit protein

vaccine delivery for local activity may induce a desired cellular immune response (Russo *et al*, 2000). Studies have demonstrated the potential of dry powders for pulmonary delivery, for example in the treatment of tuberculosis, whereby immunisation via the pulmonary route using an aerosolised spray dried form of 85B mycobacterial TB antigen microparticles enhanced protection against the infection, reducing the bacterial burden within the lungs and the spleen upon challenge in a guinea pig model (Lu *et al*, 2010).

When designing pulmonary vaccines, the inhalational device must be patient friendly whilst cost efficient to manufacture in order to economically scale up production for large immunisation projects, without causing any detrimental effects to the potency of the vaccine (Sou *et al*, 2011). Amongst the various methods of delivery, the use of pressurised metered dose inhalers (pMDIs) are popular as they offer a reliable, self contained, transportable and cheap aerosol delivery mechanism that can accommodate pulmonary drug targeting and the application of large and safe medicinal doses (Newhouse, 1991). In the present study, the aim of this chapter was to ascertain whether the DPPC based liposomal systems characterised earlier could be developed into a potential pulmonary vaccine for TB antigen delivery, to localise drug action in the lungs upon delivery via a pMDI system. In order to test these proposed liposomal adjuvants for potential pulmonary delivery, the formulations must be compatible with a solvent for delivery via a pMDI.

### ***7.2. Liposomal compatibility with ethanol***

To produce a liposomal pMDI sample, formulating liposomes in a solvent form was considered. Therefore, prior to testing the potential inhalational system for metered dose inhalation, if a medium can be used to transfer the dry pelleted liposome samples,

produced upon centrifugation, to a pressurised metered dose inhaler vial, with subsequent valve attachment and addition of a hydro-fluoroalkane (HFA) propellant, this would produce a suitable pressurised MDI suspension, to be tested and characterised further for its unique aerosolisation properties and suitability for pulmonary delivery. Indeed, utilisation of HFAs requires co-solvents, for example ethanol (Stefely, 2002) and the propellant system is a key constituent of a MDI formulation, acting as both a solvent and dispersion medium and an energy source for producing aerosol clouds upon actuation as the dose is released from the metering valve (Williams *et al*, 1998).

Lipids are compatible with solvents such as ethanol and liposomes may be prepared from ethanol-based proliposomes, in which a proliposome solution of lipids dissolved in pure ethanol is converted to liposomes upon introduction of an aqueous phase (Perrett *et al*, 1991). The addition of an aqueous phase beyond the  $T_m$  of the lipid produces such liposomes (Elhissi *et al*, 2006) and can be produced with high entrapment efficiencies for hydrophilic agents (Perrett *et al*, 1991). However, most attempts to develop proliposome technology for pulmonary delivery involve aerosolising such liposomes via nebulisation. Despite additional processing not being required, the aqueous liposomal dispersions necessary for nebulisation incur issues of stability, as during storage, the liposomal suspensions are subject to physical and chemical modifications that ultimately affect the vesicle composition, leading to eventual leakage of entrapped material (Niven *et al*, 1992; Darwis & Kellaway, 2001). Furthermore, recent studies using proliposomes for nebulisation achieved a high nebulisation output, yet further work is required to minimise losses of drug originally entrapped within such liposomes as sample sizes were reduced during nebulisation (Elhissi *et al*, 2011).

In this study, with pMDI selected as the method of liposomal delivery, an ideal solvent to be used would be a solution that provides a medium of transfer whilst being able to be removed relatively quickly. The use of ethanol allows for rapid vaporisation to occur so that contact with the vesicles is minimised, thus reducing possible detrimental effects on the system, and was therefore tested as a transfer medium. The chosen systems evaluated for their compatibility with ethanol were DDA-TDB (250-50 µg/dose), DDA-DPPC-TDB (150-100-50 µg/dose) and DDA-TDB-50%DPPC (125-25-165 µg/dose), as they represent the main adjuvant formulation and intermediate replacement or substitution with DPPC, the most prevalent phospholipid of pulmonary surfactant (Wright, 1990). These systems were tested alongside DDA liposomes and were characterised before and after ethanol exposure and upon protein adsorption to ascertain the effect of solvent on the liposomes.

### ***7.3. The effect of ethanol on the particle size and zeta potential of empty liposomes***

The empty liposomes were initially assessed for interactions with ethanol to investigate its effect on the lipid bilayers. The liposomes were prepared by lipid hydration and subjected to an equal volume of pure ethanol and then assessed for the resultant particle size, polydispersity and zeta potential over time (0-60 mins). Liposomes of DDA-TDB and partial replacement or substitution with DPPC were 500-700 nm with a polydispersity of ~0.3 and a zeta potential of 50 mV (Figure 7.1), as previously characterised (Chapter 3).

However, upon exposure to ethanol, all of the liposomal systems became significantly ( $P < 0.01$ ) smaller (200-300 nm; Figure 7.1) compared to their non-exposed counterparts, and remained at this reduced size for up to 60 minutes (Figure 7.1). The polydispersity of the liposomes ranged between 0.1-0.4, whilst the zeta potential remained in the region of 50

mV, until interaction with ethanol for 60 minutes caused a significant ( $P < 0.05$ ) decrease in zeta potential by ~30%, down to 35 mV (Figure 7.1).

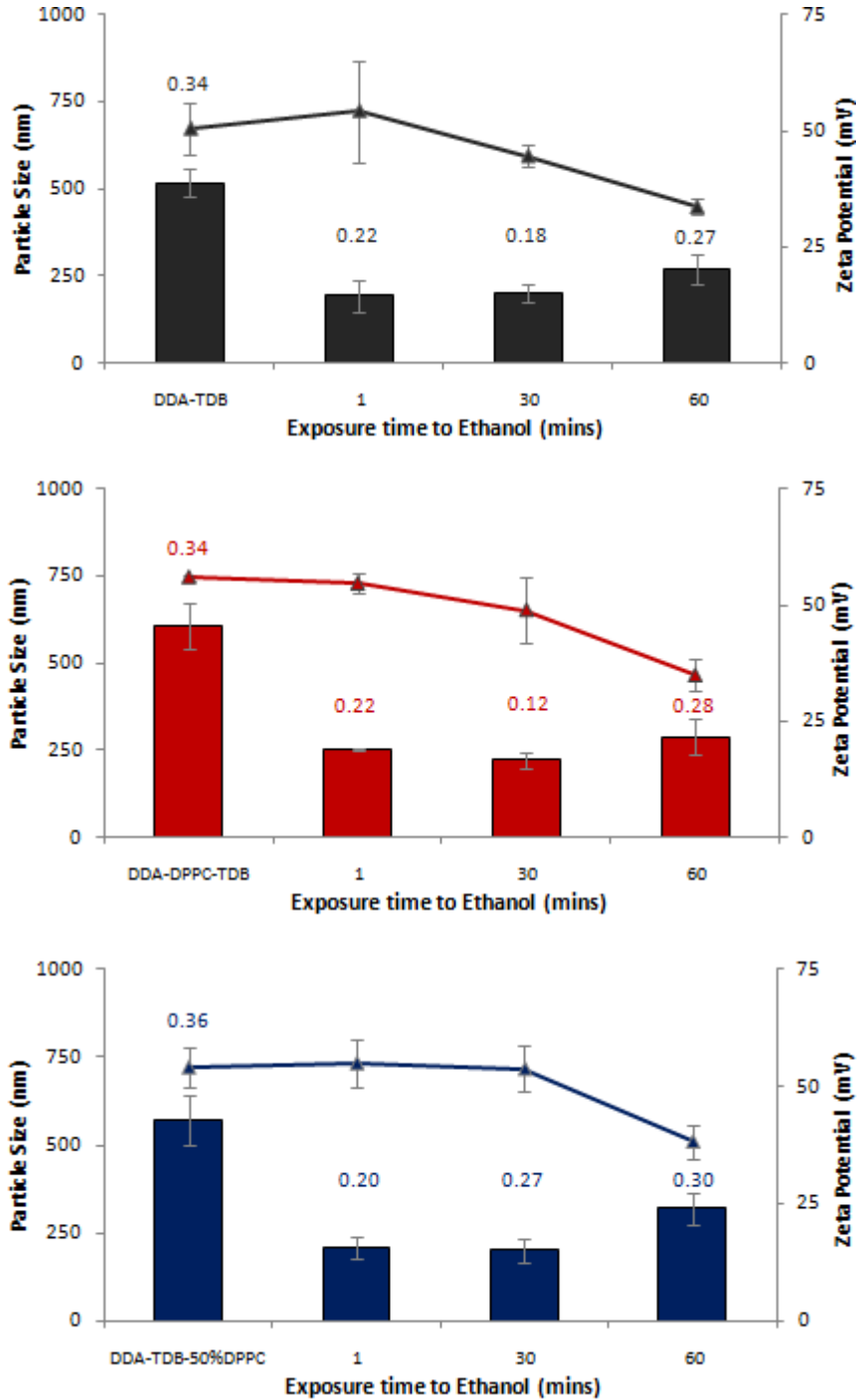


**Figure 7.1.** Effect of ethanol upon the particle size, polydispersity and zeta potential of A: DDA-TDB, B: DDA-DPPC-TDB (150-100-50  $\mu\text{g}/\text{dose}$ ) and C: DDA-TDB-50%DPPC liposomes over time. Results shown are the mean average of three experiments with error bars of the standard deviation from the mean.

It is apparent that upon exposure of the liposomal systems to ethanol, the pure solvent had interacted with and affected the vesicular structures as significantly smaller liposomes were formed. The effect of ethanol on liposomal permeability was studied by Komatsu & Okada, (1995), in which the leakage of fluorescent dye entrapped within the inner aqueous core of large unilamellar DPPC vesicles was observed. It is understood that when exposed to short chain alcohols, saturated phosphatidylcholines are capable of forming interdigitated regions, in which the methyl group within the acyl chains infiltrate the opposing monolayer. Moreover, findings indicated that the presence of ethanol at higher concentrations induced high permeability with leakage of the dye greatly increased as the original bilayer and interdigitated structure coexist with phase separation of the membrane and instability of the boundary regions, which is also the case even when the membranes were initially stabilised with cholesterol (Komatsu & Okada, 1997).

A breakdown in the spherical geometry of liposomes may also occur upon ethanol interaction with small liposomes of saturated phospholipids due to the interdigitation of ethanol molecules (Ahl *et al*, 1994). In the present study, the reduced liposomal particle size observed upon ethanol exposure demonstrates the possible effect of ethanol on the phospholipid chains of the liposomes, with such intermolecular interactions disrupting and altering the original lipid bilayer structure and may be representative of a restructure into small unilamellar vesicle formation.

In addition, alcohols have been shown to aggravate chain interdigitation of phosphatidylcholines such as DPPC or DSPC (Li *et al*, 1996), and as ethanol penetrated the liposomes, direct interaction with the pure solvent destabilised the vesicle structure

and not only affected the phospholipid acyl chain arrangements, it may have caused a secondary interaction with ethanol molecules associating to sites at the head groups of the bilayer surface (Rowe, 1983), thus affecting the original liposomal structural arrangement.

#### 7.4. Effect of ethanol exposure to liposomes adsorbed with protein

Given that particulates of a cationic nature (although smaller in size and lower in cationic charge) were still formed after exposure to ethanol, studies progressed into considering cationic liposomes with adsorbed protein. Therefore, the above outlined liposomal systems were mixed with OVA protein (which acts as a model antigen) to a final concentration of 1 mg/ml, and again the effect of ethanol exposure was considered. More specifically, the liposomal samples were adsorbed with OVA and split into two prior to ultracentrifugation, with one resultant pellet resuspended in Tris buffer and the other in pure ethanol, which was subsequently removed via nitrogen streaming and resuspended back into Tris buffer for comparison, as summarised in Figure 7.2.

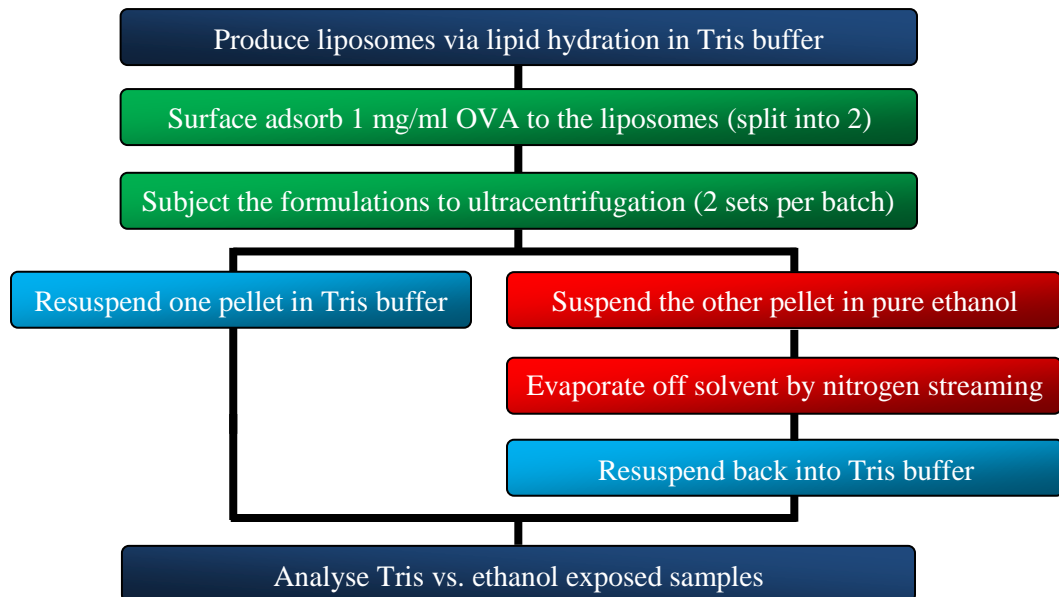


Figure 7.2. A process map summarising the experiment conducted to directly compare the effect of Tris buffer vs. ethanol on the cationic liposomes adsorbed with OVA protein.

Prior to ethanol exposure, the vesicles adsorbed with OVA in Tris buffer were between 2-3 micrometres in particle size with a neutral to slightly anionic zeta potential (Table 7.1), whilst no significant difference was apparent between the formulations. However upon exposure to ethanol, liposomes of DDA, DDA-TDB and its partial replacement or substitution with 50 mol% DPPC were all found to be significantly ( $P < 0.05$ ) smaller (~1500 nm; Table 7.1) than their Tris buffer counterparts. When considering the effect of ethanol on the cationic nature of the systems, all liposomes adsorbed with OVA were also shown to have a significantly ( $P < 0.05$ ) increased zeta potential when compared to the neutral systems saturated with OVA in Tris buffer, as exposure to ethanol generated vesicles in the region of 15-20 mV (Table 7.1), suggesting a possible loss of adsorbed protein from the surface of the liposomes and/or a re-organisation of the structures.

Subsequent morphological analysis via TEM demonstrated contrasting vesicle populations with an abundance of OVA generating aggregated particles in Tris buffer (Figure 7.3), which corroborated with the previously attained sizing data. Contrastingly, the ethanol exposed samples displayed more sparsely populated vesicles with more exposed surfaces compared to their Tris buffer counterparts (Figure 7.3). In addition, no apparent differences were observed between each of the DDA-TDB based cationic systems exposed to ethanol, with vesicles predominantly in a sub-micrometre size range, as observed in the previous measurements of particle size via DLS, with only minor traces of particle aggregation (Figure 7.3).

**Table 7.1. Particle size, polydispersity and zeta potential of liposomes adsorbed with OVA at 1 mg/ml in Tris buffer or exposed to ethanol and redispersed back into Tris buffer.** Results displayed are the mean average +/- the standard deviation of at least three independent experiments.

Formulation	Particle size (nm) (Tris buffer)	Polydispersity (Tris buffer)	Zeta potential (mV) (Tris buffer)	Particle Size (nm) (ethanol exposed)	Polydispersity (ethanol exposed)	Zeta potential (mV) (ethanol exposed)
DDA	2063.9 ± 383.6	0.60 ± 0.04	6.0 ± 3.8	909.2 ± 169.3	0.43 ± 0.01	17.6 ± 2.3
DDA-TDB (250-50 µg/dose)	2753.3 ± 410.6	0.24 ± 0.11	3.6 ± 4.3	1315.8 ± 396.7	0.49 ± 0.31	27.2 ± 3.6
DDA-DPPC-TDB (150-100-50 µg/dose)	3213.3 ± 370.2	0.59 ± 0.29	-1.9 ± 2.6	1194.1 ± 128.6	0.50 ± 0.18	14.8 ± 11.5
DDA-TDB-50% DPPC (125-25-165 µg/dose)	3589.0 ± 350.5	0.38 ± 0.15	-1.2 ± 2.0	1947.5 ± 808.3	0.42 ± 0.13	19.8 ± 11.4

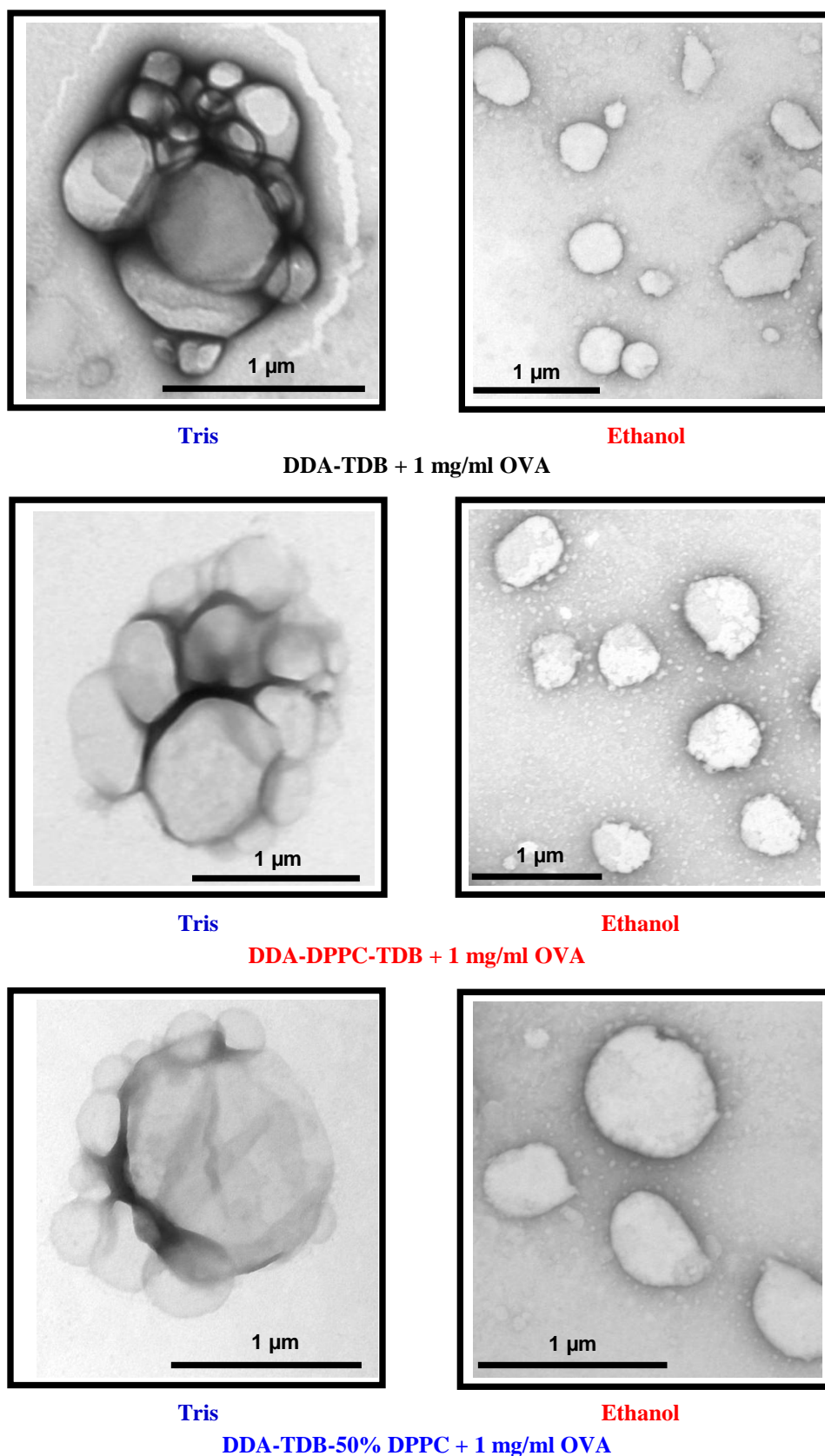


**Figure 7.3.** TEM micrographs of cationic liposomes with OVA in **Tris** buffer vs. **ethanol** exposure. All liposomes were surface adsorbed with OVA at 1 mg/ml and were prepared by lipid hydration in Tris buffer.

Holte & Gawrisch, (1997) suggested that at higher concentrations of ethanol incorporation, such as the pure form used in this study, non-specific surface binding with bilayers is induced. Thus, the causation of vesicle instability is also possible, as any bonds and intermolecular interactions contributing to maintaining the vesicle structure may be disrupted, and it is possible that exposure of the systems to ethanol has caused a restructure of the vesicles and affected the associated protein structure, therefore potentially reducing the inter particle attraction between the vesicles.

Indeed interactions of ethanol with proteins can affect their structure and function as such proteins can become unstable and poorly soluble (Pace *et al*, 2004). The addition of ethanol causes proteins in solution to precipitate out. This process occurs due to a decrease in the dielectric constant, in turn decreasing solubility. Ethanol readily associates with water to a much greater extent than it does with proteins, effectively causing dehydration of proteins at the surface (Oss, 1989). The organic solvent can continue to displace water from protein surfaces that binds into hydration layers coating the ethanol molecules. Thus, the protein molecules are exposed of hydration layers, yielding protein aggregation. Hydrogen bonding is pivotal to protein structure and important to the stabilisation of proteins, with the  $\alpha$ -helix and  $\beta$ -sheets of protein molecules recognised as fundamental structural components in the composition of proteins. Relatively weak intermolecular forces, such as hydrogen bonds and van der Waals forces, facilitate the intricate folding of proteins. However, exposure to ethanol can modify this complex protein structure and denature its original form (Mirsky & Pauling, 1936; Pauling *et al*, 1951).

Indeed a notable difference in visual appearance between the OVA solutions in Tris buffer vs. ethanol was apparent, as precipitates observable in the pure solvent demonstrated the immiscibility of protein in pure ethanol, contrasting the miscibility of OVA in Tris buffer, as it dissolved into a clear solution (Figure 7.4). When the ethanol was evaporated off and redispersed back into Tris buffer, the OVA failed to dissolve into a completely clear solution as some precipitates were present. This would suggest that upon exposure of the liposomal-protein constructs to ethanol, the proteins become insoluble and precipitate, and are therefore possibly lost from the vesicles. To investigate this further, antigen loading of the vesicles before and after ethanol exposure was investigated.

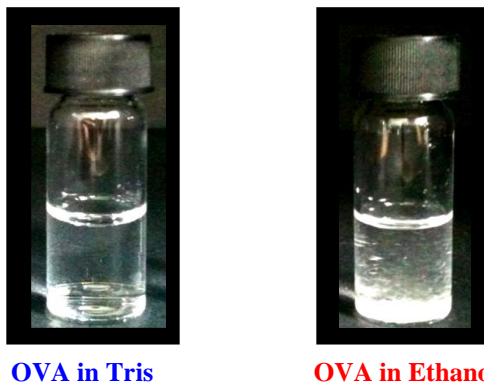


Figure 7.4. Comparison of 1 mg/ml OVA in **Tris buffer** vs. **ethanol**.

### ***7.5. Radiolabelled antigen retention***

The effect of ethanol exposure to cationic liposomes was analysed to determine the extent of resultant protein adsorption to the vesicles against identical systems in Tris buffer. OVA protein was radiolabelled with  $I^{125}$  to directly track the level of antigen retained. DDA was selected to represent the cationic liposome systems and was surface adsorbed with radiolabelled OVA to a final concentration of 1 mg/ml. Upon adsorbing the DDA liposomes with OVA- $I^{125}$ , subsequent ultracentrifugation separated the samples into

liposome associated and non-associated protein. Once the systems had undergone two ultracentrifugation steps to remove unbound material, one half of each pelleted batch was suspended in either Tris buffer or exposed to pure ethanol. The batch suspended in Tris buffer had undergone two further ultracentrifugation steps, with the ethanol samples, upon solvent removal via nitrogen streaming and reconstitution in Tris buffer, also centrifuged a further two times to allow for a direct comparison to be made between the Tris and ethanol exposed DDA-OVA/I<sup>125</sup> adsorbed systems. Gamma counts for the original total, supernatant and pellet samples were used to calculate the level of protein association.

The results in Table 7.2 show that after removal of the initial non-associated OVA, 87% of OVA was retained by the DDA liposomes, and this was not significantly changed by further incubation in Tris buffer as described above. However after exposure to ethanol, OVA retention was significantly reduced ( $P < 0.001$ ) to 24.4% (Table 7.2), demonstrating that exposure to the pure solvent resulted in protein loss from the vesicles and support that the change in zeta potential noted in Table 7.1 is a result of protein loss.

**Table 7.2. Levels of OVA/I<sup>125</sup> retention to DDA liposomes before and after exposure to ethanol.** Results represent the mean average and the standard deviation of three independent experiments.

<b>Formulation</b>	<b>OVA retained from the initial batch in Tris (%)</b>	<b>OVA retained after being redispersed in Tris (%)</b>	<b>OVA retained upon exposure to ethanol (%)</b>
DDA	87.3 ± 2.6	87.2 ± 2.6	24.4 ± 11.6

Additionally, in the context of the delivery mechanism used for inhalation, ethanol is commonly utilised to enhance the drug solubility of formulations for metered dose

inhalation, however, the volume of solvent used must be minimised as when the level of solvent introduced to the MDI rises, the aerosol particles become rougher in texture which hinders the aerosolisation performance (Johnson, 1997). In the present study, if interaction with ethanol maintained a comparable level of antigen retention to Tris buffer, this may have facilitated further development into a pulmonary delivery system via metered dose inhalation. However this was not the case, and the detrimental effect of ethanol on the liposomal structure and associated protein, later confirmed to affect the high retention of radiolabelled OVA adsorbed to the cationic vesicles, renders the use of ethanol unviable.

#### ***7.6. Drawbacks and disadvantages associated to liposomal pulmonary vaccine delivery***

Prior to continuing the development of a pulmonary TB vaccine and taking into account the efficacious potential of aerosolised antigen delivery, the obstacles associated to such a route of delivery were considered. For example, despite an immediate onset of action upon targeting the respiratory system, this period is typically limited as the delivered material may be rapidly cleared from the lung through a variety of clearance mechanisms in the upper respiratory region such as impaction, sedimentation and interception, which clears particulates and prevents deeper deposition into the lungs. It is also understood that regardless of the aerosolisation device used, patients will need regular dosing throughout the day to achieve a desired level of protection (Johnson, 1997; Joshi & Misra, 2001).

Crucially, the therapeutic and toxic drug concentration must be considered, with a compromise between pharmacological activity and safety of primary importance when formulating vaccines (Zeng *et al*, 1995). Although cationic liposomes can favourably enhance antigen retention and the resultant immunostimulatory effect, a major drawback

in the use of these cationic systems is the associated cytotoxicity which often suppresses their development into pulmonary vaccines. Li & Mitra, (1996) studied pulmonary absorption of liposome-insulin complexes and established that the capability of liposomes in facilitating pulmonary protein absorption relied upon the surface charge, concentration and acyl chain length of the lipids used. Moreover, despite the cationic liposomal systems triggering the greatest hypoglycaemic response compared to their anionic and neutral counterparts, toxicological studies demonstrated that charge inducing agents such as stearylamine, used to provide the liposomes with a positive charge, can result in the disruption of pulmonary epithelial cells (Li & Mitra, 1996). Indeed, other pulmonary studies involving positively charged liposomes have also concluded that cationic lipids are too toxic to the alveolar region (Sheule *et al*, 1997).

In the present study, although increased lipid incorporation in the reduction of cationic content or adjuvant concentration reduced cytotoxicity (chapter 5), the optimum DDA-TDB formulation induced the least macrophage cell proliferation and these particular systems may incur adverse effects upon administration to the respiratory tract. In addition, the macrophage cell line was utilised as a general model to consider the viability of the proposed immunoadjuvants, yet assessment of nanoparticle toxicity and safety elicited upon delivery to the lung provides a great challenge when developing novel systems. Indeed, when considering the fate of nanomedicines in the lungs, the use of *in vitro* cell exposure studies using pulmonary cell systems has been recognised for its potential to screen nanoparticulate toxicity. However, further development is required in order to accurately examine the biological impact of nanoparticulate delivery via the pulmonary pathway (Paur *et al*, 2011).

### ***7.7. Conclusions***

It was established from the investigation of ethanol as a possible transfer medium for a pMDI system that minimal exposure altered the properties of the liposomes and the systems adsorbed with protein. Indeed ethanol caused a restructure of the liposomes and the protein induced aggregation displayed in Tris was less apparent upon interaction with ethanol, which cleared the protein at the surface and minimised the level of inter particle attractions. Subsequent studies of DDA liposomes with radiolabelled OVA confirmed that ethanol unfavourably displaced the adsorbed antigen, as equivalent samples in Tris buffer showed a high level of radiolabelled OVA retention.

An alternative approach to using a solvent based system for pMDI is the dry powder format to produce particulates and allow for performance characterisation and development of a potential pulmonary vaccine to commence. Freeze and spray drying are two methods that could be considered to prepare liposomal dry powder formulations. Freeze drying is regarded as the method of choice for preparing liposomal dry powders, especially for liposomes encapsulating proteins, peptides or enzymes (Lu & Hickey, 2005). Spray drying is also a suitable method for preparing micron-sized powders for aerosolisation, as it can control particle formation and be easily translated to large scale production. However, upon evaluation of the use of cationic liposomal systems and their associated toxic effect upon delivery via the pulmonary route, further work into developing an aerosolised pulmonary vaccine delivery system was not undertaken.

# **Chapter 8**

## **General discussion and conclusions**

### ***8. General discussion and conclusions***

The propose of vaccination is to provide effective immunity, and with continual elucidation of immunological mechanisms such as pathogen recognition, the role of adjuvants and gene expression, an ever increasing immunological understanding has paved the way for greater research into vaccination (Bramwell & Perrie, 2005). Indeed, considerable progress has lead to the understanding that vaccination is always considered as the best control strategy against any disease (Sable *et al*, 2007a).

Tuberculosis, which is caused by the intracellular pathogen of mycobacterium tuberculosis, is no exception as over 80% of the world's population is already vaccinated against TB with the live attenuated BCG vaccine. However despite such efforts, TB is one of the most deadly infectious diseases worldwide and this predicament has worsened since the onset of the MTB and HIV co-pandemic, intensifying the need for further development of new and improved prophylactic and therapeutic interventions (Sable *et al*, 2007a). In addition, it is understood that for TB to be completely eradicated, a potent and cost effective vaccine for mass immunisation is required, and although BCG is readily available, it is estimated to prevent a mere 5% of all potential vaccine-preventable fatalities due to tuberculosis (Gupta *et al*, 2007).

Consequently, TB vaccine development remains high on the global agenda and a major advancement towards the end of the 20<sup>th</sup> century was determination of the genome sequence for the best-characterised MTB strain, H37Rv, as it fuelled the conception of novel prophylactic and therapeutic interventions. With the understanding that a promising antigen does not necessarily correlate to a proficient immunogen (Sable *et al*, 2007a), the

evolution of subunit vaccine design to enhance immunogenicity resulted in the fusion of the 6-kilodalton early secretory antigenic target (ESAT-6) to Ag85B, generating the H1 vaccine. Such a combination is promising as the proteins are highly recognised T-cell antigens during the initial stage of infection and have been established to achieve protection within animal models (Olsen *et al*, 2001). This particular fusion protein vaccine candidate has been shown to elicit potent antigen specific cellular immunity, inducing Th1 type cytokines and antibody responses in the C57BL/6 mouse model, stimulating efficient immunological memory upon delivery via DDA-MPL (Olsen *et al*, 2001), and DDA-TDB (Davidsen *et al*, 2005), which was later shown to increase monocyte infiltration at the site of injection upon H1 antigen deposition (Henriksen-Lacey *et al*, 2010a).

Whilst the fusion of early secreted TB antigens have shown potential as an alternative to BCG, a post exposure vaccine that can provide protection against the late persistent stage of infection remains a high priority (Moreno-Mendieta *et al*, 2010). The Statens Serum Institut has developed a strategy for a post-exposure vaccine by targeting mycobacteria during the latent stage of infection. The emergence of one such candidate has been established by combining H1 with Rv2660c antigen forming H56 vaccine, a therapeutic subunit vaccine that can contain the infection upon challenge (Aagaard *et al*, 2011).

Taking this into account and given that subunit vaccines can be potentiated by co-delivery with adjuvants, coupled with the promising CAF01 cationic liposomal formulation established in providing cellular immunity against TB (Davidsen *et al*, 2005), DDA-TDB formed the foundation of liposomal adjuvants tested in this study as subunit delivery systems for the H56 vaccine. The aim of this thesis was to further investigate the

physicochemical properties of DDA-TDB upon its cationic replacement or reduction in concentration by incorporating zwitterionic lipids of DPPC or DSPC, to ascertain the role of the cationic DDA lipid in the formulation. Furthermore, the DPPC based systems were assessed for possible pulmonary delivery and the characterised physicochemical and *in vitro* properties were correlated with their effectiveness *in vivo*, using the DSPC based formulations as delivery systems for the promising H56 TB vaccine.

Initial work of this thesis concentrated on extensively characterising the DDA-TDB based formulations with the key focus at this stage being the evaluation of additional lipid incorporation and its resulting physicochemical properties. With the DDA liposomal adjuvant being previously optimised for TDB incorporation at 11 mol% (5:1 weight ratio) (Davidsen *et al*, 2005), this standard formulation was retained as TDB has been shown to potentiate DDA response and outperform an aluminium based adjuvant, which still remains one of the most widely used vaccine adjuvants (Davidsen *et al*, 2005).

Our data had shown that DPPC or DSPC incorporation led to the formulations retaining a sub-micrometre particle size and a cationic zeta potential until complete DDA replacement took place. Furthermore, no difference at this stage was apparent upon the introduction of either supplementary lipid. Whilst DDA-TDB liposomes provide a cationic charge ideal for antigen absorption, possible issues of long term colloidal stability with such a combination have been countered upon TDB incorporation (Davidsen *et al*, 2005), yet despite a vast array of literature highlighting the potential of liposomal drug delivery, a lack of liposome based vaccines are currently available due to their weak physical stability in solution (Mohammed *et al*, 2010). Therefore, with incorporation of additional lipids at

the expense of DDA-TDB concentration, these formulations were subjected to stability trials, in which we observed the retention of vesicle size and zeta potential over time. The lack of aggregation or visible precipitates in both temperature conditions demonstrated that even upon increased lipid incorporation (up to 75 mol% of DPPC or DSPC), the physical stability of the systems could still be maintained. Such findings provided the springboard for further physicochemical investigation where we also discovered that the high retention of radiolabelled OVA associated to DDA-TDB, used as OVA is established as a protein standard (Huntington & Stein, 2001) and was utilised in this study as a model antigen, was reduced upon partial DDA replacement or substitution within DDA-TDB, yet upon an initial burst of protein release, levels were retained for the remainder of the experiment. In addition, the necessity of DDA in retaining antigen was clear when DSPC-TDB liposomes failed to retain OVA over time. Also, dialysis of the liposome-OVA protein complexes provided a suitable means of assessing the proposed nano-particulate systems, with iodine labelling to OVA allowing for protein release to be tracked, whilst demonstrating the level of protein retention from the systems that were not subjected to any centrifugation methods to separate liposome associated and non-associated protein, thus, mimicking an *in vivo* preparation prior to administration.

Subsequent assessment of liposomal interactions with serum proteins also demonstrated instantaneous serum induced aggregation in line with previous studies for related cationic systems (Henriksen-Lacey *et al*, 2010a; McNeil & Perrie, 2006). When DDA-TDB incorporated DPPC or DSPC, the liposomal complexes exhibited a charge dependent reaction as complete DDA replacement displayed no significant change in particle size or zeta potential upon exposure to serum proteins. These findings indicate that as a result of

serum interactions and the consequent switch to an anionic zeta potential, particularly for the cationic formulations, exposure to serum most likely induced liposome-serum complexes as opposed to serum induced vesicle disruption.

With the understanding that efficient liposome delivery is influenced by the level of protein association (Korsholm *et al*, 2007), further examination of protein adsorption properties took place after saturating the systems with 1 mg/ml OVA. Whilst all cationic systems demonstrated particle aggregation, quantification of non-adsorbed protein did differentiate between the formulations, with SDS-PAGE confirming that either incremental replacement of DDA content or DDA and TDB substitution continually decreased the level of OVA associated to the system. Korsholm *et al*, (2007), when testing the adsorption capabilities of OVA to DDA vesicles, established a high level of adsorption to such liposomes which subsequently generated active protein uptake by DCs of murine bone marrow *in vivo*, with vesicles favourably delivering antigen to the cell membranes of APCs. The targeted antigen delivery achievable demonstrates the principal role of such cationic adjuvant systems, ultimately enhancing antigen uptake and submission.

Microscopic analysis was conducted via TEM in order to examine the morphology of the liposomal systems, with images corroborating with earlier particle size analysis, displaying a heterogeneous population of spherical vesicle structures. However, whilst DPPC or DSPC lipid was assumed to be incorporated into DDA-TDB, thermodynamic analysis via DSC confirmed the nature of interactions between the multiple lipid components, as single broadened main melting peaks symptomatic of lipid interdigitation were apparent. Furthermore, DSC studies showed the first key difference between DPPC

or DSPC incorporation, with the formulations incorporating DSPC demonstrating elevated phase transition temperatures at approximately 10 °C higher than the DPPC equivalents, which can be attributed to the longer 18-carbon alkyl chains of DSPC. Interestingly, partial incorporation of DSPC, with DDA/DSPC/TDB dispersions at 150/100/50 µg/dose and substitution with 50 mol%, displayed an absence of detectable thermal events, which can be attributed to attaining an organised, intermediate liquid-ordered phase. We therefore learnt that with the behaviour observed for DDA-TDB, followed by its partial replacement or substitution, incorporation of additional lipids to a particular level was achievable without substantially hindering the resultant physicochemical properties, and at this particular stage, displayed characteristics of potential vaccine delivery systems.

The *in vitro* studies conducted strengthened the potential of the proposed liposomal immunoadjuvants as a reduced net sample concentration, DDA lipid presence and DDA-TDB concentration was observed to increase macrophage cell proliferation, and such a response is advantageous as toxicity limits the volume of cationic lipid that is offered to cells (Hofland *et al*, 1996). Therefore in this regard, although reduced cationic content and DDA-TDB dose had shown decreased antigen retention, the reduced cytotoxicity may in fact harbour an increased propensity of liposome-cell interactions and thus, increase the potential efficiency of the proposed immunoadjuvants. In addition, with an observed cationic DDA lipid and DDA-TDB concentration dependent effect upon induced phagocytic activity, levels of TNF- $\alpha$  cytokine secretion in response to the various liposomal formulations showed less variation, particularly upon DDA adjustment, as continual cationic replacement with either additional lipid elicited comparable levels of TNF- $\alpha$ . This tells us that whilst DDA presence undeniably impacts the adjuvant properties

of the formulation, as potential vaccine delivery systems, the immunopotentiating affect of TDB can still be retained within the formulation, despite further lipid incorporation and a reduced cytotoxicity, which Numata *et al*, (1985) shown *in vivo*, when TDB, a derivative of TDM, was compared to its synthetic analogue, demonstrating a reduced toxic effect whilst maintaining adjuvanticity.

The various DDA-TDB based liposomes replaced or substituted with DSPC were considered as viable subunit vaccine delivery systems to be tested *in vivo*. In consideration of the route of administration, for a targeted cell mediated immune response, it has been reported that intramuscular injection of DDA based liposomes can promote a depot effect, crucially retaining antigen-liposome complexes at the site of injection, promoting monocyte infiltration (Henriksen-Lacey *et al*, 2010a). In contrast, liposomal vaccine delivery systems applied via intravenous injection have been restricted by poor stability in the blood stream and clearance by mononuclear phagocytic system (MPS) cells of the liver and spleen (Moghimi & Patel, 1989). Taking this into account and based on previously related immunisation studies involving the H1 subunit TB vaccine adsorbed to cationic DDA based liposomes stimulating powerful Th1 type immune responses (Henriksen-Lacey *et al*, 2010a; Henriksen-Lacey *et al*, 2010b), whilst also providing additional humoral immunity specific to hepatitis B surface antigen (Vangala *et al*, 2007), intramuscular injections of the outlined DDA-TDB based systems, surface adsorbed with the proposed H56 vaccine, was the route of choice for immunological characterisation.

Having established the route of immunisation, the systems were characterised for interactions with H56 vaccine antigen prior to each immunisation. It was observed that in

dosage form, the cationic characteristics of the adjuvant delivery systems were crucially maintained (with the exception of the anionic DSPC-TDB liposomes). Indeed, the surface charge of a liposomal delivery system is a key factor influencing vital cellular interactions with such adjuvants. Hsu & Juliano, (1982) reported that an anionic charge can promote liposome-cell complexes when assessing the extent of liposomal interactions with mouse peritoneal macrophages. In this instance, macrophages interacted more favourably with negatively charged multilamellar vesicles than their cationic or neutral counterparts. In contrast, Magee *et al*, (1974) observed interactions of positively charged vesicles with cells in culture and hypothesised that cationic liposomes electrostatically bound to anionic cells, which encouraged uptake of the systems by fusion or endocytosis.

The immunisation data demonstrated the immunoadjuvant capability of the proposed subunit vaccine delivery systems, with the role of DDA presence against DSPC and the effect of DDA-TDB concentration appreciated, suggesting that even minor adjuvant adjustment was sufficient to significantly impact the resultant immune responses. Moreover, with DDA-TDB providing the peak of cellular immune responses, depending on the extent of adjuvant adjustment, polarised responses were enthused. Indeed, results were dependent upon DDA lipid presence and independent of the system's zeta potential. With DSPC continually replacing DDA or substituting DDA and TDB in the formulation, either cellular immunity, signified by IgG2b antibodies and IFN- $\gamma$  and IL-2 cytokines, or humoral, Th2 type immunity, characterised by a strong antibody response and elevated IL-5 and IL-10 cytokine production, was elicited.

Liposomal composition undoubtedly affects resultant interactions with immune system cells such as cells involved with antigen presentation (Bramwell & Perrie, 2006). The results of this thesis indicates the variety in induced immune responses from the liposomal systems, dictated by the level of DDA/DSPC incorporation, whilst initiating adaptive immunity and immunological memory, portrayed in the stronger secondary and tertiary antibody responses upon repeated immunisations of mice.

The necessity of DDA within the formulation was also recognised as DDA fused with the antigen, ensuring that activated APCs were introduced to the related antigen, differentiating effector T cells accordingly to provide a desired adaptive immune response. DDA has previously been identified as an adjuvant capable of providing protective immunity in mice upon delivery of a TB subunit vaccine (Lindblad *et al*, 1997). Furthermore, DDA based adjuvants have been tested upon the addition of selected immunostimulatory components due to their Th1 inducing capabilities for example, with MPL (Brandt *et al*, 2000), whereby vaccination of mice with a DDA based subunit TB vaccine of ESAT-6 encouragingly stimulated strong antigen specific T-cell responses together with protective immunity on par with the BCG vaccine. Later studies by Holten-Anderson *et al*, (2004), screened a variety of immunomodulators and identified DDA co-administered with TDB as a strong Th1 promoting adjuvant alongside DDA-MPL, signified by elevated ESAT-6 antigen specific interferon gamma secretion, rendering DDA an efficient adjuvant for TB subunit vaccine delivery. Recent studies have also tested additional immunopotentiators alongside DDA-TDB, whereby incorporation of a TLR3 ligand of polyinosinic-polycytidylic acid (Poly I:C) induced high CD8+ T-cell

responses and thus, may be catered for subunit vaccination against viral pathogens (Nordly *et al*, 2011).

Despite the impressive success of currently approved adjuvants for generating immunity to viral and bacterial infections, there is a necessity for improved adjuvants that enhance protective antibody responses, especially in populations that respond poorly to current vaccines. It also remains a great challenge to develop vaccines that generate strong T cell immunity using purified or recombinant vaccine antigens (Coffman *et al*, 2010). From the initial recognition of TDB potentiating DDA response and harbouring the ability to act as a subunit vaccine adjuvant delivery system, the expansion of DDA-TDB's application has continued to develop (as highlighted in chapter 1, Table 1.6) and promisingly provide protection against a variety of disease targets.

In terms of TB and the H56 vaccine antigen, it is apparent that the latency expressed protein can advantageously be maximised when combined with the H1 vaccine, as such early expressed antigens provide clonal expansion for the development of T-cell mediated immunity and protective efficacy against the advanced form of TB (Aagaard *et al*, 2011). Whilst the immunisation study conducted in this thesis strengthens the preclinical profile of this post exposure vaccine, if we compare back to the main identified vaccination strategies against TB (Chapter 1, Table 1.8), by targeting latently infected patients and combining early and latently expressed antigens, this particular candidate goes some way towards improving efficacy and preventing TB infection. However, we remain far from replacing the current live BCG vaccine in the near future, and only adjuvants that are approved and licensed for administration as vaccine products can be regarded as

successful (O'Hagan & Gregorio, 2009). Consequently, the promising immunological data attained in this thesis comes at an interesting time as we anticipate results of currently initiated clinical trials involving H56 vaccine, to establish its validity for use in humans.

Having established the immunoadjuvant capabilities of the DSPC based liposomes in an animal model, the DPPC based systems were proposed for potential pulmonary vaccine delivery. The accessibility of the lungs, coupled with the ability to prepare liposomes within a broad particle size range, whilst integrating hydrophilic or lipophilic drugs, make pulmonary vaccination via liposomal systems a potentially favourable means of therapy (Taylor & Newton, 1992; Zeng *et al*, 1995). In this study, the use of ethanol was regarded as an unsuitable transfer medium for the DPPC based cationic liposome-protein complexes and some of the formulations may be too cytotoxic if an aerosolised system was to be achieved and targeted to the respiratory tract, making application potentially unviable for pulmonary delivery and hence, further work in this area was not carried out. Indeed, current systems utilised for parenteral vaccine delivery may not be appropriate for delivery to the respiratory tract as their safety profile has yet to be established for pulmonary use, requiring further research to evaluate whether adjuvants can be safely administered to the lung (Sou *et al*, 2011).

Despite not being taken forward as a potential pulmonary vaccine in the current study, further studies of the proposed DPPC based formulations could be beneficial if alternatively developed into a dry powder format, in which case evaluating the main methods of developing dry powders such as spray and freeze drying would be of interest. Indeed, spray drying is a straightforward process that offers reasonable costs and potential

scalability (Fourie *et al*, 2008) and can be optimised to generate an abundance of stable protein based aerosolised powders, and is therefore well suited to produce antigen containing dry powdered pulmonary vaccines (Sou *et al*, 2011). In addition, freeze drying is the primary technique applied to create stable proteins and polypeptides that are otherwise physically or chemically unstable in fluid form (Manning *et al*, 1989), and when freeze drying DDA-TDB liposomes, trehalose has been shown to be an appropriate cryoprotectant providing protection during the freeze drying process and crucially, retaining its adjuvanticity (Christensen *et al*, 2007). Characterisation of the particle aerodynamic diameter is crucial (Johnson, 1997), and consideration into particle deposition within the lungs, which can be assessed *in vitro* using liquid impingers or cascade impactors (Waldrep *et al*, 1997), alongside evaluation of a suitable delivery device, would also be of great interest. Indeed, advancement of a suitable formulation for the administration of candidate antigens via inhalational vaccine delivery is still required to produce pulmonary vaccines for commercial use (Sou *et al*, 2011).

To conclude, from the results obtained in this thesis, we have shown that DDA-TDB based liposomes can be adjusted to incorporate additional lipids with varying lipid chain lengths and melting points, and suffice as competent immunoadjuvant subunit delivery systems, meeting the objective of physicochemically characterising the proposed liposomal adjuvants and testing their viability in an animal model. In addition, the viability of the proposed systems was successfully examined using a macrophage cell line to screen selected *in vitro* characteristics, prior to elucidating their resultant immunological behaviour. With immune responses invariably dictated by DDA lipid content and DDA-TDB concentration, the DSPC based liposomes retained an

extraordinary ability to elicit antigen specific cell mediated immunity, stimulating either Th1 type immune responses, vital in providing protective efficacy against TB, or upon further adjustment, Th2 type humoral immune responses. Whilst appreciating the role of DDA vs. DSPC content, it was evident that even a minimal reduction in DDA-TDB concentration can significantly alter the resultant immune response.

Overall, the results of this project suggest that we can incorporate DSPC lipid into the main DDA-TDB adjuvant yet maintain stability in terms of particle size and zeta potential, the system's structural rigidity and favourably reduce cytotoxicity. Subsequently, upon conducting the immunisation study, the adjuvant effect of DDA, immunopotentiating necessity of TDB and the ability to customise resultant immune responses based on DSPC content was appreciated, displaying the multifaceted attributes of the formulations, demonstrating that liposomes can be regarded not only as delivery systems, but also as immunostimulatory adjuvants that increase the immunogenicity of antigens (Rongen, 1997). The versatility and scope to tune the proposed adjuvant formulations provide a potential platform to facilitate the delivery of alternative subunit antigens and may be developed for other disease targets that require cell mediated or humoral immune responses. With currently ongoing clinical development of the H56 vaccine, we await results of the performance and applicability of the main DDA-TDB adjuvant, and should any issues arise, the promising immunological data obtained in this study for the DSPC based systems offer viable alternative adjuvant formulations that may be used.

Hopefully the findings presented in this thesis have increased our knowledge of physicochemical liposomal characteristics that dictate the efficacy of such subunit vaccine

delivery systems, and provided some valuable formulation advantages whilst readdressing a balance between adjuvant potency and safety. The associated stability infers longer shelf life and lessens the need for controlled conditions during storage and distribution, which can ultimately reduce production costs. In addition, a reduced cytotoxicity could signify fewer local reaction events and less pain and discomfort upon injection, while facilitating better production and transport of the formulation. Such improvements provide further possible systems to the highly promising DDA-TDB adjuvant formulation and strengthen its pre-clinical profile and possible clinical acceptability, in this particular instance, for eliciting protection against TB in response to the novel H56 vaccine.

## References

- Aagaard, C., Hoang, T., Dietrich, J., Cardona, P., Izzo, A., Dolganov, G., Schoolnik, G.K., Cassidy, J.P., Billeskov, R., Anderson, P. (2011) A multistage tuberculosis vaccine that confers efficient protection before and after exposure. *Nature Medicine*, 17 (2), pp. 189-194.
- Adams, D.O., Hamilton, T.A. (1984) The cell biology of macrophage activation. *Immunol*, 2, pp. 283-318.
- Agger, E.M., Rosenkrands, I., Hansen, J., Brahimi, K., Vandahl, B.S., Aagaard, C., Werninghaus, K., Kirschning, C., Lang, R., Christensen, D., Theisen, M., Follmann, F., Andersen, P. (2008) Cationic Liposomes Formulated with Synthetic Mycobacterial Cordfactor (CAF01): A Versatile Adjuvant for Vaccines with Different Immunological Requirements. *PLoS One*, 3 (9), pp. 1-10. Available at: <[www.plosone.org](http://www.plosone.org)> [Accessed 27 November 2008].
- Ahl, P.L., Chen, I., Perkins, W.R., Minchey, S.R., Boni, I.T., Tarasch, T.F., Janoff, A.S. (1994) Interdigitation-fusion: a new method for producing lipid vesicles of high internal volume. *Biochimica et Biophysica Acta*, 1195 (2), pp. 237-244.
- Akira, S. (2003) Mammalian Toll-like receptors. *Current Opinion in Immunology*, 15 (1), pp. 5-11.
- Akira, S., Uematsu, S., Takeuchi, O. (2006) Pathogen recognition and innate immunity. *Cell*, 124, pp. 783-801.
- Alberts, B. (2004) *Essential Cell Biology*. Taylor & Francis, UK.
- Ali, S., Minchey, S., Janoff, A., Mayhew, E. (2000) A Differential Scanning Calorimetry Study of Phosphocholines Mixed with Paclitaxel and Its Bromoacylated Taxanes. *Biophysical Journal*, 78, pp. 246-256.
- Alison, A.G., Gregoriadis, G. (1974) Liposomes as immunological adjuvants. *Nature*, 252, pp. 252.
- Anderson, P., Doherty, T.M. (2005) TB subunit vaccines—putting the pieces together. *Microbes and Infection*, 7, pp. 911-921.
- Avanti Polar Lipids, INC. (2008) [online]. Available at: <<http://www.avantilipids.com/>> [Accessed 17 June 2008].
- Avanti Polar Lipids, INC. (2009) Phase Transition Temperatures for Glycerophospholipids [online]. Available at:

<[http://www.avantilipids.com/index.php?option=com\\_content&view=article&id=1700&Itemid=419](http://www.avantilipids.com/index.php?option=com_content&view=article&id=1700&Itemid=419)>  
[Accessed 17 July 2009].

Babai, I., Samira, S., Barenholz, Y., Zakay-Rones, Z., Kedar, E. (1999) A novel influenza subunit vaccine composed of liposome-encapsulated haemagglutinin/neuraminidase and IL-2 or GM-CSF. II. Induction of TH1 and TH2 responses in mice. *Vaccine*, 17, pp. 1239-1250.

Badiee, A., Jaafari, M.R., Khamesipour, A. (2007) *Leishmania major*: Immune response in BALB/c mice immunized with stress-inducible protein 1 encapsulated in liposomes. *Experimental Parasitology*, 115, pp. 127-134.

Bangham, A.D., Standish, M.M., Watkins, J. C. (1965) Diffusion of univalent ion across the lamellae of swollen phospholipids. *Journal of Molecular Biology*, 13 (1), pp. 238-252.

Bedu-Addo, F.K., & Huang, L. (1995) Interaction of PEG-phospholipid conjugates with phospholipid: implications in liposomal drug delivery. *Advanced Drug Delivery Reviews*, 16, pp. 235-247.

Behr, M.A. (2002) BCG—different strains, different vaccines? *Lancet Infectious Diseases*, 2 (2), pp. 86-92.

Belz, G.T., Carbone, F.R., Heath, W.R., (2002) Cross-presentation of antigens by dendritic cells. *Critical Reviews in Immunology*, 22, 439-448.

Bettelli, E., Carrier, Y., Gao, W., Korn, T., Strom, T.B., Oukka, M., Weiner, H.L., Kuchroo, V.K. (2006) Reciprocal developmental pathways for the generation of pathogenic effector T<sub>H</sub>17 and regulatory T cells. *Nature*, 441, pp. 235-238.

Bettelli, E., Korn, T., Kuchroo, V.K. (2007) Th17: the third member of the effector T cell trilogy. *Current Opinion in Immunology*, 19, pp. 652-657.

Betts, J.C., Lukey, P.T., Robb, L.C., McAdam, R.A., Duncan, K. (2002) Evaluation of a nutrient starvation model of *Mycobacterium tuberculosis* persistence by gene and protein expression profiling. *Molecular microbiology*, 43 (3), pp. 717-731.

Bi, R., Zhang, N. (2007) Liposomes as a Carrier for Pulmonary Delivery of Peptides and Proteins. *Journal of Biomedical Nanotechnology*, 3 (4), pp. 332-341.

Bibi, S., Kaur, R., Henriksen-Lacey, M., McNeil, S.E., Wilkhu, J., Lattmann, E., Christensen, D., Mohammed, A.R., Perrie, Y. (2011) Microscopy imaging of liposomes: From coverslips to environmental SEM. *International Journal of Pharmaceutics*, (Epub ahead of print).

- Biltonen, R.L., Lichtenberg, D. (1993) The use of differential scanning calorimetry as a tool to characterize liposome preparations. *Chemistry and Physics of Lipids*, 64 (1-3), pp. 129-142.
- Biruss, B., Dietl, R., Valenta, C. (2007) The influence of selected steroid hormones on the physicochemical behaviour of DPPC liposomes. *Chemistry and Physics of Lipids*, 148, pp. 84-90.
- Black, M., Trent, A., Tirrell, M., Olive, C. (2010) Advances in the design and delivery of peptide subunit vaccines with a focus on toll-like receptor agonists. *Expert Review of Vaccines*, 9 (2), pp. 157-173.
- Bloom, B.R., Fine, P.E.M. (1994) The BCG experience: implications for future vaccines against tuberculosis - Tuberculosis: pathogenicity, protection, and control. *American Society for Microbiology*, pp. 531-57.
- Bolean, M., Simao, A.M.S., Favarin, B.Z., Millán, J.L., Ciancaglini, P. (2010) The effect of cholesterol on the reconstitution of alkaline phosphatase into liposomes. *Biophysical Chemistry*, 152 (1-3), pp. 74-79.
- Bordi, F., Cametti, C. (2002) Salt-induced aggregation in cationic liposome aqueous suspensions resulting in multi-step self-assembling complexes. *Colloids and Surfaces B: Biointerfaces*, 26, pp. 341-350.
- Bramwell, V.W., Perrie, Y. (2005) The rational design of vaccines. *DDT*, 10 (22), pp. 1527-1534.
- Bramwell, V.W., Perrie, Y. (2006) Particulate delivery systems for vaccines: what can we expect? *Journal of Pharmacy and Pharmacology*, 58, pp. 717-728.
- Brandt, L., Oettinger, T., Holm, A., Andersen, A.B., Andersen, P. (1996) Key Epitopes on the ESAT-6 Antigen Recognized in Mice During the Recall of Protective Immunity to *Mycobacterium tuberculosis*. *Journal of Immunology*, 157, pp. 3527-3533.
- Brandt, L., Elhay, M., Rosenkrands, I., Lindblad, E.B., Andersen, P. (2000) ESAT-6 Subunit Vaccination against *Mycobacterium tuberculosis*. *Infection and Immunity*, 68 (2), pp. 791-795.
- Brookhaven Instruments Corporation. (2004) [online]. Available at: <<http://www.bic.com>> [Accessed 11 March 2008].
- Brookhaven Instruments Corporation. (2010a) The Effect of Dispersant on Colloidal Stability and Zeta Potential [online]. Available at: <<http://www.azom.com/article.aspx?ArticleID=5340>> [Accessed 20 June 2011].

Brookhaven Instruments Corporation. (2010b) High Salt Zeta Potential Measurements of Red Blood Cells [online]. Available at: <<http://www.azom.com/article.aspx?ArticleID=5339#3>> [Accessed 20 June 2011].

Campbell, M. (2005) What Tuberculosis did for Modernism: The Influence of a Curative Environment on Modernist Design and Architecture. *Medical History*, 49, pp. 463-488.

Campos-Neto, A. (2002) Anti-leishmania vaccine. *Leishmania*, 4, pp. 169-190.

Cannon, G., Swanson, J.A. (1992) The macrophage capacity for phagocytosis. *Journal of Cell Science*, 101, pp. 907-913.

Carmona-Ribeiro AM, Chaimovich H. (1983). Preparation and characterization of large dioctadecyldimethylammonium chloride liposomes and comparison with small sonicated vesicles. *Biochimica et Biophysica Acta*, 733 (1), 172–179.

Chambers, M.A., Wright, D.C., Brisker J., Williams, A., Hatch, G., Gavier-Widén, D., Hall, G., Marsh, P.D., Hewinson, R.G. (2003) A single dose of killed *Mycobacterium bovis* BCG in a novel class of adjuvant (Novasome) protects guinea pigs from lethal tuberculosis. *Vaccine*, 22, pp. 1063–1071.

Chandel, N.S., Trzyna, W.C., McClintock D.S., Schumacker, P.T. (2000) Role of oxidants in NF-kappa B activation and TNF-alpha gene transcription induced by hypoxia and endotoxin. *J Immunol*, 165 (2), pp. 1013-1021.

Chapman, D., Urbina, J. (1974) Studies of lipid-water systems using differential scanning calorimetry. *The Journal of Biological Chemistry*, 249 (8), pp. 2512-2521.

Chonn, A., Semple, S.C., Cullis, P.R. (1991) Separation of large unilamellar liposomes from blood components by a spin column procedure: towards identifying plasma proteins which mediate liposome clearance in vivo. *Biochimica et Biophysica Acta*, 1070 (1), pp. 215-222.

Chrai, S.S., Murari, R., Ahmed, I. (2002) Liposomes (a Review). *Biopharm*, 17, pp. 1-4.

Christensen, D., Foged, C., Rosenkrands, I., Nielsen, H.M., Andersen, P., Agger, E.M. (2007a) Trehalose preserves DDA/TDB liposomes and their adjuvant effect during freeze-drying. *Biochimica et Biophysica Acta*, 1768, pp. 2120-2129.

Christensen, D., Korsholm, K.S., Rosenkrands, I., Lindenstrom, T., Anderson P., Agger, E.M. (2007b) Cationic liposomes as vaccine adjuvants. *Expert Review of Vaccines*, 6 (5), pp. 785-796.

Christensen, D., Kirby, D., Foged, C., Agger, E.M., Andersen, P., Perrie, Y., Nielsen, H.M. (2008)  $\alpha,\alpha'$ -trehalose 6,6'-dibehenate in non-phospholipid-based liposomes enables direct interaction with trehalose, offering stability during freeze-drying. *Biochimica et Biophysica Acta*, 1778 (5), pp. 1365-1373.

Christensen, D., Agger, E.M., Andreasen, L.V., Kirby, D., Andersen, P., Perrie, Y. (2009) Liposome-based cationic adjuvant formulations (CAF): Past, present, and future. *Journal of Liposome Research*, 19 (1), pp. 2-11.

Christensen, D., Foged, C., Rosenkrands, I., Lundberg, C.V., Anderson, P., Agger, E.M., Nielsen, H.M. (2010) CAF01 liposomes as a mucosal vaccine adjuvant: In vitro and in vivo investigations. *International Journal of Pharmaceutics*, 390, pp. 19-24.

Coffman, R.L., Sher, A., Seder, R.A. (2010) Vaccine Adjuvants: Putting Innate Immunity to Work. *Immunity*, 33 (4), pp. 492-503.

Cole, S.T., Brosch, R., Parkhill, J., Garnier, T., Churcher, C., Harris, D., Gordon, S.V., Eiglmeier, K., Gas, S., Barry, C.E., III, Tekaia, F., Badcock, K., Basham, D., Brown, D., Chillingworth, T., Connor, R., Davies, R., Devlin, K., Feltwell, T., Gentles, S., Hamlin, N., Holroyd, S., Hornsby, T., Jagels, K., Krogh, A., McLean, J., Moule, S., Murphy, L., Oliver, K., Osborne, J., Quail, M.A., Rajandream, M.A., Rogers, J., Rutter, S., Seeger, K., Skelton, J., Squares, R., Squares, S., Sulston, J.E., Taylor, K., Whitehead, S., Barrell, B.G. (1998) Deciphering the biology of *Mycobacterium tuberculosis* from the complete genome sequence. *Nature*, 393 (6685), pp. 537-544.

Collins F.M. (1984) Protection against mycobacterial disease by means of live vaccines tested in experimental animals. *The Mycobacteria, a Source Book*. Marcel Dekker, New York.

Cox, J.C., Coulter, A.R. (1997) Adjuvants-a classification and review of their modes of action. *Vaccine*, 15 (3), pp. 248-256.

Crowder, T.M., Louey, M.D., Sethuraman, V.V., Smyth, H.D.C., Hickey, A.J. (2001) An odyssey in inhaler formulation and design. *Pharm. Technol*, 25 (7), pp. 99-113.

Daniel, T.M. (2006) The history of tuberculosis. *Respiratory Medicine*, 100 (11), pp. 1862-1870.

Darwis, Y., Kellaway, I.W. (2001) Nebulisation of rehydrated freeze-dried beclomethasone dipropionate liposomes. *International Journal of Pharmaceutics*, 215, pp. 113-121.

Davidsen, J., Rosenkrands, I., Christensen, D., Vangala, A., Kirby, D., Perrie, Y., Agger, E.M., Andersen, P. (2005) Characterization of cationic liposomes based on dimethyldioctadecylammonium

and synthetic cord factor from *M. tuberculosis* (trehalose 6,6V-dibehenate) - A novel adjuvant inducing both strong CMI and antibody responses. *Biochimica et Biophysica Acta*, 1718, pp. 22-31.

Demetzos, C. (2008) Differential Scanning Calorimetry (DSC): A Tool to Study the Thermal Behavior of Lipid Bilayers and Liposomal Stability. *Journal of liposome Research*, 18 (3), pp. 159-173.

Denniston, K.J., Topping, J.J., Caret, R.L. (2001) *General, Organic, and biochemistry*. 3<sup>rd</sup> Ed., McGraw-Hill, USA.

Desai, T.R., Hancock, R.E.W., Finlay, W.H. (2002) A facile method of delivery of liposomes by nebulisation. *Journal of Controlled Release*, 84, pp. 69-78.

Doherty, T.M., Olsen, A.W., van, P.L., Andersen, P. (2002) Oral vaccination with subunit vaccines protects animals against aerosol infection with *Mycobacterium tuberculosis*. *Infect. Immun*, 70, pp. 3111-3121.

Edwards, K.A., Baeumner, A.J. (2006a) Analysis of liposomes. *Talanta*, 68, pp. 1432–1441.

Edwards, K.A., Baeumner, A.J. (2006b) Liposomes in analyses. *Talanta*, 68, pp. 1421–1431.

Erikäinen, H., Kauppinen, E.I. (2003) Preparation of polymeric nanoparticles containing corticosteroid by a novel aerosol flow reactor method. *International Journal of Pharmaceutics*, 263, pp. 69-83.

Elhissi, A.M.A., O'Neill, M.A.A., Roberts, S.A., Taylor, K.M.G. (2006) Calorimetric study of dimyristoylphosphatidylcholine phase transitions and steroid–liposome interactions for liposomes prepared by thin film and proliposome methods. *International Journal of Pharmaceutics*, 320, pp. 124-130.

Elhissi, A.M.A., Gill, H., Ahmed, W., Taylor, K. (2011) Vibrating-mesh nebulization of liposomes generated using an ethanol-based proliposome technology. *Journal of liposome research*, 21 (2), pp. 173-180.

Ellouz, F., Adam, A., Ciorbaru, R., Lederer, E. (1974) Minimal structural requirements for adjuvant activity of bacterial peptidoglycan derivatives. *Biochemical and Biophysical Research Communications*, 59 (4), pp. 1317-1325.

EMA, (2005) Guideline on adjuvants in vaccines for human use [online]. Available at: <<http://www.emea.eu.int>> [Accessed 17 May 2011].

Encyclopedia Britannica, Inc. (2007) Liposome [online]. Available at: <  
<http://www.britannica.com/EBchecked/topic-art/457489/92244/Phospholipids-can-be-used-to-form-artificial-structures-called-liposomes>> [Accessed 28 March 2008].

Ernst, J.D., Stendahl, O. (2006) Phagocytosis of Bacteria and Bacterial Pathogenicity. Cambridge University Press, New York.

Farhood, H., Bottega, R., Richard, M.E.P., Huang, L. (1992) Effect of cationic cholesterol derivatives on gene transfer and protein kinase C activity. *Biochimica et Biophysica Acta*, 1111 (2), pp. 239-246.

Feitosa, E., Alves, F.R., Niemiec, A., Elisabete, M., Oliveira C.D.R., Castanheira, E.M.S., Baptista, A.L.F. (2006) Cationic Liposomes in Mixed Didodecyldimethylammonium Bromide and Dioctadecyldimethylammonium Bromide Aqueous Dispersions Studied by Differential Scanning Calorimetry, Nile Red Fluorescence, and Turbidity. *Langmuir*, 22 (8), pp. 3579-3585.

Filion, M.C., Proulx, C., Bradley, A.J., Devine, D.V., Sekaly, R.P., Decary, F., Chartrand, P. (1996) Presence in peripheral blood of healthy individuals of autoreactive T cells to a membrane antigen present on bone marrow-derived cells. *Blood*, 88, pp. 2144-2150.

Filion, M.C., Phillips, N.C. (1997) Toxicity and immunomodulatory activity of liposomal vectors formulated with cationic lipids toward immune effector cells. *Biochimica et Biophysica Acta*, 1329, pp. 345-356.

Fine, P.E.M. (1995) Variation in protection by BCG: implications of and for heterologous immunity. *The Lancet*, 346 (8986), pp. 1339-1345.

Fischer, D., Li, Y., Ahlemeyer, B., Krieglstein J., Kissel, T. (2003) In vitro cytotoxicity testing of polycations: influence of polymer structure on cell viability and hemolysis. *Biomaterials*, 24, pp. 1121-1131.

Foged, C., Arigita, C., Sundblad, A., Jiskoot, W., Storm, G., Frokjaer, S. (2004) Interaction of dendritic cells with antigen-containing liposomes: effect of bilayer composition. *Vaccine*, 22, pp. 1903-1913.

Foradada, M., Manzano, A., Roig, T., Estelrich, J., Bermudez, J. (1997) Serum-liposome interaction is an oxygen-dependent process. *Biochimica et Biophysica Acta*, 1345, pp. 43-55.

Fourie, P.B., Germishuizen, W.A., Wong, Y.L., Edwards, D.A. (2008) Spray drying TB vaccines for pulmonary administration. *Expert Opinion on Biological Therapy*, 8 (7), pp. 857-863.

- Frieden, T.R., Driver, C.R. (2003) Tuberculosis control: past 10 years and future progress. *Tuberculosis*, 83 (1-3), pp. 82-85.
- Fries, L.F., Gordon, D.M., Richards, R.L., Egan, J.E., Holingdale, M.R., Gross, M., Silverman, C., Alving, C.R. (1992) Liposomal malaria vaccine in humans: a safe and potent adjuvant strategy. *Proceedings of the National Academy of Sciences of the United States of America*, 88, pp. 358-362.
- Fuldner, H.H. (1981) Characterization of a Third Phase Transition in Multilamellar Dipalmitoyllecithin Liposomes. *Biochemistry*, 20, pp. 5707-5710.
- Fultz, B., Howe, J.M. (2007) *Transmission Electron Microscopy and Diffractometry of Materials*. 3<sup>rd</sup> Ed., Springer, USA.
- Galdiero, F., Carratelli, C.R., Nuzzo, I., Bentivoglio, De Martino, L., Folgore, A., Galdiero, M. (1995) Enhanced cellular response in mice treated with a Brucella antigen-liposome mixture. *Immunology and Medical Microbiology*, 10, pp. 235-243.
- Gall, D. (1966) The adjuvant activity of aliphatic nitrogenous bases. *Immunology*, 11, pp. 369-386.
- Gelperina, S., Kisich, K., Iseman, M.D., Heifets, L. (2005) The Potential Advantages of Nanoparticle Drug Delivery Systems in Chemotherapy of Tuberculosis. *American Journal of Respiratory and Critical Care Medicine*, 172, pp. 1487-1490.
- Giatrellis, S., Nikolopoulos, G., Sideratou, Z., Nounesis, G. (2009) Calorimetric study of the interaction of binary DMTAP/DOTAP cationic liposomes with plasmid DNA. *Journal of Liposome Research*, 19 (3), pp. 220-230.
- Gilbert B.E., Wyde P.R., Wilson S.Z., Robins, R.K. (1991) Aerosol and intraperitoneal administration of ribavarin and ribavarin triacetate: pharmacokinetics and protection of mice against intracerebral infection with influenza A/WDN virus. *Antimicrob Agents Chemother*, 35 (7), pp. 1448-1453.
- Gill, P.S., Sauerbrunn, S.R., Reading, M. (1993) Modulated Differential Scanning Calorimetry. *Journal of Thermal Analysis*, 40, pp. 931-939.
- Giron, D. (2002) Applications of thermal analysis and coupled techniques in the pharmaceutical industry. *J. Thermal Anal.*, 68, pp. 335-357.
- Gluck, R., Moser, C., Metcalfe, I.C. (2004) Influenza virosomes as an efficient system for adjuvanted vaccine delivery. *Expert opinion on biological therapy*, 4 (7), pp. 1139-1145.

- Gordon, S. (2002) Pattern Recognition Receptors: Doubling Up for the Innate Immune Response. *Cell*, 111, pp. 927-930.
- Govender, L., Abel, B., Hughes, E.J., Scriba, T.J., Kagina, B.M., de Kock, M., Walzl, G., Black, G., Rosenkrands, I., Hussey, G.D., Mahomed, H., Anderson, P., Hanekom, W.A. (2010) Higher human CD4 T cell response to novel Mycobacterium tuberculosis latency associated antigens Rv2660 and Rv2659 in latent infection compared with tuberculosis disease. *Vaccine*, 29 (1), pp. 51-57.
- Gregoriadis, G. (1988) *Liposomes as Drug Carriers: Recent trends and progress*. Wiley, Chichester.
- Gregoriadis, G. (1990) Immunological adjuvants: a role for liposomes. *Immunology Today*, 11, pp. 89-97.
- Gregoriadis, G. (1991) Overview of liposomes. *Journal of Antimicrobial Chemotherapy*, 28, pp. 39-48.
- Gregoriadis, (2000) Engineering liposomes for drug delivery: progress and problems. *Trends in biotechnology*, 13 (12), pp. 527-537.
- Gregoriadis, G., McCormack, B., Obrenovic, M., Saffie, R., Zadi, B., Perrie, Y. (1999) Vaccine Entrapment in Liposomes. *Methods*, 19, pp. 156-162.
- Gregoriadis, G., Bacon, A., Caparros-Wanderley, W., McCormack, B. (2002) A role for liposomes in genetic vaccination. *Vaccine*, 20, pp. 1-9.
- Gupta, R.K. (1998) Aluminum compounds as a vaccine adjuvants. *Adv Drug Deliv Rev*, 32 (3), pp. 155-172.
- Gupta, U.D., Katoch, V.M., McMurray, D.N. (2007) Current status of TB vaccines. *Vaccine*, 25, pp. 3742-3751.
- Gutierrez, M.G., Master, S., Singh, S., Taylor, G., Colombo, M., Deretic, V. (2004) Autophagy is a defense mechanism inhibiting BCG and mycobacterium tuberculosis survival in infected macrophages. *Cell*, 119 (6), pp. 753-766.
- Harding, C.V., Collins, D.S., Kanagawa, E.R., Unanue, E.R. (1991) Liposome-encapsulated antigen engender lysosomal processing for class II MHC presentation and cytosolic processing for class I presentation. *The Journal of Immunology*, 147 (9), pp. 2860-2863.

Hart, P.D., Sutherland, I. (1977) BCG and vole bacillus vaccines in the prevention of tuberculosis in adolescence and early adult life. *Br Med J*, 2, pp. 293-295.

Henriksen-Lacey, M., Bramwell, V.W., Christensen, D., Agger, E.M., Andersen, P., Perrie, Y. (2010a) Liposomes based on dimethyldioctadecylammonium promote a depot effect and enhance immunogenicity of soluble antigen. *Journal of Controlled Release*, 142, pp. 180-186.

Henriksen-Lacey, M., Christensen, D., Bramwell, V.W., Lindstrom, T., Agger, E.M., Andersen, P., Perrie, Y. (2010b) Liposomal cationic charge and antigen adsorption are important properties for the efficient deposition of antigen at the injection site and ability of the vaccine to induce a CMI response. *Journal of Controlled Release*, 145, pp. 102-108.

Henriksen-Lacey, M., Korsholm, K.S., Andersen, P., Perrie, Y., Christensen, D. (2011a) Liposomal Vaccine Delivery Systems. *Expert Opin. Drug Deliv*, 8 (4), pp. 505-519.

Henriksen-Lacey, M., Devitt, A., Perrie, Y. (2011b) The vesicle size of DDA:TDB liposomal adjuvants plays a role in the cell-mediated immune response but has no significant effect on antibody production. *Journal of Controlled Release*, 154 (2), pp. 131-137.

Hilgers, L.A., Snippe, H., Jansze, M., Willers, J.M. (1985) Combinations of two synthetic adjuvants: synergistic effects of a surfactant and a polyanion on the humoral immune response. *Cellular Immunology*, 92 (2), pp. 203-209.

Hilgers, L.A., Snippe, H. (1992) DDA as an immunological adjuvant. *Research in Immunology*, 143 (5), pp. 494-503.

Hirota, K., Duarte, J.H., Veldhoen, M., Hornsby, E., Li, Y., Cua, D.J., Ahlfors, H., Wilhelm, C., Tolaini, M., Menzel, U., Garefalaki, A., Potocnik, A.J., Stockinger, B. (2011) Fate mapping of IL-17-producing T cells in inflammatory responses. *Nature Immunology*, 12 (3), pp. 255-263.

Hofland, H.E.J., Shephard, L., Sullivan, S.M. (1996) Formation of stable cationic lipid/DNA complexes for gene transfer. *Proceedings of the National Academy of Sciences of the United States of America*, 93, pp. 7305-7309.

Holte, L.L., Gawrisch, K. (1997) Determining Ethanol Distribution in Phospholipid Multilayers with MAS-NOESY Spectra. *Biochemistry*, 36 (15), pp. 4669-4674.

Holten-Andersen, L., Doherty, T. M., Korsholm, K. S., Andersen, P. (2004) Combination of the Cationic Surfactant Dimethyl Dioctadecyl Ammonium Bromide and Synthetic Mycobacterial Cord

Factor as an Efficient Adjuvant for Tuberculosis Subunit Vaccines. *Infection and Immunity*, 72 (3), pp. 1608-1617.

Holzer, B.R., Hatz, C., Schmidt-Sissolakt, D., Gliickt, R., Althaus, B., Egger, M. (1996) Immunogenicity and adverse effects of inactivated virosome versus alum-adsorbed hepatitis A vaccine: a randomized controlled trial. *Vaccine*, 14 (10), pp. 982-986.

Hoyrup, P., Mouritsen, O.G., Jorgensen, K. (2001) Phospholipase A2 activity towards vesicles of DPPC and DMPC-DSPC containing small amounts of SMPC. *Biochimica et Biophysica Acta*, 1515, pp. 133-143.

Hsu, M.J., Juliano, R.L. (1982) Interactions of liposomes with the reticuloendothelial system. II: Nonspecific and receptor-mediated uptake of liposomes by mouse peritoneal macrophages. *Biochimica et Biophysica Acta*, 720 (4), pp. 411-419.

Huntington, J.A., Stein, P.E. (2001) Structure and properties of Ovalbumin. *Journal of Chromatography*, 756, pp. 189-198.

Hussain, A., Arnold, J.J., Khan, M.A., Ahsan, F. (2004) Absorption enhancers in pulmonary protein delivery. *Journal of Controlled Release*, 94, pp. 15-24.

Janeway, C.A., Medzhitov, R. (2002) Innate immune recognition. *Annual Review of Immunology*, 20, pp.197-216.

Janoff, A.S. (1999) *Liposomes – Rational Design*. Marcel Dekker, INC, USA.

Johnson, K.A. (1997) Preparation of peptide and protein powders for inhalation. *Advanced Drug Delivery Reviews*, 26, pp. 3-15.

Jones, M.N. (1995) The Surface Properties Of Phospholipid Liposome Systems And Their Characterisation. *Advances in Colloid and Interface Science*, 54, pp. 93-128.

Joshi, M., Misra, A. (2001) Dry powder inhalation of liposomal Ketotifen fumarate: formulation and characterization. *International Journal of Pharmaceutics*, 223, pp. 15-27.

Kaisto, T. (2003) Special features of vesicle trafficking in skeletal muscle cells. *Oulun yliopisto*, Oulu, Finland.

Kaszuba, M., Corbett, J., Watson, F.M., Jones, A. (2010) High-concentration zeta potential measurements using light-scattering techniques. *Phil. Trans. R. Soc. A*, 368, pp. 4439-4451.

Kaufmann, S.H.E., Hussey, G., Lambert, P. (2010) New vaccines for tuberculosis. *Lancet*, 375, pp. 2110-19.

Kaufmann, S.H.E. (2010) Future Vaccination Strategies against Tuberculosis: Thinking outside the Box. *Immunity*, 33, pp. 567-577.

Kawai, T. Akira, S. (2011) Toll-like receptors and their crosstalk with other innate receptors in infection and immunity. *Immunity*, 34 (5), pp. 637-650.

Kitaa, Y., Tanakaa, T., Yoshidab, S., Oharac, N., Kanedad, Y., Kuwayamaa, S., Murakia, Y., Kanamarua, N., Hashimotoa, S., Takaia, H., Okadaa, C., Fukunagaa, Y., Sakaguchia, Y., Furukawaa, I., Yamadaa, K., Inouea, Y., Takemotoa, Y., Naitoc, M., Yamadac, T., Makoto, M., McMurrayf, D.N., Dela Cruzg, E.C., Tang, E.V., Abalosg, R.M., Burgosg, J.A., Gelberg, R., Skeikyh, Y., Reedh, S., Sakatania, M., Okadaa, M. (2005) Novel recombinant BCG and DNA-vaccination against tuberculosis in a cynomolgus monkey model. *Vaccine*, 23, pp. 2132-2135.

Kersten, G.F.A., Crommelin, D.J.A. (1995) Liposomes and ISCOMS as vaccine formulations. *Biochimica et Biophysica Acta*, 1241, pp. 117-138.

Komatsu, H., Okada, S. (1995) Increased permeability of phase-separated liposomal membranes with mixtures of ethanol-induced interdigitated and non-interdigitated structures. *Biochimica et Biophysica Acta*, 1237 (2), pp. 169-175.

Komatsu, H., Okada, S. (1997) Effects of ethanol on permeability of phosphatidylcholine:cholesterol mixed liposomal membranes. *Chemistry and Physics of Lipids*, 85, pp. 67-84.

Korsholm, K.S., Agger E.M., Foged C., Christensen D., Dietrich J., Andersen C.S., Geisler C., Andersen, P. (2007) The adjuvant mechanism of cationic dimethyldioctadecylammonium liposomes. *Immunology*, 121 (2), pp. 216-26.

Koyama, T.M., Stevens, C.R., Borda, E.J., Grobe, K.J., Cleary, D.A. (1999) Characterizing the Gel to Liquid Crystal Transition in Lipid-Bilayer Model Systems. *The Chemical Educator*, 5 (3), pp. 1-5.

Lappalainen, K., Jääskeläinen, I., Syrjänen, K., Urtti, A., Syrjänen, S. (1994) Comparison of Cell Proliferation and Toxicity Assays Using Two Cationic Liposomes. *Pharmaceutical Research*, 11 (8), pp. 1127-1131.

Leonard, J.E. (2010) Tris Buffers [online]. Available at: <<http://www.broadleyjames.com/FAQ-text/119-faq.html>> [Accessed 14 October 2010].

- Legler, G., Liillau, E., Kappes, E., Kastenholz, F. (1991) Bovine N-acetyl-beta-D-glucosaminidase: affinity purification and characterization of its active site with nitrogen containing analogs of N-acetylglucosamine. *Biochimica et Biophysica Acta*, 1080, pp. 89-95.
- Lemaire, G., Tenu, J.P., Petit, J.F., Lederer, E. (1986) Natural and synthetic trehalose diesters as immunomodulators. *Med. Res. Rev*, 6, pp. 243-274.
- Lentz, B.R., Barenholz, Y., Thompson, T.E. (1976) Fluorescence Depolarization Studies of Phase Transitions and Fluidity in Phospholipid Bilayers. *Biochemistry*, 15 (20), pp. 4521-4528.
- Li, S., Lin, H., Wang, G., Huang, C. (1996) Effects of Alcohols on the Phase Transition Temperatures of Mixed-Chain Phosphatidylcholines. *Biophysical Journal*, 70, pp. 2784-2794.
- Li, Y., Mitra, A.K. (1996) Effect of phospholipids chain length, concentration, charge, and vesicle size on pulmonary insulin absorption. *Pharmaceutical research*, 13 (1), pp. 76-79.
- Liang, C., Chou, T. (2009) Effect of chain length on physicochemical properties and cytotoxicity of cationic vesicles composed of phosphatidylcholines and dialkyldimethylammonium bromides. *Chemistry and Physics of Lipids*, 158 (2), pp. 81-90.
- Lima, K.M., Dos Santos, S.A., Rodrigues, Jr., J.M., Silva, C.L. (2004) Vaccine adjuvant: it makes the difference. *Vaccine*, 22, pp. 2374-2379.
- Lindblad, E.B., Elhay, M.J., Silva, R., Appelberg, R., Andersen, P (1997) Adjuvant Modulation of Immune Responses to Tuberculosis Subunit Vaccines. *Infection and Immunity*, 65 (2), pp. 623-629.
- Lobbecke, L., Cevc, G. (1995) Effects of short-chain alcohols on the phase behavior and interdigitation of phosphatidylcholine bilayer membranes. *Biochimica et Biophysica Acta*, 1237, pp. 59-69.
- Lonez, C., Vandenbranden, M., Ruyschaert, J. (2008) Cationic liposomal lipids: From gene carriers to cell signalling. *Progress in Lipid Research*, 47, pp. 340-347.
- Lu, D., Hickey, A.J. (2005) Liposomal Dry Powders as Aerosols for Pulmonary Delivery of Proteins. *AAPS PharmSciTech*, 6 (4), pp. 641-648.
- Lu, D., Garcia-Contreras, L., Muttill, P., Padilla, D., Xu, D., Liu, J., Braunstein, M., McMurray, D.N., Hickey, A.J. (2010) Pulmonary immunization using antigen 85-B polymeric microparticles to boost tuberculosis immunity. *The AAPS Journal*, 12 (3), pp. 338-347.

- Lv, H., Zhang, S., Wang, B., Cui, S., Yan, J. (2006) Toxicity of cationic lipids and cationic polymers in gene delivery. *Journal of Controlled Release*, 114 (1), pp. 100-109.
- Ma, Y., Zhou, D., Xie, X., Dong, B., Zhuang, Y., Zheng, M. (2009) A novel low-toxic liposomal adjuvant: Different liposome compositions regulate monocyte activation and viability. *Applied sciences in Biomedical and communication technologies*, (3), pp. 1-2.
- Mack, P.A., Griffith, J.W., Lang, C.M. (1995) N-acetyl-beta-D-glucosaminidase activity within BAL from macaques exposed to generic coal dusts. *Lung*, 173 (1), pp. 1-11.
- Mackett, M., Williamson, J.D. (1995) *Human Vaccines and Vaccination*. BIOS Scientific Publishers Ltd, Oxford.
- Mabrey, S., Sturtevant, J.M. (1976) Investigation of phase transitions of lipids and lipid mixtures by high sensitivity differential scanning calorimetry. *Proc. Natl. Acad. Sci, USA* 73 (11), pp. 3862-3866.
- Magee, W.E., Goff, C.W., Schoknecht, J., Smith, M.D., Cherian, K. (1974) The interaction of cationic liposomes containing entrapped horseradish peroxidase with cells in culture. *The Journal of Cell Biology*, 63, pp. 492-504.
- Malvern. (2008) Laser diffraction technology focus [online]. Available at: <[http://www.malvern.com/ProcessEng/systems/laser\\_diffraction/technology/technology.htm](http://www.malvern.com/ProcessEng/systems/laser_diffraction/technology/technology.htm)> [Accessed 29 March 2008].
- Manning, M.C., Patel, K., Borchardt, R.T. (1989) Stability of protein pharmaceuticals. *Pharmaceutical Research*, 6, pp. 903-918.
- Mannock, D.A., Ruthven, N.A.H.L., McElhaney, R.N. (2010) A calorimetric and spectroscopic comparison of the effects of ergosterol and cholesterol on the thermotropic phase behavior and organization of dipalmitoylphosphatidylcholine bilayer membranes. *Biochimica et Biophysica Acta*, 1798, 3, pp. 376-388.
- Manosroi, A., Thathang, K., Werner, R.G., Schubert, R., Peschka-Suss, R., Manosroi, J. (2008) Development of highly stable and low toxic cationic liposomes for gene therapy. *Arzneimittelforschung*, 58 (10), pp. 485-492.
- Mastelic, B., Ahmed, S., Egan, W.M., Giudice, G.D., Golding, H., Gust, I., Neels, P., Reed, S.G., Sheets, R.L., Siegrist, C., Lambert, P. (2010) Mode of action of adjuvants: Implications for vaccine safety and design. *Biologicals*, 38, pp. 594-601.

- Mbow, M.L., Gregorio, E.D., Valiante, N.M., Rappuoli, R. (2010) New adjuvants for human vaccines. *Current opinion in immunology*, 22, pp. 411-416.
- McAlister, S.M., Alpar, H.O., Teitelbaum, Z., Bennet D.B. (1996) Do interactions with phospholipids contribute to the prolonged retention of polypeptides within the lung? *Advanced Drug Delivery Reviews*, 19, pp. 89-110.
- McMullen, T.P.W., Lewis, R.N.A.H., McElhaney, R.N. (1993) Differential Scanning Calorimetric Study of the Effect of Cholesterol on the Thermotropic Phase Behavior of a Homologous Series of Linear Saturated Phosphatidylcholines. *Biochemistry*, 32, pp. 516-522.
- McMullen, T.P.W., McElhaney, R.N. (1995) New aspects of the interaction of cholesterol with dipalmitoylphosphatidylcholine bilayers as revealed by high-sensitivity differential scanning calorimetry. *Biochimica et Biophysica Acta*, 1234, pp. 90-98.
- McMullen, T.P.W., McElhaney, R.N. (1996) Physical studies of cholesterol-phospholipid interactions. *Current Opinion in Colloid & Interface Science*, 1, pp. 83-90.
- McNeil, S.E., Perrie, Y. (2006) Gene delivery using cationic liposomes. *Expert Opinion on Therapeutic Patents*, 16 (10), pp. 1371-1382.
- McNeil, S., Rosenkrands, I., Agger, E.M., Anderson, P., Perrie, Y. (2011) Subunit Vaccines: Distearoylphosphatidylcholine-Based Liposomes Entrapping Antigen Offer a Neutral Alternative to Dimethyldioctadecylammonium-Based Cationic Liposomes as an Adjuvant Delivery System. *Journal of Pharmaceutical Sciences*, 100 (5), pp. 1856-1865.
- Meraviglia, S., Daker, S.E., Dieli, F., Martini, F., Martino, A. (2011) T Cells Cross-Link Innate and Adaptive Immunity in Mycobacterium tuberculosis Infection. *Clinical and Developmental Immunology*, 2011, pp. 1-11.
- Mihalko, P.J., Schreier, H., Abra, R.M., (1988) Liposomes: a pulmonary perspective. In: Gregoriadis, G. *Liposomes as Drug Carriers*. Wiley, Chichester, UK.
- Mirsky, A.E., Pauling, L. (1936) On the Structure of Native, Denatured, and Coagulated Proteins. *Proc Natl Acad Sci USA*, 22 (7), pp. 439-447.
- Minor, P.D. (2002) Eradication and cessation of programmes: vaccination and public health care. *Br. Med. Bull*, 62, pp. 213-224.

Moghaddam, B., Ali, M.H., Wilkhu, J., Kirby, D.J., Mohammed, A.R., Zheng, G., Perrie, Y. (2011) The application of monolayer studies in the understanding of liposomal formulations. *International Journal of Pharmaceutics*, pp. 1-10.

Moghimi, S.M., Patel, H.M. (1989) Differential properties of organ-specific serum opsonins for liver and spleen macrophages. *Biochimica et Biophysica Acta*, 984 (3), pp. 379-383.

Mohammed, A.R., Bramwell, V.W., Kirby, D.J., McNeil, S.E., Perrie, Y. (2010) Increased potential of a cationic liposome-based delivery system: enhancing stability and sustained immunological activity in pre-clinical development. *European Journal of Pharmaceutics and Biopharmaceutics*, 76, pp. 404-412.

Morein, B., Helenius, A., Simons, K., Pettersson, R., Kaariainen, L., Schirmacher V. (1978) Effective subunit vaccines against an enveloped animal virus. *Nature*, 276, pp. 715-718.

Morein, B., Sundquist, B., Höglund, S., Dalsgaard, K., Osterhaus, A. (1984) Iscom, a novel structure for antigenic presentation of membrane proteins from enveloped viruses. *Nature*, 308, pp. 457-460.

Moreno-Mendieta, S.A., Rocha-Zavaleta, L., Rodriguez-Sanoja, R. (2010) Adjuvants in tuberculosis vaccine development. *FEMS Immunol Med Microbiol*, 58, pp. 75-84.

Myers, M.A., Thomas, D.A., Straub, L., Soucy, D.W., Niven, R.W., Kaltenbach, M., Hood, C.I., Schreier, H., Gonzalez-Rothi, R.J. (1993) Pulmonary effects of chronic exposure to liposome aerosols in mice. *Experimental lung research*, 19 (1), pp.1-19.

Nakanishi, T., Kunisawa, J., Hayashi, A., Tsutsumi, Y., Kubo, K., Nakagawa, S., Fujiwara, H., Hamaoka, T., Mayumi, T. (1997) Positively charged liposome functions as an efficient immunoadjuvant in inducing immune responses to soluble proteins. *Biochemical and Biophysical Research Communications*, 240 (3), pp. 793-797.

National Institute of Allergy and Infectious Diseases (2008) Tuberculosis in History [online]. Available at: <<http://www.niaid.nih.gov/topics/tuberculosis/Understanding/history/Pages/default.aspx>> [Accessed 17 May 2011].

Newhouse, M. (1991) Advantages of pressurized canister metered dose inhalers. *Journal of aerosol medicine*, 4 (3), pp. 139-150.

Niven, R.W., Carvajal, M.A., Schreier, H. (1992) Nebulization of liposomes. III. The effects of operating conditions and local environment. *Pharmaceutical Research*, 9 (4), pp. 515-520.

Nordly, P., Rose, F., Christensen, D., Nielsen, H.M., Andersen, P., Agger, E.M., Foged, C. (2011) Immunity by formulation design: Induction of high CD8<sup>+</sup> T-cell responses by poly(I:C) incorporated into the CAF01 adjuvant via a double emulsion method. *Journal of Controlled Release*, 150, pp. 307-317.

Numata, F., Nishimura, K., Ishida, H. Ukei, S., Tone, Y., Ishihara, C., Saiki, I., Sekikawa, I., Azuma, I. (1985) Lethal and adjuvant activities of cord factor (trehalose-6,6-di-mycolate) and synthetic analogs in mice. *Chem Pharm Bulletin (Tokyo)*, 33 (10), pp. 4544-4555.

O'Hagan, D.T., MacKichan, M.L., Singh, M. (2001) Recent developments in adjuvants for vaccines against infectious diseases. *Biomol*, 18 (3), pp. 69-85.

O'Hagan, D.T., Singh, M. (2002) Microparticles as vaccine adjuvants and delivery systems. *Expert Review of Vaccines*, 2 (2), pp. 269-283.

O'Hagan, D.T. Valiante, N.M. (2003) Recent advances in the discovery and delivery of vaccine adjuvants. *Nature Reviews. Drug Discovery*, 2 (9), pp. 727-735.

O'Hagan, D.T. (2007) MF59 is a safe and potent vaccine adjuvant that enhances protection against influenza virus infection. *Expert review of vaccines*, 6 (5), pp. 699-710.

O'Hagan, D.T., Gregorio, E.D. (2009) The path to a successful vaccine adjuvant – “The long and winding road”. *Drug Discovery Today*, 14 (11-12), pp. 541-551.

Olds, G.R., Chedid, L., Lederer, E., Mahmoud, A.A.F. (1980) Induction of resistance to schistosoma-mansoni by natural cord factor and synthetic lower homologs. *J. Infect. Dis*, 141, pp. 473-478.

Olsen, A.W., van Pinxteren, L.A.H., Okkels, L.M., Rasmussen, P.B., Anderson, P. (2001) Protection of Mice with a Tuberculosis Subunit Vaccine Based on a Fusion Protein of Antigen 85B and ESAT-6. *Infection and Immunity*, 69 (5), pp. 2773-2778.

Opanasopit, P., Nishikawa, M., Hashida, M. (2002) Factors affecting drug and gene delivery: effects of interaction with blood components. *Critical Reviews in Therapeutic Drug Carrier Systems*, 19 (3), pp. 191-233.

Oss, C.J.V. (1989) On the mechanism of the cold ethanol precipitation method of plasma protein fractionation. *Journal of Protein Chemistry*, 8 (5), pp. 661-668.

Ostro, M.J. (1983) *Interactions of Proteins and Drugs with liposomes*. Dekker, New York.

Oxman, M.N., Levin, M.J., Johnson, G.R., Schmader, K.E., Straus, S.E., Gelb, L.D., Arbeit, R.D., Simberkoff, M.S., Gershon, A.A., Davis, L.E., Weinberg, A., Boardman, K.D., Williams, H.M., Hongyuan Zhang, J., Peduzzi, P.N., Beisel, C.E., Morrison, V.A., Guatelli, J.C., Brooks, P.A., Kauffman, C.A., Pachucki, C.T., Neuzil, K.M., Betts, R.F., Wright, P.F., Griffin, M.R., Brunell, P., Soto, N.E., Marques, A.R., Keay, S.K., Goodman, R.P., Cotton, D.J., Gnann, J. W., Loutit, J., Holodniy, M., Keitel, W.A., Crawford, G.E., Yeh, S.S., Lobo, Z., Toney, J.F., Greenberg, R.N., Keller, P.M., Harbecke, R., Hayward, A.R., Irwin, M.R., Kyriakides, T.C., Chan, C.Y., Chan, I.S.F., Wang, W.W.B., Annunziato, P.W., Silber, J.L. (2005) A vaccine to prevent herpes zoster and postherpetic neuralgia in older adults. *The New England Journal of Medicine*, 352 (22), pp. 2271-2284.

Pace, C.N., Treviño, S., Prabhakaran, E., Scholtz, J.M. (2004) Protein structure, stability and solubility in water and other solvents. *Phil. Trans. R. Soc. Lond. B*, 359, pp. 1225-1235.

Pandey, R., Khuller, G.K. (2005) Antitubercular inhaled therapy: opportunities, progress and challenges. *Journal of Antimicrobial Chemotherapy*, 55, pp. 430-435.

Parham, P. (2005) *The Immune System*. 2<sup>nd</sup> Ed., Garland Science, New York.

Parida, S.K., Kaufmann, S.H.E. (2010) Novel tuberculosis vaccines on the horizon. *Current opinion in immunology*, 22, pp. 374-384.

Parthasarathy R., Gilbert B., Mehta, K. (1999) Aerosol delivery of liposomal all-trans retinoic acid to the lungs. *Cancer Chemother Pharmacol*, 43 (4), pp. 277-283.

Pauling, L., Corey, R. B., Branson, H. R. (1951) The structure of proteins: two hydrogen-bonded helical configurations of the polypeptide chain. *Proc. Natl Acad. Sci. USA*, 37, pp. 205-211.

Paur, H., Cassee, F.R., Teeguraden, J., Fissan, H., Diabate, S., Aufderheide, M., Kreyling, W.G., Hanninen, O., Kasper, G., Riediker, M., Rothenrutishauser, B., Schmid, O. (2011) In-vitro cell exposure studies for the assessment of nanoparticle toxicity in the lung—A dialog between aerosol science and biology. *Journal of aerosol science*, 42 (10), pp. 668-692.

Perkin Elmer, (2010) *Differential Scanning Calorimetry (DSC)* [online]. Available at: <[http://las.perkinelmer.com/content/Manuals/GDE\\_DSCBeginnersGuide.pdf](http://las.perkinelmer.com/content/Manuals/GDE_DSCBeginnersGuide.pdf)> [Accessed 14 September 2010].

- Perrett, S., Golding, M., Williams, W.P. (1991) A simple method for the preparation of liposomes for pharmaceutical applications: characterization of the liposomes. *The Journal of Pharmacy and Pharmacology*, 43 (3), pp. 154-161.
- Perrie, Y. (2006) Vaccines: an overview and update. *Pharm. J*, 276, pp. 209-213.
- Perrie, Y., Frederik, P.M., Gregoriadis, G. (2001) Liposome-mediated DNA vaccination: the effect of vesicle composition. *Vaccine*, 19, pp. 3301-3310.
- Perrie, Y., Mohammed, A.R., Kirby, D.J., McNeil, S.E., Bramwell, V.W. (2008) Vaccine adjuvant systems: Enhancing the efficacy of sub-unit protein antigens. *International Journal of Pharmaceutics*, 364, pp. 272-280.
- Pierce Biotechnology Inc. (2005) Protein Assay Technical Handbook. USA.
- Pimm, M.V., Baldwin, R.W., Polonsky, J., Lederer, E. (1979) Immunotherapy of an ascitic rat hepatoma with cord factor (trehalose-6, 6V-dimycolate) and synthetic analogs. *Int. J. Cancer*, 24 (6), pp. 780-785.
- Plotkin, S.A. (2005) Vaccines: Past, present and future. *Nature Medicine*, 11 (4), pp. 5-11.
- Promega. (2007) Technical Bulletin - CellTiter 96<sup>®</sup> AQueous One Solution Cell Proliferation Assay. USA.
- Pulendran, B., Ahmed, R. (2006) Translating innate immunity into immunological memory: implications for vaccine development. *Cell*, 124, pp. 849-863.
- Quesniaux, V.F., Jacobs, M., Allie, N., Grivennikov, S., Nedospasov, S.A., Garcia, I., Olleros, M.L., Shebzukhov, Y., Kuprash, D., Vasseur, V. (2010) TNF in host resistance to tuberculosis infection. *Current Directions in Autoimmunity*, 11, pp. 157-179.
- Ramon, G. (1924) Sur la toxine et sur l'anatoxine diphtheriques. *Ann Inst Pasteur*, 38 (1).
- Rappuoli, R. (2001) Reverse vaccinology, a genome-based approach to vaccine development. *Vaccine*, 19 (17-19), pp. 2688-2691.
- Relyveld, E.H., Bizzini B., Gupta, R.K. (1998) Rational approaches to reduce adverse reactions in man to vaccines containing tetanus and diphtheria toxoids. *Vaccine*, 16, pp. 1016-1023.
- Rescigno M, Granucci F, Ricciardi-Castagnoli P. (1999) Dendritic cells at the end of the millennium. *Immunology and Cell Biology*, 77 (5), pp. 404-10.

- Robinson, J.P., Babcock, G.F. (1998) Phagocyte Function: A guide for research and clinical evaluation. John Wiley and Sons Ltd, USA.
- Romoren, K., Thu, B.J., Bols, N.C., Evensen, O. (2004) Transfection efficiency and cytotoxicity of cationic liposomes in salmonid cell lines of hepatocyte and macrophage origin. *Biochimica et Biophysica Acta*, 1663, pp. 127-134.
- Rosenberg, I.M. (2005) Protein analysis and purification: benchtop techniques. 2<sup>nd</sup> Ed., Birkhauser, Boston.
- Rawicz, W., Olbrich, K.C., McIntosh, T., Needham, D., Evans, E. (2000) Effect of Chain Length and Unsaturation on Elasticity of Lipid Bilayers. *Biophysical Journal*, 79, pp. 328-339.
- Rongen, H.A.H., Bult, A., van Bennekom, W.P. (1997) Liposomes and immunoassays. *Journal of Immunological Methods*, 204, pp. 105-133.
- Reed, S.G., Bertholet, S., Coler, R.N., Friede, M. (2008) New horizons in adjuvants for vaccine development. *Trends in immunology*, 30 (1), pp. 23-32.
- Rowe, E. (1983) Lipid Chain Length and Temperature Dependence of Ethanol-Phosphatidylcholine Interactions. *Biochemistry*, 22 (14), pp. 3299-3305.
- Russo, D.M., Kozlova, N., Lakey, D.L., Kernodle, D. (2000) Naive human T cells develop into Th1 effectors after stimulation with mycobacterium tuberculosis-infected macrophages or recombinant Ag85 proteins. *Infect Immun*, 68 (12), pp. 6826-6832.
- Ryan, K.J., Ray, C.G. (2003) Sherris medical microbiology: an introduction to infectious diseases. 4<sup>th</sup> Ed., McGraw-Hill, USA.
- Sable, S.B., Kalra, M., Verma, I., Khuller, G.K. (2007a) Tuberculosis subunit vaccine design: The conflict of antigenicity and immunogenicity. *Clinical Immunology*, 122, pp. 239-251.
- Sable, S.B., Bonnie, B., Plikaytis, B.B., Shinnick, T.M. (2007b) Tuberculosis subunit vaccine development: Impact of physicochemical properties of mycobacterial test antigens. *Vaccine*, 25, pp. 1553-1566.
- Scheule, R.K., St George, J.A., Bagley, R.G., Marshall, J., Kaplan, J.M., Akita, G.Y., Wang, K.X., Lee, E.R., Harris, D.J., Jiang, C., Yew, N.S., Smith, A.E., Cheng, S.H. (1997) Basis of pulmonary toxicity associated with cationic lipid-mediated gene transfer to the mammalian lung. *Human gene therapy*, 8 (6), pp. 689-707.

- Seder, R.A., Hill, A.V.S. (2000) Vaccines against intracellular infections requiring cellular immunity. *Nature*, 406, pp. 793-798.
- Senior, J., Gregoriadis, G. (1982) Stability of small unilamellar liposomes in serum and clearance from the circulation: The effect of the phospholipid and cholesterol components. *Life Sciences*, 30 (24), pp. 2123-2136.
- Sharma, A., Sharma, U.S. (1997) Review – Liposomes in drug delivery: progress and limitations. *International Journal of Pharmaceutics*, 154, pp. 123-140.
- Sichina, W.J. (2000) DSC as Problem Solving Tool: Characterization of Consistency of PFA Resins [online]. Available at:  
<[http://las.perkinelmer.com/Content/applicationnotes/app\\_thermalconsistencyofpfaresins.pdf](http://las.perkinelmer.com/Content/applicationnotes/app_thermalconsistencyofpfaresins.pdf)>  
[Accessed 3 December 2010].
- Siddiqui, W.A., Taylor, D.W., Kan, S.C., Kramer, K., Richmond-Crum, S.M., Kotani, S., Shiba T., Kusumoto, S. (1978) Vaccination of experimental monkeys against *Plasmodium falciparum*: a possible safe adjuvant. *Science*, 201 (4362), pp. 1237-1239.
- Sigma. (2009) Technical Bulletin  $\beta$ -N-Acetylglucosaminidase Assay Kit. Saint Louis, Missouri.
- Sisk, R.B., Wang, Z.Q., Lin, H.N., Huang, C.H. (1990) Mixing behavior of identical molecular weight phosphatidylcholines with various chain-length differences in two-component lamellae. *Biophys J*, 58 (3), pp. 777-783.
- Silverstein, S.C., Steinman, R.M., Cohn, Z.A. (1977) Endocytosis. *Annu Rev Biochem*, 46, pp. 669-722.
- Smith, J.G., Walzem, R.L., German, J.B. (1993) Liposomes as agents for DNA transfer. *Biochimica et Biophysica Acta*, 1154 (3-4), pp. 327-340.
- Smith, I. (2003) *Mycobacterium tuberculosis* pathogenesis and molecular determinants of virulence. *Clinical microbiology reviews*, 16 (3), pp. 463-496.
- Smith-Palmer, T., Pelton, R., Somasundaran, P. (2006) *Encyclopaedia of Surface and Colloid Science*. 2<sup>nd</sup> Ed., Taylor & Francis Group, USA.
- Sompayrac, L. (2008) *How the Immune System Works*. 3<sup>rd</sup> Ed., Blackwell Publishing, USA.
- Sosnik, A., Carcaboso, A.M., Glisoni, R.J., Moretton, M.A., Chiappeta, D.A. (2010) New old challenges in tuberculosis: Potentially effective nanotechnologies in drug delivery. *Advanced Drug Delivery Reviews*, 62, pp. 547-559.

Sou, T., Meeusen, E.N., de Veer, M., Morton, D.A.V., Kaminskas, L.M., McIntosh, M.P. (2011) New developments in dry powder pulmonary vaccine delivery. *Cell*, 29 (4), pp. 191-198.

Spargo, B.J., Crowe, L.M., Ionedo, T., Beaman, B.L., Crowe, J.H. (1991) Cord factor (α,α-trehalose 6,6'-dimycolate) inhibits fusion between phospholipid vesicles. *Proceedings of the National Academy of Sciences of the United States of America*, 88, pp. 737-740.

SSI, (2010) Tuberculosis vaccine research – concept and results [online]. Available at: <<http://www.ssi.dk/English/RandD/Research%20Departments/Department%20of%20Infectious%20Disease%20Immunology/Tuberculosis%20Vaccine%20Research/Concept%20and%20results.aspx>> [Accessed 14 September 2010].

Stefely, J.S. (2002) Novel Excipients for Inhalation Drug Delivery: Expanding the Capability of the MDI [online]. Available at: <<http://www.drugdeliverytech.com/ME2/dirmod.asp?sid=&nm=&type=Publishing&mod=Publications%3A%3AArticle&mid=8F3A7027421841978F18BE895F87F791&tier=4&id=BB5D9B03746342A6ABB038EE55035478>> [Accessed 12 May 2011].

Stenesh, J. (1998) *Biochemistry*. University of Chicago Press, USA.

Storni, T., Kundig, T.M., Senti, G., Johansen, P. (2005) Immunity in response to particulate antigen-delivery systems. *Advanced Drug Delivery Reviews*, 57, pp. 333-355.

Stumpo, R., Kauer, M., Martin, S., Kolb, H. (2003) IL-10 induces gene expression in macrophages: partial overlap with IL-5 but not with IL-4 induced genes. *Cytokine*, 24, pp. 46-56.

TA Instruments, (2011) Nano DSC [online]. Available at: <<http://www.tainstruments.com/main.aspx?siteid=11&id=264&n=1>> [Accessed 24 January 2011].

Taylor, K.M.G., Newton, J.M., (1992) Liposomes for controlled delivery of drugs to the lung. *Thorax*, 47 (4), pp. 257-259.

Taylor, K.M.G., Morris, R.M. (1995) Thermal analysis of phase transition behaviour in liposomes. *Thermochimica Acta*, 248, pp. 289-301.

Taylor, K.M.G., Craig, D.Q.M. (2003) *Liposomes: A Practical Approach*. Oxford University Press, UK.

Taylor, K., Nguyen, A., Stéphenne, J. (2009) The need for new vaccines. *Vaccine*, 27, pp. 3-8.

- Thomas, D.A., Myres, M.A., Wichert, B., Schreier, H., Gonzalez-Rothi, R.J. (1991) Acute effects of liposome aerosol inhalation on pulmonary function in healthy human volunteers. *Chest*, 99 (5), pp. 1268-1270.
- Vangala, A., Kirby, D., Rosenkrands, I., Agger, E.M., Andersen, P., Perrie, Y. (2006) A comparative study of cationic liposome and niosome-based adjuvant systems for protein subunit vaccines: characterisation, environmental scanning electron microscopy and immunisation studies in mice. *J. Pharm. Pharmacol*, 58, pp. 787-799.
- Vangala, A., Bramwell, V.W., McNeil, S., Christensen, D., Agger, E.M., Perrie, Y. (2007) Comparison of vesicle based antigen delivery systems for delivery of hepatitis B surface antigen. *Journal of Controlled Release*, 119, pp. 102-110.
- Vassalli, A. (1992) The Pathology of Tumor Necrosis Factors. *Annual Review of Immunology*, 10, pp. 411-452.
- Vautier, S., Sousa, M.D.G., Brown, G.D. (2010) C-type lectins, fungi and Th17 responses. *Cytokine & Growth Factor Reviews*, 21 (6), pp. 405-412.
- Velinova, M., Read, N., Kirby, C., Gregoriadis, G. (1996) Morphological observations on the fate of liposomes in the regional lymph nodes after footpad injection into rats. *Biochimica et Biophysica Acta*, 1299 (2), pp. 207-215.
- Vitas, A.I., Diaz, R., Gamazo, C. (1996) Effect of Composition and Method of Preparation of Liposomes on Their Stability and Interaction with Murine Monocytes Infected with *Brucella abortus*. *Antimicrobial Agents and Chemotherapy*, 40 (1), pp.146-151.
- Vogel, F.R., Powell M.F. (1995) A compendium of vaccine adjuvants and excipients. Plenum Press, New York.
- Waldrep, J.C., Arppe, J., Jansa, K.A., Knight, V. (1997) High dose cyclosporin A and budesonide-liposome aerosols. *International Journal of Pharmaceutics*, 152 (1), pp. 27-36.
- Wang, C., Muttill, P., Lu, D., Beltran-Torres, A.A., Garcia-Contreras, L., Hickey, A.J. (2009) Screening for Potential Adjuvants Administered by the Pulmonary Route for Tuberculosis Vaccines. *The AAPS Journal*, 11 (1), pp. 139-147.
- Webb C.E., Jones, J.D.C. (2004) *Handbook of Laser Technology and Applications*. Taylor & Francis, UK.

- Werling, D., Jungi, T.W. (2003) TOLL-like receptors linking innate and adaptive immune response. *Veterinary Immunology and Immunopathology*, 91, pp. 1-12.
- WHO. (1993) World Health Organization declares tuberculosis a global emergency. *Soc. Prevent. Med*, 38, pp. 251-252.
- WHO. (2008) Priorities for vaccine evaluations for prequalification [online]. Available at: <<http://www.who.int/en/>> [Accessed 2 December 2008].
- WHO. (2010a) Tuberculosis [online]. Available at: <<http://www.who.int/mediacentre/factsheets/fs104/en/>> [Accessed 17 May 2011].
- WHO. (2010b) 2010/2011 Tuberculosis Global Facts [online]. Available at: <<http://www.who.int/en/>> [Accessed 17 May 2011].
- WHO. (2010c) Global tuberculosis control 2010 [online]. Available at: <[http://www.who.int/tb/publications/global\\_report/2010/en/index.html](http://www.who.int/tb/publications/global_report/2010/en/index.html)> [Accessed 17 May 2011].
- Williams, R.O., Repka, M., Liu, J., (1998) Influence of propellant composition on drug delivery from pressurized metered-dose inhaler. *Drug development and industrial pharmacy*, 24 (8), pp. 763-770.
- Wright, J.R. (1990) Clearance and recycling of pulmonary surfactant. *American Journal of Physiology*, 259 (2), pp. 1-12.
- Yan, W., Chen, W., Huang, L. (2007) Mechanism of adjuvant activity of cationic liposome: Phosphorylation of a MAP kinase, ERK and induction of chemokines. *Molecular Immunology*, 44, pp. 3672-3681.
- Yan, W., Huang, L. (2009) The effects of salt on the physicochemical properties and immunogenicity of protein based vaccine formulated in cationic liposome. *International Journal of Pharmaceutics*, 368, pp. 56-62.
- Yu, H., Jiang, X., Shen, C., Karunakaran, K.P., Jiang, J., Rosin, N.L., Brunham, R.C. (2010) Chlamydia muridarum T-Cell Antigens Formulated with the Adjuvant DDA/TDB Induce Immunity against Infection That Correlates with a High Frequency of Gamma Interferon (IFN- $\gamma$ )/Tumor Necrosis Factor Alpha and IFN- $\gamma$ /Interleukin-17 Double-Positive CD4 T Cells. *Infection and Immunity*, 78 (5), pp. 2272-2282.

Zeng, X.M., Martin, G.P., Marriot, C. (1995) The controlled delivery of drugs to the lung. *International Journal of Pharmaceutics*, 124, pp. 149-164.

Zhang, X., Zhang, Z. (2001) *Progress in Transmission Electron Microscopy: Concepts and techniques*. Springer, New York.

**Table A.1. DDA-TDB based immunoadjuvant formulations in which the main liposomal system was either substituted or replaced with DPPC or DSPC lipid.** The formulations are displayed in order of DDA content, with the highest level of cationic presence at the top.

	<b>Formulation</b>	<b>DDA/Lipid/TDB (<math>\mu\text{g}/\text{dose}</math>)</b>	<b>DDA/Lipid/TDB (<math>\text{mg}/\text{ml}</math>)</b>
Decreasing cationic content ↓	DDA-TDB	250/0/50	1.25/0.00/0.25
	+25% DPPC	188/82/36	0.94/0.41/0.18
	+25% DSPC	188/88/36	0.94/0.44/0.18
	DDA-LIPID-TDB	150/100/50	0.75/0.50/0.25
	+50% DPPC	125/165/25	0.62/0.83/0.13
	+50% DSPC	125/175/25	0.62/0.88/0.13
	DDA-LIPID-TDB	100/150/50	0.50/0.75/0.25
	DDA-LIPID-TDB	100/0/50	0.50/0.00/0.25
	+75% DPPC	62/246/14	0.31/1.23/0.07
	+75% DSPC	62/264/14	0.31/1.32/0.07
	DDA-LIPID-TDB	50/200/50	0.25/1.00/0.25
	DDA-LIPID-TDB	10/240/50	0.05/1.20/0.25
	DDA-LIPID-TDB	0/250/50	0.00/1.25/0.25

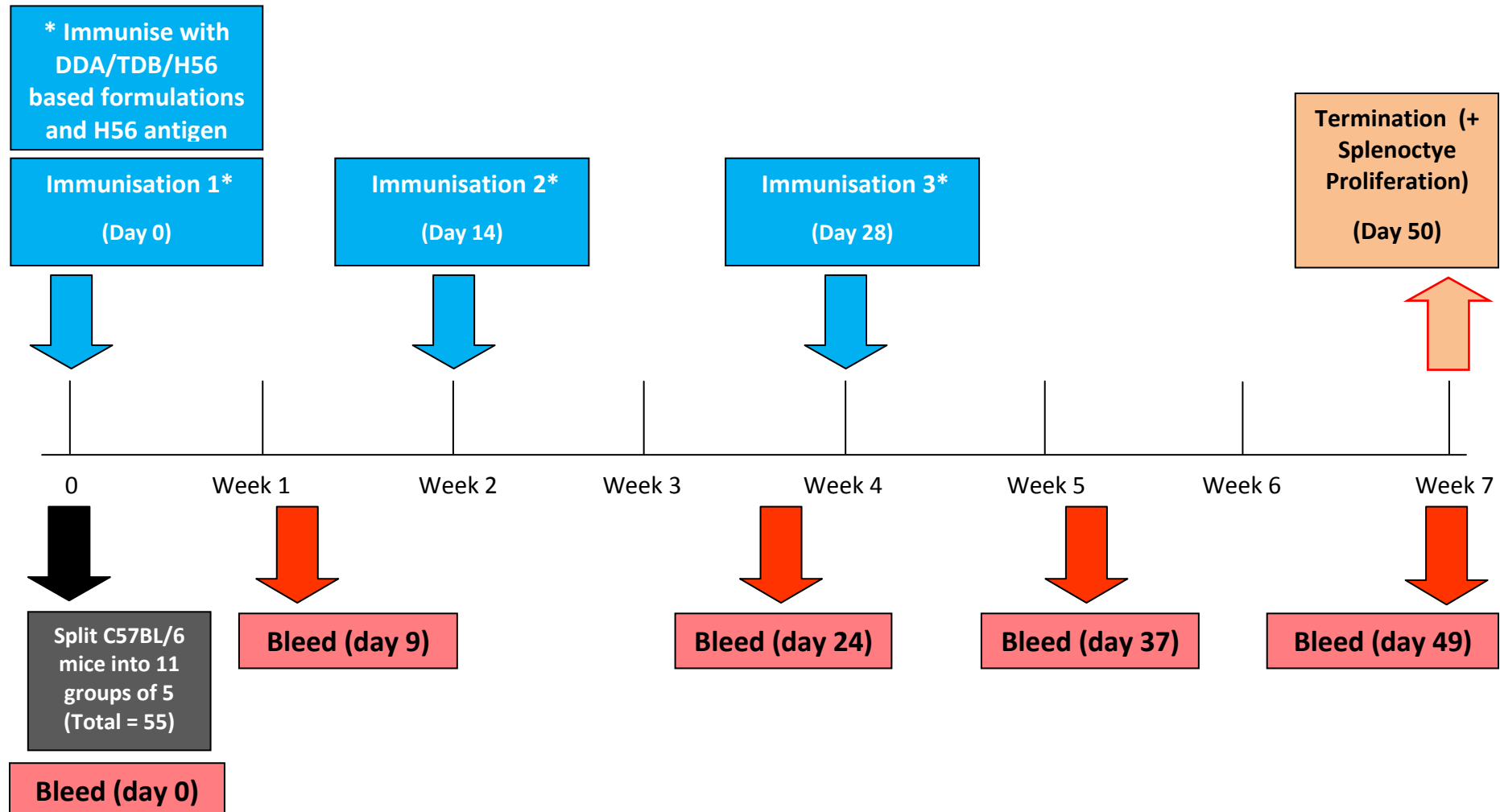


**Figure A.1. Full vaccine immunisation study timeline.** Vaccine preparations were made with liposomes incorporating H56 vaccine. All mice, with the exception of the naive group, were immunised intramuscularly with the proposed vaccine three times, with two week intervals between each immunisation, prior to termination after 7 weeks.